BMR JOURNAL of Australian Geology & Geophysics

VOLUME 3, NUMBER 1, MARCH 1978

BMR Journal of Australian Geology & Geophysics Volume 3, (1)

Department of National Development, Australia

Minister: The Hon. K. E. Newman, M.P.
Secretary: A. J. Woods

Bureau of Mineral Resources, Geology and Geophysics

Director: L. C. Noakes, O.B.E.
Editor, BMR Journal: J. F. Truswell

The BMR Journal of Australian Geology and Geophysics is a quarterly journal of research and related activities. Contributions are from officers of the BMR, from BMR officers working in collaboration with others, or requested work sponsored by the BMR. In addition to articles the Journal may include shorter notes and discussion of papers published in it. Discussion of papers is invited from anyone.

Annual subscription to the Journal is at the rate of $10 (Australian). Individual numbers, if available, cost $3. Subscriptions, etc., made payable to the Receiver of Public Moneys in Australian dollars, should be sent to the Director, Bureau of Mineral Resources, Geology & Geophysics, P.O. Box 378, Canberra, A.C.T. 2601, Australia. The Journal can also be obtained from the offices of the Department of National Development in Sydney and Melbourne.

Other matters concerning the Journal should be sent to the Director, marked for the attention of the Editor, BMR Journal.

BMR JOURNAL of Australian Geology & Geophysics

Volume 3, Number 1
March 1978

AUSTRALIAN GOVERNMENT PUBLISHING SERVICE
CANBERRA 1978

Front cover:

Obsidian daggers from Lou Island, in St Andrew Strait, northern Papua New Guinea. The blades were flaked from rhyolitic lava flows by the ancestors of the present-day inhabitants of Lou Island. This number contains a paper on the geochemistry of the St Andrew Strait rhyolites. Trace-element compositions have been used to determine the ancient trading routes of obsidian in Melanesia.

Photograph: W. R. Ambrose and D. Marcovic, Research School of Pacific Studies, Australian National University. Cover design, P. Corrigan.

ISSN 0312-9608

Printed by Graphic Services Pty Ltd, 516-518 Grand Junction Road, Northfield, S.A. 5085

Proterozoic microfossils from the Roper Group, Northern Territory, Australia

C. J. Peat[1], M. D. Muir[2], K. A. Plumb, D. M. McKirdy[3], & M. S. Norvick[4]

The Roper Group (minimum age approximately 1300 x 10^6yr) is a shallow water sequence of sandstone, siltstone, and shale, with minor, sub-economic oolitic ironstone. The depositional environments of the Group as a whole, range from fluvial, through deltaic or estuarine, to marine, and a number of different environments of deposition for the ironstones can be recognised. Shales from the McMinn Formation at the top of the Group have yielded an assemblage of microfossils. The microbiota includes algal cells and filaments, large acritarchs and giant filaments of uncertain affinity. A probable life cycle and an example of endospory may indicate that some of the organisms are eukaryotic. The flora is very advanced for its geological age, but this is probably because most other Precambrian microbiotas come from carbonate, stromatolitic environments, where simpler and more conservative forms would have predominated. The microfossils are in a particularly good state of preservation because of the low degree of thermal metamorphism which the sediments have undergone. Geochemical and petrographic studies of the organic matter indicate that its composition and level of organic maturation are appropriate for the generation of oil. The rank of the organic matter is locally increased by proximity to dolerite sills which intrude the Group as a whole.

Introduction

The rocks of the Roper Group crop out extensively in the eastern part of the Northern Territory from about 17°S to northern Arnhem Land (Fig. 1). The sequence comprises mainly sandstone and shale, with minor amounts of sub-economic oolitic ironstone near the top of the Group. The ironstone was drilled by BHP in the 1950s, and an account of its petrography was given by Cochrane & Edwards (1960). Among other lithologies reported in the drill core, were fine-grained black and green shale and siltstone, some of which were analysed by Hoering (1967), who described the low degree of thermal maturity of the organic matter. Norvick (1970) subsequently examined some of the shales for organic-walled microfossils, and briefly reported on an assemblage of spheroids.

The present studies are an elaboration of these preliminary findings and are intended to elucidate the environments of deposition, to describe the varied and abundant microfossil assemblages, and to examine the degree of thermal maturity of the soluble and insoluble organic matter, and to determine how the extensive intrusion of dolerite sills has affected the microfossils and the other organic matter.

Some of the drill-core material was collected by K. A. Plumb in 1972, and the remaining samples were collected by M. D. Muir and C. J. Peat in 1975, from the drill core stored at Sherwin Creek (and now the

1. Department of Geology, Royal School of Mines, Prince Consort Road, London SW7 2BP, U.K.
2. Formerly of Department of Geology, Royal School of Mines, Prince Consort Road, London SW7 2BP, U.K., present address BMR.
3. Formerly of BMR, present address South Australia Department of Mines, P.O. Box 151, South Australia 5063.
4. Formerly of the BMR, present address Exploration Division, British Petroleum, Aberdeen, U.K.

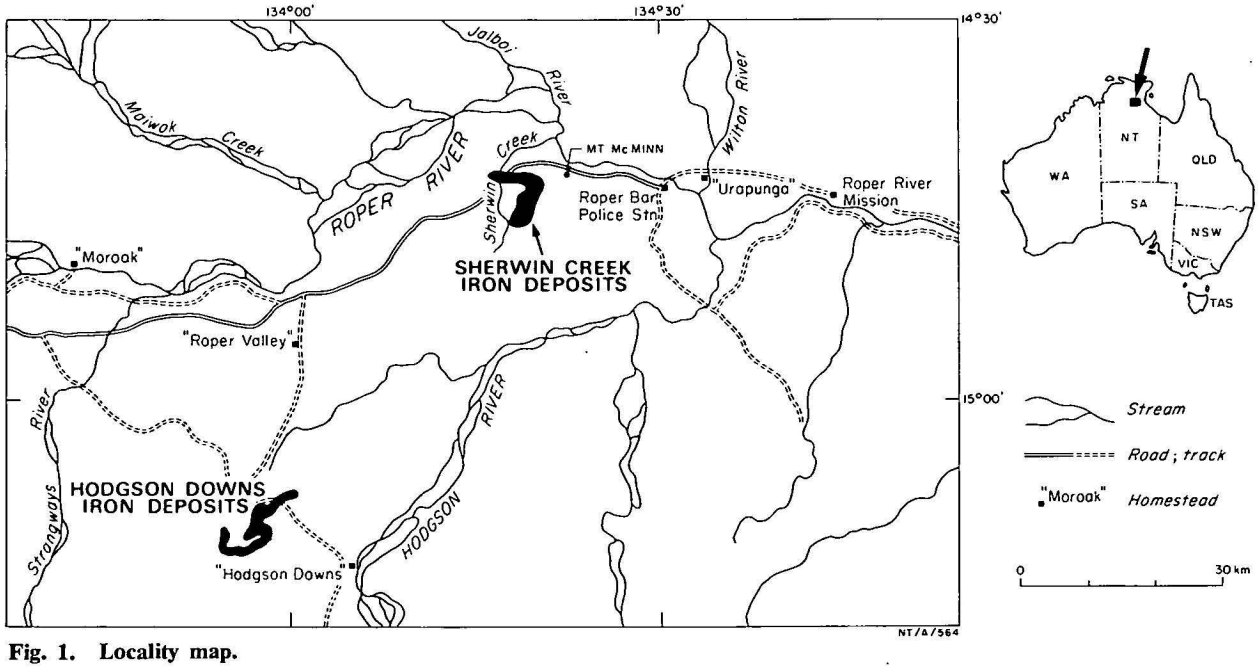

Fig. 1. Locality map.

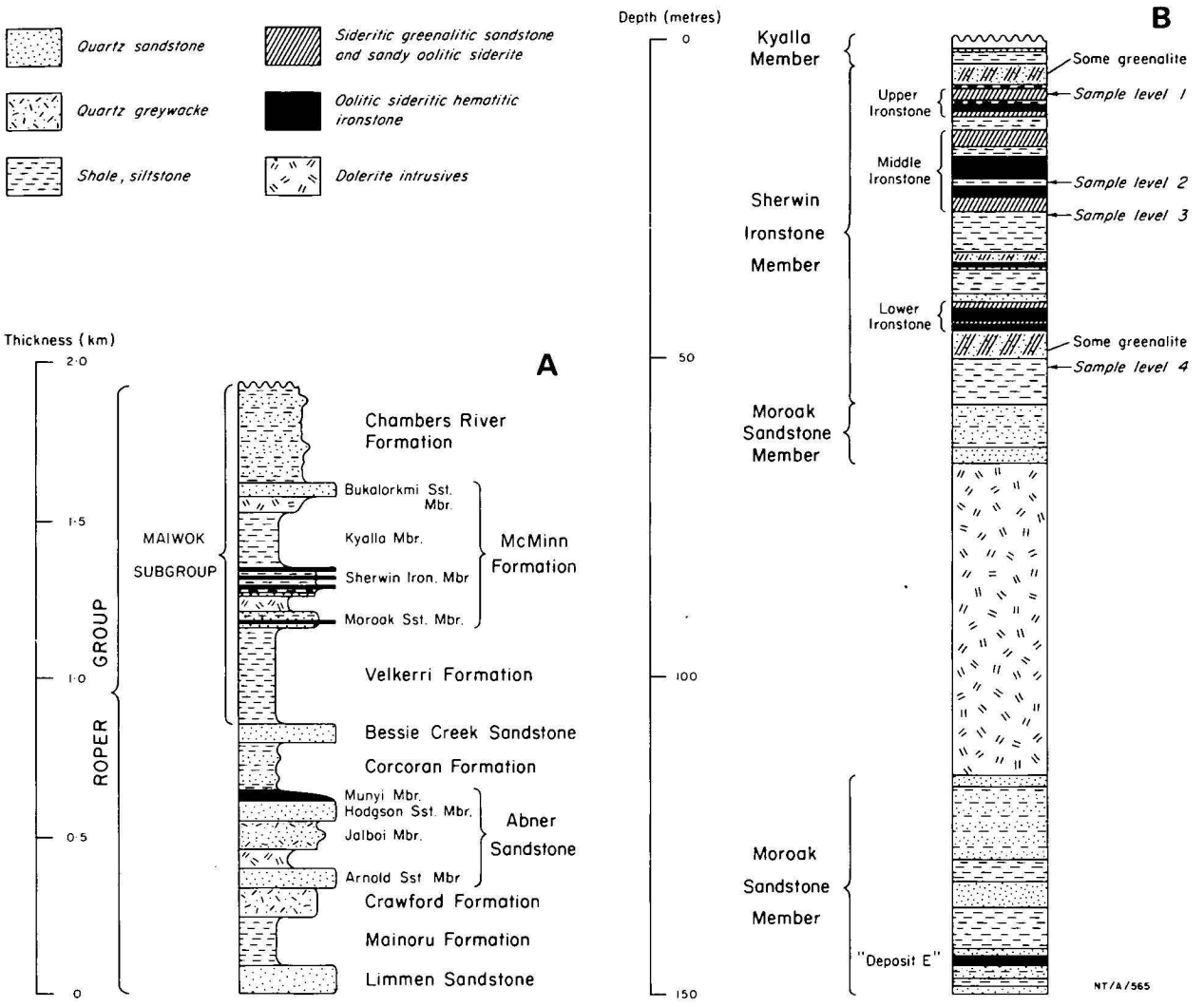

Figure 2a. Schematic column of the stratigraphy of the Roper Group at Roper River. b. Schematic lithological log BHP DDH B7—Sherwin Creek iron deposit.

property of the Northern Territory Department of Mines). Surface outcrop samples are too weathered to be used for micropalaeontology or organic geochemistry. The slides prepared for this paper are now in Peat's working collection, but will eventually be deposited in the CPC, BMR. Additional reference information, recorded in the form MAC DDH B7 74'2-9-1257-067, which means *M*aceration from *D*iamond *D*rill *H*ole number *B7*, sample depth *74'2"* slide number *9* prepared from this macerate, microscope stage co-ordinates *125.7* x *06.7*, prefix TS means thin section—is housed with the slides. In a few cases a similar form of reference is used in this text.

Geology

The Roper Group is the youngest sequence of the McArthur Basin and unconformably overlies the older successions: the carbonate-rich McArthur Group and its equivalents, which in turn overlie the quartz arenite/basic volcanic suite of the Tawallah Group and its equivalents (Plumb & Derrick, 1976). The McArthur Group is a rich source of microfossils from different facies (Love & Zimmerman, 1961; Love, 1965; Croxford, 1973; Hamilton & Muir, 1974; Muir, 1974, 1976; Oehler, J. H., 1977; Oehler, D. Z., in preparation).

The Roper Group comprises an unstable shelf association of mica-rich siltstone, shale and quartz greywacke, alternating with well-sorted pure quartz sandstone (Fig. 2a). The quartz sandstones are characterised by abundant medium-scale high-angle cross-beds, and ripple and rill marks. The interbedded quartz greywacke/siltstone sequences have a spectacular abundance and variety of sedimentary structures—medium to small-scale low-angle cross-beds, ripple marks, rill marks, swash marks, shale clasts, mud cracks, flute casts, brush and tool marks, braided channel casts, step moulds, current scours (toroids), crystal casts (?gypsum) and slump folds. Glauconite is a common constituent. Thick shales and siltstones are generally laminated, have calcareous interbeds, and range through black, grey, grey-green, olive-green and brown in colour.

At Roper River the Roper Group is up to 1.9 km thick (Dunn, 1963) and dolerite sills intrude at several levels; elsewhere the group is up to 5 km thick (Plumb & Derrick, 1976). The major units are continuous over wide areas, but while the quartz sandstones are characteristically laterally uniform the other units display significant lateral facies changes.

The lutite-rich Maiwok Sub-Group (Fig. 2a) is only recognised in the Maiwok Sub-Basin, around Roper River (Dunn, 1963): the equivalent beds crop out very

poorly elsewhere and are mapped as Cobanbirini Formation (Plumb & Derrick, 1976). Four members have been recognised in the McMinn Formation, but regionally they interfinger and their contacts are gradational.

At Sherwin Creek (Fig. 2b) the Moroak Sandstone Member comprises blocky, fine to medium-grained red and grey friable quartz sandstone and interbedded flaggy sandstone, siltstone and black shale. Coarse-grained sandstone is locally present at the base. Upward-fining sequences are repeated throughout the Member. Cross-beds and ripple marks are abundant; flute casts, scour and fill structures, desiccation cracks, distorted sandstone dykes (Conybeare & Crook, 1968, p. 188) clay pellets, and small slumps are common. The blocky sandstones decrease in abundance up section, and the lutites increase up to the overlying Kyalla Member.

The Kyalla Member comprises mainly flaggy interbedded variegated grey, olive-green and brown shale, micaceous siltstone and fine-grained sandstone. Interbeds of blocky sandstone and black carbonaceous shale (sometimes pyritic) occur near the base; carbonates are locally important towards the top of the sequence. Sedimentary structures include ripple marks, flute casts, current lineations, brush and tool marks, mud cracks and clay pellets. Sandstone dykes have not been found in the Kyalla Member.

Discontinuous bands of sub-economic ironstone at or near the base of and interfingering with the Kyalla Member are mapped together as the Sherwin Ironstone Member. Up to three major bands of ironstone are found (a fourth minor band is present within the Moroak Sandstone Member), comprising combinations of hematite oolites, greenalite oolites and granules, chamosite and quartz grains, set in a matrix of siderite. The siderite partially replaces the greenalite and hematite, and in weathered outcrop is itself replaced by silica (Cochrane & Edwards, 1960). Interbeds of fine-grained chloritic sandstone and black micaceous pyritic carbonaceous shale, studded with greenalite granules, occur within and separating the ironstone bands. Cross-beds are present in the hematite oolite beds, and intraformational ironstone conglomerates are observed locally.

The rocks adjacent to the dolerite sills show little visible contact metamorphism, although one sample from DDH B7 about 13 m above the dolerite did show slight recrystallisation. Organic remains and fossils are noticeably darker from samples near to sills but these changes have not yet been quantified. An unsuccessful attempt to obtain a Rb-Sr isotopic age from a suite of the fossiliferous shales may be attributable to slight thermal metamorphism by the dolerite (Webb, 1973).

Depositional environment

Detailed sedimentological studies have not yet been carried out on the Roper Group, but the overall association of mineralogical textures and sedimentary structures suggests alternating shallow-marine, transitional and fluviatile environments for the Group as a whole.

The regional setting of the basin (Plumb & Derrick, 1976) is that of a broad epicontinental shelf (of the order of 400 x 600 km) probably bordered by land on most sides. A variety of local environments is to be expected in such a setting from open shelf, barrier systems, tidal channels and flats to lagoons, estuaries, rivers and lakes. Local areas of restricted circulation are common in estuaries, lagoons and sea-floor depressions.

The repeated upward-fining sequences and the structures indicating strong current action and periodic desiccation suggest a fluviatile origin for the Moroak Sandstone Member. The degree of sorting and paucity of coarse material indicates a distant source area and the most likely environment would seem to be near the outer limit of fluvial influence, perhaps extending into tidal channels. In comparison, the types of lutite in the Kyalla Member and their regularly interbedded rock types, laminations and desiccation features indicate restricted or transitional marine environments (barred basins, lagoons or tidal flats). The vertical progression of facies therefore points to the Sherwin Ironstone Member being deposited in a shallow restricted marine environment at or near to the interface with terrestrial or fluvial influence.

The Sherwin Ironstone Member contains all of the four facies or iron formation—sulphides, carbonate, silicate, and oxide—described by James (1954), and they are all closely interbedded and intermixed. For example, oxides (hematite) and silicate (greenalite) occur in carbonate (siderite) cement, and greenalite occurs in pyritic black shale sulphide). These facies were each supposed to require distinctly different physico-chemical conditions for their precipitation, but recent studies (Curtis, 1977) have shown that the facies could easily be the result of changing rates of sedimentation and differential diagenesis.

The microfossils are best preserved within black pyritic carbonaceous and micaceous shales; most of the organisms probably lived as free-floating plankton, and were then transported or dropped into their present positions with other detritus. Some colonies are preserved in their positions of growth (Fig. 7h, i) but most of the other forms, judging by their attitudes in the sediment and varied preservation, had been washed around or recycled for some time before being deposited.

Age of the Roper Group

A recent attempt to obtain a direct estimate of the isotopic age of the fossiliferous shales was unsuccessful, perhaps due to rehomogenisation of the rocks during intrusion of the dolerite sills (Webb, 1973). The best estimate of the age of the Roper Group is still that of McDougall and others (1965). Glauconite ages from the Crawford Formation range from 1100 to 1280 x 10^6 years old by the K-Ar method and 1270-1390 x 10^6 years old by the Rb-Sr method, so 1390 x 10^6 years is regarded as a minimum age for the Formation. K-Ar mineral ages of pyroxenes and plagioclases from the dolerite sills range from 1095 to 1280 x 10^6 years, so 1280 x 10^6 years is regarded as a minimum estimate for the end of deposition of the Roper Group.

Although these data are not good when taken in isolation, they are broadly consistent with the overall pattern of the latest ages available for the McArthur Basin and Mount Isa Region (Plumb & Sweet, 1974; Plumb & Derrick, 1976) and it seems reasonable to conclude that the Roper Group is somewhere between 1300 and 1400 x 10^6 years old.

The Roper Group has commonly been assigned to the Adelaidean (Dunn, Plumb & Roberts, 1966), but the age of the type Adelaidean is now the subject of further investigation. There is no agreement yet on whether this age is about 1400 m.y. (Thomson, 1966) or less than 900 m.y. (Cooper & Compston, 1971; Cooper, 1975; Preiss, 1976). The microfossils from the McMinn Formation cannot be correlated with any material from the Adelaide Geosyncline at this stage.

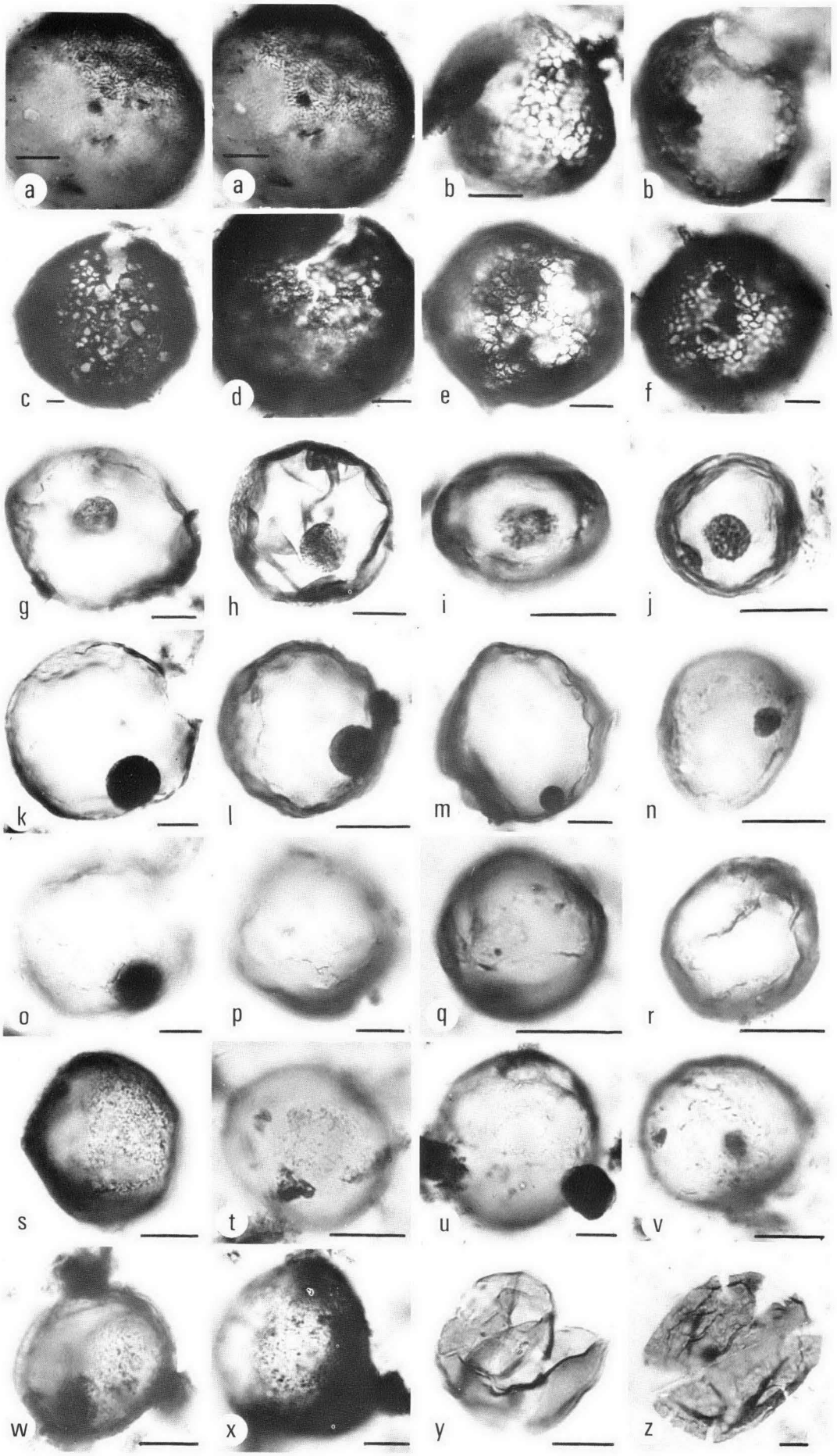
a
a
b
b
c
d
e
f
g
h
i
j
k
l
m
n
o
p
q
r
s
t
u
v
w
x
y
z

Palaeontology

The presence of animals in the Roper Group has been suggested on dubious grounds. No specimens of the '*Beltanella*-type' jellyfish (cf Dunn, 1964) are known, and Peat and Muir found no further examples at the original locality in the Limmen Sandstone along the East bank of Flying Fox Creek between 14°7′S, 133°43′E and 14°9′S, 133°14′E. Other reports of '*Beltanella*-type' jellyfish in the Lower Proterozoic Katherine River Group (Rix, 1965) have not been confirmed. Triact sponge spicules reported from the Vizard Formation near the base of the McArthur Group in the Urapunga Sheet area (Dunn, 1963, 1964) are now believed to be volcanic shards, while 'Impressions of groups of radiating acicular spines' (Dunn, 1964) on the surface of cherts from the Mount Rigg Group or the McArthur Group are probably crystal casts (cf Cloud, 1976). The question of trace fossils is open, but all of the structures found so far can be adequately explained as of sedimentary or diagenetic origin.

Microfossils were first discovered by standard palynological maceration of drill-core (DDH-U37-120′ to 166′, 134°15′E, 14°45′S) samples of carbonaceous shales (Norvick, 1970), which McKirdy and others (in prep.) were using to study the organic geochemistry of the McMinn Formation. The area was drilled by the Broken Hill Proprietary Company Limited between 1958 and 1961 to prospect the Sherwin Ironstone Member; the core now belongs to the Northern Territory Department of Mines (Cochrane & Edwards, 1960; Canavan, 1965). Fourteen samples were collected by Plumb in 1972 and sent to Muir in London. Results from these samples were so exciting that the core was extensively resampled by Muir and Peat in 1975 (367 samples) Some of this material has yet to be examined, but observations to date are of sufficient interest to provoke this preliminary report. Our intention is to indicate the diversity and evolutionarily advanced nature of the microbiota rather than the taxonomic and nomenclatural problems which it has presented.

The fossils are morphologically grouped as spheres, filaments, and colonial aggregations, and are most likely of bacterial and algal affinity. Intimately connected clusters of cells and filaments are excluded from the Group Acritarcha (Downie and others, 1963), but we feel that all microfossils of the type described here are best dealt with informally in a morphological scheme of classification. There are few instances, especially in the Precambrian, where the assignment of fossil genera is not questionable at the Order level. No new names are proposed here although some of the fossils represent new types.

The fossils illustrated are described from petrographic thin sections and standard palynological macerations (surface contamination removed by grinding, 10% HCl, 40% HF, washed, no oxidation or staining, residues mounted in glycerine jelly). All of the fossils except Figures 3a, 7b and 7c have been found in thin sections, but macerates generally photograph better and it is these pictures which are presented. Filaments, especially the organic sheaths (Fig. 7a), are broken up during maceration, and even when common in thin sections of the same rock it is rare to find fragments longer than 40 μm in macerations. New and modified preparative techniques for scanning and transmission electron microscopy have been developed by Peat, but have not yet been extensively applied. Cell wall ultrastructure may provide a basis for classification (Kjellstrom, 1968; D. Z. Oehler, 1976).

The forms illustrated in this report demonstrate the breakup of intimately connected clusters of cells to produce sphaeromorph acritarchs, the release of other sphaeromorphs by the equatorial splitting of disphaeromorphs and the production of filamentous and netromorph-like structures from others. A possible sample of endospory is described and some filaments are compared with experimentally fossilised material. Most of the fossils can be compared with forms described from Late Precambrian and Early Cambrian rocks (Naumova, 1960; Timofeev, 1966; Vidal, 1976). Unfortunately many genera are invalid or obscure and we are not yet in a position to evaluate them. It will be some time before any coherent systematic treatment can be presented.

Spheres have two kinds of surface reticulation: type I is very fine with elongate surface cells (Fig. 3a) while type II is coarser with more or less equidimensional cells (Fig. 3b-f). The spheres with type II reticulation have a very distinctive appearance, but the reticulate pattern is sometimes almost obscured by a granular texture (Fig. 3d, e). They resemble *Favosophaeridium* Timofeev (1966), especially *F. scandicum* and *F. michailovskyi* (cf. Timofeev, 1966, Plate VIII fig. 3; LXXIV, fig. 7; XLI, fig 3; LXXXVIII, fig. 3). One sphere with type II reticulation has been examined in the scanning electron microscope and we were surprised to find that the surface was merely dented. Either the cell wall is thin with pattern on the inside or an ornamented sphere has a thin membraneous cover. The pattern is too fine and regular to be the result of pyrite infilling (Neves & Sullivan, 1964), and pyrite framboids have not been found. The granular texture may be the result of partial decay of the thinner parts of the wall: in some cases extensive recycling of material occurred prior to fossilisation and this will have given rise to darkened and partially decayed specimens (Fig. 3c). Two specimens (e.g. Fig. 3b) out of the 22 found have an opening which suggests a cyclopyle.

Many smooth spheres (Fig. 3g-n, Fig. 4 various pictures) contain opaque or granular inclusions similar to the 'spots' and 'granulars' of Schopf (1974). There is only one spot or granule in a sphere, though sometimes spots are surrounded by a granular area (Fig. 4q). Large spheres do not necessarily have large spots (Fig. 3 l, m), nor do inclusions occur in every cell of a cluster. The left big sphere of Figure 4t contains a granular, while the others contain spots. While the granulars in small spheres usually lack a regular outline (Fig. 3i), those in larger spheres (Fig. 3g, h) are usually spherical, or disc-shaped in flattened specimens. The simplest explanation of these inclusions is that they are carbonised cytoplasmic remnants preserved in various stages of coalescence. There does seem to be continuum from a dispersed granulation to discrete spots in our material; many plasmolysed cells, including blue-green

Figure 3. Spheres.
(a) Type I reticulate surface at two focal planes; (b-f) Type II reticulate surface; two focal planes of same specimen in *b* showing possible cyclopyle; (g-j) spheres with granular inclusions; (k-n) spheres with opaque inclusions; (o-x) surface textures of spheres. *o* is surface of *k*, *p* is surface of *m*; (y) opening by median split; (z) radial splitting of a more rigid wall due to compression. Bar scale is 10 μm long.

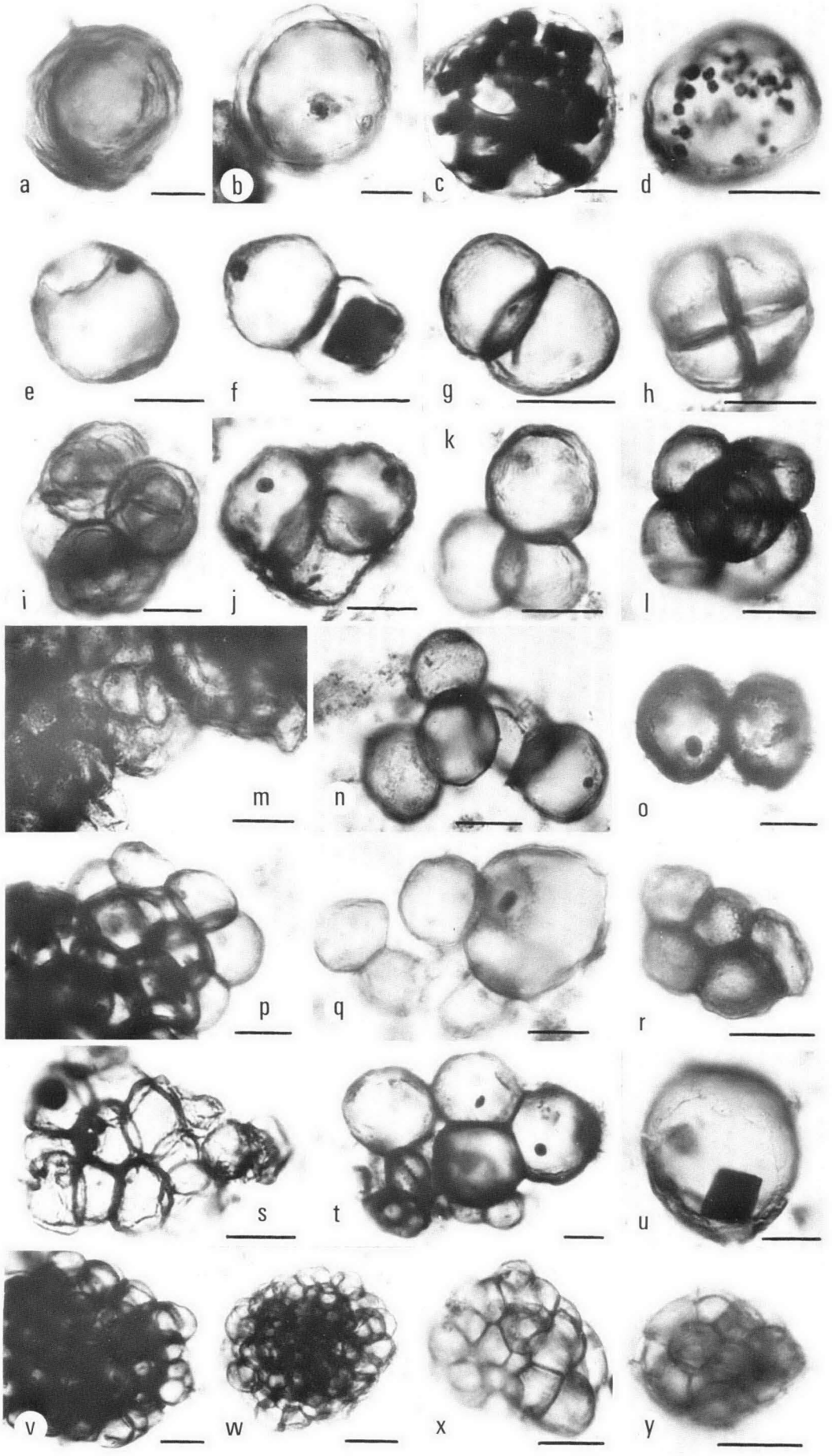
a
b
c
d
e
f
g
h
i
j
k
l
m
n
o
p
q
r
s
t
u
v
w
x
y

algae, exhibit similar structures when dying and before decomposition (Knoll & Barghoorn, 1975; Golubic & Barghoorn, 1977).

Spots in cells from the Bitter Springs cherts have been shown to have a distinct dense microstructure in the transmission electron microscope (D. Z. Oehler, 1976) and have been interpreted as remnants of pyrenoids. The congealing properties of cytoplasm have not been studied, but it does seem that an original, densely carbonaceous structure such as a pyrenoid (dense protein), fat globule (volutin) or storage granule (starch) would be most likely to give rise to a spot, or act as the nucleus for its formation. Spots and granules alone are not adequate grounds for supposing the presence of eukaryotic cells (Knoll & Barghoorn, 1975; Golubic & Hofmann, 1976; Hofmann, 1976; Schopf & Oehler, 1976). Better evidence is provided by large sphaeromorph acritarchs and the existence of life cycles like the one described below. For the future it is difficult to envisage any generally applicable way of differentiating prokaryotic and eukaryotic unicells, especially as biochemical evidence is beginning to point to a gradual, polyphyletic evolution of eukaryotes from prokaryote and protoeukaryotic stocks (Bonen & Doolittle, 1976).

Among the non-reticulate spheres, surface texture varies from smooth or shagreen-like (Fig. 3o, p) to distinctly granular (Fig. 3s, x). The polygonal areas on some fossils (Fig. 3q, r) could be due to wrinkling, the rupture of the outer of a series of membranes, or caused by mechanical disturbance of a hardened layer of mucilage, any of which could have occurred at any time during deposition, diagenesis, recycling, maceration or mounting. Figure 3 is very similar to a form described from the Torridonian by Cloud & Germs (1971, figs. 9, 10), referred by them to *Protosphaeridium* cf. *P. parvulum* Timofeev (1966). Some forms have a distinctive crinkly surface (Fig. 6r) but this pattern is part of a continuum varying from a linear surface granulation (Fig. 3v) to microfolds (Fig. 6 o. Compare this with Cloud & Germs, 1971, fig. 8). Larger wrinkles than those shown in Figure 6u in turn become indistinguishable from much-folded sphaeromorphs which are, nonetheless, different from Figure 6r. A variability map which plots morphological features in diagrammatic form as used for the Leiofusidae (Combax and others, 1967) is probably the only satisfactory way of dealing with these variations.

Sheets of cells occur within thin membranes (Fig. 5a) and free (Fig. 5b, c). The cells grow larger (Fig. 5d) and can be expected to give rise to clumps of sphaeromorphs (Fig. 5e, possibly even Fig. 5f). It seems reasonable to suggest that individual spheres (from Fig. 5e) may grow and develop endospores in their turn. We have seen one example (not figured; MAC DDH M14 250'8-18-1270-216) of a cell sheet inside an opened valve, but this could have been an accident of preparation. The regular occurrence of sphaeromorph acritarchs in clumps has already been suggested as evidence for their formation as endospores (Downie, 1973). These fossils could also represent the remains of colonies of volvocacean algae such as *Pandorina* and Eudorina (see Kazmierczak, 1976), but could equally be endosporulating pleurocapsalean cyanophytes (Golubic, 1976).

Large aggregations of pale unstructured organic matter containing dark inclusions (Fig 5t-w) are common. The pale material is interpreted as mucilage in which degraded vegetative algal cells are embedded, as in the living genus *Aphanocapsa* (e.g. Desikachary, 1959). The cells may be arranged along twisted ribbons of mucilage (Fig. 5t), in folded sheets (Fig. 5u) or in large rounded aggregations up to 200 μm across (TS DDH B8-143'0-7-1017-071, not illustrated) that may resemble flattened spheres.

Disphaeromorph acritarchs (Fig. 5g) are not rare, but they are usually flattened and slightly degraded (Fig. 5h, i) which makes them superficially similar to some Pteromorphs (Downie and others 1963). The thin outer test opens by a median split to release a dark, much folded, orange-brown sphaeromorph (Fig. 5j). Sphaeromorphs and empty valves (Fig. 5k) are common. Many of the larger Sphaeromorphs open by median splits, and in thin sections it is often especially difficult to tell whether a circular body is a flattened sphere or a simple valve.

The thin empty valves eventually separate and curl up, either through being rolled about with the sediment or because of internal strains (Eisenack, 1958). When tightly rolled they resemble Netromorphs. Mädler (1963) seems to have mistaken at least some rolled valves for Netromorphs when describing *Lancettopsis lanceolata* (Taf 28, figs. 4-8; Taf 29, figs. 1-3) which he later considered to be a juvenile stage of *Campenia gigas* (Mädler, 1969).

Large thin-walled flattened sphaeromorphs occur regularly in macerates and thin sections and range up to 600 μm in diameter (Fig. 6b). Spheres of this size are not uncommon in Late Precambrian and Cambrian deposits Timofeev, 1966, 1970a, b; Roblot, 1964) and some of macroscopic size (greater than 500 μm diameter) have been arbitrarily selected for inclusion in the genus *Chuaria* (Ford & Breed, 1973).

The breakdown of large sphere is inferred to be due to the action of bacteria, although no convincing bacterial fossils have been found. Filamentous fossils have not been found in association with decaying spheres, so there is no firm evidence of fungal attack. Decay has taken place after some compaction of the fossils, and has proceeded over the whole surface at once. The thin wall of the spheres disappears first, leaving only the thicker folds behind (Fig. 6a, c, d). In some horizons the commonest fossils are 'fronds' (Fig. 6e-h) resulting from recycled material. These fronds were originally interpreted as partially degraded remains of iron bacteria or filamentous algae (Peat, 1975). Similar structures have been illustrated and described as *Microtaenia* sp. by Lopukhin (1975, 1976), and Pflug (1967) noted that they could be formed in the sediment by the compaction of organic debris in thin laminae. The interpretation advanced here implies a planktonic source of large organic remains, most likely acritarchs, with recycling of material and bacterial activity. Sometimes spheres become rolled up in fronds (Fig. 6h) when they resemble some of the Phycomycetes described by Timofeev (1970a, b).

Giant filaments (Fig. 6i-n) have only been found in short fragments, thought these seem to show apical (Fig. 7i, j) and medial regions (Fig. 6k), and remains of cells (Fig. 6 l, n). Most fragments are of the Figure 7k-type,

Figure 4. Small spheres and cells in various configurations.
(a) tangentially folded sphere; (b) double-walled sphere with granular inclusion; (c, d, f, u) infilling of spheres by iron sulphides; (e-h, j-l, n, o, q, t) small spheres in various arrangements and, probably, stages of growth; (i, m) cells showing division within a common sheath; (p, v-y) colonies of closely-packed small cells. Scale bar is 10 μm long.

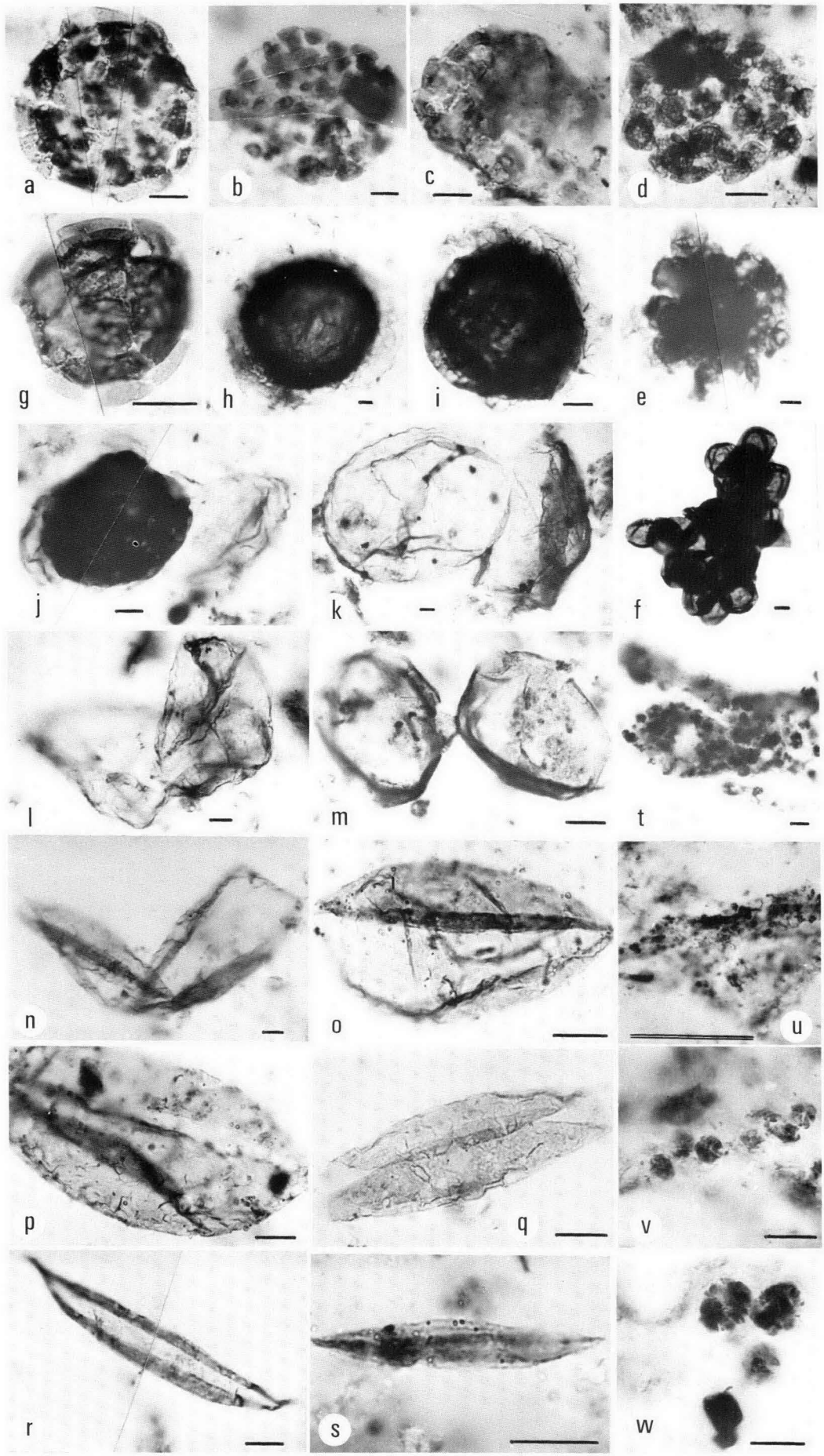
a
b
c
d
g
h
i
e
j
k
f
l
m
t
n
o
u
p
q
v
r
s
w

and all wide pieces were lumped together as broadly similar. Closer examination has shown that Figure 6m is not a tightly twisted ribbon, but a join between two large cells which are unlikely to be of Cyanophyoean affinity. Further, apical fragments Figure 6i, and 6j, can probably be referred to different species of *Lyngbya,* though at 120 μm wide, Figure 6j is 40 μm wider than the 16-80 μm range of *L. majuscula* (Desikachary, 1959). *Lyngbya majuscula,* the largest known extant species, has also been used for experiments in simulated fossilisation (J. H. Oehler, 1976): the similarity between Oehler's material and our fossils in both the light and scanning electron microscopes is very striking. Similar-looking striated tubes ranging from 200 μm to 5000 μm across have been found in the Vendian and described as primitive Deuterostomata (Pogonophora) by Sokolov (1967). Narrower tubes from Late Precambrian and Cambrian rocks have been referred to the algae and illustrated as *Oscilatorites wernadskyi* and *O. sp.* (Timofeev, 1966). We are not yet certain of the affinities of our material, but the possibility of giant blue-green algae in the Precambrian is of considerable interest.

Granular organic filaments (Fig. 7a) are common, sometimes branch, and are occasionally found with a thin (0.5 μm wide) denser strand running down the centre (Fig. 7d, e). In one instance (Fig. 7f) thin strands are seen with only traces of surrounding material, and at high magnification they can be seen to be segmented like a string of beads. This segmentation could be an artifact of preservation, though it is reasonable to assume a filament of small, perhaps shrunken cells embedded in a thick sheath, as has been shown in some larger specimens from the Devonian (Fairchild and others, 1973, although Schopf (1975) now has reservations about the biogenicity of these). Wide granular filaments are here regarded as sheaths, and their preservation varies from finely granular (Fig. 7a) to opaque, brittle, carbonised or encrusted ribbons (Fig. 7g). In the scanning electron microscope the ribbons have no distinctive features. Crystal growth within the sheaths is common (Fig. 7a): similar structures have been described as heterocysts (Schopf, 1972, figs. 46-49). Sometimes sheaths are expanded into round structures (Fig. 7d) or flat sheets (Fig. 7j) or replaced by pyrite (Fig. 7j). The effects are considered to be diagenetic rather than reflecting any original structures: the pyrite crystals need not have formed each within a cell as occurs in some Devonian filaments (Wicander & Schopf, 1974).

Filamentous colonies are rare (Fig. 7h, i), though from their three-dimensional arrangement some of them were growing in the sediment at the time of fossilisation. These two colonies resemble the genera *Eoastrion* (Barghoorn & Tyler, 1965) and *Metallogenium* (Kuznetsov and others, 1963), as well as manganese-rich forms from the McArthur Group (Muir and others, 1974), and a colony described as 'Gunflintia-like' by Licari & Cloud (1968, fig. 10).

Comparisons

Of the 18 well-preserved microfossil assemblages so far reported from non-USSR Precambrian deposits (Schopf, 1975) only two are found in shales, and none of the structures found in them (Allison & Moorman, 1973; Hoorman, 1974) at all comparable to the Roper Group forms, except that some have been doubtfully interpreted as multicellular and planktonic. Neither of these biotas is reported to contain filaments. However, filaments and large (greater than 70 μm diameter) aggregates of spheroidal unicells have been reported from the Belcher Islands, Hudson Bay (older than 1.8 x 10^9 years—Hofmann, 1974, 1976), and wide (16 μm) filaments have been found in the Altyn Formation of Montana (c. 1.3 x 10^9 years—White, 1974).

The nearest assemblages in age to the Roper Group are the Skillogalee Dolomite (Schopf & Barghoorn, 1969; Knoll and others, 1975), Beck Springs Dolomite (Cloud and others, 1969) and Boorthanna (Schopf & Fairchild, 1973) floras. The River Wakefield and Dismal Lakes Groups have so far only been mentioned in abstract (Schopf and others, 1974). The Skillogalee and Beck Springs microbiotas contain only thin (.05 μm wide) filaments or sheaths and 5-25 μm diameter spherical cells, sometimes in clumps. None of these assemblages contains microfossils like the larger Roper Group forms, except for a large (35 x 290 μm) 'ascus-like' structure from the Skillogalee, which is only comparable in size. Large colonies are uncommon in the slightly older stromatolitic McArthur Group (Croxford and others, 1973; Muir, 1974, 1976) and Bungle Bungle Dolomite (Diver, 1974) assemblages. Small (15 μm diameter) colonies from the Bungle Bungle are regarded as allochthonous (Diver, 1974).

The striking difference between the Roper Group shale flora and these contemporaneous chert floras seems most likely to be a result of extensive sampling of the stromatolitic carbonate facies with an almost total neglect of the shelf facies across the beach. This inference is supported by the mass of Russian data on shale sequences (e.g. Timofeev, 1966) and studies of the clastic Torridonian rocks of Scotland (Diver, pers. comm.; Downie, pers. comm.) and the Nonesuch Shale of Michigan (Muir, unpublished data) which show that diverse assemblages and complex large fossils occur in these younger Precambrian sediments.

Multicellular structures which apparently show cellular differentation have been demonstrated in the Amelia Dolomite (c. 1.6 x 10^9 years—Muir, 1976) and macroscopic algae preserved as impressions have been described from the Belt Series of Montana (c. 1.3 x 10^9 years—Walter and others, 1976). Structures of a lichen-like level of organisation have been reported from the Witwatersrand Reef Deposits (c. 2.6 x 10^9 years—Hallbauer & Van Warmelo, 1974; Hallbauer, 1975), though this interpretation has been challenged (Cloud, 1976) and the preparation techniques were undoubtedly severe.

Gnilovskaya (1971) has described megascopic algae from the Vendian of the Russian Platform, and macroscopic algae (*Laminarites* sp.) have long been known from the Lower Cambrian Blue Clays of the Soviet Union (Timofeev, 1966). The general similarity of the Eastern European clastic floras to the Roper Group forms has already been noted.

It therefore seems likely that the development of the megascopic, multicellular level of organisation had taken

Figure 5. Cells and endospores.
(a-d) sheets of cells embedded in mucilage, within a thin membrane; (e-f) suggested further development of *d*; (g-s) the thin outer membrane of some Dsiphaeromorphs *g-i* opens by a median split, releasing a sphaeromorph *j* and producing a pair of valves *k-m*. The valves fall apart and curl up *n-r* eventually giving rise to netromorph-like bodies *s;* (t-w) cellular remains in ribbons and sheets of mucilage. Scale bar is 10 μm long.

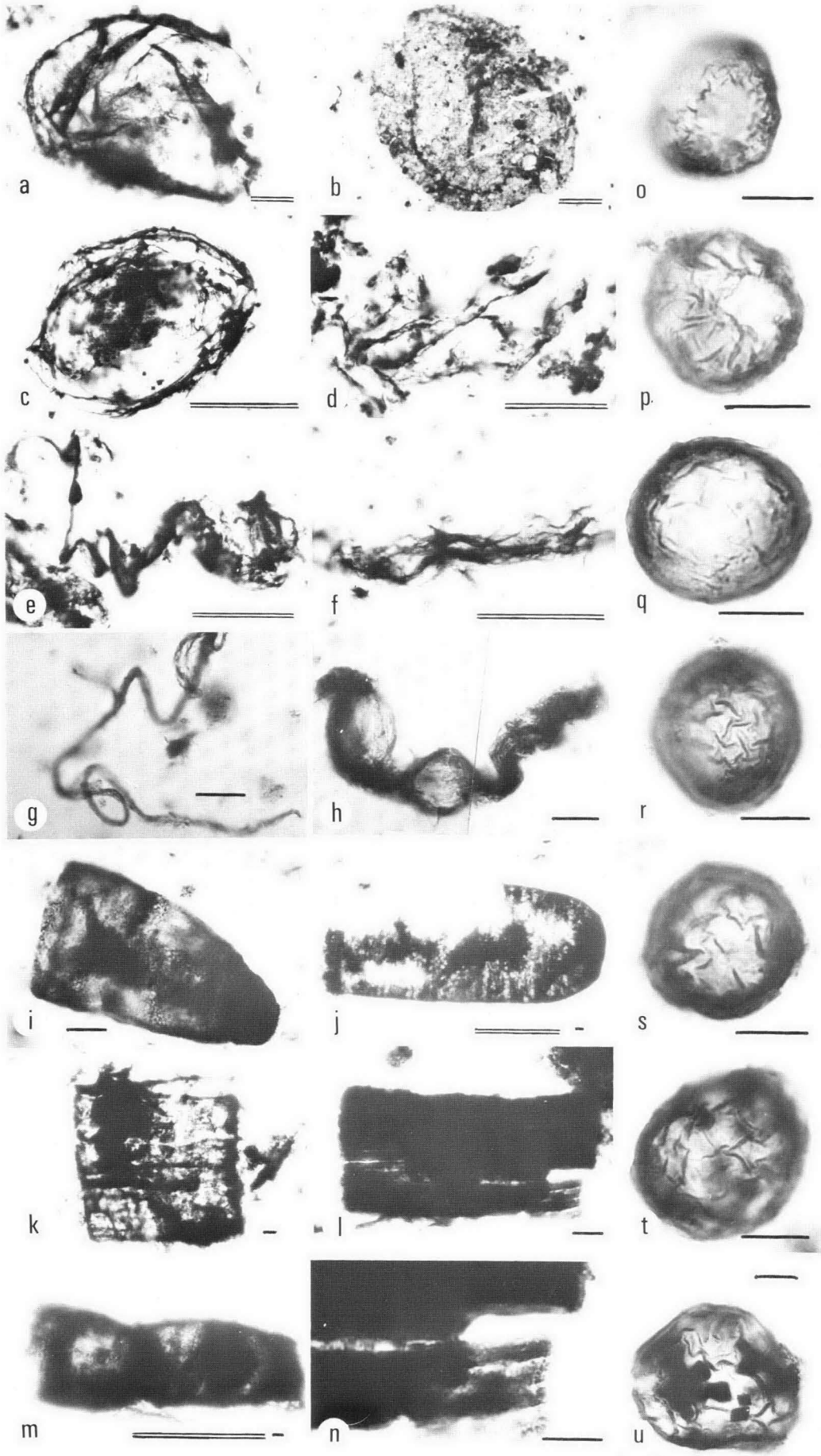
a
b
o
c
d
p
e
f
q
g
h
r
i
j
s
k
l
t
m
n
u

Sample level	Distance above sill (m)	EOM yield	Total hydrocarbons	Saturates	Kerogen H/C ratio	Kerogen C (daf)	Kerogen matrix R_o max.	Kerogen colour
1	55	38–56 mg/gC	58–73% EOM	47–59% EOM	0.86	81.2%	0.47%	dark brown
2	46	16–20	49–69	19–42	0.65	81.9	0.82	greyish brown
3	38	7–12	30–72	19–32	0.53–0.59	80.7–83.4	1.07–1.27	grey brown
4	18	6– 9 (29–32)	27–62 (62–81)	12–33 (25–74)	0.36–0.40	85.5–86.8	1.17	brownish grey

Sample Level 1 includes Samples C4/43, and C5/29. Sample Level 2 includes Samples B8/143 and C11/28. Sample Level 3 includes A9/72, A10/65, B8/173, C3/101, C5/82, C6/80, C6/85. Sample Level 4 A10/121, B7/167, C5/155, C6/154. Where A, B, and C with the accompanying digits are drill hole numbers. The last numbers (after the oblique lines) are depths in feet. All samples at a particular sample level are at the same distance above a dolerite sill.

Table 1. Sherwin Ironstone organic geochemistry.

place by the Middle Precambrian, rather than being a relatively recent innovation. The recent concentration of effort on the investigation of black stromatolitic cherts has given us much information on one restricted ecological niche, but a distorted picture of Precambrian evolution as a whole. The investigation of other Precambrian shale sequences is a vital preliminary to the dating of significant evolutionary events and the future development of a Precambrian Biostratigraphy.

Geochemistry

The organic geochemistry of the McMinn Formation has been studied using core material from the Kyalla Member in the 37-50 m interval of DDH U37 from the Hodgson Downs area, and from other core material in the Sherwin Ironstone, near Sherwin Creek. The samples are listed in Table 1. A detailed account of this work will be published elsewhere (McKirdy, Kantsler, McHugh, & Tardif, in preparation).

The preservation of recognisable microfossils in ancient sediments is thought to depend, among other things, on the lack of metamorphic alteration (Gray & Boucot, 1975). Indeed, low-grade metamorphism has been invoked to explain the poor preservation of many Precambrian microfossil assemblages (e.g. Muir & Hall, 1974; Muir & Grant, 1976; Muir and others, 1977). Rarely are morphologically intact remains of microorganisms found in rocks metamorphosed above lower greenschist facies (Bliss, 1977). To the authors' knowledge, however, there has been no previous attempt to correlate rigorously the state of preservation of the microfossils in a Precambrian formation with its degree of incipient metamorphism. Preliminary organic geochemical analysis of both the extractable organic matter (EOM) and kerogen in 16 samples of carbonaceous shale from the fossiliferous McMinn Formation has provided quantitative evidence of their stage of diagenesis and incipient metamorphism. Both the Kyalla Member (1 sample) and the Sherwin Ironstone Member (15 samples) have been examined. The latter was sampled at four different heights (18, 38, 46 and 55 metres, respectively) above a dolerite sill in the Sherwin Creek area. Hence, the organic matter in this suite may be expected to show some effects of contact metamorphism. The Kyalla Member sample comes from the Hodgson Downs locality, some 70 km south-southwest, where it is less closely associated with intrusive dolerites. Field evidence indicates that at neither locality has the Roper Group been buried by more than 1 km of cover.

Kyalla Member

Kerogen isolated from the single sample of Kyalla Member carbonaceous shale (total organic carbon, 1.66%) is pale yellow-brown and includes both structural and amorphous organic matter. Elemental analysis of the kerogen (73.6% C dry, ash-free; atomic H/C = 1.17; atomic O/C = 0.13), indicates a low rank, broadly equivalent to that of a high-volatile bituminous coal. Although its H/C and O/C values would classify it as a liptinite, infrared spectrometry (IR) and pyrolysis-hydrogenation gas chromatography (PHGC) reveal a highly aliphatic structure, more like that of alginite. The hydrogen-rich composition of the organic matter is consistent with the presence of abundant algal microfossils and acritarchs in the shale, and imparts to the rock a significant potential for generating liquid hydrocarbons.

The associated EOM (561 ppm, 45 mg/g organic C) contains 25.3% saturated hydrocarbons. This, in conjunction with the rank of the kerogen, suggests that the Kyalla shale at Hodgson Downs has matured to the stage of diagenesis at which oil generation occurs (early mesodiagenesis: Foscolos and others, 1976). The shale is somewhat silty and interbedded with silts and sandstones, a situation which favours primary migration of hydrocarbons.

The stable carbon isotopic composition of the Kyalla kerogen ($\delta^{13}C_{PDB} = -30.2‰$) falls at the lighter (i.e. more negative) end of the range for unmetamorphosed Precambrian organic matter (−31 to −19‰: Eichmann & Schidlowski, 1975). Lower $\delta^{13}C_{PDB}$ values (between −30 and −40‰) have been reported from Precambrian organic matter (Hoering, 1967; Hoefs & Schidlowski, 1967; Eichmann & Schidlowski, 1975; Barghoorn and others, 1977), but in most instances these occurrences comprise (at least in part) 'mobilised' organics. The latter are enriched in ^{12}C because during diagenesis or incipient metamorphism ^{12}C-^{12}C bonds rupture more frequently than ^{13}C-^{13}C bonds (McKirdy & Powell, 1974).

Petrographic examination of the shale in polished section under reflected light confirmed the presence of both a primary alginite component in the kerogen and secondary 'mobilised' organic matter. Indeed, most of the optically recognisable organic matter comprises either long coalified algal filaments, or spherical aggregates of thucolite-type material (A. J. Kantsler, pers.

Figure 6. Pseudofilaments, giant filaments and spheres.
(a-h) large sphaeromorphs *b* are gradually eroded *a*, *c*, *d* to fronds and filamentous structures *e-g*. Spheres are sometimes trapped and rolled up in these fronds *h*; (i-n) giant filaments. *i-k* may be sheath material: convincing cellular remnants are rare *l*, *n*. *m* and *i* may represent different species; (o-u) spheres with crinkly surfaces. Single scale bar is 10 μm long double scale bar is 100 μm long.


a
b
g
c
h
i
d
e
f
j

Sample level		EXTRACTABLE ORGANIC MATTER Yield mg/gC	Composition % saturates	% total h'cs	$\delta^{13}C_{PBD}$ ‰	KEROGEN C d.a.f. %	H/C atomic	R_o max.[1] %	Colour
1	Proximity to sill	38–56	47–59	58–73		81.2	0.85	0.47	dark brown
2		16–20	19–42	49–69	–31.7	81.9	0.65	0.82	greyish brown
3		7–12	19–32	30–72	–31.5	80.7–83.4	0.53–0.59	1.07–1.27	grey brown
4		6–9 (29–32)	12–33 (25–74)	27–62 (62–81)	–31.2	85.5–86.8	0.36–0.40	1.17	brownish grey

1. Reflectivity measurements made on compact matrix material rather than discrete phytoclasts.

Table 2. Summary of organic geochemistry of silty shales of the Sherwin Ironstone Member adjacent to a dolerite sill, Sherwin Creek area.

comm., 1976). The thucolite is present as spheres (10-50 μm in diameter) surrounding zircon grains. In most cases, the organic matter is massive and structureless, suggesting an origin from migrating liquid hydrocarbone which have been polymerised by ionising radiation emanating from the zircons.

Sherwin Ironstone Member

This suite of carbonaceous silty shales (total organic carbon, 0.35-0.87%), because of its proximity to the underlying dolerite sill, shows contact metamorphic effects. Approaching the sill, there is a progressive increase in the level of organic maturation (Table 2). Organic matter at sample level 1 (110% sill thickness above sill contact) is the least affected (lowest rank), whereas that at sample level 4 (37% sill thickness above contact) is the most altered (highest rank).

The degree of coalification of the kerogen increases regularly towards the sill, as shown by the trends in carbon content (percent, d.a.f.), H/C atomic ratio, matrix reflectivity, and colour (Table 2). Its elemental composition also changes, possibly via a series of coalification jumps, from that of liptinite at level 1, through micrinite at levels 2 and 3, to semifusinite at level 4, where cooking of the dispersed organic matter appears to have taken place (McKirdy, and others, in preparation). Alteration of the chemical structure of the kerogen is evident from IR and PHGC data (not reproduced here) which indicate a progressive shortening of aliphatic chains and a loss of alkyl groups, accompanied by increased condensation and aromatisation of the kerogen 'nucleus'. At the four levels sampled, carbon isotopic fractionation as a result of contact metamorphism of the kerogen has been slight (0.5‰), but in the expected direction, viz. enrichment of the residual kerogen in ^{13}C (McKirdy & Powell, 1974). Greater metamorphic adjustment of kerogen $\delta^{13}C$ values may have occurred closer to the sill.

Both the yield and hydrocarbon content of the EOM decrease towards the sill (see Table 2). The anomalous values (in brackets) for EOM yield, total hydrocarbons and saturates in two samples at sample level 4 (B 7/167 and A10/121) suggest that they contain migrated hydrocarbons which presumably originated from shales lower in the sequence (i.e. closer to the upper sill contact). The effect of contact metamorphism on the saturated hydrocarbon fraction of the shales has been to markedly increase the proportion of branched and cyclic hydrocarbons at the expense of normal (i.e. straight-chain) alkanes, by catalytic cracking reactions.

Conclusions

The state of diagenesis of both microfossils and kerogen indicates that the rocks have undergone little or no thermal metamorphism, except near to the dolerite sills. Fossils from samples only 10 cm from a sill do not look more carbonised than individuals from further away, even though there has been marked geochemical activity and migration of organic compounds.

Recently, there has been considerable debate on how to recognise the pro- or eukaryotic affinities of organic-walled microfossils (Knoll & Barghoorn, 1975; Schopf & Oehler, 1976; Runnegar, 1977). Although the origin of the eukaryotic cell is of considerable biological interest, there is so far no way of being sure that a microfossil species is eukaryotic. Most discussions on this topic implicitly assume that Precambrian prokaryotes were the same as present-day ones, and that prokaryotes have less genetic variability than eukaryotes because meiotic sexual reproduction is not a part of their life cycle. Such a simplistic view is unwarranted at this stage, and there is no evidence to support either premise. Indeed, from a general point of view it seems most likely that the eukaryotes evolved gradually rather than overnight, and possibly by way of a number of proto-eukaryotic stocks, now extinct.

It is also possible that early prokaryotes were much more morphologically variable than living ones, and that they were much more abundant in the absence of eukaryotic competitors. In the Roper Group assemblage, the presence of the very large cyanophytic filaments might be taken as the basis for arguing that all the large spheroids are also gigantic cyanophytes. However, Schopf (1977) has presented data showing that extant unicellular cyanophytes range in size up to about 50 μm, although the vast majority (about 85%) are under 10 μm in diameter. Nonetheless, it might be possible that Precambrian cyanophytic unicells could have been considerably larger, especially in view of the (presumed) lack of competition. The large filaments, however, are coated by sheath-like material, which is a typical cyanophytic characteristic, whereas the large unicells have no

Figure 7. Filaments.
(a) finely granular organic sheath disrupted by crystal growth; (b, c) cellular filaments, type I, *b* and type II, *c;* (d-f) thin filaments *f*, usually found in sheaths *d*, *e* of type *a:* (g) carbonised sheaths; (h-i) encrusted colonies, *Eoastrion* sp.; (j) organic sheath replaced by pyrite. The expansion of the sheath to the right of figure is probably an artefact of preservation. Single scale bar is 10 μm long: double scale bar is 100 μm long.

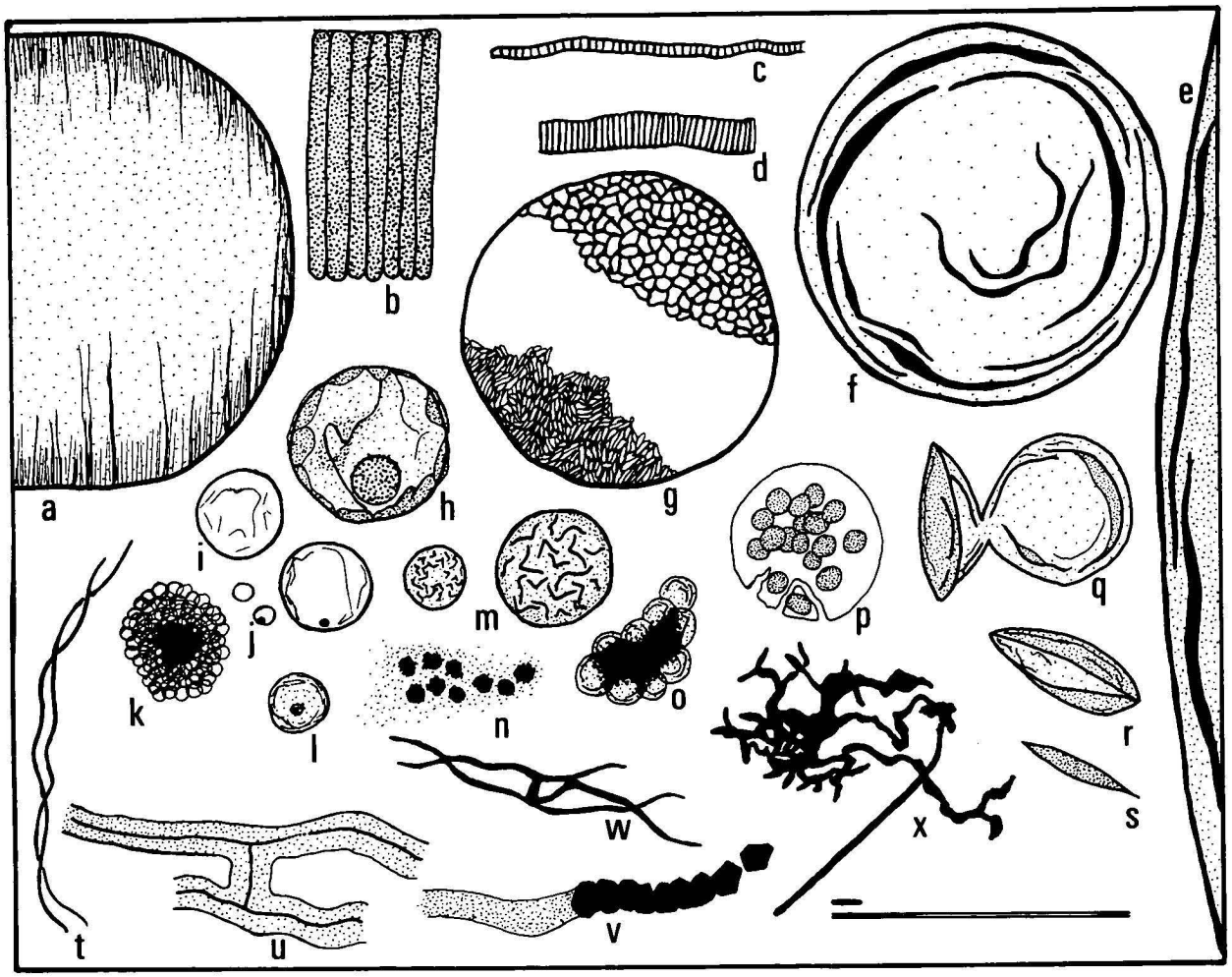

Figure 8. Scale plan to show relative size of microfossils.
(a) giant sheath, fig. 6b; (b) giant cells, fig. 6l; (c) cellular filament type II, fig. 7c; cellular filament type I, fig. 7b; (e) large sphaeromorph, fig. 6a, b; (f) medium sized sphaeromorph, fig. 5k; (g) spheres with reticulate surfaces, fig. 3a-f; (h, l) spheres with granular inclusions, fig. 3h, j; (i) smooth sphere, fig. 3p; (j) small spheres, fig. 4k, q; (k) colony of small cells, fig. 4w; (m) spheres with crinkled surfaces, fig. 60-u; (n) cell remnants in mucilage, fig. 5t-w; (o) cluster of sphaeromorphs, fig. 5f; (p) sheet of cells in membrane, fig. 5a-d; (q-s) valves of opened disphaeromorphs, fig. 5k-s; (t) thin filaments, fig. 7f; (u) thin filaments in sheaths, fig. 7d-e; (v) sheath replaced by pyrite, g. 7j; (w, x) *Eoastrion* sp., fig. 7h, i. Single scale bar is 10 μm long, double scale bar is 100 μm long. Figure references are to relevant illustrations in this paper.

such sheath material, and therefore lack this particular cyanophytic feature.

On this basis it is clear that there is no way of proving conclusively that the Roper Group microfossils are pro or eukaryotic. However, the occurrence of single large spheres within membranes which open by median splits, and the probable development of sheets of cells within membranes do make a eukaryotic origin most likely.

If the radiometric age data are accepted, these fossils are the oldest and most convincing eukaryotes yet discovered. Morphologically, this assemblage most resembles later Precambrian biotas from the Baltic, and palaeontologically, it would suggest an Upper Riphaean age (c. 950-680 m.y.). We have already commented on the neglect of the shale facies in Precambrian micropalaeontology, and it is likely that this assemblage only seems anomalous because there few other shale assemblages of similar age to compare with it.

The recent concentration of effort on the investigation of black stromatolitic cherts has given us much information on one restricted ecological niche, but may have produced a distorted picture of Precambrian evolution as a whole. The investigation of other Precambrian shale sequences is a vital preliminary to the dating of significant evolutionary events, and the future development of Precambrian biostratigraphy.

Acknowledgements

We wish to thank the Northern Territory Department of Mines, Darwin, for letting us sample the McMinn Formation core.

Muir and Peat thank the Natural Environment Research Council for supporting their work and for financing fieldwork in Australia, the Bureau of Mineral Resources for generous logistic support and Mr A. Adams for assistance in the field.

McKirdy acknowledges support from a Commonwealth Public Service Post-Graduate Scholarship.

Figures 1 & 2 were drawn by R. R. Melsom and B. Holden.

References

ALLISON, C. W., & MOORMAN, M. A., 1973—Microbiota from the Late Proterozoic Tindir Group, Alaska. *Geology*, **1**, 65-8.

BARGHOORN, E. S., & TYLER, S. A., 1965—Microorganisms from the Gunflint Chert. *Science*, **147**, 563-77.

BLISS, G. M., 1977—The micropalaeontology of the Dalradian. Unpublished Ph.D. thesis, University of London.

BONEN, L., & DOOLITTLE, W. F., 1976—Partial sequences of 16S rRNA and the phylogeny of blue-green algae and chloroplasts. *Nature*, **261**, 669-73.

CANAVAN, F., 1965—Iron ore deposits of Roper Bar. *In* MCANDREW, J. (Editor), GEOLOGY OF AUSTRALIAN ORE DEPOSITS. 2nd edition, 212-15. *8th Commonwealth Mining and Metallurgical Congress, Melbourne.*

CLOUD, P., 1976—Beginnings of biospheric evolution and their biogeochemical consequences. *Paleobiology*, **2**, 351-87.

CLOUD, P. E., & GERMS, A., 1917—New pre-Palaeozoic nannofossils from the Stoer Formation (Torridonian), Northwest Scotland. *Geological Society of America Bulletin*, **82**, 3469-74.

CLOUD, P. E., LICARI, G. R., WRIGHT, L. A., & TROXEL, B. W., 1969—Proterozoic eukaryotes from Eastern California. *Proceedings of the National Academy of Science, USA*, **62**, 623-30.

COCHRANE, G. W., & EDWARDS, A. B., 1960—The Roper River oolitic ironstone formations. *Mineragraphic Investigation, CSIRO Technical Paper* **1**, *Melbourne.*

COMBAZ, A., LANGE, F. W., & PANSART, J., 1967—Les *'Leiofusidae'* Eisenack, 1938. *Review of Palaeobotany and Palynology*, **1**, 291-307.

CONYBEARE, C. E. B., & CROOK, K. A. W., 1968—Manual of sedimentary structures. *Bureau of Mineral Resources, Australia—Bulletin*, **102**.

COOPER, J. A., 1975—Isotopic datings of the basement-cover boundaries within the Adelaide 'Geosyncline'. *Geological Society of Australia, 1st Geological Convention, Adelaide, May 1975*, Abstract, 12.

COOPER, J. A., & COMPSTON, W., 1971—Rb-Sr dating within the Houghton Inlier, South Australia. *Journal of the Geological Society of Australia*, **17**, 213-20.

CROXFORD, N. J. W., JANECEK, J., MUIR, M. D., & PLUMB, K. A., 1973—Microorganisms of Carpentarian (Precambrian) age from the Amelia Dolomite, McArthur Group, Northern Territory, Australia. *Nature*, **245**, 28-30.

CURTIS, C. D., 1977—Sedimentary geochemistry: environments and processes dominated by involvement of an aqueous phase. *Philosophical Transactions of the Royal Society of London, Series A*. In press.

DESIKACHARY, T. V., 1959—CYANOPHYTA. *Indian Council of Agricultural Research, New Delhi.*

DIVER, W. L., 1974—Precambrian microfossils of Carpentarian age from Bungle Bungle Dolomite of Western Australia. *Nature*, **247**, 361-2.

DOWNIE, C., 1973—Observations on the nature of the Acritarchs. *Palaeontology*, **16**, 239-59.

DOWNIE, C., EVITT, W. R., & SARJEANT, W. A. S., 1963—Dinoflagellates, Hystrichospheres and the classification of the Acritarchs. *Stanford University Publication, Geological Science I.*

DUNN, P. R., 1963—Urapunga, N.T. 1:250 000 Geol. Ser. *Bureau of Mineral Resources, Australia, Explanatory Notes*, **SD/53-10**.

DUNN, P. R., 1964—Triact spicules in Proterozoic rocks of the Northern Territory of Australia. *Journal of the Geological Society of Australia*, **11**, 195-7.

DUNN, P. R., PLUMB, K. A., & ROBERTS, H. G., 1966—A proposal for time-stratigraphic subdivision of the Australian Precambrian. *Journal of the Geological Society of Australia*, **13**, 593-608.

EICHMANN, R., & SCHIDLOWSKI, M., 1975—Isotopic fractionation between coexisting organic carbon-carbonate pairs in Precambrian sediments. *Geochimica et Cosmochimica Acta*, **39**, 585-95.

EISENACK, A., 1958—*Tasmanites* Newton 1875 und *Leiosphaeridia* n.g. ab. gattungen der hystrichosphaeridea. *Palaeontographica, Abteilung A*, **110** (1-3), 1-19.

FAIRCHILD, T. R., SCHOPF, J. W., & FOLK, R. L., 1973—Filamentous algal microfossils from the Caballos Novaculite, Devonian of Texas. *Journal of Paleontology*, **47**, 946-52.

FORD, T. D., & BREED, W. J., 1973—The problematical Precambrian fossil *Chuaria*. *Palaeontology*, **16**, 535-50.

FOSCOLAS, A. E., POWELL, T. S., & GUNTHER, P. R., 1976—The use of mineralogical, inorganic and organic indicators for evaluating the degree of diagenesis and generating potential of shales. *Geochimica et Cosmochimica Acta*, **40**, 953-66.

GNILOVSKAYA, M. B., 1971—The oldest aquatic plants of the Vendian of the Russian Platform (Late Precambrian). *Palaeontological Journal*, **5**, 372-378 (in Russian).

GOLUBIC, S., & BARGHOORN, E. S., 1977—Interpretation of microbial fossils with special reference to the Precambrian. *In* FLUGEL, E. (Editor), FOSSIL ALGAE, 1-14. *Springer-Verlag*, Berlin.

GOLUBIC, S., & HOFMANN, H. J., 1976—Comparison of Holocene and mid-Precambrian Entophysalidaceae (Cyanophyta) in stromatolitic algal mats: cell division and degradation. *Journal of Paleontology*, **50**, 1074-82.

GOLUBIC, S., 1976—Organisms that build stromatolites. *In* WALTER, M. R. (Editor), STROMATOLITES. *Elsevier Scientific Publishing Co., Amsterdam*, 113-26.

GRAY, J., & BOUCOT, A., 1975—Color change in pollen and sporesia review. *Bulletin of the Geological Society of America*, **86**, 1019-33.

HALLBAUER, D. K., 1975—The plant origin of the Witwatersrand carbon. *Minerals Science and Engineering*, **7**, 111-31.

HALLBAUER, D. K., & VAN WARMELO, K. T., 1974—Fossilised plants in thucolite from Precambrian rocks of the Witwatersrand, South Africa. *Precambrian Research*, **1**, 199-212.

HAMILTON, L. H., & MUIR, M. D., 1974—Precambrian microfossils from the McArthur River lead-zinc-silver deposit, Northern Territory, Australia. *Mineralium Deposita*, **9**, 83-6.

HOEFS, T., & SCHIDLOWSKI, M., 1967—Carbon isotope composition of carbonaceous matter from the Precambrian of the Witwatersrand System. *Science*, **155**, 1096-7.

HOERING, T. C., 1967—The organic geochemistry of Precambrian rocks. *In* ABELSON, P. H. (Editor), RESEARCHES IN GEOCHEMISTRY. *Wiley, New York*, 2, 89-111.

HOFMANN, H. J., 1974—Mid-Precambrian prokaryotes (?) from the Belcher Islands, Canada. *Nature*, **249**, 87-8.

HOFMANN, H. J., 1976—Precambrian microflora, Belcher Islands, Canada: significance and systematics. *Journal of Paleontology*, **50**, 1040-73.

JAMES, H. L., 1954—Sedimentary facies of iron-formation. *Economic Geology*, **49**, 235-93.

KAZMIERCZAK, J., 1976—Devonian and modern relatives of the Precambrian Eosphaera: possible significance for the early eukaryotes. *Lethaia*, **9**, 39-50.

KJELLSTROM, G., 1968—Remarks on the chemistry and ultrastructure of the cell-wall of some Palaeozoic leiospheres. *Geologisk Forenskrift Stockholm Fordhandlung*, **90**, 221-8.

KNOLL, A. H., & BARGHOORN, E. S., 1975—Precambrian eukaryotic organisms: a reassessment of the evidence. *Science*, **190**, 52-4.

KNOLL, A. H., BARGHOORN, E. S., & GOLUBIC, S., 1975—*Paleopleurocapsa wopfnerii* gen et sp. nov.: a late Precambrian alga and its modern counterpart. *Proceedings of the National Academy of Science, USA*, **72**, 2488-92.

KUZNETSOV, S. I., IVANOV, M. V., & LYALIKOVA, N. N., 1963—INTRODUCTION TO GEOLOGICAL MICROBIOLOGY. OPPENHEIMER, C. H. (Editor). *McGraw Hill, New York.*

LICARI, G. R., & CLOUD, P. E., 1968—Reproductive structures and taxonomic affinities of some nannofossils from the Gunflint Iron Formation. *Proceedings of the National Academy of Science, USA*, **59**, 1053-60.

LOPUKHIN, A. S., 1975—Structures of biogenic origin from early Precambrian rocks of Euro-Asia. *Origins of Life*, **6**, 45-57.

LOPUKHIN, A. S., 1976—Probable ancestors of Cyanophyta in sedimentary rocks of the Precambrian and Palaeozoic. *Geologisk Forenskrift Stockholm Forhandlung*, **98**, 297-315.

LOVE, L. G., 1965—Microorganic material with diagenetic pyrite from the lower Proterozoic Mt Isa shale and a Carboniferous shale. *Proceedings of the Yorkshire Geological Society*, **35**, 187-202.

LOVE, L. G., & ZIMMERMAN, D. O., 1961—Bedded pyrite and microorganisms from the Mt Isa shale. *Economic Geology*, **56**, 873-96.

MCDOUGALL, I., DUNN, P. R., COMPSTON, W., WEBB, A. W., RICHARDS, J. R., & BOFINGER, V. M., 1965—Isotopic age determinations on Precambrian rocks of the Carpentaria region, Northern Territory Australia. *Journal of the Geological Society Australia*, **12**, 67-90.

MCKIRDY, D. M., KANTSLER, A. J., MCHUGH, D. J., & TARDIF, J. W., in preparation—Geochemical and petrographic studies of organic matter in the Proterozoic McMinn Formation, Northern Territory.

MCKIRDY, D. M., & POWELL, T. G., 1974—Metamorphic alteration of carbon isotopic composition in ancient sedimentary organic matter: new evidence from Australia and South Africa. *Geology*, **2**, 591-5.

MADLER, K., 1963. Die figurierten organischen Bestandteile der Posidonienschiefer. *Beiheft Geologisches Jahrbuch*, **58**, 287-406.

MADLER, K. A., 1969—Tasmanites und verwandte planktonformen aus dem posidonienschiefer-Meer. *Proceedings of the 1st International Conference on Planktonic Microfossils, Geneva, 1967*, **2**, 375-7.

MOORMAN, M. A., 1974—Microbiota of the late Proterozoic Hector Formation, Southwestern Alberta, Canada. *Journal of Paleontology*, **48**, 524-39.

MUIR, M. D., 1974—Microfossils from the middle Precambrian McArthur Group, Northern Territory, Australia. *Origins of Life*, **5**, 105-18.

MUIR, M. D., 1976—Proterozoic microfossils from the Amelia Dolomite, McArthur Basin, Northern Territory. *Alcheringa*, **1**, 143-58.

MUIR, M. D., & GRANT, P. R., 1976—Micropalaeontological evidence from the Onverwacht Group, South Africa. *In* WINDLEY, B. F. (Editor), THE EARLY HISTORY OF THE EARTH. *Wiley Interscience*, 595-604.

MUIR, M. D., GRANT, P. R., BLISS, G. M., DIVER, W. L., & HALL, D. O., 1977—A discussion of biogenicity criteria in a geological context, with examples from a very old greenstone belt, a late Precambrian deformed zone and tectonised Phanerozoic rocks. *In* PONNAMPERUMA, C. (Editor), GEOCHEMISTRY OF THE ARCHAEAN. *Academic Press, New York*, 155-70.

MUIR, M. D., & HALL, D. O., 1974—Diverse microfossils in Precambrian Onverwacht Group rocks of South Africa. *Nature*, **252**, 5482, 376-8.

MUIR, M. D., SPICER, R. A., GRANT, P. R., & GIDDENS, R., 1974—X-ray microanalysis in the SEM for the determination of elements in modern and fossil microorganisms. *8th International Congress of Electron Microscopy, Canberra*, **2**, 104-5.

NAUMOVA, S. N., 1960—Sporovo-pyl'cevye kompleksy Rifeiskih i nizhnekembriyskih otlozeniy SSSR. *21st International Geological Congress*, **8**, 109-17.

NEVES, R., & SULLIVAN, H. J., 1964—Modification of fossil spore exines associated with the presence of pyrite crystals. *Micropaleontology*, **10**, 443-52.

NORVICK, M. S., 1970—Palynological report on late Precambrian samples from South Australia and Northern Territory. *Bureau of Mineral Resources, Australia*, Palynological File No. 240 (unpublished).

OEHLER, D. Z., 1976—Transmission electron microscopy of organic microfossils from the Late Precambrian Bitter Springs Formation of Australia: techniques and survey of preserved ultrastructure. *Journal of Paleontology*, **50**, 90-106.

OEHLER, D. Z., in preparation—Microflora of the middle Proterozoic Balberinni Dolomite (McArthur Group) of Australia. *Alcheringa* (submitted for publication).

OEHLER, J. H., 1976—Experimental studies in Precambrian paleontology: structural and chemical changes in blue-green algae during simulated fossilisation in synthetic chert. *Geological Society of America Bulletin*, **87**, 117-29.

OEHLER, J. H., 1977—Precambrian microfossils and associated mineralization in the McArthur deposit, Northern Territory, Australia. *Alcheringa*, **1**, 315-49.

PEAT, C. J., 1975—Microfossils from the Roper Group. *Geological Society of Australia, 1st Geological Convention, Adelaide, May 1975*, Abstract, 17.

PFLUG, H. D., 1967—Structured organic remains from the Fig Tree Series (Precambrian) of the Barberton Mountain Land (South Africa). *Review of Palaeobotany & Palynology*, **5**, 9-29.

PLUMB, K. A., & DERRICK, G. M., 1976—Geology of the Proterozoic rocks of the Kimberley to Mount Isa region. *In* KNIGHT, C. L. (Editor), ECONOMIC GEOLOGY OF AUSTRALIA AND PAPUA NEW GUINEA, I. METALS. *Australasian Institute of Mining & Metallurgy, Melbourne*, 217-52.

PLUMB, K. A., & SWEET, I. P., 1974—Regional significance of recent correlations across the Murphy Tectonic ridge, Westmoreland area. *In*: Recent technical and social advances in the North Australian Minerals Industry, 199-207. *Australasian Institute Mining Metallurgy, North West Queensland Branch.*

PREISS, W. V., 1976—Intercontinental correlations. *In* WALTER, M. R. (Editor), STROMATOLITES, *Elsevier, Amsterdam*, 359-70.

RIX, P., 1965—Milingimbi, N.T. 1:250 000 Geological Series. *Bureau of Mineral Resources, Australia, Explanatory Notes* **SD/53-2**.

ROBLOT, M. M., 1964—Sporomorphes du Precambrien Armoricain. *Annales Palaeontologiques*, **50**, 105-10.

RUNNEGAR, B., 1977—Panel of experts discuss evidence for Precambrian eukaryotes at 25th International Geological Congress, Sydney, August, 1976. *Alcheringa*, **1**, 311-14.

SCHIDLOWSKI, M., EICHMANN, R., & JUNGE, C. E., 1975—Precambrian sedimentary carbonates: carbon and oxygen isotope geochemistry and implications for the terrestrial oxygen budget. *Precambrian Research*, **2**, 1-69.

SCHOPF, J. W., 1972—Precambrian Paleobiology. *In* PONNAMPERUMA, C. (Editor), EXOBIOLOGY, FRONTIERS OF BIOLOGY, **23**. *North Holland, Amsterdam, Elsevier, New York*, 16-61.

SCHOPF, J. W., 1974—The development and diversification of Precambrian life. *Origins of Life*, **5**, 119-35.

SCHOPF, J. W., 1975—Precambrian paleobiology: problems and perspectives. *Annual Review of Earth & Planetary Sciences*, **3**, 213-49.

SCHOPF, J. W., 1977—Are the oldest 'fossils', fossils? *Origin of Life*, **7**, 19-36.

SCHOPF, J. W., & BARGHOORN, E. S., 1969—Microorganisms from the late Precambrian of South Australia. *Journal of Paleontology*, **43**, 111-18.

SCHOPF, J. W., & FAIRCHILD, T. R., 1973—Late Precambrian microfossils: a new biota from Boorthanna, South Australia. *Nature*, **242**, 537-8.

SCHOPF, J. W., HORODYSKI, R. J., FAIRCHILD, T. R., & DONALDSON, J. A., 1974—Late Precambrian microfossils: discovery of four new stromatolitic biotas. *American Journal of Botany*, **61** (supplement 5), Abstract, 19.

SCHOPF, J. W., & OEHLER, D. Z., 1976—How old are the Eukaryotes? *Science*, **193**, 47-49.

SOKOLOV, B. S., 1967—Drevneyshiye pogonofory. *Doklady Akademia Nauk SSR*, **177**, 201-4 (in Russian).

THOMSON, B. P., 1966—The lower boundary of the Adelaide System and older basement relationships in South Australia. *Journal of the Geological Society of Australia*, **13**, 203-28.

TIMOFEEV, B. V., 1966—Mikropaleofitologicheskoe issledovanie drevnikh svit. *Izdatiye Nauka Moskva.*

TIMOFEEV, B. V., 1970a—Une decouverte de Phycomycetes dans le Precambrien. *Review of Palaeobotany Palynology*, **10**, 79-81.

TIMOFEEV, B. V., 1970b—Sphaeromorphida geants dans le Precambrien avance. *Review of Palaeobotany Palynology*, **10**, 157-60.

VIDAL, G., 1976—Late Precambrian microfossils from the Visingso Beds in Southern Sweden. Fossils & Strata, **9**. *Universitets forlaget, Oslo.*

WALTER, M. R., OEHLER, J. H., & OEHLER, D. Z., 1976—Megascopic algae 1300 million years old from the Belt Supergroup, Montana: a reinterpretation of Walcotts' *Helminthoidichnites. Journal of Paleontology*, **50**, 872-81.

WEBB, A. W., 1973—AMDL Report An. 1814/73. Unpublished.

WHITE, B., 1974—Microfossils from the late Precambrian Altyn Formation of Montana. *Nature*, **247**, 452.

WICANDER, E. R., & SCHOPF, J. W., 1974—Microorganisms from the Kalkberg limestone (Lower Devonian) of New York State. *Journal of Paleontology*, **48**, 74-7.

The Stratigraphic and Tectonic development of the Manokwari Area, Irian Jaya

G. P. Robinson and Nana Ratman

The Manokwari area lies in the northeastern extremity of the Kepala Burung region in the western part of Irian Jaya.

In 1976 the area was investigated at the start of an ongoing mapping programme which will be carried out as an Indonesian-Australian integrated geological survey of Irian Jaya.

Ten mappable units have been recognised in the area, ranging in age from Silurian to Holocene. The Silurian to Devonian metamorphics crop out in the southern mountainous region, and consist mainly of fine-grained low-grade regionally metamorphosed sedimentary rocks. Along the length of the mountain front these rocks have been intruded and partially assimilated in places by a number of late Permian to middle Triassic granodiorite bodies and a middle Miocene diorite body. Basalt and andesite flow breccia, tuff, and volcaniclastic sediments occur to the southeast, and are probably Oligocene to Miocene in age. Massive algal-foraminiferal biomicrite of Miocene age forms a number of elongate ridges to the northeast of the volcanics and probably unconformably overlies them. In the northeastern part of the area soft, well-bedded mudstone, siltstone and sandstone of late Miocene to Pleistocene age is unconformably overlain by Pleistocene raised reefs. Surrounded by the western part of the extensive alluvial plain is a symmetrical mountain of ?Pliocene agglomerate. Immediately to the south, at the edge of the mountain front is an area of uplifted, dissected, and northerly-tilted coarse alluvium and fanglomerate.

The Manokwari area is situated amid a complex array of crustal plates and sub-plates which formed as a result of complicated interaction between the Australian and Pacific Plates and the island arcs and ocean basins of the Indonesian Archipelago. The two major structural elements within the Manokwari Sheet, the Sorong and Ransiki Fault Zones, are continent-island arc collision sutures which have subsequently undergone sinistral transcurrent faulting.

Introduction

This paper is based on field work carried out in September and October 1976 at the beginning of an ongoing mapping program funded by the Australian Development Assistance Bureau to assist the Indonesian Government to undertake the systematic geological mapping of the province of Irian Jaya (Fig. 1). The 1976 field work in Kepala Burung involved the following geologists from the Geological Survey of Indonesia (GSI): H. Sumadirdja (party leader), N. Ratman, Kastowo and M. Masria. The BMR team consisted of D. S. Trail (party leader), R. J. Ryburn, G. P. Robinson, P. E. Pieters, and D. S. Hutchison.

The first map showing the general geology of Irian Jaya including the Manokwari area appears in Visser & Hermes (1962). An economic geological investigation of the northeastern part of the Kepala Burung region of Irian Jaya was carried out between 1959-1962 by the 'Foundation Geological Investigation Netherlands New Guinea' and a lengthy report was published (d'Audretsch and others, 1966). This report includes geological compilation maps at scales of 1:100 000 and 1:250 000.

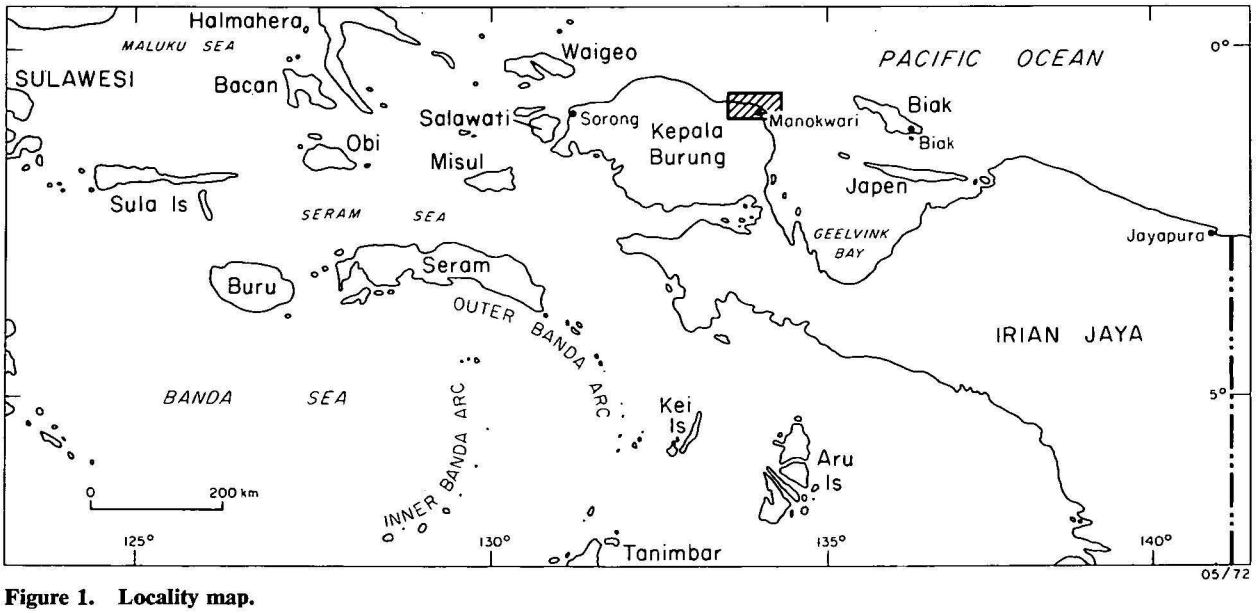

Figure 1. Locality map.

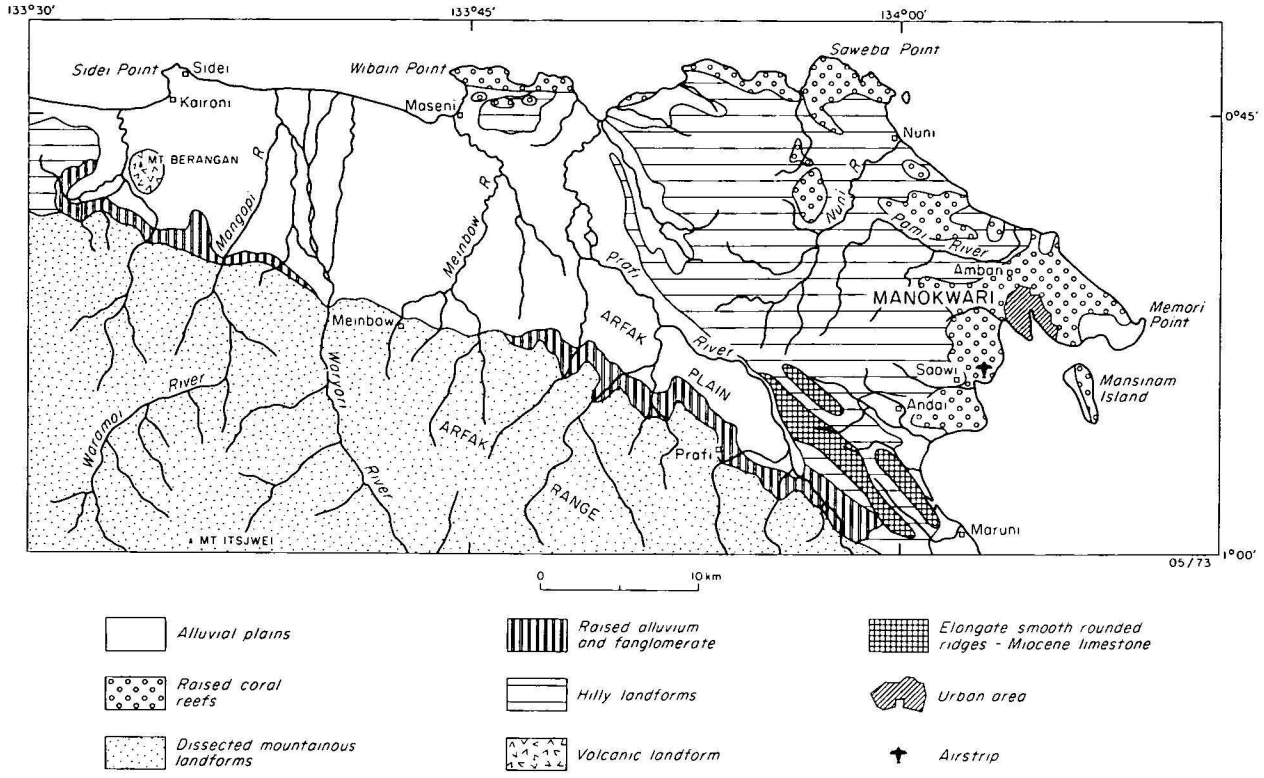

Figure 2. Physiographic units in the Manokwari area.

The main physiographic units in the Manokwari area are shown in Figure 2, the three most important units being a southern zone of dissected mountainous landforms and a northeastern zone of hilly landforms, separated by a wide alluvial plain zone.

The Geological Survey of Indonesia will publish a 1:250 000 scale geological map of the Manokwari Sheet area and accompanying explanatory notes. A detailed account of the geology of the Manokwari 1:250 000 Sheet is to be found in Robinson & Ratman (1977).

Stratigraphy

In the Manokwari area ten mappable units have been recognised, ranging in age from Silurian to Holocene. The stratigraphic thickness is possibly about 8000 m excluding the metamorphic rocks, which may be many thousands of metres thick. The Silurian to Devonian metamorphics (Kemum Formation) crop out in the southern mountainous region, and consist mainly of fine-grained low-grade regionally metamorphosed sedimentary rocks. Along the length of the mountain front these rocks have been intruded and partially assimilated in places by a number of granodiorite, diorite and gabbro bodies comprising the Wariki Granodiorite (late Permian to middle Triassic) and the Lembai Diorite (middle Miocene). Basalt and andesite flow breccia, tuff, and volcaniclastic sediments (Arfak Volcanics) occur in the southeastern part of the area, and are probably Oligocene to Miocene in age. The Arfak Volcanics may conformably overlie the subsurface Imskin Formation, an upper Eocene to middle Miocene fine-grained marine limestone unit (Visser & Hermes, 1962; Rahardjo, 1975).

Massive algal-foraminiferal biomicrite of Miocene age (Kais Formation) forms a number of elongate ridges to the northeast of the volcanics, and probably unconformably overlies the volcanics. In the northeastern part of the area, soft, well-bedded mudstone, siltstone and sandstone (Befoor Formation) of late Miocene to Pleistocene age is unconformably overlain by Pleistocene raised reefs (Manokwari Limestone). Surrounded by the western part of the extensive alluvial plain is a symmetrical mountain of ?Pliocene agglomerate, Mount Berangan. Immediately to the south, at the edge of the mountain front is an area of uplifted, dissected, and northerly-tilted coarse alluvium and fanglomerate. Details of the stratigraphy and structure of the Manokwari area are shown in Figures 3 and 4, and Table I.

Tectonic development

The Manokwari area is situated amid a complex array of crustal plates and sub-plates (Fig. 5). Fundamentally the present plate configuration is the result of complicated interaction between the northerly moving Pacific Plate and the island arcs and ocean basins of the Indonesian Archipelago. Thus the major structural feaures, including those which are no longer active, must be thought of in terms of constantly changing plate and island arc interaction. The Ransiki Fault Zone and the Sorong Fault Zone, both of which occur in the Manokwari area, may be understood in this light. Both are continent-island arc collision sutures which have subsequently undergone sinistral transcurrent faulting. The Ransiki Fault Zone represents a continent-island arc Miocene collision suture between the essentially metamorphic and granitic continental rocks of Kepala Burung and the Oligocene island arc volcanics of the Arfak Mountains. The Ransiki Fault may represent a sinistral transcurrent fault, formerly easterly-trending, formed at a time when the Kepala Burung region had not yet undergone clockwise rotation. The Sorong Fault Zone probably originated in the same way as a sinistral

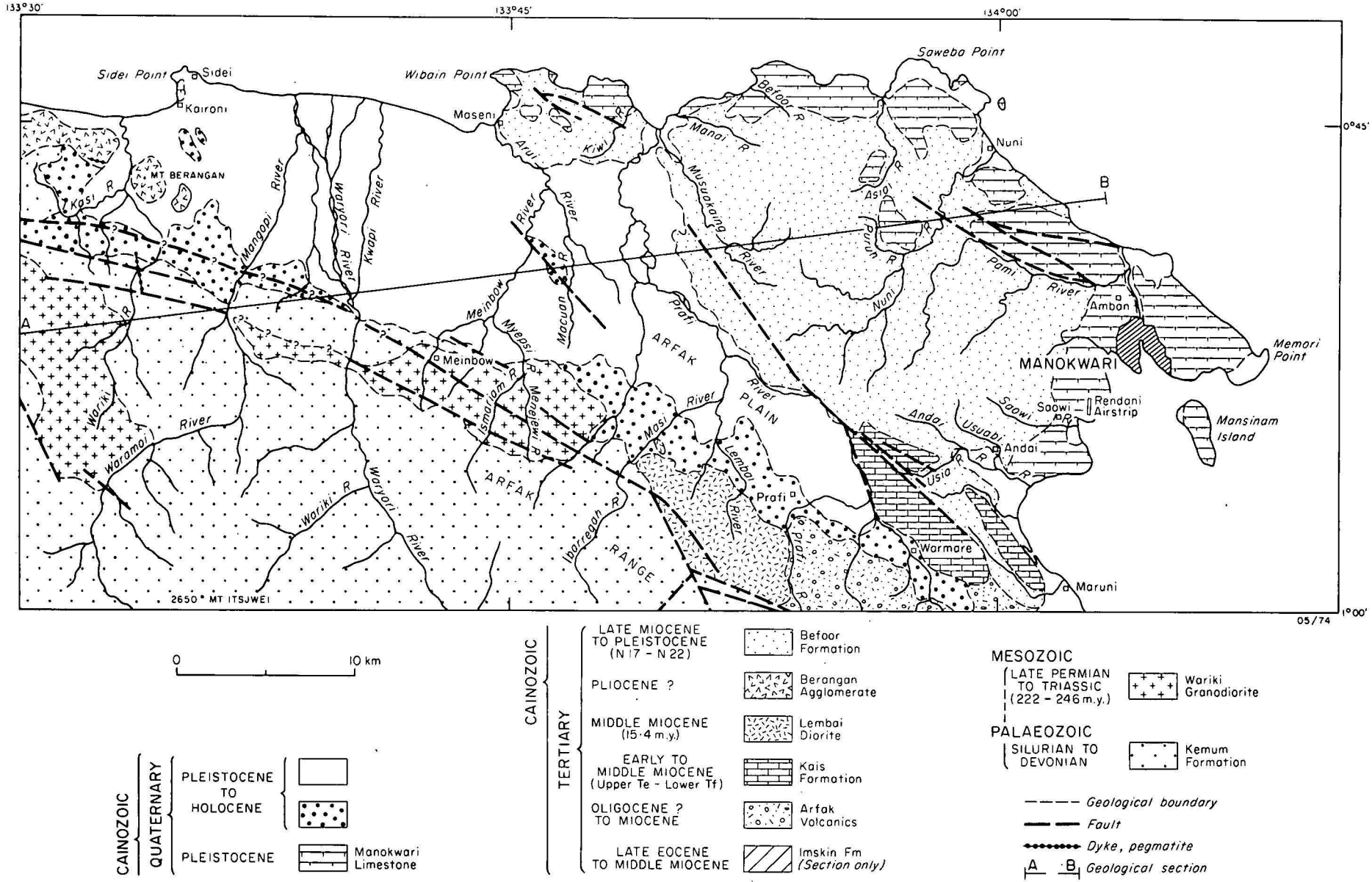

Figure 3. Simplified geology of the Manokwari area.

Table 1: Stratigraphy

Age	*Rock unit*	*Lithology*	*Thickness (m)*	*Topography and distribution*	*Remarks*
Pleistocene to Holocene	Qa	Coarse gravel, sand, fine silt, and mud; becomes finer to N. Most clasts from Psk. River terraces in places; alluvium and beach deposits	400	N of mountain zone, 20 km wide in E, 8 km wide in W. Exposed along large braided river courses	Appear to truncate and partly overlie the northern edge of Qf. Accumulated in shallow graben between mountainous landforms in S part of area and hilly landforms to E.
	Qf	Coarse alluvium and fanglomerate. Locally massive, very poorly sorted conglomerate and boulder beds, interbedded with well-bedded dark yellowish orange clay	400	Dissected N-dipping flatirons to N of mountain front. Cliffs up to 25 m high along mountain front	Represent alluvial fan deposits which accumulated along mountain front. N primary depositional dip accentuated by uplift and N tilting. Unconformably overlies Psk, Toa, and Tmk. Nonconformably overlies Pwg and Tpld
Pleistocene	Manokwari Limestone Qpm	Massive, cavernous, resistant algal-foraminiferal biomicrite, calcirudite, calcilutite and calcarenite; greyish yellow to white; heavily contaminated by terrigenous detritus in places	800	Raised reefs around coastal areas near Manokwari and capping low hills in NE part of area	Fringing reef complexes contaminated in places by terrigenous detritus and subsequently uplifted. Unconformably overlies Tpb
Late Miocene to Pleistocene (N17-N22)	Befoor Formation Tpb	Soft, friable and porous sandstone, siltstone and mudstone. Well-bedded, locally current lamination and large-scale cross-bedding. Usually weakly calcareous. Mudstone strongly calcareous, with planktonic forams. Rarely bivalves and calcarenite	1600	Hilly region of low relief, rounded ridges and small streams in NE part of area	Shallow water marine to estuarine environment of deposition. Sediment source is Psk and Toa. Unconformably overlies Tmk and Toa and is unconformably overlain by Qpm. Planktonic forams give a late Miocene to Pleistocene age
Pliocene?	Berangan Agglomerate Tpbr	Basaltic to andesitic agglomerate; clasts of porphyritic, scoriaceous low-silica andesite, with 2% plagioclase phenocrysts 3 mm long	900	Symmetrical humped mountain 900 m high in NW part of area	Accumulated as a result of explosive volcanic activity. Geomorphology and porous nature of volcanics suggests a Pliocene age.
Middle Miocene	Lembai Diorite Tpld	Medium dark grey and olive grey diorite, coarse; locally grades into gabbro. Numerous acidic veins and dykes. At the contact zone Psk schist and phyllite shows various stages of complete replacement		Throughout length of Lembai River and in lower reaches of Ibarregah River in SE part of area	Acidic veins with blended contacts and considerable digestion and hybridization of the surrounding diorite suggests a highly mobile magma during and after late hydrothermal emplacement. Shows assimilation textures and structures at contact with Psk. Dated by K-Ar method as 15.4 m.y.
Early to Middle Miocene (upper Te-lower Tf)	Kais Formation Tmk	Massive yellowish grey to white algal-foraminiferal biomicrite; resistant, non-porous and brittle; possibly fringing or barrier reef	500	Elongate SE-trending ridges in SE part of area	Fringing or barrier reef environment of deposition. Unconformably overlies Toa. Unconformably overlain by Tpb. Larger Foraminifera suggest early to middle Miocene age
Oligocene? to Miocene	Arfak Volcanics Toa	Basalt and andesite flow breccia, tuff, rubble slides, paraconglomerate and turbidite deposits	3000	Far SE corner of area. Includes part of far N foothills of Arfak Range	Deposits formed by breaking up of lava flows as they descended submarine slopes. Possibly conformably overlie Tei and are unconformably overlain by Tmk
Late Eocene to Middle Miocene	Imskin Formation (section only) Tei	Well-bedded, dense, reddish or light grey aphanitic limestone. Locally abundant pelagic Foraminifera. A few moderately resistant marl beds	2000	Subsurface only	Deep water marine environment. Probably conformably overlain by Toa. Age from pelagic Foraminifera
Late Permian to Triassic	Wariki Granodiorite Pwg	Granodiorite with planar fabric in places and very coarse light grey granite. Some pegmatite		Upper reaches of Wariki R	Probably emplaced as a highly viscous magma. Post-consolidation shear truncates pegmatite dykes. Thermal metamorphism and minor hydrothermal alteration in contact zone. K-Ar age of late Permian to middle Triassic.
Silurian to Devonian	Kemum Formation Psk	Black to medium grey slate, quartzite, siliceous argillite, metachert and phyllite in E; dark grey to black mica schist in W, locally with andalusite and pyrite. Small-scale slumping in places. A few metamorphosed micromonzonite dykes		Deeply dissected mountainous landforms drained by large braided rivers. In SW part of area	Deep water marine environment. Unconformably overlain by Qf. Intruded by Pwg and Tpld. Silurian age based on graptolites and Devonian age based on ostracods

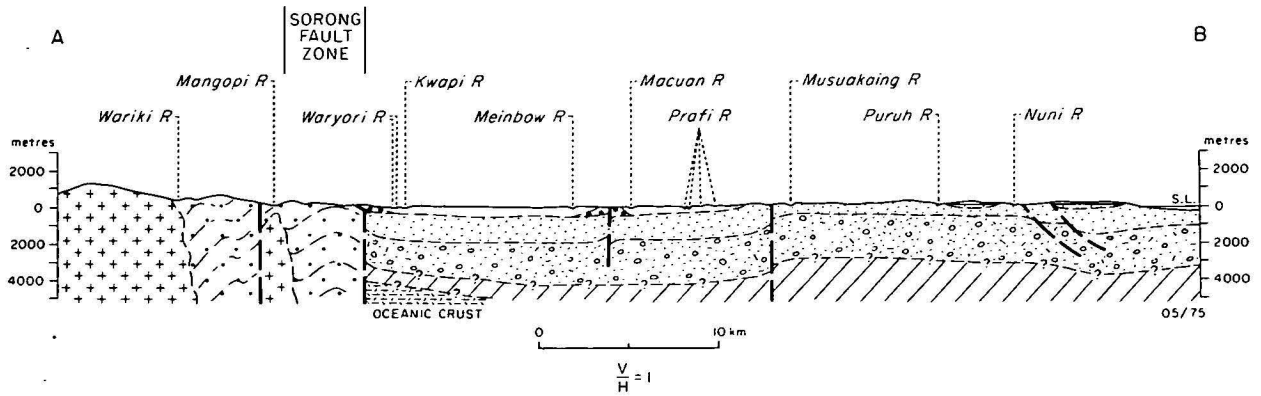

Figure 4. Simplified cross-section of the Manokwari area (location of section shown on Fig. 3).

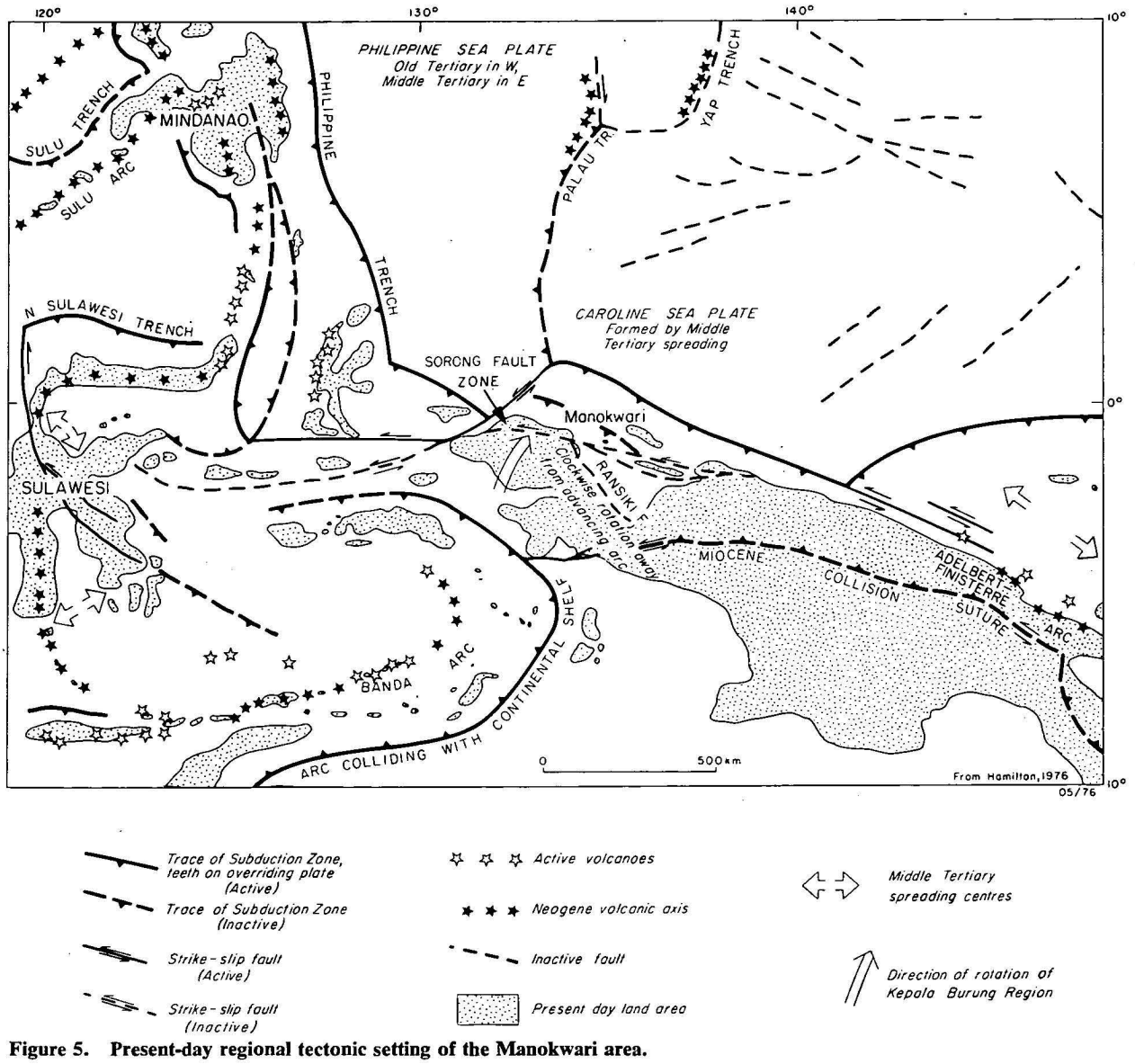

Figure 5. Present-day regional tectonic setting of the Manokwari area.

transcurrent fault, representing a continental-island arc collision suture formed after Kepala Burung had rotated in a clockwise direction, thus imparting a southeastern trend to the Ransiki Fault Zone. The presence of Kemum metamorphics to the north of the present Sorong Fault Zone west of the Manokwari area suggests that the Sorong Fault Zone was once much wider, and that sinistral transcurrent movement has since taken place recently only along the southern edge of the previously wide fault zone.

The development of the Ransiki Fault Zone, the clockwise rotation of Kepala Burung, and the formation of the Sorong Fault Zone truncating the Ransiki Fault Zone are shown diagramatically in Figure 6. It should be noted that in this hypothetical structural development of the Kepala Burung region two factors might have

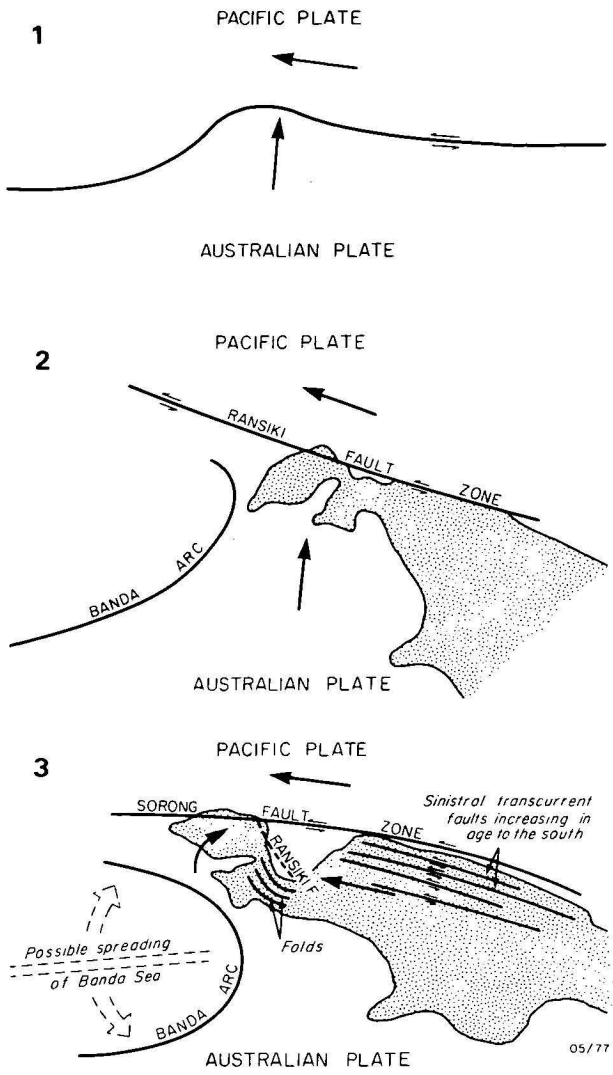

Figure 6. Hypothetical structural evolution of the Manokwari region.

contributed to bring about clockwise rotation. The first of these was the westerly movement of northern Irian Jaya and Papua New Guinea, caused by sinistral movement on numerous parallel transcurrent faults—thus forcing the southwesterly side of Kepala Burung against the Banda Arc. The second factor may have been the possibility of spreading in the Banda Sea, thereby increasing the stresses between Kepala Burung and the Banda Arc. Although there is as yet no definite evidence for crustal spreading in the Banda Sea, the area is the site of an undation (and, consequently, as the result of gravity, a spreading centre) according to Van Bemmelen (1949). Hamilton (personal communication, 1977) also considers it likely that spreading has taken place in this area.

Sequence of events

A thick pile of fine-grained terrigenous muds, bedded cherts, and occasional fine-grained greywacke sandstone and siltstone was deposited in a deep-sea evironment in Siluro-Devonian times. During the Permian these deposits were folded, faulted, and intruded by the Wariki Granodiorite. Either in the late Cretaceous or early Eocene the Australian Plate began to move northwards and collided with the west-northwesterly moving Pacific Plate. The collision suture between the plates was bent in a northerly direction by the Australian Plate and ultimately ruptured, the northeast part becoming the Ransiki Fault Zone and the southwest part the Banda Arc. As a result of this plate interaction an Oligocene volcanic arc (Arfak Volcanics) developed on the northeastern edge of the Ransiki Fault Zone. Coral reefs (Kais Formation) developed along the edge of this island arc in Miocene times. At the end of the Miocene, sinistral movements in northern Papua New Guinea and Irian Jaya (caused by the northwesterly movement of the Pacific Plate) forced the Kepala Burung region against the Banda Arc. This northwesterly movement, together with a possible northeasterly-directed stress associated with a spreading centre in the Banda Sea, caused the clockwise rotation of Kepala Burung. The Ransiki Fault assumed its present northwesterly trend.

In the Pliocene the terrain, consisting mainly of the Kemum Formation and Wariki Granodiorite, was uplifted and marine and estuarine muds, silts, and sands (Befoor Formation) were laid down on the northern side of the emergent area. During this uplift the Lembai Diorite was intruded into the western edge of the island arc environment near the Ransiki Fault, and explosive volcanic activity (Berangan Agglomerate) took place near the north coast. Uplift and associated tensional fracturing continued to the south, particularly in the Arfak Mountains to the southeast throughout Pliocene and Pleistocene times. Fringing reefs (Manokwari Limestone) were successively uplifted throughout the Pleistocene. At the edge of the mountain front coarse alluvium and fanglcmerate accumulated during uplift, and subsequently became dissected and tilted to the north.

Acknowledgements

Ratman publishes with the permission of the Director, Geological Survey of Indonesia. BMR participation in the Irian Jaya project is under the auspices of the Australian Development Assistance Bureau, Department of Foreign Affairs, whose Director has agreed to the publication of this account.

The figures were drawn by R. R. Melsom and G. Butterworth.

References

CAROZZI, A. V., 1960—MICROSCOPIC SEDIMENTARY PETROGRAPHY. *Wiley, New York.*

D'AUDRETSCH, F. C., KLUIVING, R. B., & OUDEMANDS, W., 1966—Economic geological investigations of NE Vogelkop (Western New Guinea). *Koninklijk Nederlands Geologisch Mijnbouwkundig Genootschap, Verhandelingen, Geologische serie,* **23**, *Staatsdrukkerij en Uitgeverijbedrijf, 's-Gravenhage.*

HAMILTON, WARREN, 1976—Subduction in the Indonesian Region. *5th Annual Convention of the Indonesian Petroleum Association* (unpublished).

RAHARDJO, TJIPTO, 1975—Geologi dan stratigrafi daerah timur—Muturi, cekungan Bintuni—Kepala Burung, Irian Jaya. *Pertamina Unit V,* 1, 2A, 2B (unpublished).

ROBINSON, G. P., & RATMAN, N., 1977—Explanatory notes on the Manokwari 1:205 000 sheet, Irian Jaya. *Bureau of Mineral Resources, Australia, Record* **1977/32.**

VAN BEMMELEN, R. W., 1949—THE GEOLOGY OF INDONESIA: **1a**, General Geology, **1b**, Portfolio; Vol. **11**, Economic Geology. *The Hague, Staatsdrukkerij/Martinus Nijhoff.* (Monograph on the geology of Indonesia; reprinted in 1970.)

VISSER, W. A., & HERMES, J. J., 1962—Geological results of the exploration for oil in Netherlands New Guinea. *Koninklijk Nederlands Geologisch Mijnbouwkundig Genootschap Verhandelingen, Geologische serie,* **20**, *Staatsdrukkerij en Uitgeverijbedrijf, 's-Gravenhage.*

BMR Journal of Australian Geology & Geophysics, 3, 1978, 25-33

Triassic environments in the Canning Basin, Western Australia

John D. Gorter

A review of the lithology, sedimentary structures and palaeontology, supplemented by original investigations, suggests that the Triassic system in the Canning Basin can be subdivided into four broad environmental episodes. The sequence records a slow transgression culminating in the Smithian, when the riverine plain in the southeastern Fitzroy Graben was drowned. The resulting shallow embayment in the Fitzroy Graben supported a much impoverished marine biota, made up of species tolerant of reduced saline conditions caused by substantial run-off of fresh water from surrounding streams. A regression began in the Spathian and continued throughout the later Triassic, although there were minor transgressions with marine incursions: the environment evolved into a low-relief coastal alluvial plain, with meandering streams and lakes. A general trend to increasing aridity is evident, with an increase red beds, and is correlated with the withdrawal of the Blina Sea. Finally in Ladinian time the region became an area of non-deposition and remained so until the early Jurassic.

Introduction

Triassic rocks in the Canning Basin (Fig. 1) have been described by Veevers & Wells (1961), McKenzie (1961), and Yeates and others (1975), and divided into four named onshore formations, and their unnamed offshore equivalents. Available interpretations of the depositional environment of the Canning Basin Triassic rocks are based only on the contained fauna and flora, or on lithological studies of small areas. This study integrates all known palaeontological, lithological and geochemical properties of the rocks into an assessment of the depositional environments of the Basin during the Triassic. The rocks are regarded as a genetically related sequence, and to represent an extended environmental episode.

Previously published information has been supplemented by examination of cores and cuttings, interpretation of subsidised logs of petroleum exploration wells, and subsidised seismic data. This information is assembled fully elewhere (Gorter, in prep.); this paper represents a synthesis drawn from that data.

Stratigraphy

Four formations have been formally defined in the onshore Canning Basin (Fig. 2). They are discussed fully by Veevers & Wells (1961), Yeates and others (1975), and Gorter (in prep.). None of the offshore units have been formalised and are here referred to as 'Beds', generally named after the well in which they were first penetrated.

Facies and environmental significance

It proved possible to distinguish five broad depositional environments in terms of facies. A facies is considered to denote the sedimentary record of an environment, or group of closely related environments. Facies were defined on the basis of a combination of textural, compositional, structural and palaeontological characteristics (Selley, 1970). The small number of samples, extensive erosion, and the lack of adequate palaeontological information probably results in an incomplete list of facies types, and a sketchy areal distribution.

Examination of all available measured sections and borehole data allows the construction of a diagrammatic lithological section (Fig. 3). Log analyses, especially the gamma-ray curve, aided determination of sedimentary succession. Named formations were broken down into facies groups, and all lithological parameters are listed along with the suggested environment of deposition and, broadly, the fossil content.

Facies I—Fluviatile

This facies is characterised by high-angle cross-bedding, dominance of sandstone, frequent conglomerate, upward fining, and absence of marine fossils. A combination of these characters is compatible with deposition in a fluviatile regime (Allen, 1965), and, where upward-fining cycles are present, a meandering stream origin is suggested (Allen, 1965; 1970). Such cycles are present in the Millyit Sandstone and Culdiva Sandstone (Yeates and others, 1975), the Bedout Beds (2938 m to 2997 m from the gamma-ray curve). Finer clastics usually top the upward-fining sequences and are interpreted as overbank deposits (Allen, 1965).

Facies II—Transgressive

This facies is also characterised by a general fining upward sequence, however high-angle cross-bedding is absent, and glauconite and marine fossils (acritarchs and lingulids) are present. The facies is recognised in the basal Blina Shale (e.g. Blackstone No. 1, Meda No. 1, Langoora No. 1, BMR Lucas No. 13), and the 4A Beds in BMR Wallal No. 4A. The content of coarse clastics decrease upwards, and megaspores (in Blackstone No. 1, and Meda No. 1 (P. J. Jones, pers. comm.)) become scarcer.

Facies III—Marine

The marine facies is characterised by common marine fossils, a preponderance of laminated green and grey siltstone, claystone or shale, sandstone stringers, and glauconite. In Blackstone No. 1 this facies contains abundant foraminifera with conodonts. The facies is recognised in the Blina Shale (Blackstone No. 1, Langoora No. 1, Meda No. 1), lowermost Bedout Beds (Bedout No. 1, 2997 m to 3020 m) and Keraudren Beds (3124-3630 m in Keraudren No. 1). The marine facies grades downwards into the transgressive facies in all known sections, except at Bedout No. 1 where it directly overlies weathered Upper Permian basalt (BOC, 1971). Probably the Bedout High (Fig. 1) was inundated late in the transgression when coarser clastic deposits were not available from any nearby source area.

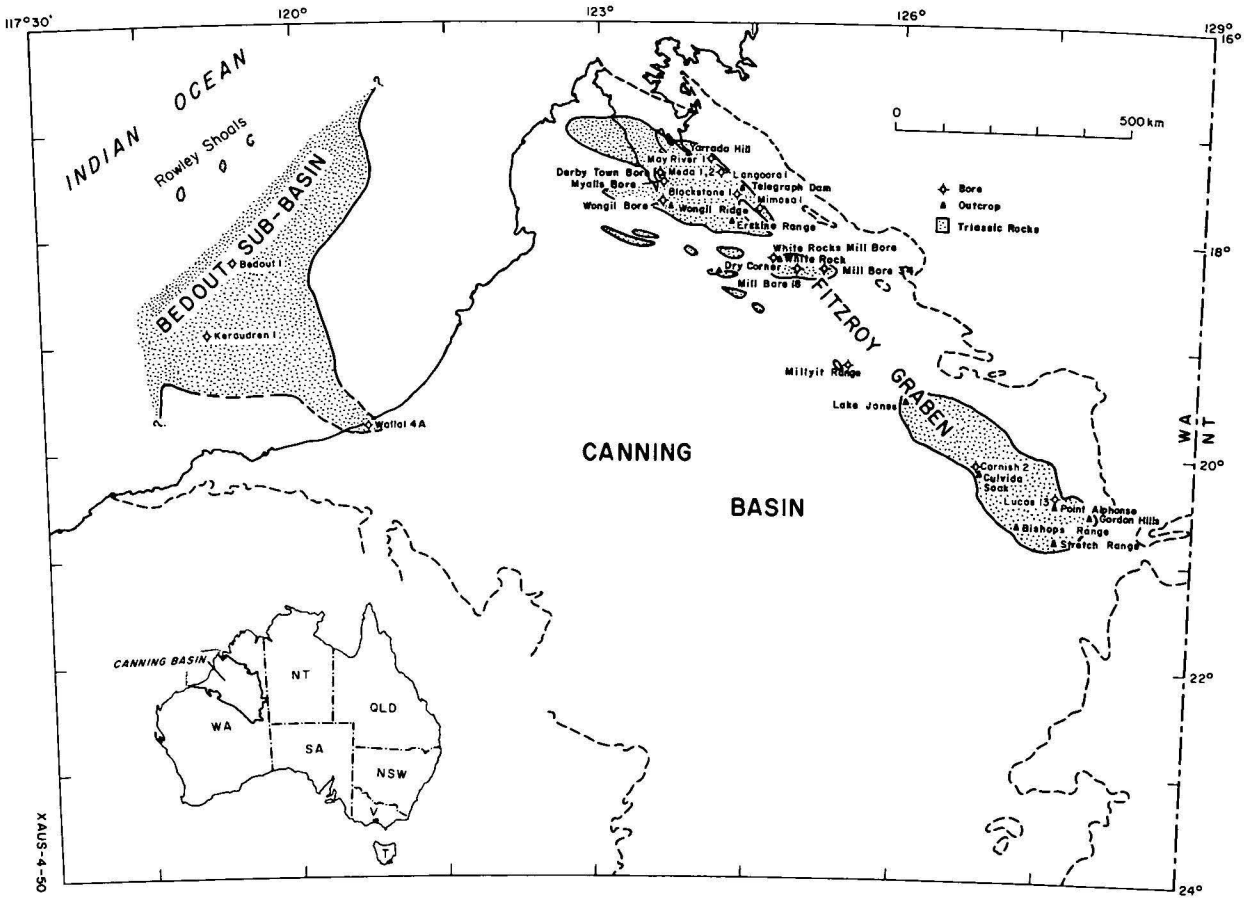

Figure 1. Locality map, showing known limit of preserved Triassic rocks.

Facies IV—Regressive

The major characteristics of this facies is a coarsening upwards trend, coupled with a decrease of marine fossils and an increase in land plants. The vertical sequence may terminate in two distinct sub-facies: regression may be accomplished by coastal aggradation (Sykes, 1974; Walker & Harms, 1975; Andrews & Laird, 1976) where a shoaling sequence is overlain by coastal plain deposits; or by delta progradation (Coleman & Gagliano, 1965). Shoaling sequences (Facies IVa) are apparent in the upper part of the Blina Shale (e.g. at Erskine Hill (McKenzie, 1961)) and the lower Bedout Beds (Bedout No. 1 from 2911 to 2938 m), and deltaic channels (Facies IVb) by upward-coarsening sandstones (2960-3124 m in Keraudren No. 1).

The regressive sequences at the top of the Blina Shale are notable for the lack of massive sandstone bodies. This absence is thought to be due to deposition in a shallow environment with a low tidal range and little wave agitation. In such an environment winnowing of mud from the sediment would not result in the build up of sandbars or beaches (Walker, 1972). Alternatively, sand supply may have been low, suggesting a subdued hinterland. However, the presence of much sand and conglomerate in the under and overlying fluviatile sequences suggests that lack of winnowing was the major factor in the absence of sand bodies in the upper Blina Shale.

At Erskine Hill, the basal massive cross-bedded sandstone (McKenzie, 1961) may represent a prograding distributary of a deltaic system advancing over the upper Blina Shale. The lithological association is similar to that of estuarine sands (Land, 1972), except for the lack of marine shelly fossils. Prograding distributary sands are also interpreted in the Keraudren Beds (between 2960-3124 m in Keraudren No. 1 from the gamma-ray curve pattern), and the upper Bedout Beds 2911 m to 2938 m in Bedout No. 1). These progradational sand bodies are included in Facies IVb, and always overlie Facies III with basal scour. In the Fitzroy Graben IVb always gives way to Facies I, but at Keraudren No. 1, it is overlain by a possible lacustrinal facies (Facies V).

Facies V—Lacustrinal

This facies is recognised only at Keraudren No. 1 (2801-2960 m and 2460-2568 m), and is characterised by thin-bedded and laminated claystone, and minor sandstone. It may also contain calcilutite (2825-2864 m in Keraudren No. 1). No marine fossils are present, but spores and pollen (Ingram, 1974), and coal, may occur. The claystones are multi-coloured, suggesting deposition under alternating humid to arid climate (Falke, 1971); humid conditions are also suggested by the presence of coal, and drier conditions by dolomite.

Pickard & High (1972) state that deposits bounded either by fluviatile units, as at Keraudren No. 1, or unconformities, and the presence of a non-marine fauna in sediments that could be ascribed either to a marine or lacustrinal origin, is suggestive of lacustrine deposition. A similar stratigraphic position between continental deposits was also stated to be characteristic of lacustrine deposits by Greiner (1974). The common presence of iron sulphides, and siliceous and calcitic cements (Hematite, 1974) also suggests lacustrine sediments (Picard & High, 1972).

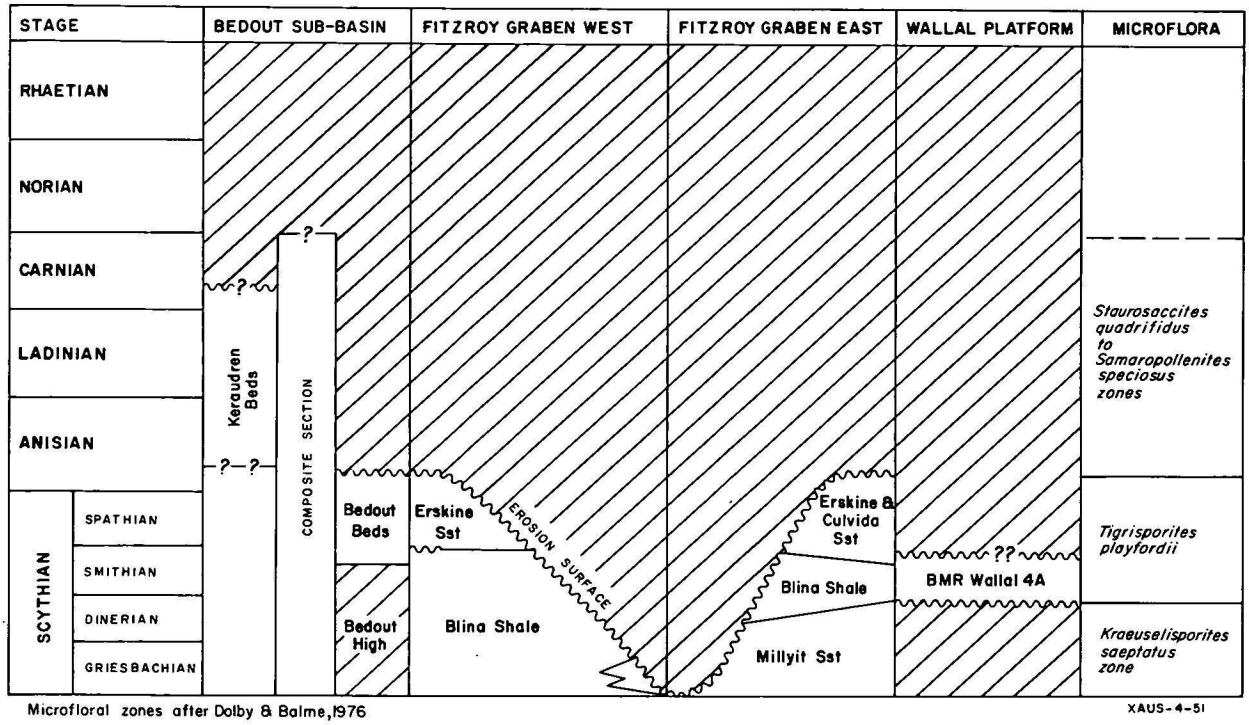

Figure 2. Age and correlation of Triassic rocks in the Canning Basin.

Biofacies

An extensive literature search for the environmental tolerances of each element of the flora and fauna preserved within the Triassic rocks of the Canning Basin (autecology of Ager, 1963; Gorter, in prep., Appendix 2) was undertaken. The combined biota (synecology of Ager, 1963) of each lithofacies is considered on its overall ecological implications, and is termed biofacies (Table 1). Each biofacies is considered in the light of the significant contained fossils—fossils whose ecological limits are reasonably well known—and is then used to reconstruct a picture of the Triassic environmental succession.

Palaeogeography

Four palaeogeographic maps (Fig. 4a-d) were drawn to illustrate the environmental changes through the Triassic, and depict the interpreted distribution of the major depositional environments at a given point in time.

The Fitzroy Embayment (Griesbachian to Dienerian)

At the commencement of the Triassic the seas transgressed the basin. The full extent of this transgression is unknown because of subsequent erosion, but seismic data suggest that the Fitzroy Graben and Bedout Subbasin were flooded. The beginning of the transgression (Fig. 4a) is marked in the onshore basin by fine-grained sandstone and siltstone (basal Blina Shale) which often contain glauconite and numerous acritarchs. In the northwestern Fitzroy Graben the sea was flanked by low-lying land, which supported a coastal plant community of lycopods, cycads, ferns, and conifers. In the southeastern area shallow-marine sediments interfingered with fluviatile sediments (Millyit Sandstone) derived from the erosion of Palaeozoic rocks. The area around the fluviatile systems supported a *Dicroidium* vegetation with small waterside herbs, equisetaleans and other hydrophytic plants occupying billabongs, ponds and river-bank niches. Higher ground surrounding the shallow sea was the habitat of a glossopterid-conifer and cycad-ginkgoalean community, which also contained ferns, and *Dicroidium*.

A shallow sea also occupied the Bedout Sub-basin, but probably did not inundate elevated areas such as the Bedout High (Fig. 4a).

Facies I rocks are represented by the Millyit Sandstone, which was deposited in meandering rivers. The riverine plain supported a flora of ferns, equisetaleans, cycads, glossopterids, conifers and peltasperms (Paten & Price, 1975; White & Yeates, 1976) and rare *Dicroidium* sp. G. J. Retallack (personal communication) has suggested that some of the fossils identified as *Dicroidium* may be misidentifications of the basal Triassic plant *'Thinnfeldia' callipteroides* or similar plants (Townrow, 1966).

Facies II is represented by the basal Blina Shale and the 4A Beds; little is known of the palaeontology of the latter unit. However, both units contain acritarchs characterised by forms which indicate shallow marine, nearshore environments (Sarjeant, 1974). These acritarchs occur in great numbers: such swarms are interpreted by Dolby & Balme (1976) to indicate immature ecosystems, as is to be expected in transgressive conditions. The occurrence together in the Blina Shale of lingulids and conchostracans, both indicative of brackish water (Tasch, 1975), further emphasises the transitional nature of the facies.

The poorly diversified microfloral assemblage (*Kraeueselisporites saeptatus* zone of Dolby & Balme, 1976) represents plants that grew in a specialised coastal environment (Balme, 1969a), which Dolby & Balme (1976) suggest developed following the early Triassic transgression of an older peneplained surface. The broad tidal flats formed were colonised by halophytic lycopod and coastal gymnosperm groups—represented by *Lunatisporites* and other taeniate bisaccate pollens—hydrophytic plants, such as *Equisetum* (Batten, 1974), and ferns indicating moist conditions.

BIOTA	Facies I	Facies II	Facies III	Facies IVa	Facies IVb	Facies V
Ammonoids						
Conodonts			x			
Forams			x			
Bryzoa			x			
Acritarchs		x	x			
Lingulids		x	x	x		
Bivalves				x		
Gastropods						x
Fish	?	x	x	m/f		x
Amphibians			?	m/f		
Reptiles			?	m/f		
Conchostraca		x	x	x		x
Pleuromids	1		x	x		x
Equisetaleans	?	?	?	x	x	?
Seleginellids		x	x	x		
Peltasperms	x					
Ferns	x	x	x		x	x
Cycads	x	x				x
Corystosperms	2	x	x		?	x
Coniferales	x	x	x	x	x	x

x—present; ?—probably present; m/f—marine and freshwater forms present; 1—caving suspected in cutting samples in Bedout 1; 2—recorded from top of the Millyit Sandstone.

Table 1. Check list of fossils recorded from Triassic rocks of the Canning Basin.

The Blina Sea (Smithian)

The major transgressive phase, which began in the early Triassic, culminated in the Smithian Sub-stage, and was probably contemporaneous with similar transgressions in the Carnarvon and Perth Basins (McTavish & Dickins, 1974). During this transgression the Bedout High was inundated (Bedout Beds—Facies III), the Wallal Platform was flooded (4A Beds), and the river systems of the Fitzroy Graben drowned (Figure 4b).

The marine Facies III is characterised by the presence of forms with wide ecological tolerance. The arenaceous foraminifer *Ammodiscus* is recorded from warm and cold-water deposits (Crespin, 1958), and presumably had wide tolerance. The acritarchs are of the same genera present in Facies II, while lingulids and conchostracans also occur. The presence of conchostracans in the Blina Shale suggests that influx of fresh water into the shallow sea had not ceased with the drowning of the eastern rivers. Seasonal flooding of rivers, and the flushing of fresh-water biota (reptiles, amphibians, fish, and plants) into the marine environment (see Cockbain, 1974) could explain the anomalous admixture of marine and fresh-water organisms (Table 1). Hyposalinity of the water is further suggested by the rarity of stenohaline invertebrates and the presence of lingulids indicating the presence of nearby river systems. Connections with the open sea are shown by the presence of marine fish, microplankton, conodonts, and ammonoids. The dominant microplankton are forms which Sarjeant (1974) suggests indicate inshore, partially enclosed environments in an immature ecosystem (Dolby & Balme, 1976). The abundance of U-shaped burrows of *Diplocraterion* is probably indicative of subtidal environments (Sellwood, 1970).

Of the two identifiable conodont genera present, *Neohindeodella* is euryhaline, while *Neogondolella* was extremely sensitive to increased salinities, but could tolerate slightly brackish water (Kazur, 1972). This ability to inhabit waters with lowered salinity is compatible with the presence of lingulids and conchostracans, especially if the latter were washed into the marine environment by flooding.

The microflora, although inadequately sampled in this facies, is broadly comparable to the *Tigrisporites playfordii* Assemblage zone in the Carnarvon Basin, which Dolby & Balme (1976) believe, because of the high number of acritarchs, represents the maximum Smithian transgression. Of the plant types represented in the microflora of the Canning Basin, the majority are ferns and conifers, although *Equisetum* remains are also present. The conifers are of the type designated 'coastal flora' by Balme (1969a). However, it is possible that some of these conifer pollen and fern spores may represent upland communities, rather than reflecting the vegetation in the immediate vicinity of the marine environment (Chaloner & Muir, 1968).

In the western sub-basin, the Bedout High was partially transgressed, as shown by the shallow marine sediments (Facies III) at the base of the Bedout Beds. The local vegetation on emergent parts of the Bedout High included conifers, some of Araucarian type, ferns, and *Dicroidium*. The shore-face was inhabited by coastal lycopods, and probably by equisetaleans, although there are no equisetalean spores reported in the microflora. Between 3124-3630 metres in Keraudren No. 1 the interpretation of Facies III (Marine) is consistent with the presence of acritarchs (Hematite, 1974).

The retreat of the Blina Sea (Spathian to mid-Anisian)

In latest Scythian time the sea receded from the Bedout High, the Wallal Platform and onshore Canning Basin (Fig. 4c). The transition from shallow marine to continental deposition (Facies IV) is represented by deposits of the upper Blina Shale, Lower Erskine Sandstone, upper Bedout Beds, and possibly the lower part of the Culvida Sandstone. These transitional deposits are of interest for the plant communities were undergoing ecological change. The lower Scythian *Taeniaesporites* (= *Lunatisporites*) Microflora (Balme, 1964) gave way to the *Falcisporites* Microflora (Helby, 1973) in later Scythian time. The characteristic *Pleuromeia-Cylostrobus-Aratrisporites* assemblage represents an opportunistic group which rapidly colonised the new coastal mud-flat niche resulting from the retreat of the sea (Balme & Helby, 1973).

As the sea regressed westwards the coastal plain became the site of meandering stream deposition and, by early Middle Triassic time, a continental climatic regime became established in the Fitzroy Graben.

Facies IVa, the regressive facies, is present in the upper Blina Shale, and also contains the *T. playfordii* Assemblage, but lacks the abundant acritarch element. This microflora marks the first appearance of *Aratrisporites* in abundance in the Canning Basin, and indicates the introduction of the pleuromeid complex. The first appearance of *Aratrisporites*, considered by some to be the microspore of the megaspore *Cylostrobus* (Potonié, 1970), although not confined to that genus, and borne by the coastal lycopod *Pleuromeia* (Retallack, 1975) occurs in this facies. *Pleuromeia* first occurs in the Erskine Sandstone at Yarrada Hill (Brunnschweiler, 1957; Retallack, 1975). Balme (1963) suggested that *Pleuromeia* was a plant adapted to more desert-like conditions than earlier lycopods. However, Retallack (1975) has suggested that *Pleuromeia* grew in monotypic stands along the waters edge, and also in shallow water, much like the modern coastal mangrove. Probably, as suggested by Balme & Helby (1973), the pleuromeid complex represents an opportunistic plant group that rapidly colonised the new ecological

PERIOD/ FORMATION	LITH-OLOGY	FOSSILS	SEDIMENTARY STRUCTURES	MINERALOGY	COLOUR	ENVIRONMENTS
JURASSIC						
KERAUDREN V			Laminated		Multicoloured	Lacustrine
KERAUDREN I				Trace pyrite cement	Light grey, minor multi.	Meandering stream, overbank
KERAUDREN V		F,	Laminated, thin bedded	Trace pyrite and calcite, dolomite	Multicoloured	Lacustrine
KERAUDREN IVb				Pyrite, calcite cement, carbon	Grey, multi-coloured in part	Prograding distributary channels - prodelta
KERAUDREN III			Thin bedded, laminated, thickness increases with depth	Trace siliceous, calcitic cement, kaolinitic in part	Grey	Shallow marine or bay
KERAUDREN I				Trace to common kaolinite, pyrite or calcite	Grey, white, black/brown clays	Meandering streams and overbank deposits
			SAMPLING GAP			
BEDOUT IVb					Grey/green when fresh	Prograding distributaries
BEDOUT I ERSKINE I CULVIDA I			, clay pellet conglomerate	Kaolintic	Greenish grey, black, red in part	Meandering stream and overbank
BLINA, IVa BEDOUT, IVa ERSKINE, IVb			Cross laminated, thick bedded, laminated, slump and flow, , coquina,	Pyrite	Green, grey, black	IVa shoaling sequence - shallow marine to tidal flat IVb prograding channels, tidal flat channels
BEDOUT, III BLINA, III		F,	Laminated,	Glauconitic, pyrite, calcite, chert	Green, grey/ green and grey	Shallow marine
BLINA, II 4A, II MILLYIT, I		F, S	Laminated, thin to massive, bedding, coquina poor to well bedded, trough cross bedded,	Glauconitic, ?collophane, pyrite	Black, grey green white, grey, black	Transgressive marine Meandering streams and overbank

XAUS-6-52

Claystone	Conodonts	Bioturbation
Siltstone	Foraminifera	Ripples
Sandstone	Bryozoa	Scour
Conglomerate	Lingulids	Mud cracks
Limestone	Conchostracans	Crossbeds
Coal	S Shell	Up fining
Wood	F Fish	Down fining
Plants	Tetrapods	Unconformity
Megspores	Gastropods	Spores /pollen
Acritarchs	Diplocraterion	

Figure 3. Summary chart of lithology, fossils, sedimentary structures, mineralogy, rock colouration and interpreted sedimentary environments of the Triassic rocks of the Canning Basin.

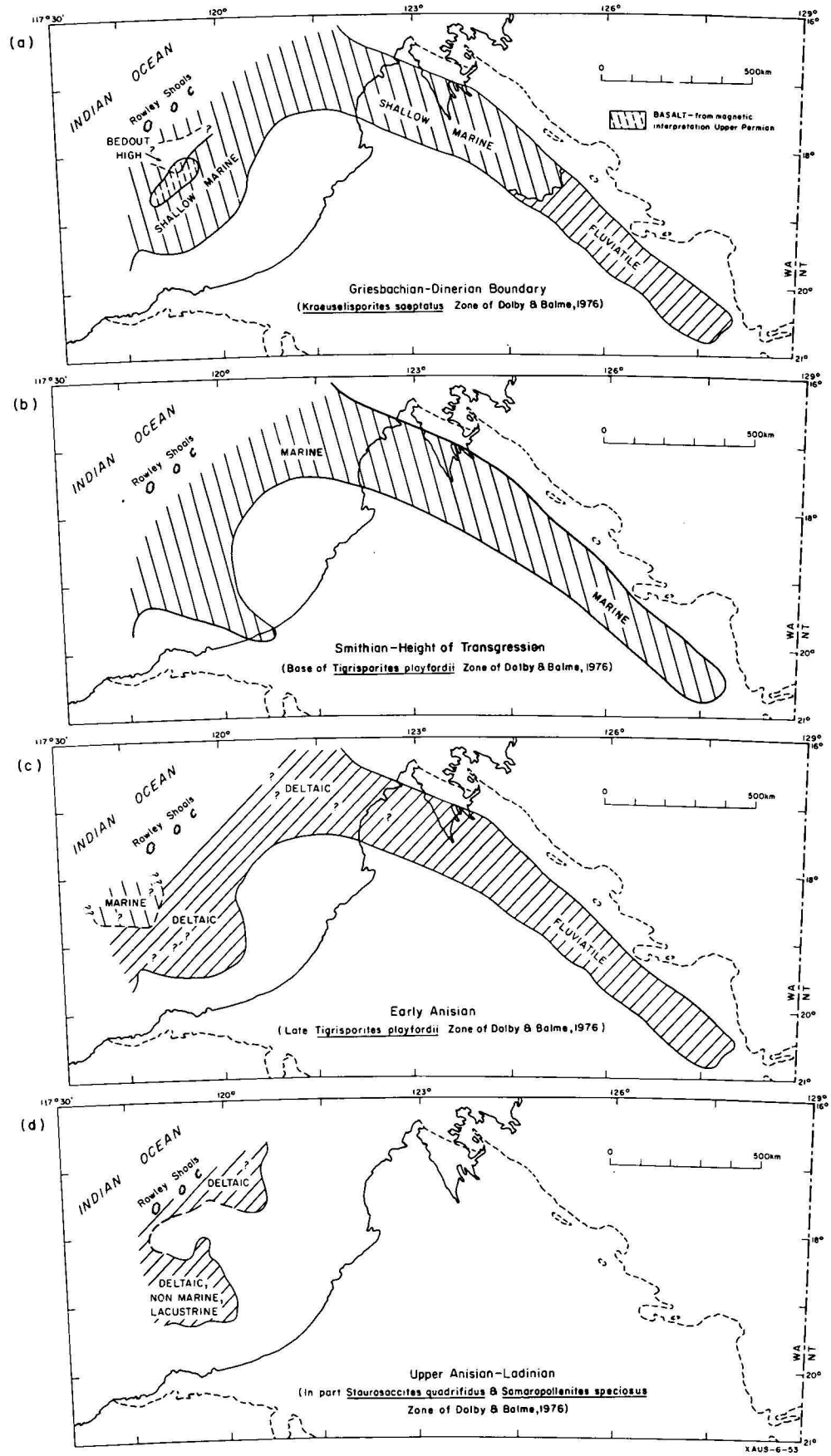

Figure 4. Palaeogeography. A. Griesbachian-Dinerian boundary (*Kraeuselisporites saeptatus* Zone); B. Height of Smithian transgression (base of *Tigrisporites playfordii* Zone); C. Early Anisian (late *Tigrisporites playfordii* Zone); D. Late Anisian-Ladinian (in part *Staurosaccites quadrifidus* and *Samaropollenites speciosus* Zones. Zones from Dolby & Balme, 1976.

niche after the retreat of the sea. Kauffman (1970) noted that environmental crisis associated with regression is often accompanied by rapid changes in environmental parameters, and accelerated evolution at the species level. This is reflected by the rapid diversification of *Aratrisporites* apparent in younger rocks.

The *Tigrisporites playfordii* Assemblage 1 Zone is more diversified than the preceding microflora. Certainly the macroflora represented in the upper Blina Shale (Facies IVa), and lower Erskine Sandstone (Facies IVb), reflects a greater plant diversity, especially in the several species of *Dicroidium* present. A similar situation in the Carnarvon Basin is suggested by Dolby & Balme (1976, p. 131) who state 'these modifications coincide, in broad terms, with the culmination of marine transgression in the Smithian and mark the recolonization of coastal areas by more diverse gymnosperm and cryptogram groups'. The corystosperm *Falcisporites* is the dominant pollen type in the non-marine strata of the Canning Basin, but is subordinate to *Aratrisporites* and other pteridophyte spores in the marginal marine sediments.

The upper Blina Shale (Facies IVa) contains a diverse faunal assemblage. Conchostracans are abundant, sometimes forming coquinas, and are associated with *Lingula* (McKenzie, 1961), bivalves (Casey & Wells, 1960), and *Diplocraterion*. This association of brackish, freshwater, and marine fossils indicates that environments were intimately associated. Freshwater and marine fish are also present, represented by marine Icthyosaurs and non-marine Capitosaurid reptilians. Marine (*Erythrobatrachus*, Cosgriff & Garbut, 1972) and fluviatile (*Blinasaurus*, Cosgriff, 1969) amphibians (Cosgriff, 1974) are found in this facies, further attesting to the alternating environment. This interplay of marine and non-marine fauna is best explained in the context of semi-emergent tidal flats formed during regression of the sea, which were periodically inundated by flooding of streams during seasonal periods of high rainfall. The streams probably entered the sea all year round, but high discharge may have caused ephemeral sheet flooding (Cockbain, 1974) of the tidal flats, and dilution of seawater, as suggested by the low diversity of stenohaline forms.

A seasonal climate is also supported by the presence of the lung fish *Ceratodus*, probably with a climatic range of 11-31°C (Shaeffer, 1970), which may have inhabited ephemeral streams away from the coastal area.

Distributaries on the tidal flats are represented by Facies IVb (e.g. lower Erskine Sandstone), and are distinguished by the lack of animal fossils and the presence of plant remains. Pterophytic plants included *Equisetum*, ?*Schizoneura* and coastal lycopods with associated conifers.

The coastal plain (mid-Anisian to Ladinian)

Middle and lower Upper Triassic rocks in the Bedout Sub-basin reflect the marshy and deltaic environment of that time (Fig. 4d). Fluviatile and lacustrine sediments were deposited on a deltaic plain which was occasionally transgressed by a shallow sea. The climate was probably semi-arid in the Bedout Sub-basin (red beds, dolomite), and continental in the Fitzroy Graben.

Triassic deposition came to a close with tectonism during the late Triassic, when movement on the bounding faults of the Fitzroy Graben produced east-west anticlinal structures and north-south faulting (Smith, 1968); and also uplift in the Bedout Sub-basin.

Lower Middle Triassic Facies I rocks in the Bedout Sub-basin (3630-3844 m, Keraudren No. 1 well) contain no marine fossils, fine upwards and are partly carbonaceous or kaolinitic. The sediments represent meandering stream deposits and the predominant green colour suggests a humid (reducing conditions) climatic regime in the sub-basin. Fluviatile deposition (Facies I) occurs above 2810 metres, with fining upwards cycles, minor coal, and multi-coloured claystone suggesting continental deposition, although no fossils are recorded.

In Facies I rocks of the Erskine Sandstone *Dicroidium* and related plants are dominant, ginkgoaleans make their first appearance. Fossils are rare in this facies, probably because of oxidising conditions inherent in a continental environment. Glossopterids are reported (White & Yeates, 1976), but could probably be better assigned to the Triassic plant *Chiropteris* which has similar venation. Conifers and corystosperms are also prominent in Facies I of the Keraudren Beds and Bedout Beds. Representatives of the pleuromeid complex (*Aratrisporites*) are also present in the latter two units but the occurrence of *Aratrisporites* in the Bedout Beds is questionable because of the possibility of caving. Overbank deposits in the Culvida Sandstone show that the plant communities during the early Middle Triassic were dominated by *Dicroidium*, and contained hydrophytic plants (e.g. *Equisetum*) which probably grew in billabongs or ponds; and conifers, ginkgoes and cycads, probably of upland habitat.

Facies IVb is recognised in Keraudren No. 1 between 2960 and 3124 metres. Arenaceous foraminifera occur in several horizons (Hematite, 1974), and bryozoan fragments occur at 2960 metres. Coarsening upwards cycles between 2955 and 3035 metres are interpreted as progradational channels. Claystone above the uppermost channel contains bryozoans, interpreted as resulting from avulsion of the river, causing a switch in the locus of sedimentation.

The lacustrinal facies (Facies V) is only recognised in Keraudren No. 1. The sequence above the progradational facies (2960 m) contains a dolomitic calcilutite unit from which conchostracans, fish and gastropods were collected from cutting samples. The microflora included ferns, corystosperms and conifers. *Aratrisporites* is present, suggesting a coastal plain site for the lake, or, alternatively, the pleuromeids may by this time have colonised inland lakes, as in the Russian Moscow Basin (Strok & Gorbatkina, 1977). However, as *Aratrisporites* has recently been isolated from lycopod cones other than *Cylostrobus* (Retallack, pers. comm., 1977), this record of *A.* sp. may not necessarily indicate the presence of *Pleuromeia*. It is possible that lycopods occupied distributary channels in lake deltas, as suggested by Retallack (1976) in the Sydney Basin. As suggested by the contained microflora, the hinterland was vegetated by *Dicroidium* (*Falcisporites*), conifers (*Guthoerlisporites*), ferns, and possibly cycads. The upper deposits in Keraudren No. 1 (2460-2568 m) are interpreted as possible lake deposits with a lack of marine fossils, and fine grainsize. The shores of the lake probably supported lycopodian stands, with a mixed *Dicroidium*-conifer vegetation occupying higher land.

Conclusions

From the above description of the sedimentary history of the Triassic succession of the Canning Basin and the contained biota some conclusions of the general history of the area and the effect of the overall transgression-regression on the biota may be drawn.

The sequence records a slow transgression culminating in the Smithian, when the riverine plain in the south-eastern Fitzroy Graben was drowned. The resulting shallow embayment in the Fitzroy Graben supported a much impoverished marine biota, made up of those species which could tolerate reduced saline conditions caused by substantial run-off of fresh water from streams around the shallow sea. A regression began in the Spathian and continued throughout the later Triassic, although there were minor transgressions with marine incursions: the environment changed into a low-relief coastal alluvial plain, with meandering streams and locally developed lakes. A general trend to increasing aridity is also evident, with an increase in red beds, and is correlated with the withdrawal of the Blina Sea. Finally from Ladinian time the area became an area of non-deposition until the early Jurassic.

The major transgressive-regressive cycle is of great interest as it accompanies, or perhaps resulted in, the transition from the early Triassic *'Thinnfeldia' callipteroides* flora to the later Triassic flora, dominated by *Dicroidium,* and the coeval development of a *Pleuromeia* flora in the coastal mud-flat area left by the retreating sea. Aspects of this transition have been touched on by Retallack (1975) in the Sydney Basin, and similar situations are recorded by Kauffman (1970) in North America, and Chaloner & Muir (1968) from Europe. Detailed palynology and macrofloral collections are not yet available from the Triassic rocks of the Fitzroy Graben or Bedout Sub-basin, but what is known supports the concept of floral change in response to climatic fluctuation and the transgressive-regressive cycle. Similar floral transitions can be expected at any major eustatic event (see Gussow, 1976). Further study of this problem and its application is recommended.

Acknowledgements

I would like to thank the several colleagues who contributed discussion and first-hand knowledge to this review, in particular Drs P. J. Jones and E. M. Truswell, and Messrs R. R. Towner and A. N. Yeates. Dr K. A. W. Crook (Australian National University) and Mr G. J. Retallack (University of New England, Armidale) have critically read the manuscript. Text figures were drawn by John Gallagher of the Geological Drawing Office, BMR.

References

AGER, D. V., 1963—Principles of paleoecology; an introduction to the study of how and where animals and plants lived in the past. *McGraw-Hill, New York.*

ALLEN, J. R. L., 1965—Fining-upward sequences in alluvial successions. *Journal of Geology,* **4**, 229-46.

ALLEN, J. R. L., 1970—Studies on fluviatile sedimentation: a comparison of fining upward cyclothems, with special reference to coarse-member composition and interpretation. *Journal of Sedimentary Petrology,* **40**, 293-323.

ANDREWS, P. B., & LAIRD, M. G., 1976—Sedimentology of a Late Cambrian regressive sequence (Bowers Group), Northern Victoria Land, Antarctica. *Sedimentary Geology,* **16**, 21-44.

BALME, B. E., 1963—Plant microfossils from the Lower Triassic of Western Australia. *Palaeontology,* **6**, 12-40.

BALME, B. E., 1964—The palynological record of Australian pre-Tertiary floras. *In* CRANWELL, L. M. (Editor), ANCIENT PACIFIC FLORAS, THE POLLEN STORY. *Hawaii University Press, 10th Pacific Science Congress Series.*

BALME, B. E., 1969a—The Permian-Triassic boundary in Australia. *Special Publication of the Geological Society of Australia,* **2**, 99-111.

BALME, B. E., 1969b—The Triassic System in Western Australia. *APEA Journal,* **11**, 67-78.

BALME, B. E., & HELBY, R., 1973—Floral modifications at the Permian-Triassic boundary in Australia. *In* LOGAN, A., & HILLS, L. V. (Editors), THE PERMIAN AND TRIASSIC SYSTEMS AND THEIR MUTUAL BOUNDARY. *Canadian Society of Petroleum Geologists, Memoir* **2.**

BATTEN, D. J., 1974—Wealdean palaeoecology from the distribution of plant fossils. *Proceedings of the Geological Association,* **85**, 433-58.

BOCAL (BOCAL PTY LTD), 1971—Bedout No. 1 Well Completion report. *Bureau of Mineral Resources, Australia,* File 71/435 (unpublished).

BOCAL (BOCAL PTY LTD), 1971—Bedout No. 1 Well com-File 17/435 (unpublished).

BRUNNSCHWEILER, R. O., 1957—The geology of the Dampier Peninsula, Western Australia. *Bureau of Mineral Resources, Australia, Report* **13.**

CASEY, J. N., & WELLS, A. T., 1960—Regional geology of the north-east Canning Basin, Western Australia. *Bureau of Mineral Resources, Australia, Record* **1960/110** (unpublished).

CHALONER, W. G., & MUIR, M., 1968—Spores and floras. *In* MURCHISON, D. G., & WESTOLL, T. S. (Editors), COAL AND COAL-BEARING STRATA. *Oliver & Boyd, London.*

COCKBAIN, A. E., 1974—Triassic conchostracans from the Kockatea Shale. *Annual Report of the Western Australian Department of Mines for 1973,* 146-8.

COLEMAN, J. M., & GAGLIANO, S. M.—Sedimentary structures: Mississippi River deltaic plain. *In* MIDDLETON, G. V. (Editor), PRIMARY SEDIMENTARY STRUCTURES AND THEIR HYDRODYNAMIC INTERPRETATION. *Society of Economic Paleontologists and Mineralogists, Special Publication* **12**, 133-49.

COSGRIFF, J. W., 1969—*Blinasaurus,* a brachiopod genus from Western Australia and New South Wales. *Journal of the Royal Society of Western Australia,* **52**, 65-88.

COSGRIFF, J. W., 1974—Lower Triassic Temnospondyli of Tasmania. *Geological Society of America Special Paper,* **149**, 1-134.

COSGRIFF, J. W., & GARBUTT, N. K., 1972—*Erythrobatrachus noonkanbahensis,* a Trematosaurid species from the Blina Shale. *Journal of the Royal Society of Western Australia,* **55**, 5-18.

CRESPIN, I., 1958—Permian Foraminifera of Australia. *Bureau of Mineral Resources, Australia, Bulletin* **48.**

DOLBY, J. H., & BALME, B. E., 1976—Triassic palynology of the Carnarvon Basin, Western Australia. *Review of Palaeobotany and Palynology,* **22**, 105-68.

FALKE, H., 1971—Zur Palaogeographie des Kontinentalen Perms in Suddentchland. *Abhandlungen des Hessischen Landesamtes für Bodenforschung,* **60**, 223-34.

GORTER, J. D., in prep.—Review of Triassic palaeoenvironments in the Canning Basin, Western Australia. *Bureau of Mineral Resources, Australia, Record* **1978/1.**

GRIENER, H., 1974—The Albert Formation of New Brunswick: a Paleozoic lacustrine model. *Geologische Rundschau,* **63**, 1102-13.

GUSSOW, W. C., 1976—Sequence concepts in petroleum engineering. *Geotimes, September 1976,* 16-17.

HELBY, R. J., 1973—Review of the Late Permian and Triassic palynology of New South Wales. *Geological Society of Australia, Special Publication* **4**, 141-55.

HEMATITE, 1974—Keraudren No. 1 well completion report. *Bureau of Mineral Resources, Australia,* File 73/240 (unpublished).

INGRAM, B. S., 1974—Palynology report. *In* HEMATITE—Keraudren No. 1 well completion report. *Bureau of Mineral Resources, Australia,* File 73/240 (unpublished), Appendix 2.

KAUFFMAN, E. G., 1970—Population systematics, radiometrics and zonation—a new biostratigraphy. *Proceedings of the North American Paleontological Convention, Chicago, Section F*, 612-66.

KOZUR, H., 1976—Paleoecology of the Triassic conodonts and its bearing on multi-element taxonomy. *Geological Association of Canada, Special Paper* **15**, 313-24.

LAND, C. B., JR, 1973—Stratigraphy of Fox Hills Sandstone and associated formations, Rock Springs Uplift and Wamsutter Arch area, Sweetwater County, Wyoming: a shoreline-estuary sandstone model for the Late Cretaceous. *Quarterly Journal of the Colorado School of Mines*, **67**, 1-69.

MCKENZIE, K. G., 1961—Vertebrate localities in the Triassic Blina Shale of the Canning Basin, Western Australia. *Journal of the Royal Society of Western Australia*, **44**, 69-76.

MCTAVISH, R. A., & DICKINS, J. M., 1974—The age of the Kockatea Shale (Lower Triassic), Perth Basin—a reassessment. *Journal of the Geological Society of Australia*, **21**, 195-202.

PATEN, R., & PRICE, P., 1975—Palynological study of cores cut in BMR stratigraphic drillholes. Appendix C. *In* YEATES, A. N., CROWE, R. W. A., TOWNER, R. R., WYBORN, LESLIE A. I., & PASSMORE, VIRGINIA L., Notes on the geology of the Gregory Sub-basin and adjacent areas of the Canning Basin, Western Australia. *Bureau of Mineral Resources, Australia, Record* **1975/77** (unpublished).

PICARD, M. D., & HIGH, L. R., JR., 1972—Criteria for recognizing lacustrine rocks. *In* RIGBY, J. K., & HAMBLIN, W. K. (Editors)—RECOGNITION OF ANCIENT SEDIMENTARY ENVIRONMENTS. *Society of Economic Paleontologists and Mineralogists Publication* **16**.

POTONIE, R., 1970—Synopsis der Guttungen der Sporae dispersae. *Beihefte zum Geologischen Jahrbuch*, **87**.

RETALLACK, G. J., 1975—The life and times of a Triassic lycopod. *Alcheringa*, **1**, 3-29.

RETALLACK, G. J., 1976—Triassic palaeosols in the upper Narrabeen Group, New South Wales. I. Features of the palaeosols. *Journal of the Geological Society of Australia*, **32**, 383-99.

SARJEANT, W. A. S., 1974—FOSSIL AND LIVING DINOFLAGELLATES. *Academic Press, London.*

SELLEY, R. C., 1970—ANCIENT SEDIMENTARY ENVIRONMENTS. *Chapman & Hall, London.*

SELLWOOD, B. W., 1970—The relation of trace fossils to small scale sedimentary cycles in the British Lias. *In* CRIMES, T. P., & HARPER, J. C. (Editors)—TRACE FOSSILS. *Geological Journal, Special Issue* **3**, 489-504.

SCHAEFFER, B., 1970—Mesozoic fishes and climate. *Proceedings of the North American Paleontological Convention, Chicago, Section D*, 376-88.

SMITH, S. G., 1968—Tectonics of the Fitzroy wrench trough, Western Australia. *American Journal of Science*, **266**, 766-76.

STROK, N. I., & GORBATKINA, T.Ye., 1977—Geologic history of the central and western parts of the Moscow Syncline during the early Triassic. *International Geology Review*, **19**, 810-16.

SYKES, R. M., 1974—Sedimentological studies in southern Jameson Land, East Greenland. II. Offshore estuarine regressive sequences in the Neill Klinter Formation (Pliensbachian-Toarcian). *Bulletin of the Geological Society of Denmark*, **23**, 213-24.

TASCH, P., 1975—Non-marine arthropoda of the Tasmanian Triassic. *Proceedings of the Royal Society of Tasmania, Paper* **109**, 97-106.

TOWNROW, J. A., 1966—On *Lepidopteris madagascarensis* Carpentier (Peltaspermacae). *Journal of the Proceedings of the Royal Society of New South Wales*, **98**, 203-14.

WALKER, R. G., 1972—Upper Devonian marine-non-marine transition, southern Pennsylvania. *Pennsylvania Geological Survey, Report* **G62**, 1-25.

WALKER, R. G., & HARMS, J. C., 1975—Shorelines of weak tidal activity: Upper Devonian Catskill Formation. Central Pennsylvania. *In* GINSBURG, R. N. (Editor), TIDAL DEPOSITS. A RECENT CASEBOOK OF RECENT AND FOSSIL COUNTERPARTS. *Springer-Verlag, Berlin.*

WHITE, M. E., & YEATES, A. N., 1976—Report on the 1972 and 1973 collections of plant fossils from the Canning Basin, Western Australia. *Bureau of Mineral Resources, Australia, Record* **1976/18** (unpublished).

YEATES, A. N., CROWE, R. W. A., TOWNER, R. R., WYBORN, LESLEY A. I., & PASSMORE, VIRGINIA, L., 1975—Notes on the geology of the Gregory Sub-basin and adjacent areas of the Canning Basin, Western Australia. *Bureau of Mineral Resources, Australia, Record* **1975/77** (unpublished).

The Proterozoic and Palaeozoic rocks of The Granites-Tanami region, Western Australia and Northern Territory, and interregional correlations

D. H. Blake

The Granites-Tanami region links the mainly Proterozoic areas of northwestern and central Australia. It is made up of two main tectonic units: *The Granites-Tanami Block*, which consists of metasediments and metavolcanics of the Lower Proterozoic Tanami Complex, younger Lower Proterozoic sedimentary and acid volcanic rocks, and 1820-1710 m.y. old granites; and the *Birrindudu Basin*, which contains the mainly clastic sedimentary rocks of the Carpentarian Birrindudu Group, dated at about 1560 m.y., and the Adelaidean Redcliff Pound Group, which was probably deposited less than 1000 m.y. ago, and their possible stratigraphic equivalents. The Proterozoic rocks are overlain by Early Cambrian Antrim Plateau Volcanics and younger Palaeozoic non-marine sediments. Five major phases of tectonic activity, ranging in age from Lower Proterozoic (1960 m.y.) to early Carboniferous (Alice Springs Orogeny), can be recognised.

The Proterozoic and Palaeozoic rocks are correlated with similar rocks in the Kimberley region to the northwest, the Victoria River region to the north, the Arunta Block and Amadeus Basin to the south, the Tennant Creek region to the east, and the Canning Basin to the west. The best substantiated correlations are the Tanami Complex with the Halls Creek Group of the Kimberley region, and the Redcliff Pound Group with the Heavitree Quartzite and Bitter Springs Formation of the Amadeus Basin. The latter correlation indicates that when these units were deposited the Birrindudu and Amadeus Basins were interconnected.

Introduction

The Granites-Tanami region is an area of Proterozoic and subordinate Palaeozoic rocks, largely covered by Cainozoic superficial deposits, which links the mainly Proterozoic areas of northwestern and central Australia. It is situated between the Kimberley region (Western Australia) and Victoria River region (Northern Territory) to the northwest and north, and the Arunta Block and Amadeus Basin to the south and southeast (Fig. 1), and is separated from the Proterozoic Tennant Creek region to the east by the Palaeozoic Wiso Basin; to the west it is bounded by the Phanerozoic Canning Basin.

Relatively little was known about the geology of the region before it was mapped at 1:250 000 scale between 1971 and 1973 by the Bureau of Mineral Resources (BMR) and the Geological Survey of Western Australia (GSWA). Goldfields, now abandoned, at The Granites and Tanami were described by Hossfeld (1940), and a published account of The Granites goldfield was also given by Hall (1953). The Western Australian part of the region was briefly examined during a reconnaissance survey of the Canning Basin in 1955-56 (Veevers & Wells, 1961; Casey & Wells, 1964). The 1971-73 survey was carried out by D. H. Blake, I. M. Hodgson, and P. A. Smith (BMR), and P. C. Muhling (GSWA). Results of this survey have been published or are in preparation as a BMR Bulletin (Blake, Hodgson, & Muhling, in prep.), as Explanatory Notes and maps for the eight 1:250 000 Sheet areas mapped (Blake, 1975, 1977; Blake, Passmore, & Muhling, 1977; Blake & Yeates, 1977; Hodgson, 1975, 1976, 1977; Crowe & Muhling, in press), and as a BMR Report (Blake, Hodgson, & Smith, 1975).

The Granites-Tanami region is made up of two major Precambrian tectonic units: The Granites-Tanami Block (Geological Society of Australia, 1971), which consists of Lower Proterozoic[1] metamorphosed and unmetamorphosed sedimentary and volcanic rocks, and Lower Proterozoic and Carpentarian granites; and the Birrindudu Basin (Blake & Hodgson, 1975; Blake and others, 1975,

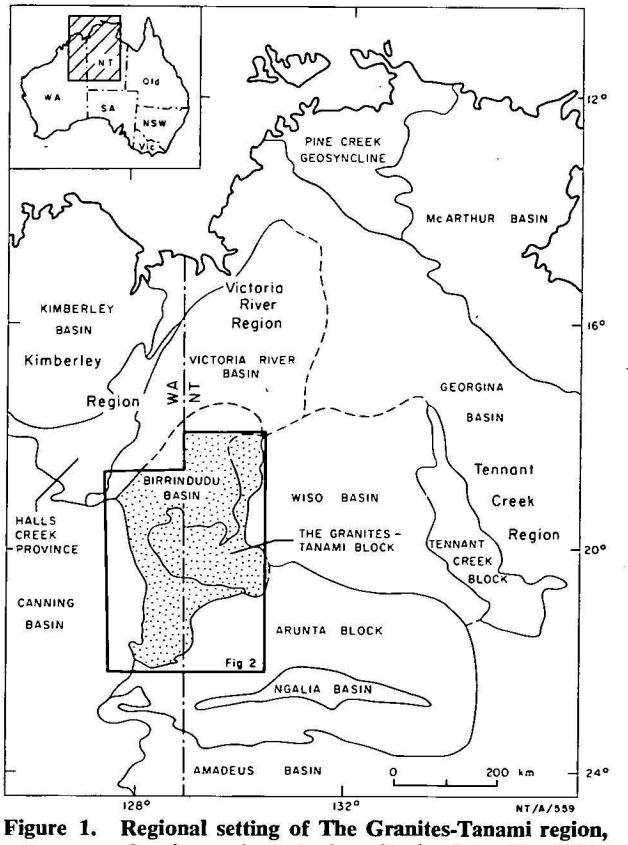

Figure 1. Regional setting of The Granites-Tanami region, showing main tectonic units (mainly after GSA, 1971).

1. **Subdivisions of the Precambrian presently adopted by BMR are Lower Proterozoic = 2300 to 1770 m.y. ago, Carpentarian = 1770 to 1400 m.y. ago, Adelaidean = 1400 to 570 m.y. ago; all Precambrian ages quoted are based on Rb-Sr geochronology using 1.39 $\times$ $10^{-11}yr^{-1}$ as the decay constant of Rb^{87}.**

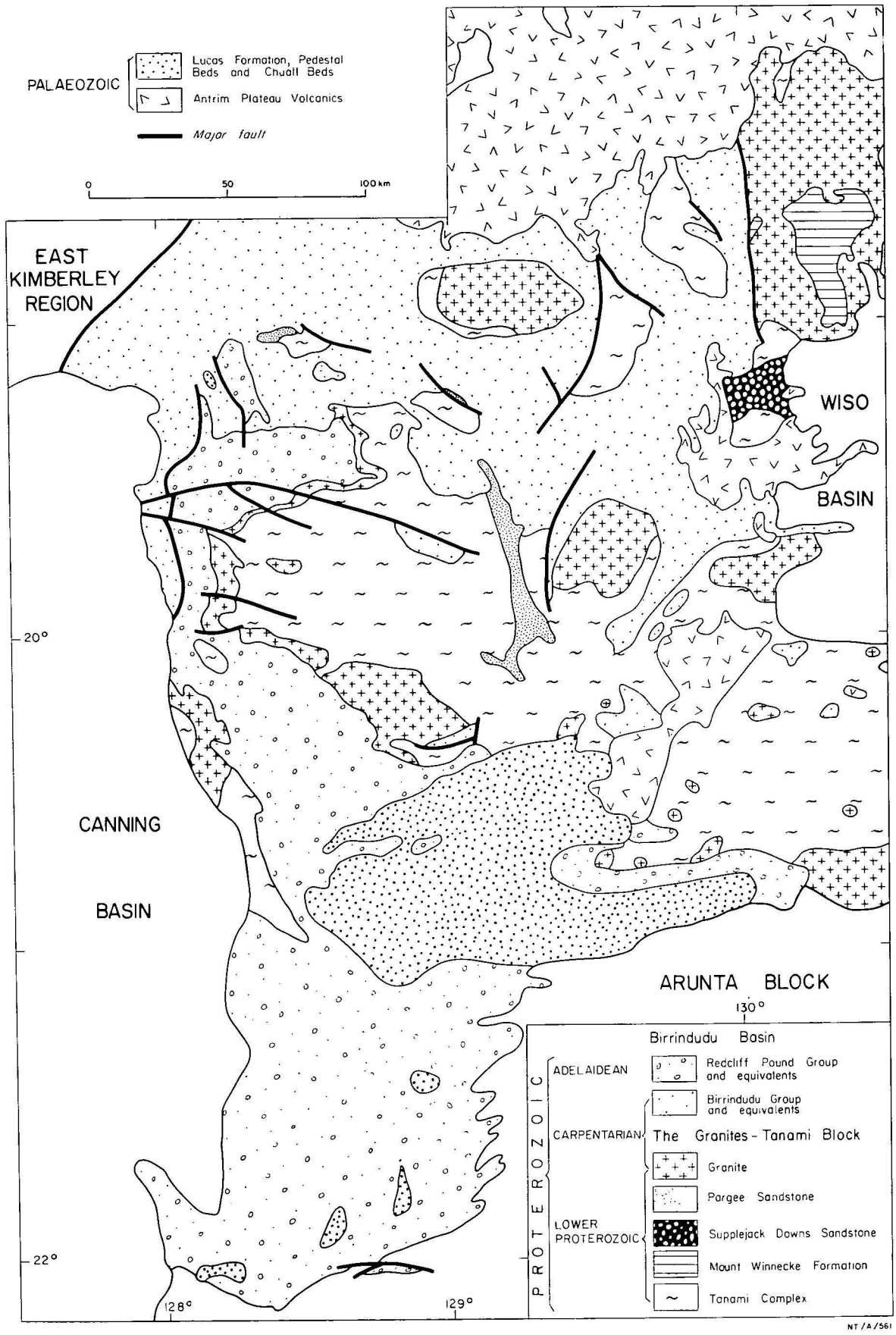

Figure 2. Geological map of The Granites-Tanami region.

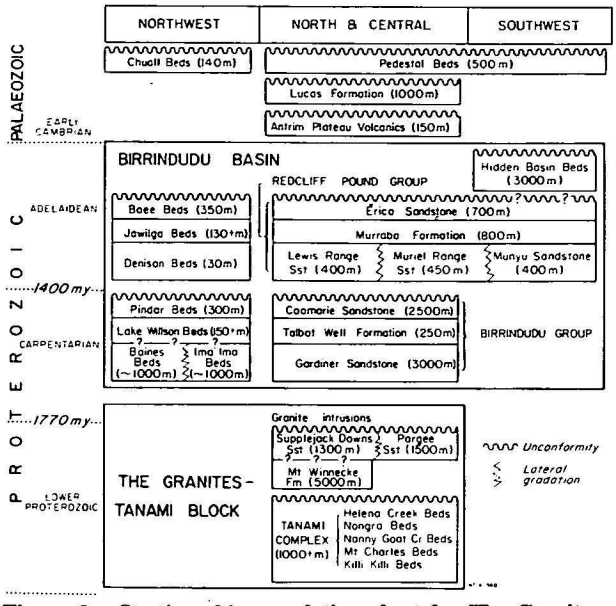

Figure 3. Stratigraphic correlation chart for The Granites-Tanami Block, Birrindudu Basin and overlying Palaeozoic rocks (with maximum thickness in metres) in The Granites-Tanami region.

and in prep.), which contains unmetamorphosed Carpentarian and Adelaidean sedimentary rocks (Plumb & Derrick, 1975, give an alternative definition of the Birrindudu Basin which excludes the Adelaidean rocks). The distribution of the main rock units is shown in Figure 2, and the stratigraphy is summarised in Figure 3.

The Proterozoic rocks of the region are overlain by Early Cambrian subaerial basalt lavas in the northeast and by younger, probably non-marine, Palaeozoic sedimentary rocks in the central and western parts.

The post Palaeozoic is represented by a few scattered outcrops of probably Mesozoic, non-marine sedimentary rocks, and by a widespread cover of Cainozoic superficial continental sediments which locally reach thicknesses of more than 100 m.

Correlations between The Granites-Tanami region and adjoining and nearby regions are discussed in this paper, and are summarised in Figure 4.

The Granites-Tanami region

Lower Proterozoic and Carpentarian rocks of The Granites-Tanami Block

The oldest rocks exposed in The Granites-Tanami Block are tightly to isoclinally folded and commonly cleaved low-grade metasediments and metavolcanics of the **Tanami Complex.** Main rock types present are greywacke, siltstone, lithic and sublithic arenite (nomenclature of Pettijohn, Potter, & Siever, 1972), and shale, all of which are schistose to phyllitic, and also basic and acid volcanics, quartzite, and thin-banded chert. The Tanami Complex is probably several thousands of metres thick, but because of overall poor exposures, lack of marker beds, and unknown structural complexities, no sequences have been established within it. Five sub-units, the Mount Charles, Killi Killi, Nanny Goat Creek, Nongra, and Helena Creek Beds, have been mapped; these are distinguished by different proportions of constituent rock types and geographic separation, and they may be lateral equivalents of one another. The Mount Charles Beds are the hosts to the mineralisation in The Granites and Tanami goldfields.

The Tanami Complex is intruded by late Lower Proterozoic and early Carpentarian granites, and is overlain unconformably by late Lower Proterozoic, Carpentarian, and Adelaidean sedimentary rocks. Four of the granites intruding the Tanami Complex have been isotopically dated (Page, Blake, & Mahon, 1976): Winnecke Granophyre at 1802 ± 15 m.y.; The Granites Granite at 1780 ± 24 m.y.; Slatey Creek Granite at 1770 ± 62 m.y.; Lewis Granite at 1720 ± 8 m.y.

Three formations younger than the Tanami Complex, but older than any of the Birrindudu Basin rocks, are also considered to be part of The Granites-Tanami Block. These formations, which may be more or less lateral equivalents, are the Pargee and Supplejack Downs Sandstones and the Mount Winnecke Formation. They have been deformed into several large, tight, upright folds, but they do not appear to have been regionally metamorphosed. The **Pargee Sandstone** consists of interbedded sublithic, lithic, and quartz arenite, conglomerate, and greywacke which crop out in the western and central parts of The Granites-Tanami Block. It is unconformable on the Tanami Complex, and is overlain unconformably by Carpentarian and Adelaidean sedimentary rocks of the Birrindudu Basin succession. The **Supplejack Downs Sandstone** is composed mainly of quartz and sublithic arenite, and is confined to the northeast. It lies unconformably on the Tanami Complex and possibly conformably on the Mount Winnecke Formation, and is inferred to be overlain unconformably by Carpentarian Birrindudu Basin rocks. Outcrops of the **Mount Winnecke Formation** are also confined to the northeast. This unit is made up mainly of porphyritic acid lava, sublithic arenite, and tuffaceous sandstone and siltstone. It is intruded by the high-level Winnecke Granophyre, which is considered to be comagmatic with the acid lava (Blake and others, 1975; in prep.; Page and others, 1976). Rb-Sr geochronology indicates that both the acid lava of the Mount Winnecke Formation and the Winnecke Granophyre crystallised about 1800 m.y. ago, late in the Lower Proterozoic.

Carpentarian and Adelaidean rocks of the Birrindudu Basin

The Granites-Tanami Block is overlain unconformably by unmetamorphosed sedimentary rocks, mainly sandstone, of the Birrindudu Basin succession. This succession comprises the Carpentarian Birrindudu Group and the Adelaidean Redcliff Pound Group, and possible stratigraphic equivalents in the north, northwest, and southwest (Fig. 3).

The **Birrindudu Group** is exposed extensively in the north of the Granites-Tanami region, but is absent in the south. It has mainly moderate dips. Three formations make up the group; the Gardiner Sandstone at the base, the conformably overlying Talbot Well Formation, and the Coomarie Sandstone at the top. The **Gardiner Sandstone** consists of quartz-cemented and locally iron-stained sublithic arenite and subordinate quartz arenite, conglomerate, shale, siltstone, glauconitic sandstone, and dolomitic sandstone. Cross-bedding is almost ubiquitous in the arenites, and ripple marks and shale pellets are common locally. One or two marker bands of glauconitic sandstone are present near the top of the formation. K-Ar and Rb-Sr dating of glauconite from these bands indicates that the Gardiner Sandstone was probably deposited about 1560 m.y. (Page & others,

1976). Conglomerate at the base of the formation at one locality (Killi Killi Hills) contains uranium and rare-earths (Blake and others, in prep.). The succeeding **Talbot Well Formation** consists of chert, arenite, siltstone, shale, and some carbonate. The chert is commonly stromatolitic (as also is the carbonate), indicating that it represents silicified carbonate rocks. The overlying **Coomarie Sandstone,** like the Gardiner Sandstone, is formed mainly of cross-bedded sublithic arenite. The presence of glauconite and stromatolites indicates that the Birrindudu Group is probably at least partly marine.

Possible stratigraphic equivalents of the Birrindudu Group, mainly cross-bedded arenite, form isolated exposures in the north and northwest. They are mapped as **Limbunya** Group in the Birrindudu 1:250 000 Sheet area (Blake, 1975) and as **Baines, Ima Ima, Lake Willson** and **Pindar Beds** in the Billiluna 1:250 000 Sheet area (Blake and others, 1977); the Lake Willson Beds include some stromatolitic chert.

The Adelaidean **Redcliff Pound Group** crops out in the north, centre, and southwest of the region. It comprises the Munyu, Muriel Range, and Lewis Range Sandstones, which are laterally equivalent basal formations, the overlying Murraba Formation, and the Erica Sandstone, the yougest formation. Compared with those of the Birrindudu Group, these formations are generally not as steeply dipping, and the predominant rock-type present, sandstone, is generally better sorted, more friable (less silicified), and more ironstained. The Redcliff Pound Group is correlated with the Heavitree Quartzite and Bitter Springs Formation of the Amadeus Basin (see below), hence it is probably less than 1000 m.y. old.

The **Munyu Sandstone** is the basal formation in the south, where it lies unconformably on rocks of the Arunta Block. It consists of cross-bedded quartz arenite, accompanied by subordinate conglomerate near the base and carbonate near the top; the carbonate rocks contain thin lenses and laminae of dark grey chert, and show vague, possibly stromatolitic, fine banding. The **Muriel Range Sandstone** crops out in the eastern-central part of the Birrindudu Basin, unconformably overlying rocks of The Granites-Tanami Block. The main rock types of this formation are cross-bedded and ripple-marked sublithic and quartz arenite. These are mainly thin to very thin-bedded, and commonly have bedding planes crowded with shale pellets. The **Lewis Range Sandstone** is exposed in the western, central, and northern parts of the Birrindudu Basin. It is unconformable on The Granites-Tanami Block and, in the north, also on the Birrindudu Group. The main rock type of this unit is cross-bedded, and commonly ripple-marked, quartz arenite.

The **Murraba Formation** is inferred to overlie the three basal formations conformably; however, its lower contact is nowhere exposed. The formation consists of thinly interbedded chert-granule conglomerate, sublithic and quartz arenite, siltstone, shale, mudstone, pebble conglomerate, and dolomite. Cross-bedding, ripple marks, and bedding planes with shale pellets are all very common; mud-cracks, indicating periodic subaerial conditions during deposition, occur locally. The predominant rock type of the overlying **Erica Sandstone** is cross-bedded sublithic arenite. Rare glauconite in the Erica Sandstone and the presence of carbonates in the Munyu Sandstone and Murraba Formation suggest that the Redcliff Pound Group is probably at least partly marine.

Possible stratigraphic equivalents of the Redcliff Pound Group are the **Hidden Basin Beds** in the southwest, a unit of mainly quartz and sublithic arenites which appears to overlie Erica Sandstone, possibly conformably, and the **Denison, Jawilga,** and **Boee Beds** in the northwest. The last three units are similar to the Lewis Range Sandstone, Murraba Formation, and Erica Sandstone, respectively, in lithology and inter-relationships.

Palaeozoic rocks of The Granites-Tanami region

Flat-lying to gently dipping Palaeozoic rocks, probably non-marine, form scattered outcrops in several parts of the region, and unconformably overlie Proterozoic rocks. The oldest are basalt lavas and subordinate interlayered sedimentary rocks of the **Antrim Plateau Volcanics,** which crop out in the northeast quadrant. This unit is probably Early Cambrian (Bultitude, 1976). The only fossils known within it are stromatolites. The other Palaeozoic units are the Lucas Formation and the Pedestal and Chuall Beds; these may be Devonian, but they are unfossiliferous, and their ages are uncertain. The **Lucas Formation** occupies a broad and relatively shallow basin in the central part of the region, and is thought to be lacustrine (Blake and others, in prep.). It consists of sandstone, siltstone and mudstone, which are commonly calcareous, and minor limestone and dolomite. The **Pedestal Beds** are exposed in the central and southern parts of the region, and overlie the Antrim Plateau Volcanics and Lucas Formation, in both cases probably unconformably. The main rock type, quartzose to lithic sandstone with a generally abundant clayey matrix, is locally accompanied by conglomerate, shale, and siltstone. Cross-bedding, ripple marks, and shale-pellet horizons are common in both this unit and the Lucas Formation. The **Chuall Beds** consist of friable quartzose to lithic sandstone, and are confined to a small area in the northwest; they are similar in lithology, and probably in age, to the Pedestal Beds.

Tectonism

Five major phases of tectonic activity have been recognised in The Granites-Tanami region. The first phase caused the tight to isoclinal folding and low-grade regional metamorphism of the Tanami Complex and also of the Halls Creek Group in the east Kimberley region to the northwest—where the regional metamorphism has been dated at 1960 m.y. (Dow & Gemuts, 1969). The second phase probably took place at the end of the Lower Proterozoic and early in the Carpentarian, the time of granite emplacement in The Granites-Tanami Block. The Pargee and Supplejack Downs Sandstones and the Mount Winnecke Formation were folded during this phase. Most of the deformation of the Birrindudu Group in the northern part of the Birrindudu Basin took place during the third phase, some time between about 1550 and 1000 m.y. ago, before the deposition of the Redcliff Pound Group. The effects of the fourth phase are evident in the south, where it resulted in the development of mainly open folds in the Redcliff Pound Group. This phase may have taken place about 600 m.y. ago, at the time of the Petermann Ranges Orogeny (Forman & Shaw, 1973). The fifth phase has been recognised only in the southeast, where the Palaeozoic Pedestal Beds overlying the Arunta Block are folded and faulted; this phase was probably part of the Alice Springs Orogeny, which took place during the late Devonian-early Carboniferous (Stewart, 1971; Armstrong & Stewart, 1975).

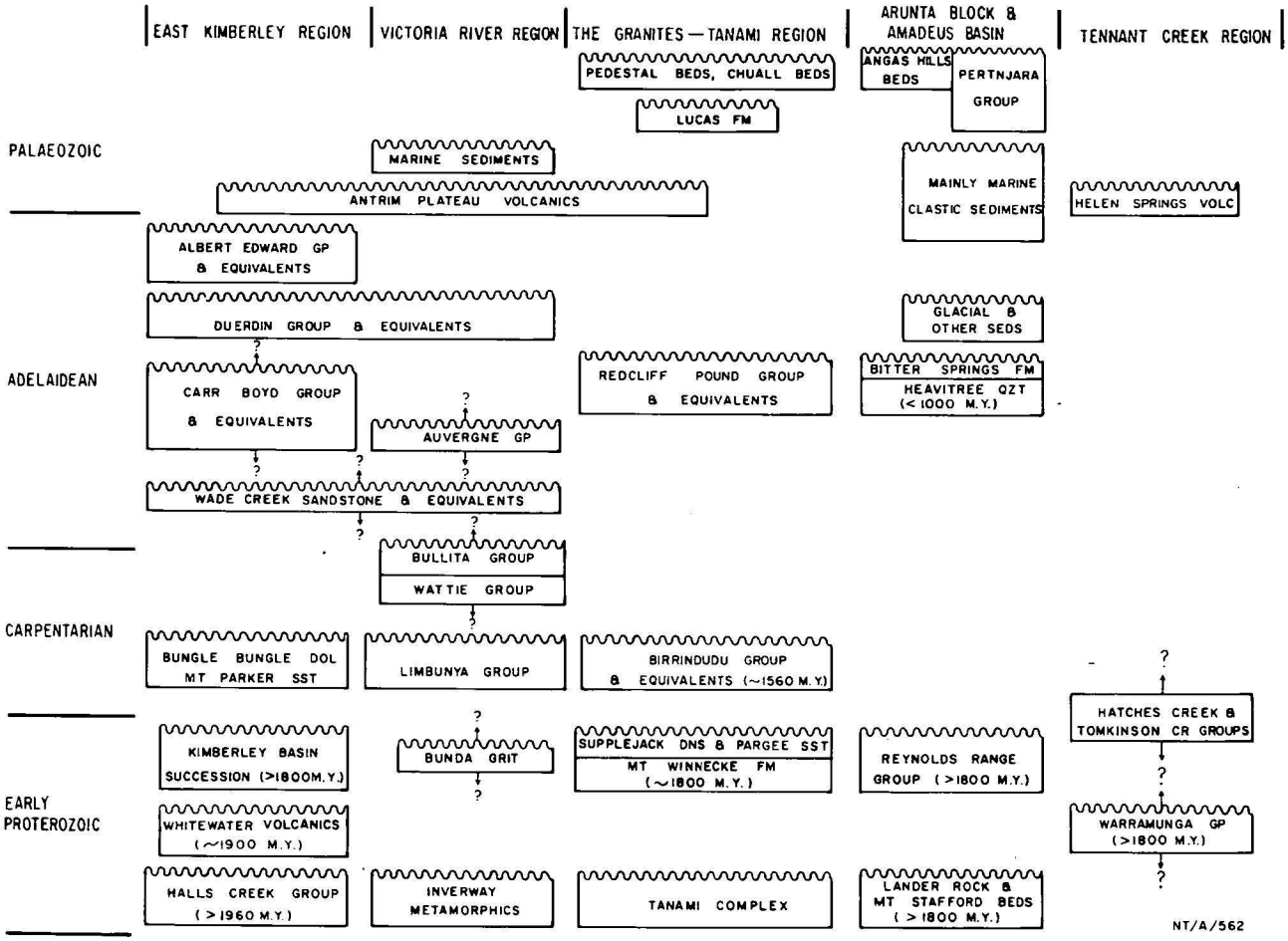

Figure 4. Stratigraphic correlation chart for The Granites-Tanami and nearby regions.

Inter-regional correlations

Correlatives of rocks in The Granites-Tanami Block

The oldest rocks of The Granites-Tanami Block, those of the **Tanami Complex,** are correlated with the **Halls Creek Group** of the Halls Creek Province in the adjoining Kimberley region to the northwest (Dow & Gemuts, 1969; Plumb & Gemuts, 1976). Both units include thick sequences of metagreywacke, siltstone, and basic volcanics, which are tightly to isoclinally folded and regionally metamorphosed to greenschist facies. The Halls Creek Group is older than 1960 m.y. (the age of its regional metamorphism), but probably younger than 2200 m.y. (Page, 1976); hence an Archaean age for the Halls Creek Group, as suggested by Dow & Gemuts (1969) and Gellatly (1971), is now considered unlikely. The Tanami Complex is also probably the same age as the **Inverway Metamorphics,** the oldest unit exposed in the Victoria River region to the north (Sweet and others, 1974; Sweet, 1977); the Inverway Metamorphics consist of schist, some of which represents metamorphosed acid volcanics.

To the south and southeast of The Granites-Tanami Block the Tanami Complex grades into somewhat higher grade, but still mainly greenschist facies, metasediments which are mapped as part of the Arunta Block (Blake, 1977; Hodgson, in press; Blake and others, in prep.). These higher grade rocks are now quartzite, micaceous and chloritic schist, and quartzo-feldspathic gneiss. They are probably correlatives of the **Lander Rock** and **Mount Stafford Beds** (Shaw & Stewart, 1975), which were involved in regional metamorphisms dated at about 1800 and about 1700 m.y. ago (Stewart & Warren, 1977).

Another possible correlative of the Tanami Complex is the **Warramunga Group** of the Tennant Creek Block. The Warramunga Group consists of rocks which are similar in lithology, metamorphic facies, and structure to those of the Tanami Complex; it is at least as old as 1810 m.y. and is possibly older than 1900 m.y. (Black, 1977).

The three younger Lower Proterozoic formations of The Granites-Tanami Block, the **Pargee** and **Supplejack Downs Sandstones** and the **Mount Winnecke Formation,** have no definite correlatives in adjacent regions. The Mount Winnecke Formation is the only one of the three that has been isotopically dated; it contains acid lavas which, together with the comagmatic Winnecke Granophyre, are dated at about 1800 m.y. These acid volcanics appear to be younger than those of the **Whitewater Volcanics** of the Kimberley region, which are probably about 1900 m.y. old (Page, 1976), and slightly older than those of the **Cliffdale Volcanics,** the unit which defines the base of the Carpentarian (Dunn, Plumb, & Roberts, 1966): the Cliffdale Volcanics form part of the Murphy Tectonic Ridge, 800 km to the east, and are dated at 1770 ± 20 m.y. (Plumb & Sweet, 1974; Mitchell, 1976). The acid volcanics of the Mount Winnecke Formation could, however, be similar in age to those of the Warramunga Group if this group can be shown to be younger than gneiss in the Tennant Creek Block dated at 1920 ± 60 m.y. (Black, 1977). Other possible equivalents of the Mount Winnecke Formation and also of the Pargee and Supplejack Downs Sandstones are the

Bunda Grit of the Victoria River region (Sweet, 1977), units of the Kimberley Basin succession to the northwest (Plumb & Derrick, 1975), the **Reynolds Range Group,** which is unconformable on Lander Rock Beds in the Arunta Block (Shaw & Stewart, 1975), and the **Hatches Creek** and **Tomkinson Creek Groups,** which unconformably overlie the Warramunga Group in the Tennant Creek Block (Black, 1977).

Granites similar in age to those of The Granites-Tanami Block (1820-1710 m.y.) are known in the Arunta and Tennant Creek Blocks (Stewart & Warren, 1977; Black, 1977). Granitic units of the east Kimberley region are somewhat older (Dow & Gemuts, 1969).

Correlatives of rocks in the Birrindudu Basin

The Birrindudu Basin succession in The Granites-Tanami region comprises the Carpentarian Birrindudu Group and the Adelaidean Redcliff Pound Group, and their possible correlatives in the northwest and southwest. The most likely stratigraphic equivalents of the Birrindudu Group in adjacent regions are the **Mount Parker Sandstone** and **Bungle Bungle Dolomite** of the east Kimberley region (Dow & Gemuts, 1969; Plumb & Gemuts, 1976), and the **Limbunya Group** of the Victoria River region (Sweet, 1977). The Mount Parker Sandstone is similar in overall lithology to the Gardiner Sandstone, the basal formation of the Birrindudu Group; similarly, it is separated from underlying Lower Proterozoic rocks by a marked angular unconformity. However, the Mount Parker Sandstone is generally better sorted than the Gardiner Sandstone, and is not known to include any glauconitic sandstone. Both units are overlain conformably by formations containing stromatolitic chert and carbonates—the Mount Parker Sandstone by the Bungle Bungle Dolomite, and the Gardiner Sandstone by the Talbot Well Formation (the middle unit of the Birrindudu Group), additional evidence supporting their correlation. The Mount Parker Sandstone and Bungle Bungle Dolomite are similar in lithology and sedimentary structures to the Limbunya Group, and are regarded as equivalents of this group by Sweet (1977).

The lower part of the **Redcliff Pound Group** is correlated with the **Heavitree Quartzite** and the conformably overlying **Bitter Springs Formation,** the two oldest units of the Amadeus Basin succession (Wells and others, 1970). The Heavitree Quartzite is known to overlie migmatite dated at 1076 ± 50 m.y. (Marjoribanks & Black, 1974), and hence is probably younger than 1000 m.y. (Wells, 1976). The **Munyu Sandstone,** the basal formation of the Redcliff Pound Group in the south of the Birrindudu Basin, and the Heavitree Quartzite crop out only 30 km apart in the Webb 1:250 000 Sheet area (Blake, 1977); both formations here are unconformable on metamorphic rocks of the Arunta Block, consist mainly of strikingly similar quartz-rich sandstone, and show comparable fold structures. The upper part of the Munyu Sandstone includes carbonates similar to those found in the Bitter Springs Formation, hence the upper Munyu Sandstone, together with part or all of the overlying **Murraba Formation** (the middle formation of the Redcliff Pound Group), which also includes some carbonate beds, are probable correlatives of the Bitter Springs Formation.

The Bitter Springs Formation is overlain unconformably by late Adelaidean glacial rocks (Wells and others, 1970) which may be correlatives of the **Duerdin Group** glacials of the east Kimberley and Victoria River regions (Dow & Gemuts, 1969; Sweet, 1977). No comparable glacial rocks have been found in The Granites-Tanami region, however, as the youngest Proterozoic rocks exposed here, the Redcliff Pound Group and its equivalents, are of pre-Duerdin Group age.

Possible correlatives of the Redcliff Pound Group north of The Granites-Tanami region are thick sequences of sandstone, siltstone, and shale forming the upper parts of the **Carr Boyd** and **Fitzmaurice Groups** in the east Kimberley and Victoria River regions, respectively (Dow & Gemuts, 1969; Plumb & Derrick, 1975; Sweet, 1977).

No equivalents of the Birrindudu Basin sediments appear to be present in the Tennant Creek area, although a possible correlation between the **Birrindudu** and **Tomkinson Creek Groups** cannot be completely ruled out at present: the Tomkinson Creek Group overlies the Warramunga Group unconformably, is not known to be intruded by granite, and may be younger than the 1800 m.y. tectonism that affected the Tennant Creek Block (Black, 1977).

Correlatives of Palaeozoic rocks

The Lower Cambrian Antrim Plateau Volcanics, represented mainly by basaltic lavas, extends southwards into The Granites-Tanami region from more extensive outcrops in the east Kimberley and Victoria River regions. Similar basic volcanics of probably the same age, the **Helen Springs Volcanics,** are exposed in the north of the Tennant Creek region (Bultitude, 1976). The volcanics are older than the oldest rocks exposed in the Canning Basin to the west and Wiso Basin to the east, and there are no volcanic equivalents in the Amadeus Basin.

The other Palaeozoic units in The Granites-Tanami region are the unfossiliferous, non-marine, sedimentary rocks of the **Lucas Formation, Pedestal Beds,** and **Chuall Beds.** These are tentatively regarded as correlatives of the lithologically similar, non-marine, **Pertnjara Group** of the Amadeus Basin (Wells and others, 1970), which is Devonian (Playford, Jones & Kemp, 1976). The basal unit of this group is the **Parke Siltstone** which, like the Lucas Formation, is considered to be lacustrine. Previously, Casey & Wells (1964) had suggested, on the basis of lithology, airphoto-pattern, and structure, that the Lucas Formation was possibly a correlative of the Permian Noonkanbah Formation of the Canning Basin succession; however, this correlation is considered unlikely as the Noonkanbah Formation is a fossiliferous marine unit. A possible Canning Basin equivalent of both the Pedestal Beds, which overlie the Lucas Formation, and the Chuall Beds is the non-marine **Knobby Sandstone,** a Devonian unit which unconformably overlies Birrindudu Basin sediments in the northwest (Blake and others, 1977). Some probable equivalents of the Pedestal Beds are present to the south of the region, in the Webb 1:250 000 Sheet area; these are the lithologically similar **Angas Hills Beds,** which unconformably overlie Arunta Block and Amadeus Basin rocks (Blake, 1977).

Conclusions

The following implications can be drawn from the interregional correlations.

1. During the Lower Proterozoic, sometime between 1960 m.y. and 2200 m.y., when the sedimentary rocks of the Tanami Complex were laid down within The Granites-Tanami Block, sediments of similar lithology were being deposited in the Kimberley region, in the Arunta Block, and perhaps also in the Tennant Creek

Block. Evidently greywacke-type sediments were deposited over a very wide area at this time, covering much of present-day central and northern Australia. The greywacke sedimentation was accompanied by local basic and acid volcanism.

2. The Lower Proterozoic Tanami Complex and its correlatives were intruded by granites and subjected to regional metamorphisms at various times in the different areas.

3. Correlatives of the Carpentarian Birrindudu Group were probably deposited to the north and possibly to the east of The Granites-Tanami region, but not, apparently, within the Arunta Block to the south.

4. The Birrindudu Group and Adelaidean Redcliff Pound Group were separated by a time interval of about 600 m.y.

5. The correlation of the Redcliff Pound Group with the Heavitree Quartzite and Bitter Springs Formation indicates that during the deposition of these units the Birrindudu and Amadeus Basins were interconnected.

6. Early in the Cambrian much of northern Australia, including the northern part of The Granites-Tanami region, was overlain by basaltic lavas.

7. Unfossiliferous non-marine Palaeozoic sediments within The Granites-Tanami region may be Devonian, similar in age to the Pertnjara Group of the Amadeus Basin.

Acknowledgements

I am grateful to I. M. Hodgson, B. S. Oversby, K. A. Plumb, and A. J. Stewart for their critical comments on the manuscript. The text figures were drawn by Gwen Bates and Andrew Retter.

References

ARMSTRONG, R. L., & STEWART, A. J., 1975—Rubidium-strontium dates and extraneous argon in the Arltunga Nappe Complex, Northern Territory. *Journal of the Geological Society of Australia* **22**, 103-15.

BLACK, L. P., 1977—A Rb-Sr geochronological study in the Proterozoic Tennant Creek Block, central Australia. *BMR Journal of Australian Geology & Geophysics*, **2**, 111-22.

BLAKE, D. H., 1975—Birrindudu, N.T.—1:250 000 Geological Series. *Bureau of Mineral Resources, Australia—Explanatory Notes* **SE/52-11**.

BLAKE, D. H., 1977—Webb, Western Australia—1:250 000 Geological Series. *Bureau of Mineral Resources, Australia—Explanatory Notes* **SF/52-10**.

BLAKE, D. H., & HODGSON, I. M., 1975—Precambrian Granites-Tanami Block and Birrindudu Basin—Geology and mineralization. *In* KNIGHT, C. L. (Editor), ECONOMIC GEOLOGY OF AUSTRALIA AND PAPUA NEW GUINEA: I. METALS. *Australasian Institute of Mining and Metallurgy—Monograph Series* **5**, 417-20.

BLAKE, D. H., HODGSON, I. M., & MUHLING, P. C., in prep. —Geology of The Granites-Tanami region, Northern Territory and Western Australia. *Bureau of Mineral Resources, Australia—Bulletin* **197**.

BLAKE, D. H., HODGSON, I. M., & SMITH, P. A., 1975—Geology of the Birrindudu and Tanami 1:250 000 Sheet areas, Northern Territory. *Bureau of Mineral Resources, Australia—Report* **174**.

BLAKE, D. H., PASSMORE, V. L., & MUHLING, P. C., 1977—Billiluna, W.A.—1:250 000 Geological Series. Second edition. *Bureau of Mineral Resources, Australia—Explanatory Notes* **SE/52-14**.

BLAKE, D. H., & YEATES, A. N., 1977—Stansmore, Western Australia—1:250 000 Geological Series. Second edition. *Bureau of Mineral Resources, Australia—Explanatory Notes* **SF/52-6**.

BULTITUDE, R. J., 1976—Flood basalts of probably early Cambrian age in northern Australia. *In* JOHNSON, R. W. (Editor), VOLCANISM IN AUSTRALASIA, *Elsevier, Amsterdam*, 1-20.

CASEY, J. N., & WELLS, A. T., 1964—The Geology of the north-east Canning Basin, Western Australia. *Bureau of Mineral Resources, Australia—Report* **49**.

CROWE, R. W. A., & MUHLING, P. C., in press—Lucas, W.A.—1:250 000 Geological Series. Second edition. *Bureau of Mineral Resources, Australia—Explanatory Notes* **SF/52-2**.

DOW, D. B., & GEMUTS, I., 1969—Geology of the Kimberley region, Western Australia: the east Kimberley. *Bureau of Mineral Resources, Australia, Bulletin* **106**.

DUNN, P. R., PLUMB, K. A., & ROBERTS, H. G., 1966—A proposal for time-stratigraphic subdivision of the Australian Precambrian. *Journal of the Geological Society of Australia*, **13**, 593-608.

FORMAN, D. J., & SHAW, R. D., 1973—Deformation of the crust and mantle in central Australia. *Bureau of Mineral Resources, Australia, Bulletin* **144**.

GELLATLY, D. C., 1971—Possible Archaean rocks of the Kimberley region, Western Australia. *Geological Society of Australia, Special Publication* **3**, 93-101.

GEOLOGICAL SOCIETY OF AUSTRALIA, 1971—Tectonic map of Australia and New Guinea 1:5 000 000. *Geological Society of Australia, Sydney.*

HALL, G., 1953—The Granites goldfield. *In* EDWARDS, A. B. (Editor), GEOLOGY OF AUSTRALIAN ORE DEPOSITS (1st Edition). *Australasian Institute of Mining and Metallurgy, Melbourne*, **1**, 317-21.

HODGSON, I. M., 1975—Tanami, N.T.—1:250 000 Geological Series. *Bureau of Mineral Resources, Australia—Explanatory Notes* **SE/52-15**.

HODGSON, I. M., 1976—The Granites, N.T.—1:250 000 Geological Series. *Bureau of Mineral Resources, Australia—Explanatory Notes* **SF/52-3**.

HODGSON, I. M., 1977—Highlands Rocks, N.T.—1:250 000 Geological Series. *Bureau of Mineral Resources, Australia —Explanatory Notes* **SF/52-7**.

HOSSFELD, P. S., 1940—The gold deposits of the Granites-Tanami district, central Australia. *Aerial Geological and Geophysical Survey of North Australia—Northern Territory Report* **43**.

MARJORIBANKS, R. W., & BLACK, L. P., 1974—Geology and geochronology of the Arunta Complex, north of Ormiston Gorge, central Australia. *Journal of the Geological Society of Australia*, **21**, 291-9.

MITCHELL, J., 1976—Precambrian geology of the Westmoreland region, Northern Territory, Part III: Cliffdale Volcanics. *Bureau of Mineral Resources, Australia, Record,*. **1976/34** (unpublished).

PAGE, R. W., 1976—Reinterpretation of isotopic ages from the Halls Creek Mobile Zone, northwestern Australia. *BMR Journal of Australian Geology and Geophysics*, **1**, 79-81.

PAGE, R. W., BLAKE, D. H., & MAHON, M. W., 1976—Geochronology and related aspects of acid volcanics, associated granites, and other Proterozoic rocks in The Granites-Tanami region, northwestern Australia. *BMR Journal of Australian Geology and Geophysics*, **1**, 1-13.

PETTIJOHN, F. J., POTTER, P. E., & SIEVER, R., 1972—SAND AND SANDSTONE. Springer-Verlag, Berlin.

PLAYFORD, G., JONES, B. G., & KEMP, E. M., 1976—Palynological evidence for the age of the synorogenic Brewer Conglomerate, Amadeus Basin, central Australia. *Alcheringa*, **1**, 235-43.

PLUMB, K. A., & DERRICK, G. M., 1975—Geology of the Proterozoic rocks of the Kimberley to Mount Isa region. *In* KNIGHT, C .L. (Editor), ECONOMIC GEOLOGY OF AUSTRALIA AND PAPUA NEW GUINEA: I. METALS. *Australasian Institute of Mining and Metallurgy—Monograph Series* **5**, 217-52.

PLUMB, K. A., & GEMUTS, I., 1976—Precambrian geology of the Kimberley region, Western Australia. *25th International Geological Congress—Guidebook, Excursion* **44C**.

PLUMB, K. A., & SWEET, I. P., 1974—Regional significance of recent correlations across the Murphy Tectonic Ridge, Westmoreland area. *In* Recent technical and social advances in the north Australian minerals industry, 199-206. *Australasian Institute of Mining and Metallurgy, North West Queensland Branch.*

SHAW, R. D., & STEWART, A. J., 1975—Arunta Block—regional geology. *In* KNIGHT, C. L. (Editor), ECONOMIC GEOLOGY OF AUSTRALIA AND PAPUA NEW GUINEA: I. METALS. *Australasian Institute of Mining and Metallurgy —Monograph Series 5*, 437-42.

STEWART, A. J., 1971—Potassium-argon dates from the Arltunga Nappe Complex, Northern Territory. *Journal of the Geological Society of Australia,* **17**, 205-11.

STEWART, A. J., & WARREN, R. G., 1977—The mineral potential of the Arunta Block, central Australia. *BMR Journal of Geology & Geophysics,* **2**, 21-34.

SWEET, I. P., 1977—The Precambrian geology of the Victoria River region, Northern Territory. *Bureau of Mineral Resources, Australia, Bulletin* **168**.

SWEET, I. P., MENDUM, J. R., BULTITUDE, R. J., & MORGAN, C. M., 1974—The geology of the southern Victoria River region, Northern Territory. *Bureau of Mineral Resources, Australia, Report* **167**.

VEEVERS, J. J., & WELLS, A. T., 1961—The geology of the Canning Basin, Western Australia. *Bureau of Mineral Resources, Australia, Bulletin* **60**.

WELLS, A. T., 1976—Geology of the Late Proterozoic-Palaeozoic Amadeus Basin. *25th International Geological Congress—Guidebook, Excursion* **48A**.

WELLS, A. T., FORMAN, D. J., RANFORD, L. C., & COOK, P. J., 1970—Geology of the Amadeus Basin, central Australia. *Bureau of Mineral Resources, Australia, Bulletin* **100**.

Lithological correlations of Adelaidean glaciogenic rocks in parts of the Amadeus, Ngalia, and Georgina Basins

W. V. Preiss[1], M. R. Walter, R. P. Coats[1], & A. T. Wells

Adelaidean glaciogenic sediments, representing two major glaciations, are widespread in three central Australian basins. Recognition of distinguishable marker dolomites, identical to those found above lower and upper tillites in the Adelaide Geosyncline, South Australia, has led to a revision of the Adelaidean stratigraphy of the Amadeus Basin. There the earlier glaciation is represented by the Areyonga Formation. The term Areyonga Formation is here restricted to the previously unnamed lower member (diamictite, conglomerate, sandstone, siltstone, dolomite) as originally defined in the central-western sections, where it is discontinuous; and corresponds to the whole of what has been mapped as Areyonga Formation in the extreme east. In each area it is capped by a sequence of thinly laminated, dark grey dolomite and siltstone. The former upper sandstone member of the Areyonga Formation lies with inferred disconformity on various older units. It is probably a non-glacial lateral equivalent of the glaciogenic Olympic Formation (formerly Member) in the east, which records the younger of the two glaciations. The Olympic Formation is overlain by a typical upper marker dolomite, which is pink to buff-coloured, laminated and flaggy.

A thin lower tillite, with typical lower marker dolomite, was recognised for the first time in the Ngalia Basin. It lies below a shale sequence beneath the upper tillite (Mount Doreen Formation), which has a typical upper marker dolomite. In the Georgina Basin, the diamictites and varved siltstones of the Field River Beds, recording the earlier glaciation, are capped by an identical lower marker dolomite. Glacials at Central Mount Stuart and at Nancy Hill are of uncertain stratigraphic position, but lithological associations suggest a comparison with the earlier of two Sturtian (lower) tillites in South Australia.

These correlations indicate remarkable persistance of certain marker lithologies, and the recurrence of extremely similar lithologic successions, across much of the late Precambrian platform. Presently available isotopic and biostratigraphic data are imprecise and subject to many doubts and qualifications, but are consistent with the view that each glaciation was approximately synchronous in the basins considered.

New nomenclature for some upper Adelaidean units in the Amadeus and Ngalia Basins is formalised in the Appendix.

Introduction

New data on the stratigraphy of the late Precambrian (Adelaidean) tillites of the Adelaide Geosyncline has prompted a reassessment of their correlatives in central Australia. Since 1964, when officers of the Geological Survey of South Australia first visited BMR field parties working in the Amadeus Basin, a dispute has existed concerning the correlation of tillites within the basin. During that field trip, R. P. Coats recognised the similarity of a marker 'cap' dolomite above the Olympic Member (upper tillite) of the Pertatataka Formation (Amadeus Basin) to the Nuccaleena Formation above the upper tillites of the Adelaide Geosyncline (Mirams and others, 1964). That observation was consistent with currently accepted correlations, but in addition Coats believed that the whole of the Areyonga Formation as originally defined in the Ellery Creek section is a correlative of the Olympic Member, and not the lower tillite as it was then interpreted by BMR geologists. During the last three years M. R. Walter has been studying the Adelaidean stratigraphy of the southern Georgina Basin, where one or more tillites also occur.

Stimulated by the work of the International Geological Correlation Programme Working Group on Upper Precambrian Correlations, a joint field trip was undertaken in July 1977, in an attempt to clarify the correlation of the glaciogenic sequences in the three Adelaidean basins of central Australia—the Amadeus, Ngalia and Georgina. The recognition during that trip of the significance of a distinctive 'cap' dolomite comparable with that at the base of the Tapley Hill Formation in the Adelaide Geosyncline has resolved correlation difficulties in the Amadeus Basin, and the discovery of the same sequence in the Ngalia Basin has revealed a previously unrecognised lower tillite in that basin. Subsequent stratigraphic drilling and detailed mapping in the southern Georgina Basin by Walter, C. J. Simpson and P. J. Kennewell led to the recognition of the same 'cap' dolomite. Field work for this project was limited to the northern Amadeus Basin, southern and southwestern Georgina Basin, and the Naburula Hills in the Ngalia Basin. Most emphasis has been placed on the Amadeus Basin in this paper; the Adelaidean stratigraphy of the other two basins is described in more detail in publications in preparation. It is now possible to suggest with increased confidence a series of lithological correlations between these basins.

Glacial sequences comparable with those described here are well known from the Adelaide Geosyncline, as is discussed below, and also on King Island (Jago, 1974, and pers. comm., 1977), in the Duchess area of northwestern Queensland (de Keyser, 1972), in the Kimberley region of northwestern Australia (Dow & Gemuts, 1969; Coats & Preiss, in prep.) and in the Officer Basin of South and Western Australia (Krieg, 1973; Lowry and others, 1972). They are extensively developed on other continents, e.g. Africa (Kröner, 1977). The worldwide synchroneity or diachroneity of these glacial events is currently a subject for vigorous research and debate. The isotopic data are still equivocal. Here we are con-

1. Geological Survey of South Australia, P.O. Box 151, Eastwood, S.A. 5063.

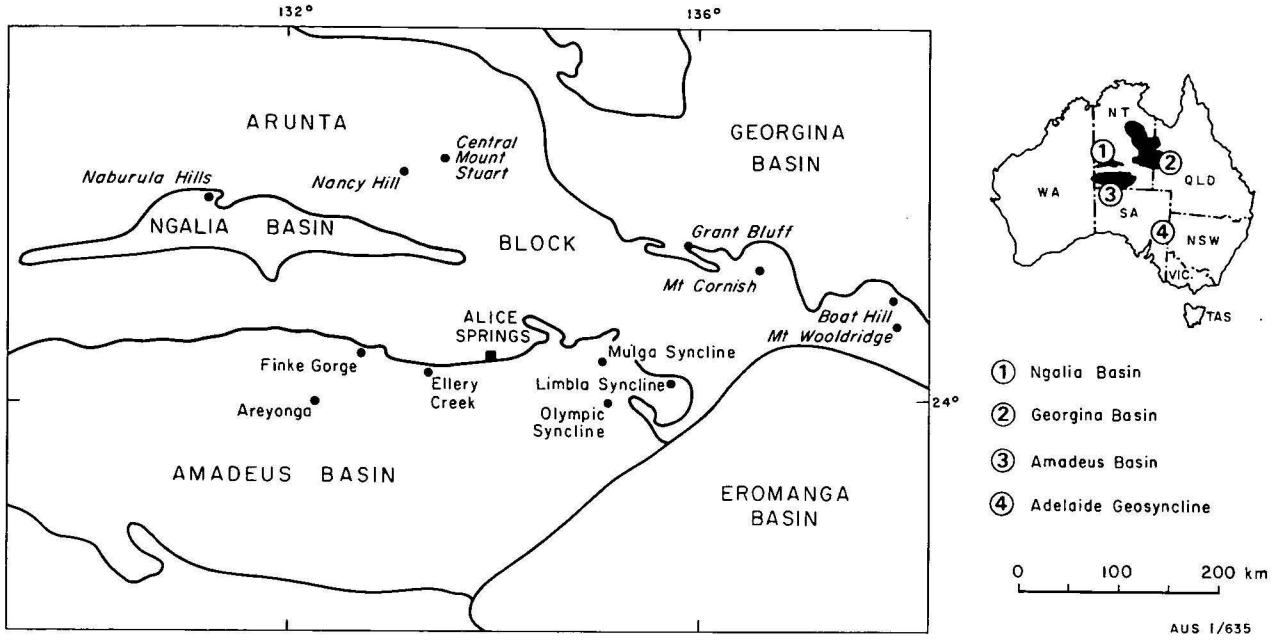

Figure 1. Locality map. Basin outlines are taken from the Tectonic Map of Australia and New Guinea, 1971.

cerned only with the lithological correlations which provide a framework for chronostratigraphic interpretations.

Stratigraphic discussion

Amadeus Basin

Wells and others (1967, 1970) have described the stratigraphy and geological history of this basin. In our study, Adelaidean sections were examined in five areas along the northern margin of the basin, particular emphasis being given to the search for marker dolomites above the tillites; the observations made are summarised in Table 1.

The key to the correlation of the tillite-bearing units lies, we believe, in the persistence of the distinctive marker dolomites. The dark, thinly laminated silty dolomite that caps the lower diamictite of the Areyonga Formation at Ellery Creek is lithologically identical to the dolomite overlying the Areyonga Formation in the Limbla Syncline. It is also identical to the dolomite at the base of the Tapley Hill Formation, capping the Sturt Tillite, in South Australia, and to a dolomite capping a newly discovered lower tillite in the Ngalia Basin (see below). This confirms the view that the diamictites and associated conglomerates and sandstones of the *lower member* of the Areyonga Formation (Prichard & Quinlan, 1962) represent an earlier glaciation. Inspection of the sections (Table 1) and the reconstructed cross-section (Fig. 4) shows that the upper sandstone member of the Areyonga Formation is persistent between Areyonga and the Mulga Syncline. In the west, the lower member was observed only in the Ellery Creek and Areyonga areas: as noted by Prichard & Quinlan (1962), it is a laterally impersistent unit, preserved only in depressions in the pre-Areyonga erosion surface. The upper member in other places transgresses over it on to the underlying Bitter Springs Formation. In the most easterly sections, only the diamictite member of the Areyonga Formation is present. It is suggested that the base of the upper sandstone member is a disconformity which has cut down to various levels in the underlying units (the lower marker cap dolomite at Ellery Creek, the lower diamictite member at Areyonga, and the Bitter Springs Formation at the Finke River and in the Mulga Syncline). In view of this probable break *within* the Areyonga Formation as presently defined, it is redefined in the Appendix to restrict the name to the lower diamictite member.

The stratigraphic position of the upper sandstone member remains uncertain. A major facies change occurs between the Mulga Syncline and the Limbla Syncline (Figs. 3, 4); the sandstone has no lithological equivalent in the east. Instead the Areyonga Formation (which we believe is here equivalent *in toto* to the western lower member) is overlain by a sequence that commences with the lower marker cap dolomite and passes up into a sequence of fine clastics, carbonates, sandstones, and finally an upper glacial horizon. The latter red diamictite of the Olympic Member shows close similarity to the Marinoan tillite of the Elatina Formation of South Australia, and both are capped by identical pink dolomites (Nuccaleena Formation in South Australia), here referred to as the upper marker cap dolomite. Wells (1969) suggested that the Olympic Member is disconformable on the underlying Limbla Member, since clasts of the latter are found reworked in it. We propose that the Olympic Member be raised to formation status.

In the more westerly sections, the clastic sequence above the Areyonga Formation has been defined as the Pertatataka Formation (Prichard & Quinlan, 1962). The only member that has been previously differentiated in the central-western region is the Julie Member. In our opinion, as this member is extremely persistent throughout the basin, it should be regarded as a formation. We here distinguish three other members: a lower member I of red, green and grey siltstone, shale and fine sandstone, a middle member II of white quartzite with clay galls and an upper member III of red and green shale, siltstone and sandstone. A thin, weathered pink dolomite at the base of member I at Areyonga is a possible correlative of the upper marker cap dolomite. Member II is a likely facies variant of the Cyclops Member defined in the east, and the Waldo Pedlar Member

Areyonga-Katapata Gap

LATE ADELAIDEAN

Pertatataka Formation

Julie Member

Dolomite, pale grey, flaggy, laminated

unnamed member III

Siltstone, red, finely micaceous, platy; bands fine-grained sandstone

unnamed member II

Sandstone, white, coarse-grained, cross-bedded, with clay galls

unnamed member I

Sandstone, dark red, fine-grained, with load structures; siltstone, green, red, shaly, micaceous; interbeds fine sandstone, sole marks, ripple marks. At Areyonga: thin pink dolomite at base

Areyonga Formation

upper sandstone member

Sandstone, white to pale grey, medium to coarse, cross-bedded, with pebble trains; red siltstone; pale brown sandstone, medium-grained, feldspathic

lower diamictite member

Diamictite, massive green-grey, silty mudstone matrix, clasts red, white quartzites, Bitter Springs and basement lithologies

——— disconformity ———

EARLY ADELAIDEAN

Bitter Springs Formation

Dolomite, gritty, and siltstone, red and green, shaly. Dolomite, pale grey with pale chert, sandstone interbeds

Finke River

LATE ADELAIDEAN

Pertatataka Formation

Julie Member

Dolomite, buff, flaggy to blocky, pale grey chert; interbeds coarse feldspathic sandstone, red siltstone

unnamed member III

Siltstone, shale, red, green & grey, micaceous; interbeds coarse sandstone, granule-bearing red siltstone

unnamed member II

Sandstone, white, siliceous, fine to medium, cross-bedded, with clay galls

unnamed member I

Siltstone, green, red; shale, laminated, dark grey; siltstone, shale, dark green, red, finely micaceous

Areyonga Formation

upper sandstone member

Sandstone, white, medium to coarse, feldspathic, cross-bedded

——— disconformity ———

EARLY ADELAIDEAN

Bitter Springs Formation

Dolomite, pale grey, blocky, cryptalgal lamination, white chert

Ellery Creek

LATE ADELAIDEAN

Pertatataka Formation

Julie Member

Dolomite, pale grey, thick-bedded, part laminated

members not recognised

Siltstone, red, with granules

Quartzite, grey, medium grained

Siltstone, shale, dark red and green, flaser bedding, small scale cross-lamination

Areyonga Formation

upper sandstone member

Dolomite, pink, massive, with small stromatolite bioherms, sandy at base

Sandstone, pale grey, medium grained, cross-bedded (10-20 cm sets), siliceous; clay galls

Sandstone, white, feldspathic, medium to coarse-grained, cross-bedded

lower marker cap dolomite

Dolomite, dark grey, silty, very thinly, evenly laminated, as lenses in dark grey silty shale, very thinly laminated

lower diamictite member

Diamictite, massive, with green silty mudstone matrix; interbeds fine-grained green sandstone, dolomitic arkose, conglomerate, pale brown-weathering dolomite

——— disconformity ———

EARLY ADELAIDEAN

Bitter Springs Formation

Dolomite, pale grey, cherty

Mulga Syncline

LATE ADELAIDEAN

Pertatataka Formation

Julie Member

Dolomite, limestone, oolitic, laminated, dolomitic fine-grained sandstone

unnamed member III

Siltstone, olive green, poorly bedded and shaly. 50 cm dark brown dolomite

Cyclops Member

Sandstone, fine-grained, pale grey and greenish, platy, very thinly, evenly bedded

unnamed member I

Shale, dark red, pale green

Areyonga Formation

upper sandstone member

Sandstone, white, feldspathic, coarse-grained, with quartz and feldspar pebble trains; minor pale green shale

——— disconformity ———

EARLY ADELAIDEAN

Bitter Springs Formation

Siltstone, dark green, platy; dolomite, dark pink and brownish grey, laminated

Limbla-Olympic Synclines

LATE ADELAIDEAN

Pertatataka Formation

Julie Member

(Not examined in this study)

Waldo Pedlar Member

Sandstone, pale brown, very thinly bedded, laminated

Sandstone, fine-grained, grey-green platy to blocky, with current lineation, ripple marks, micaceous in lower part

Interval no outcrop

upper marker cap dolomite

Dolomite, pink-buff, cream weathering, flaggy, laminations 1-2 mm thick

Olympic Member

Arkose, pale brown, fine-grained

Dolomite, pale brown and dark grey, gritty

Diamictite, dark red-brown silty matrix, massive. Clasts red and white quartzites, porphyry, amygdaloidal volcanics, basement and Bitter Springs lithologies

Arkose, pale grey, pebbly; polymict conglomerate; red micaceous siltstone, pale grey-green siltstone, sandstone

Limbla Member

Sandstone, pale brown, fine-grained, festoon cross-bedded

Limestone, pale grey, gritty, oolitic, cross-bedded

Interval no outcrop. (Siltstone observed by Wells *et al.*, 1967)

Ringwood Member

Dolomite, limestone, greenish and brownish weathering; stromatolite bioherms; interbedded green siltstones near base

unnamed siltstone member

Siltstone, grey-green, calcareous, flaggy; platy green shale; dark grey dolomite bands in upper part

lower marker cap dolomite

Dolomite, dark grey, olive-green weathering, very thinly laminated, as lenses in greenish weathered platy shale

Areyonga Formation

Diamictite, massive olive-green silty matrix; clasts volcanics, red quartzites, granites, Bitter Springs lithologies; fine-grained greenish sandstone; conglomerate; medium-grained arkose dolomitic diamictite

——— disconformity ———

EARLY ADELAIDEAN

Bitter Springs Formation

Sandstone, red, with shaly partings, salt casts

Sandstone, massive, white, coarse, cross-bedded

Siltstone, red; fine sandstone

Dolomite, silicified; basic volcanics

Table 1. Stratigraphic sections across the Northern Amadeus Basin (using previously accepted formal nomenclature)

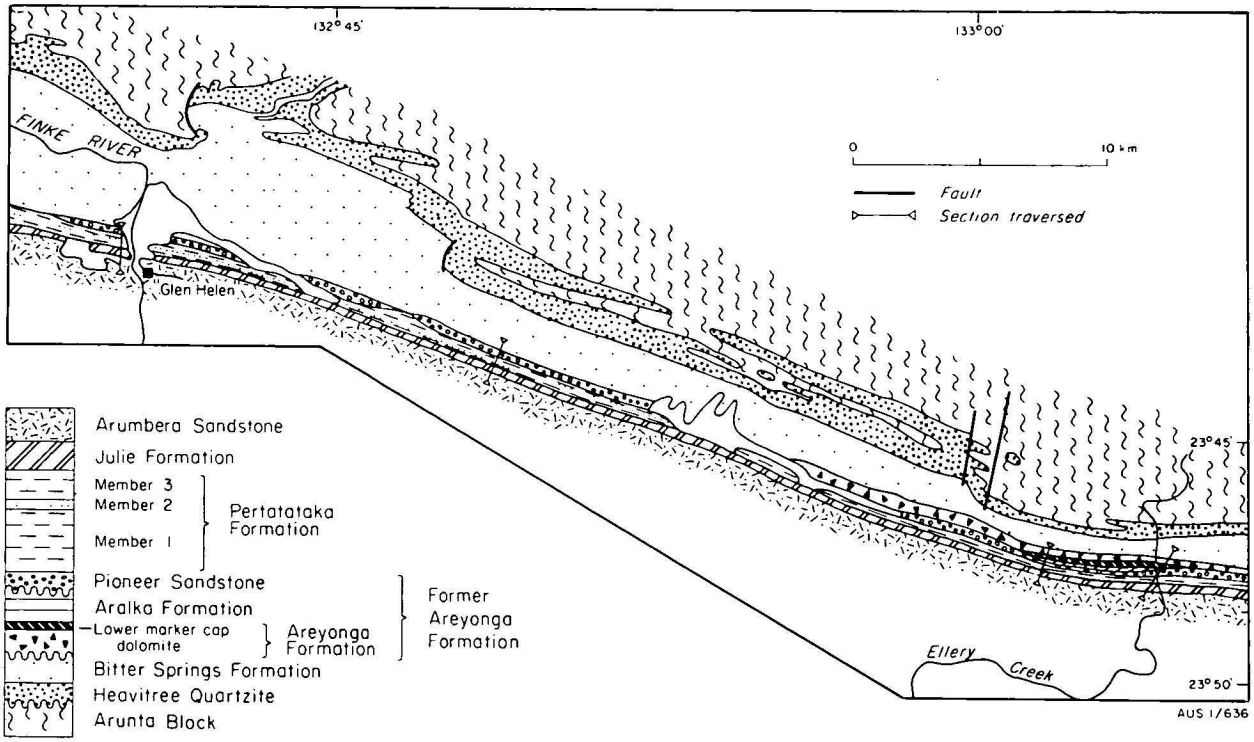

Figure 2. Simplified geological locality map, Finke River to Ellery Creek, Amadeus Basin. Modified from Quinlan & Forman (1968). The Areyonga Formation as redefined in this paper is restricted to the Ellery Creek area; elsewhere the newly defined Pioneer Sandstone rests on the Bitter Springs Formation.

may also be in part equivalent. The upper Waldo Pedlar Member is here considered to be a lithological correlative of the Cyclops Member.

Although it cannot be proved, the upper sandstone member of the Areyonga Formation as previously defined may be a facies variant of the tillitic Olympic Formation, in a manner analogous to the relationship between the Elatina Formation sandstones in the west and the Marinoan tillites in the east in the Adelaide Geosyncline. Equivalence of the thin dolomite at the base of member I at Areyonga with the upper marker cap dolomite would support this view. The pink dolomite at Ellery Creek, above the sandstone member, differs in being more massive, sandy at its base, and in containing stromatolites and red cherts; it may be a lateral variant of the upper marker cap dolomite, although this is not certain.

We propose that the upper sandstone member of the former Areyonga Formation be redefined as a new formation, the Pioneer Sandstone (see Appendix). The inclusion of a more silicified sandstone with clay galls in the top of the Pioneer Sandstone is supported by photo-interpretation; the lithologically similar quartzitic Member II of the Pertatataka Formation seen at Finke River and Areyonga (Table 1) appears to lens out between Finke River and Ellery Creek. It follows from this that the term Pertatataka Formation, defined as the sequence overlying the Pioneer Sandstone (and now excluding the Julie Formation) should be restricted in the eastern sections to the sequence above the upper glacials (Olympic Formation). A new name is then required for the interval between the Areyonga and Olympic Formations—the Aralka Formation (see Appendix). The Limbla and Ringwood Members then become part of the Aralka Formation. Table 2 summarises the new stratigraphic nomenclature and correlations and the cross-section (Fig. 4) illustrates rock relationships across the northern Amadeus Basin.

Ngalia Basin

Wells (1972) has described the stratigraphy and geological history of this region. The base of the Adelaidean succession in the Ngalia Basin is marked by the extensive Vaughan Springs Quartzite, correlated with the Heavitree Quartzite of the Amadeus Basin. In the Naburula Hills area (Fig. 5) the quartzite has been completely eroded, and the granitic basement is directly overlain unconformably by a partly glacial sequence, the Mount Doreen Formation (Wells, 1972). As defined, this formation includes a tillite capped by a pink dolomite and red shale. Wells (1972) correlated the tillite with the upper glacials of the Olympic Member (Formation) in the Amadeus Basin, a correlation with which we concur. However, green shales underlying the tillite were also included in the same formation. We restrict the term Mount Doreen Formation to the upper glacial sediments (diamictite, minor conglomerate, dolomite, red shale) and define new formations for the underlying units.

A brief traverse through these underlying beds at the type section revealed a previously unrecognised basal diamictite (2 m thick) with a green silty matrix, resting unconformably on granite. This diamictite is overlain by a typical lower marker cap dolomite, and is readily correlated with the Areyonga Formation of the Amadeus Basin. The green shale and siltstone (carbonaceous near the base) between this Areyonga equivalent and the tillite of the Mount Doreen Formation would then correlate with the Aralka Formation (see Appendix) in the eastern Amadeus Basin (Table 2). The new name Rinkabeena Shale is proposed for this unit (see Appendix). The contact between the upper

WEST-CENTRAL AMADEUS BASIN	EASTERN AMADEUS BASIN	NORTHERN NGALIA BASIN	ADELAIDE GEOSYNCLINE
Julie Formation	Julie Formation		Wonoka Formation
Pertatataka Formation Member III Member II	Pertatataka Formation Member III Cyclops Member, Waldo Pedlar Member	hiatus	Bunyeroo Formation ABC Range Quartzite
Member I	Member I	Mount Doreen Formation red shale member	Brachina Formation
local dolomite	upper marker cap* dolomite	upper marker cap* dolomite member	Nuccaleena Formation
Pioneer Sandstone	Olympic Formation	diamictite member	Elatina Formation
— inferred disconformity —	——— disconformity ———	— inferred disconformity —	—— local disconformity ——
hiatus	Aralka Formation Limbla Member unnamed siltstone Ringwood Member	hiatus	Trezona Formation Enorama Shale Etina Formation
	unnamed siltstone	Rinkabeena Shale	Tapley Hill Formation
lower marker cap* dolomite	lower marker cap* dolomite	lower marker cap* dolomite	lower marker cap dolomite
Areyonga Formation	Areyonga Formation	Naburula Formation	Sturt tillite and equivalents
——— disconformity ———	——— disconformity ———	——— non-conformity ———	——— disconformity ———
hiatus	hiatus	hiatus	Yudnamutana Subgroup, Pualco Tillite, ironstones ——— disconformity ———
Bitter Springs Formation	Bitter Springs Formation		Burra Group

* Coats and Preiss express the alternative view that the cap dolomites should not be included with the underlying tillites. In each basin, they are clearly post-glacial; they overlie the tillites with sharp contacts and they grade up into or are interbedded in the overlying shale/siltstone sequences.

Table 2. Revised nomenclature and correlation table.

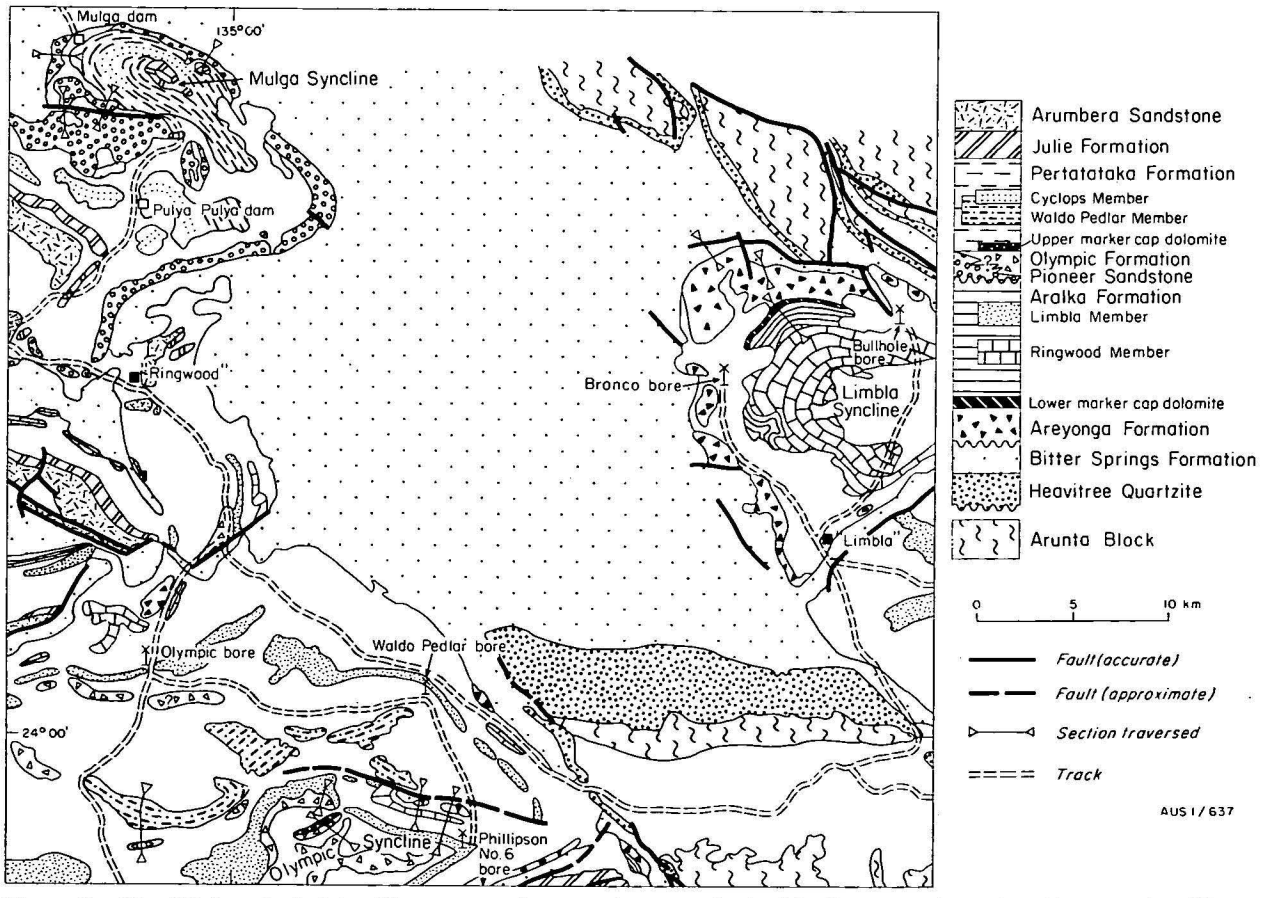

Figure 3. Simplified geological locality map, northeastern Amadeus Basin. Modified from Shaw (1968), Shaw & Milligan (1969), Cook (1969), and Wells (1969). The newly defined Pioneer Sandstone and Aralka Formation are present in this area. Major facies changes occur between the Pioneer Sandstone in the Mulga Syncline and the Olympic Formation in the Olympic Syncline.

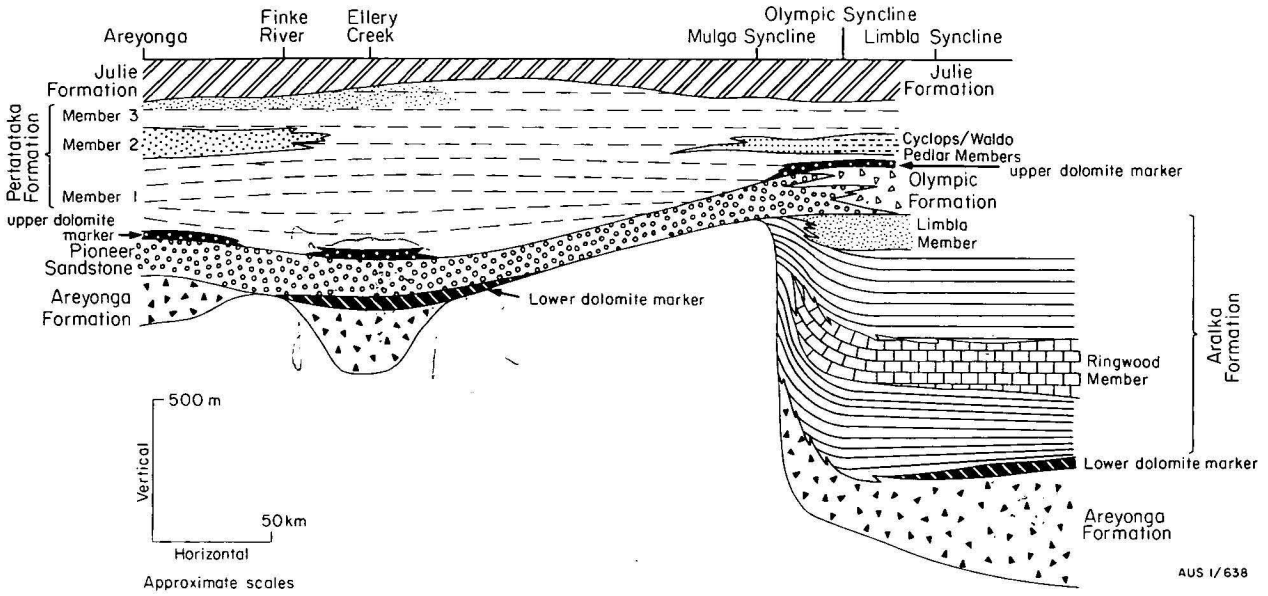

Figure 4. Stratigraphic relationships, northern Amadeus Basin. The Bitter Springs Formation forms the basement to the units depicted. The lithological symbols are as used on Figures 2 and 3. Thicknesses are taken from published sources.

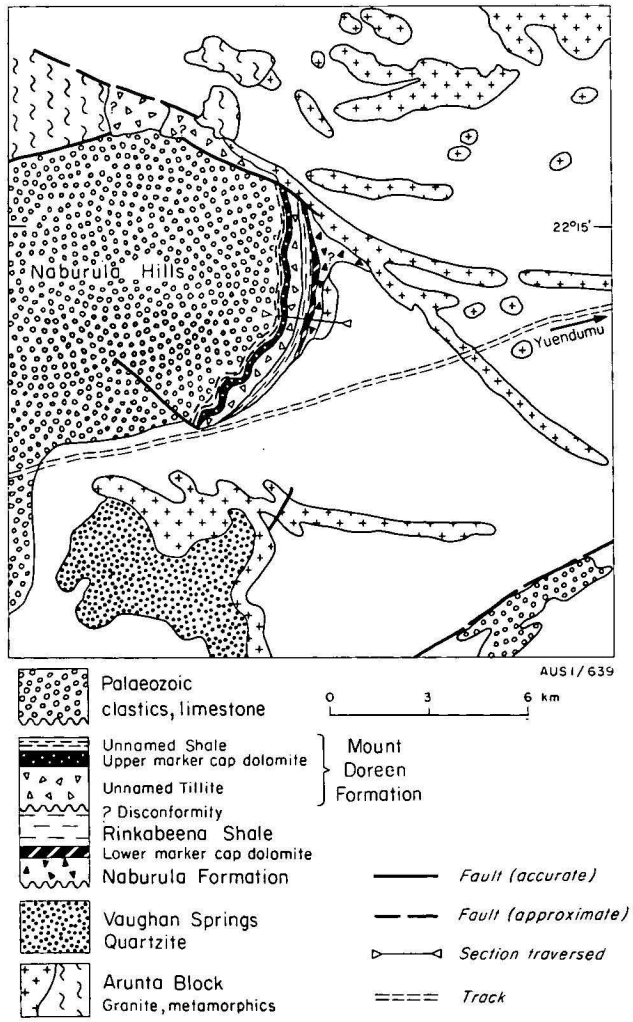

Figure 5. Simplified geological locality map, northern Ngalia Basin. Modified from the Mount Doreen 1:250 000 Sheet (Wells, 1972). The Rinkabeena Shale and Naburula Formation are defined in this paper.

diamictite and the underlying green shale is sharp, and since no equivalents of the Ringwood and Limbla Members are present, is probably disconformable. The new name Naburula Formation is proposed for the lower diamictite and overlying cap dolomite in this area (see Appendix). The red shale at the top of the Mount Doreen Formation is unconformably overlain by the Ordovician Djagamara Formation (Wells, 1972). Table 2 summarises the correlations between the Amadeus and Ngalia Basins.

Georgina Basin

A thick sequence of Adelaidean to Early Cambrian sediments is poorly exposed in the southern Georgina Basin in the Tobermory, Hay River and Mt Whelan 1:250 000 Sheet areas. As a result of recent work in this area the Field River Beds (Smith, 1963a), overlain by the Grant Bluff Formation, can be subdivided into six formations:

6. Pebbly pale grey and medium brown arkose— 150 m
5. Yellow-brown stromatolitic dolomite— 90 m
4. Interbedded red-brown siltstone, shale and dolomite.
3. Red-brown arkose, siltstone and shale.

— disconformity —

2. Diamictite and olive-grey siltstone (1500 m), locally overlain by grey siltstone and shale with thin beds of grey dolomite (less than 100 m).
1. Arkose and stromatolitic dolomite (both are absent locally).

— non-conformity —

granite, gneiss, schist

The dolomite and shale cap at the top of unit 2 has been observed at two localities (7 km SE of Mount Wooldridge, Hay River 1:250 000 Sheet area and Boat Hill, 6 km ESE of Christmas Creek Bore, Tobermory 1:250 000 Sheet area). Elsewhere, unit 3 lies directly on diamictite (e.g. 2 km WSW of Black Stump Dam in Hay River drill hole no. 7). Units 2 and 3 appear to be structurally conformable at all localities except Boat Hill, where there may be an angular uncon-

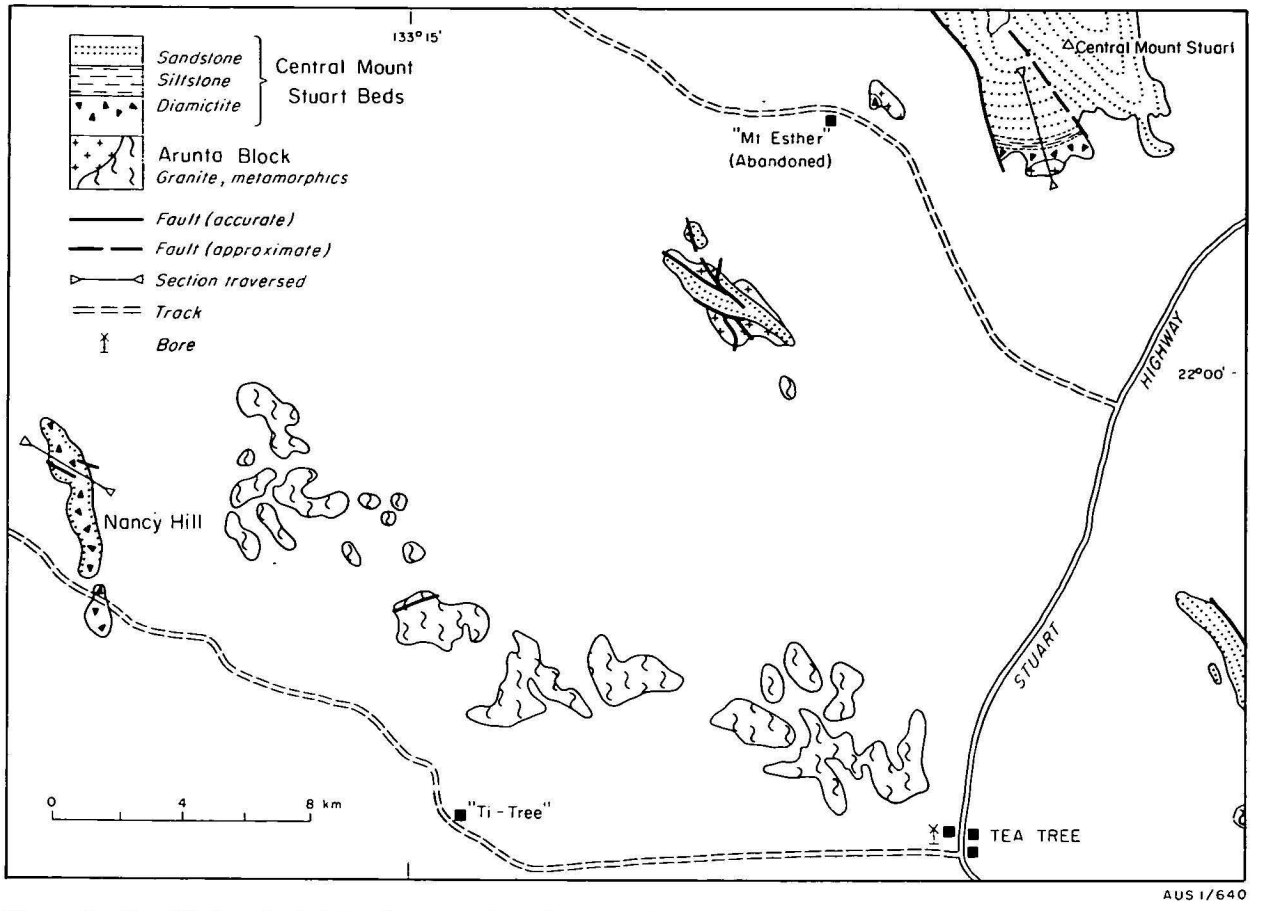

Figure 6. Simplified geological locality map, Central Mount Stuart area. Modified from Offe & Stewart (1974), and Evans (1972).

formity, although that is not clear due to the small extent of the exposure. Because of the local absence of the cap sequence, this contact is interpreted as a disconformity. Hay River no. 7 penetrated a possible fossil weathering horizon at the top of unit 2.

At Mount Cornish in the southwestern Georgina Basin, the presently defined Mount Cornish Formation (Smith, 1963b), resting unconformably on granitic basement of the Arunta Block, contains a basal arkosic grit and dolomite member, overlain by glaciogene sediments. The latter contain no carbonate interbeds, and we therefore suggest that the dolomitic sequence is unrelated to the glacials and that it should be separated from the Mount Cornish Formation. In view of some lithologic similarity (pale and dark grey cryptalgal laminated dolomites with cherty blebs) we suggest that it may be a correlative of the Bitter Springs Formation of the Amadeus Basin. The Mount Cornish Formation (in its restricted sense) consists of cyclic alternations of green, well-laminated siltstones and diamictites with a massive, green, silty matrix and abundant pebbles to boulders of quartzite, granite and gneiss. The siltstones have extremely uniform, even, graded, fine sandy laminations 1-3 mm thick, alternating with fine silt laminations, and are interpreted as varves. The glacial sequence is at least 1800 m thick in this section, and its top is not exposed.

In a section 2 km east of Grant Bluff, the Mount Cornish Formation is extremely reduced; lenticular remnants of diamictite, less than a metre thick, occur in depressions in the underlying granite basement. The diamictite is capped by a very thin dark grey laminated dolomite (possible lower marker cap dolomite). These basal beds are disconformably overlain by the massive Oorabra Arkose, which elsewhere transgresses on to the basement.

The Mount Cornish Formation of the Huckitta area and unit 2 of the Hay River area are correlated with the Areyonga Formation (*sensu stricto*) of the Amadeus Basin. The overlying arkoses and siltstones (Oorabra Arkose on Huckitta, and units 3 and 4 on Hay River) may be correlatives of the Pertatataka Formation and Pioneer Sandstone of the Amadeus Basin.

At Central Mount Stuart (Fig. 6), granitic basement is unconformably overlain by a diamictite (3.5 m thick) of the Central Mount Stuart Beds, with a dark red-brown ferruginous matrix and small pebbles and cobbles of granite. The only lithological comparison that can be made is with the ferruginous diamictites of the Holowilena Ironstone, which records an earlier Sturtian glaciation (i.e. pre-Sturt Tillite) in the Adelaide Geosyncline. The diamictite is overlain by thin, pale grey, very recrystallised limestones, and locally, by a brown, flaggy dolomite. Their contact with the diamictite is sharp and possibly partly erosional, with a few pebbles incorporated at the base. The diamictite occurs only very locally around the base of Central Mount Stuart; elsewhere the remainder of the Central Mount Stuart Beds rests directly on the basement.

A sequence unconformably overlying basement schists and identified in Evans (1972) as Central Mount Stuart Beds was examined at Nancy Hill, 34 km WSW of Central Mount Stuart. It comprises a much thicker glacial component. The basal member is a conglomerate with a quartzitic matrix and scattered, mostly rounded pebbles

of quartzite, quartz and minor shale. A cross-bedded, coarse quartzite separates this from a second pebbly horizon—a diamictite with a sandy matrix and white quartzite cobbles up to 20 cm in diameter. The diamictite is capped by white orthoquartzite. Stratigraphically higher, immediately north of Nancy Hill, two further, more convincingly tillitic diamictite horizons occur interbedded in laminated grey siltstones and orthoquartzites. The matrix of the latter diamictites contains a greater proportion of clay and resembles a greywacke, and the clasts include a greater variety of rock types, including pegmatites; some boulders are striated. Interbedded siltstones are grey, finely laminated, with slaty cleavage, and in places contain pebbles. The uppermost sandy diamictite is capped by thick-bedded medium-grained pinkish grey orthoquartzite. The predominant sandy greywacke-like matrix and close association with orthoquartzites suggests that the best lithological comparison for the Nancy Hill tillite occurrence is with the earlier Sturtian tillites of South Australia (Pualco Tillite and Yudnamutana Subgroup).

Synthesis and comparison with other basins

Lithological comparison of tillite-bearing sequences in central Australian basins with late Adelaidean sections in the Adelaide Geosyncline, South Australia, indicates remarkable persistence of certain marker lithologies, and the recurrence of extremely similar lithologic successions across much of the late Precambrian platform. We suggest that these features indicate considerable interconnection between these basins (later disrupted by Palaeozoic tectonism), and that precise lithological correlations can be made between the basins. The Adelaide Geosyncline contains by far the thickest, and possibly the most complete record of Adelaidean sedimentation.

Of particular significance are the thin carbonate markers that cap glacial horizons in all the basins. The very thinly, evenly laminated dark grey silty dolomites intercalated in thinly laminated dark grey shales (lower marker cap dolomite) were first recognised capping the Sturt Tillite and its equivalents (Appila Tillite, Wilyerpa Formation and other unnamed tillites) in the Adelaide Geosyncline, where they mark the base of the Tapley Hill Formation. Identical dolomites have now been recognised in the Amadeus, Ngalia, and southern Georgina Basins, in each case capping a lower (Sturtian) tillite. Upper (Marinoan) tillites are also widespread, occurring in the Adelaide Geosyncline, eastern Amadeus Basin and Ngalia Basin. In each case they are capped by identical laminated, pink flaggy dolomites that grade into overlying shale-siltstone sequences.

Certain lithologic features of the tillites themselves also appear to be distinctive. A red, silty matrix is common though not exclusive in the Marinoan tillites. The equivalents of the Sturt Tillite tend to have an olive-green silty mudstone matrix, and are commonly associated with green laminated siltstones. The earlier Sturtian glacials of South Australia characteristically have a greywacke-like matrix, and are associated with orthoquartzites and with iron formations; the latter have not been found associated with younger tillites. The stratigraphic position of ironstones in the deposits of an earlier of two Sturtian glacial phases and overlain unconformably by tillites of the later phase finds a striking parallel outside Australia in the Rapitan Group of northwestern Canada (Young, 1976, p. 139).

Independent chronostratigraphic data relevant to the debate about the synchroneity of the glacial events are very limited. The whole of the Adelaidean succession in the Amadeus Basin is younger than 1076 ± 50 m.y. (Marjoribanks & Black, 1974), the age of the latest recorded basement event. Other dates are subject to considerable question. The age of the Pertatataka Formation was interpreted as approximately 790 m.y. by Compston & Arriens (1968), and 730 ± 45 m.y. by Compston & Taylor (1969); these age determinations are based on samples of shales and coarser clastic sediments spanning almost the whole thickness of the Pertatataka Formation or its equivalent, and thus may not be registering a sedimentary or diagenetic age (Walter, 1972, p. 38); there is no independent evidence of a metamorphic event of this age. Compston & Arriens (1968) quoted shale age determinations for the Field River Beds of either 790 m.y. or 600 m.y. The use of stromatolites in the correlation of these late Adelaidean units is discussed by Walter (1972), and Preiss (1977). The Adelaidean in the Adelaide Geosyncline may be younger than 850 ± 50 m.y. (Preiss, 1977). The available data are consistent with the view that there may have been two glacial events that were approximately synchronous throughout southern and central Australia.

Acknowledgements

We wish to thank the Directors of our two institutions for permitting this joint study. M. R. Walter's work in the Georgina Basin is an aspect of the BMR's Georgina Basin Project. A. J. Stewart took an active part in discussions on Amadeus Basin stratigraphy, and C. J. Simpson assisted with the photo-interpretation of the Finke River-Ellery Creek area. D. J. Belford, J. H. Shergold, A. J. Stewart and G. E. Wilford critically read the manuscript of this paper and made many helpful suggestions. The figures were drawn by M. Steele and R. Bates. The paper is published with the permission of the Director of the Department of Mines, Adelaide.

References

COMPSTON, W., & ARRIENS, P. A., 1968—The Precambrian geochronology of Australia. *Canadian Journal of Earth Sciences*, **5**, 561-83.

COMPSTON, W., & TAYLOR, S. R., 1969—Rb-Sr study of impact glass and country rocks from the Henbury meteorite crater field. *Geochimica et Cosmochimica Acta*, **33**, 1037-43.

COOK, P. J., 1969—Rodinga, N.T.—1:250 000 geological series, *Bureau of Mineral Resources, Australia — Explanatory Notes*, **SG/53-2**.

DE KEYSER, F., 1972—Proterozoic tillite at Duchess, northwestern Queensland. *Bureau of Mineral Resources, Australia, Bulletin* **125**, 1-6.

DOW, D. B., & GEMUTS, I., 1969—Geology of the Kimberley Region, Western Australia: the East Kimberley. *Geological Survey of Western Australia, Bulletin* **120**.

EVANS, T. G., 1972—Napperby, N.T.—1:250 000 geological series, *Bureau of Mineral Resources, Australia—Explanatory Notes*, **SG/53-9**.

JAGO, J. B., 1974—The origin of Cottons Breccia, King Island, Tasmania. *Transactions of the Royal Society of South Australia*, **98**, 13-28.

KRIEG, G. W., 1973—Everard, S.A.—1:250 000 geological series, *Geological Survey of South Australia—Explanatory Notes*, **SG/53-13**.

KRÖNER, A., 1977—Non-synchroneity of late Precambrian glaciations in Africa. *Journal of Geology*, **85**, 289-300.

LOWRY, D. C., JACKSON, M. J., VAN DE GRAAFF, W. J. E., & KENNEWELL, P. J., 1972—Preliminary results of geological mapping in the Officer Basin, Western Australia, 1971: *Geological Survey of Western Australia, Annual Report* 1971, 50-56.

MARJORIBANKS, R. W., & BLACK, L. P., 1974—Geology and geochronology of the Arunta Complex, north of Ormiston Gorge, central Australia. Journal of the Geological Society of Australia, **21**, 291-9.

MIRAMS, R. C., COATS, R. P., & DALGARNO, C. R., 1964—Report on visit to Amadeus Basin, September, 1964. *Department of Mines, South Australian Geological Survey Report* **59/99** (unpublished).

OFFE, L. A., & STEWART, A. J., 1974—Mount Peake, N.T.—1:250 000 geological series, *Bureau of Mineral Resources, Australia* (preliminary edition), **SF/53-5**.

PREISS, W. V., 1977—The biostratigraphic potential of Precambrian stromatolites. *Precambrian Research*, **5**, 207-19.

PRITCHARD, C. E., & QUINLAND, T., 1962—The geology of the southern half of the Hermannsburg 1:250 000 sheet. *Bureau of Mineral Resources, Australia, Report* **61**.

QUINLAN, T., & FORMAN, D. J., 1968—Hermannsburg, N.T.—1:250 000 geological series, *Bureau of Mineral Resources, Australia—Explanatory Notes*, **SF/53-13**.

SHAW, R. D., 1968—Hale River, N.T.—1:250 000 geological series, *Bureau of Mineral Resources, Australia—Explanatory Notes*, **SG/53-3**.

SHAW, R. D., & MILLIGAN, E. N., 1969—Illogwa Creek, N.T.—1:250 000 geological series, *Bureau of Mineral Resources, Australia—Explanatory Notes*, **SF/53-5**.

SMITH, K. G., 1963a—Hay River, N.T.—1:250 000 geological series, *Bureau of Mineral Resources, Australia—Explanatory Notes*, **SF/53-16**.

SMITH, K. G., 1963b—Huckitta, N.T.—1:250 000 geological series, *Bureau of Mineral Resources, Australia—Explanatory Notes*, **SF/53-11**.

SMITH, K. G., 1972—Stratigraphy of the Georgina Basin. *Bureau of Mineral Resources, Australia, Bulletin* **111**.

WALTER, M. R., 1972—Stromatolites and the biostratigraphy of the Australian Precambrian and Cambrian. *Special Papers in Palaeontology*, **11**, *The Palaeontological Association, London*.

WELLS, A. T., 1969—Alice Springs, N.T.—1:250 000 geological series, *Bureau of Mineral Resources, Australia—Explanatory Notes*, **SF/53-14**.

WELLS, A. T., 1972—Mount Doreen, N.T.—1:250 000 geological series, *Bureau of Mineral Resources, Australia—Explanatory Notes*, **SF/52-12**.

WELLS, A. T., MOSS, F. J., & SABITAY, A., 1972—The Ngalia Basin Northern Territory—recent geological and geophysical information upgrades petroleum prospects. *Australian Petroleum Exploration Association Journal*, **12**, 144-51.

WELLS, A. T., STEWART, A. J., & SKWARKO, S. K., 1966—Geology of the southeastern part of the Amadeus Basin, Northern Territory. *Bureau of Mineral Resources, Australia, Report* **88**.

WELLS, A. T., RANFORD, L. C., STEWART, A. J., COOK, P. J., & SHAW, R. D., 1967—Geology of the northeastern part of the Amadeus Basin, Northern Territory. *Bureau of Mineral Resources, Australia, Report* **113**.

WELLS, A. T., FORMAN, D. J., RANFORD, L. C., & COOK, P. J., 1970—Geology of the Amadeus Basin, Central Australia. *Bureau of Mineral Resources, Australia, Bulletin* **100**.

YOUNG, G. M., 1976—Iron-formation and glaciogenic rocks of the Rapitan Group, Northwest Territories, Canada. *Precambrian Research*, **3**, 137-58.

Appendix: Stratigraphic nomenclature

JULIE FORMATION (Variation of published name)

Amadeus Basin

Proposers: W. V. Preiss, M. R. Walter, R. P. Coats, & A. T. Wells.

The Julie Member of Wells and others (1967) is upgraded to formation status because of its wide distribution and usefulness as a mappable unit. It is comparable in these criteria with other formations in the Amadeus Basin.

PERTATATAKA FORMATION (redefinition of unit)

Amadeus Basin

Proposers: W. V. Preiss, M. R. Walter, R. P. Coats, & A. T. Wells.

The Pertatataka Formation of Prichard & Quinlan (1962) is redefined because the original definition has not been followed by subsequent authors (apparently unknowingly). To revert to the original definition would cause considerable confusion. The type section as originally designated (5 km west of Ellery Creek) is retained.

The top of the Pertatataka Formation is taken as the base of the Julie Formation (former Julie Member), i.e. at the incoming of the first carbonate. The base of the Formation is put at the top of the Pioneer Sandstone. The Formation is predominantly red and green siltstone, shale, and felspathic sandstone.

OLYMPIC FORMATION (Variation of name)

Amadeus Basin

Proposers: W. V. Preiss, M. R. Walter, R. P. Coats, & A. T. Wells.

The Olympic Member of Wells and others (1967) is upgraded to formation status because of the redefinition of the Pertatataka Formation, and the recognition of the Pioneer Sandstone, a probable correlative of the Olympic Formation. This allows the lower boundary of the Pertatataka Formation to be placed at the same stratigraphic position throughout the northern Amadeus Basin.

PIONEER SANDSTONE (new name)

Amadeus Basin

Proposers: W. V. Preiss, M. R. Walter, R. P. Coats, & A. T. Wells.

Derivation of name: Pioneer Creek, which flows into Ormiston Creek near Glen Helen Tourist Camp, Hermannsburg 1:250 000 Sheet area.

Distribution: The formation is exposed on the Henbury, Hermannsburg, Alice Springs, and probably Rodinga 1:250 000 Sheet areas.

Type section: Sandstone with minor dolomite in the bed of Ellery Creek, 1.0–1.3 km south of Ellery Creek Big Hole (lat. 23°47′24″S, long. 133°04′12″E) Hermannsburg 1:250 000 Sheet area.

The base is the first sandstone above the Areyonga Formation; the top is the top of the pink dolomite into which the sandstone grades.

Lithology: Sandstone, felspathic, white to brown, friable, medium to coarse, cross-bedded. The uppermost 8 m are silicified and outcrop prominently. Erosional scours in the uppermost sandstone are filled with lenses of dolomite about 10 cm thick; this is pink, and contains erect columnar stromatolites. The sandstone grades up into pinkish grey dolomite with red chert nodules and lenses. In much of the Alice Springs 1:250 000 Sheet area the formation is conglomeratic.

Thickness: 170 metres in the type section, and similar elsewhere.

Relationships and boundary criteria: Overlies the Areyonga Formation and Bitter Springs Formation with inferred disconformity. Conformably overlain by the Pertatataka Formation.

Age: The Pioneer Sandstone is a probable correlative of the Olympic Formation, the upper tillite of the Amadeus Basin. By correlation with the Adelaide Geosyncline, it is late Adelaidean.

Synonymy: This is the upper member of the Areyonga Formation of Prichard & Quinlan (1962), and subsequent authors.

ARALKA FORMATION (new name) *Amadeus Basin*

Proposers: W. V. Preiss, M. R. Walter, R. P. Coats, & A. T. Wells.

Derivation of name: Mount Aralka on the Hale River 1:250 000 Sheet area (lat. 24°00′57″S, long. 135°29′08″E).

Distribution: The formation is known in outcrop on the Alice Springs, Illogwa Creek, Hale River and Hermannsburg 1:250 000 Sheet areas; it is confined to the northeastern part of the Amadeus Basin.

Type section: The type section ASR 4 lies 6.4 km southeast of Ringwood Homestead (lat. 23°53′S, long. 135°02′E).

The shale sequences in the formation are mostly obscured but the Ringwood and Limbla Members are well exposed.

The type section is:

TOP

144 m Limbla Member—festoon cross-laminated sandstone in upper half; pebbly and sandy calcarenite in lower half.

333 m concealed—siltstone and shale sequence with minor sandstone interbeds inferred from partial exposures elsewhere.

166 m Ringwood Member—dolomite and calcarenite, mostly thin-bedded, in part pisolitic and stromatolitic.

376 m ± concealed—siltstone and shale sequence with subordinate sandstone interbeds inferred from partial exposures elsewhere.

Lithology: The sequence of rock types in the type section ASR 4 is shown in Wells and others (1967, Plate 10), and in addition is described in the text of the report.

Thickness: The thickness in the type section is about 1020 m. The formation thickens gradually eastwards from the type section, but thins rapidly westwards.

Relationships and boundary criteria: The formation conformably overlies the Areyonga Formation, and is disconformably overlain by the Olympic Formation. The upper boundary is exposed in the type section, but the lower boundary is concealed.

A stratotype lower boundary is present on the north flank of the Limbla Syncline (lat. 23°47′30″S, long 135°17′30″E) where the upper marker cap dolomite of the Areyonga Formation is in contact with shale of the Aralka Formation.

A stratotype upper boundary is present in the northwest part of the Olympic Syncline (lat. 21°01′40″S, long. 135°02′30″E) where cross-laminated sandstone of the Limbla Member is in contact with dark red-brown, poorly laminated siltstone and light green-grey, locally gritty, siltstone, of the Olympic Formation.

A disconformable contact with the Bitter Springs Formation is inferred in areas where the Areyonga Formation is absent.

Age: The Aralka Formation lies between formations that are considered to be Adelaidean in age.

Synonymy: The Aralka Formation was originally included in the basal part of the Pertatataka Formation by Wells and others (1967). The Olympic Formation (formerly Olympic Member of the Pertatataka Formation) is postulated to be laterally continuous with the Pioneer Sandstone (formerly the upper unit of the Areyonga Formation). Hence it was concluded that the interval between the Olympic and Areyonga Formation in the northeast part of the Amadeus Basin is a previously unrecognised separate formation, older than the Pertatataka Formation, and should be formalised.

AREYONGA FORMATION (redefinition of unit) *Amadeus Basin*

Proposers: W. V. Preiss, M. R. Walter, R. P. Coats, & A. T. Wells.

Prichard & Quinlan (1962) recognised two members in the Areyonga Formation in its type section. A disconformity has now been recognised separating these members. The upper member is redefined as the Pioneer Sandstone (new name). The name Areyonga Formation is restricted to the lower member, with which it is conventionally associated. The top of the Areyonga Formation in the type section at Ellery Creek is taken as the top of a dark grey silty shale with lenses of regularly laminated dolomite. The redefined Areyonga Formation is 250 m thick, and consists of diamictite, sandstone, dolomitic arkose, conglomerate and dolomite, with dolomitic silty shale at the top.

Distribution: Locally present in outcrop on the Hermannsburg and Henbury 1:250 000 Sheet areas; more widespread on the Illogwa Creek, Hale River and to a lesser extent, Alice Springs and Rodinga 1:250 000 Sheet areas.

MOUNT DOREEN FORMATION (redefinition of unit) *Ngalia Basin*

Proposer: A. T. Wells.

The original definition of the Mount Doreen Formation is here amended because it is now believed that a disconformity is present in its lower part. The formation was described (Wells and others, 1972) as consisting of red shale at the top followed in the middle by thin beds of pink dolomite then diamictite, and green shale at the base. The disconformity occurs between the diamictite and underlying green shale. The shale is here defined as the Rinkabeena Shale; the name Mount Doreen is retained for the upper part of the sequence.

The lower boundary of the formation is taken as the contact between diamictite of the Mount Doreen Formation with green shale of the Rinkabeena Shale.

RINKABEENA SHALE (new name) *Ngalia Basin*

Proposer: A. T. Wells.

Derivation of name: The name of the formation is derived from Rinkabeena Bore (2130:4868) in the eastern part of the Ngalia Basin on the Napperby 1:250 000 Sheet area.

Distribution: Outcrops extend intermittently around the eastern closure of the Naburula Syncline, and approximately follow the trend of the Patmungala and Gum Creeks in their headwaters.

The Rinkabeena Shale is known from a shallow stratigraphic drillhole in the Davis Gap area, and it probably occurs in the Vaughan Springs Syncline, but outcrops here are too poor to be certain of its identification.

Thickness: The Rinkabeena Shale is about 100 m thick in the type section. The shale is not sufficiently well exposed to obtain any information on regional changes in thickness.

Lithology: The formation consists of a very uniform sequence of green shale, with subordinate interbeds of siltstone.

Type section: The type section of the Rinkabeena Shale is located in the headwaters of Patmungala Creek at 7387:5334 to 7393:5332.

The type section consists predominantly of shale, with some interbeds of siltstone. The formation is in places slightly calcareous, especially towards its base.

Stratigraphic relationships: In the type section the Rinkabeena Shale is overlain, probably disconformably, by the Mount Doreen Formation, and it conformably overlies the Naburula Formation.

Age: Stratigraphic relationships and regional correlations suggest that the Rinkabeena Shale is late Adelaidean in age. It is correlated with the basal part of the Aralka Formation in the eastern part of the Armadeus Basin.

Synonymy: A mappable unit of shale that was originally included in the

basal part of the Mount Doreen Formation. It is probably separated from the diamictite of the Mount Doreen Formation by a disconformity.

NABURULA FORMATION (new name) *Ngalia Basin*

Proposer: A. T. Wells.

Derivation of name: The name is derived from the Narubula Hills in the central northern part of the Ngalia Basin. (Grid ref. of Naburula Hills approx. 7250–7400; 5300–5400) on the Mount Doreen 1:250 000 Sheet area.

Distribution: Outcrops extend intermittently around the eastern closure of the Naburula Syncline. Diamictite overlying the Vaughan Springs Quartzite in the Vaughan Springs Syncline is referred to the Naburula Formation.

Type section: The type section is located in the headwaters of Patmungala Creek at 7398:5334. The type section is—

TOP

0.2 m *Dolomite* — thin-bedded, fine-grained, green-grey, deeply weathered, iron-stained.

0.5 m *Shale*—dark grey to black, well-bedded.

0.2 m *Dolomite*—as above.

3.7 m *Shale*—dark grey to black, well-bedded.

0.2 m *Dolomite*—yellow-brown and dark brown, fine-grained, deeply weathered.

0.9 m *Shale and Siltstone*—yellow-brown, poorly exposed.

2.1 m *Diamictite* — matrix, green-brown, angular grains of feldspar and quartz; clasts of granite, quartzite, quartz, quartz-mica schist, silicified yellow-grey siltstone, vein quartz with tourmaline, feldspar porphyry, spotted blue-grey hornfels, quartz granule grit. The erratics are commonly striated and faceted, and closely fractured. The diamictite shows incipient cleavage.

Lithology: The formation comprises three dominant rock types, a basal diamictite, overlain by black shale, which is in turn overlain by interbedded dolomite and shale.

Thickness: The Naburula Formation is 8 m thick in the type section. The formation is not sufficiently well exposed to obtain any information on regional changes in thickness.

Stratigraphic relationships: In the type section the formation unconformably overlies Precambrian basement granite, and is conformably overlain by the Rinkabeena Shale.

Age: Stratigraphic relationships and regional correlations suggest that the formation is late Adelaidean in age.

Synonymy: A mappable unit of thin diamictite, shale, and dolomite that has not been previously differentiated, and only partly described.

Hot-spot volcanism in St Andrew Strait, Papua New Guinea: geochemistry of a Quaternary bimodal rock suite

R. W. Johnson, I. E. M. Smith[1], & S. R. Taylor[2]

Four distinct volcanic rock types are found above a conjectured mantle hot spot in St Andrew Strait, northern Papua New Guinea. Hypersthene-normative basalts on Baluan Island are geochemically similar in most respects to those on oceanic islands and, together with voluminous alkali-rich rhyolites on Tuluman, Lou, and Pam Islands, constitute a strongly bimodal rock suite. The rhyolites are regarded as partial melts of basaltic crust isotopically similar to the basalts of Baluan, though with lower Sr, Rb, and Ba contents. In contrast, quartz-tholeiite basalts in the Fedarb Islands are isotopically distinct from the Baluan basalts. Dacite is also present in the Fedarb Islands, but not all of its geochemical features are consistent with a derivation by crystal fractionation from Fedarb quartz tholeiite. Like Iceland, St Andrew Strait may be underlain by a hot mantle diapir that has produced basaltic magmas as well as partial melting of basaltic crust.

Introduction

The Quaternary volcanic islands of St Andrew Strait are about 35 km southeast of Manus Island, the largest of the Admiralty group, in northern Papua New Guinea (Fig. 1). They provide a striking example of contrasting rhyolitic and basaltic activity over a possible mantle 'hot spot' (Johnson & Smith, 1974). Additions to the felsic component of this bimodal rock suite have taken place as recently as 1953-57, when Tuluman volcano produced rhyolitic pumice and lava flows (Reynolds & Best, 1976).

Major and trace-element analyses have been obtained for 28 samples of lava flows from the St Andrew Strait islands (Tables 1-5). The major-element data were discussed by Johnson & Smith (1974) in their account of the geology of the islands, and the purpose of this complementary paper is to evaluate the trace-element data, and to update the petrological conclusions of the earlier account. Sample localities are plotted in Figure 1, and described in Table 6 (see also Johnson & Davies, 1972).

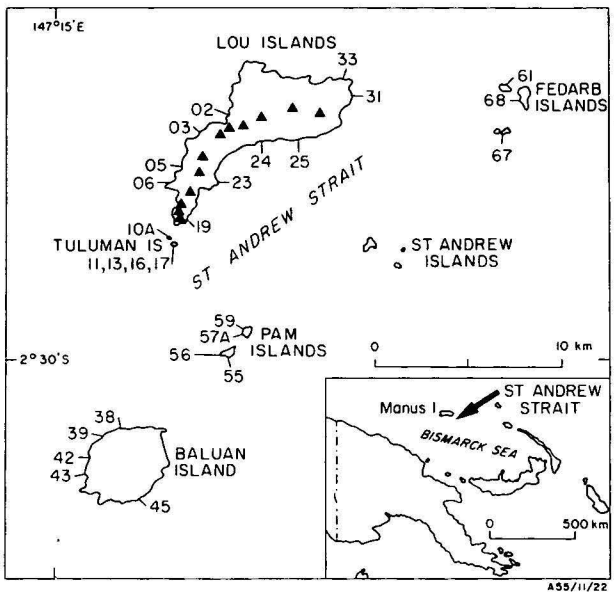

Figure 1. Islands of St Andrew Strait, showing localities of samples listed in Table 6. Triangles represent volcanic centres of Lou Island, numbered 1-12 anticlockwise. The St Andrew Islands are coral.

Analytical methods

Most of the major and trace-element abundances listed in Tables 1-4 were determined by X-ray spectrometry using an automated Philips PW1220 spectrometer. Si, Ti, Al, Fe, Mn, Mg, Ca, K, and P were determined in glass discs prepared by the fusion method of Norrish & Hutton (1969). The trace elements were measured on rock-powder pellets using the methods of Norrish & Chappell (1967). FeO was determined by titration against potassium dichromate solution (Peck, 1964). H_2O- was measured after heating at 110°C, and H_2O+ and CO_2 were determined by collecting volatiles lost from the sample at 1050°C. The major-element analyses of samples 31, 05, and 56 in Table 1 were supplied by The Australian Mineral Development Laboratories.

Rare-earth elements (REE), U, Th, Cs, and Hf in nine samples (Table 5) were determined by spark source mass spectrography using the method described by Taylor & Gorton (1977). Precision and accuracy of the method are considered to be about ± 5% relative deviation. Tm and Lu were not measured, and the reported values are those obtained by interpolation. REE chondrite values used for normalisation in Figures 3, 5 and 6 are Leedey chondrite data (Masuda, Nakamura & Tanaka, 1973) divided by 1.20 (Sun & Hanson, 1976a).

Magma types and tectonic setting

Four magma types are represented in the St. Andrew Strait islands; no two of them are found on the same island.

(1) Alkali-rich rhyolites on Tuluman, Lou, and Pam Islands comprise the 'TLP series' (Johnson & Smith, 1974), and are the most voluminous rock type exposed in the area. These rocks are characterised by peralkalinity indices (PI = mol. $(Na_2O + K_2O)$/mol. Al_2O_3) almost equal to one (0.87-0.94).

(2) Basalts on Baluan Island are olivine and hypersthene-normative. Some are aphyric; others are rich in plagioclase phenocrysts.

(3) Quartz-tholeiite basalts are exposed only in a 35 m-high cliff on the southwestern side of Sivisa Island, the largest of the Fedarb group.

(4) Dacite crops out on the other three smaller Fedarb Islands, which are possibly parts of the same lava

1. Department of Geology, Australian National University, Canberra, ACT 2600. Present address: Department of Geology, University of Toronto, Toronto, Canada.
2. Research School of Earth Sciences, Australian National University, Canberra, ACT 2600.

flow. PI values are 0.73-0.76, and Na_2O/K_2O values are much greater than those of the TLP rocks.

Rocks intermediate in composition between basalt and dacite-rhyolite have not been found on the St Andrew Strait islands, but large proportions of the volcanoes are below sea-level and of unknown composition, and a careful search for included blocks has yet to be made.

The composition of the sea floor underlying the volcanoes is also unknown. However, there is now a consensus that the Bismarck Sea is a marginal basin (e.g. Karig, 1973), and that sea-floor spreading is at present taking place in at least one sector of a zone of shallow seismicity that crosses the Bismarck Sea east-west, passing about 80 km south of St Andrew Strait (Taylor, 1975; Connelly, 1976). By analogy with other marginal basins (e.g. the Lau Basin; Hawkins 1976), therefore, the Bismarck Sea is probably underlain by tholeiitic basalt.

The St Andrew Strait islands straddle the northwestern end of the Willaumez-Manus Rise, which separates two depressions in the Bismarck Sea—an eastern one characterised by thin sediment and rough topography, and a smoother western one covered by thicker sediments (Connelly, 1974). The pattern of magnetic anomalies in the depressions is complex, and although a crude east-west trend has been reported there is no evidence that anomalies are arranged systematically parallel to, and increasing in age from, the zone of seismicity (Connelly, 1974, 1976; Taylor, 1975; Willcox, 1976). The age of the crust beneath St Andrew Strait is therefore unknown, although most, if not all, of the basin is likely to be Cainozoic. Calculated crustal thicknesses beneath the Bismarck Sea are mostly in the range 19-25 km (Willcox, 1976). The thickest crust is reported to be at the margins of the sea and beneath the Willaumez-Manus Rise, corresponding with lower Bouguer gravity anomalies (+120-150 mgals). Beneath St Andrew Strait the estimated crustal thickness is 24-25 km.

TLP series

Mineralogy and major-element chemistry

TLP rocks are obsidian, pitchstone, pumice, and fine-grained lava. Phenocrysts of sodic plagioclase, clinopyroxene, orthopyroxene, and iron-titanium oxides are present in a few rocks, but rarely in amounts exceeding about 1 percent. In thin sections of samples more coarsely crystalline than usual, grains of amphibole, potash feldspar, and high-temperature polymorphs of silica can also be seen; biotite and apatite are accessory phases.

The phenocrysts in two samples have been analysed with the electron microprobe. The analysed feldspars are all oligoclase ($An_{27.9\text{-}19.6}$ $Ab_{68.3\text{-}75.0}$ $Or_{3.4\text{-}5.4}$), and the pyroxenes are augite ($Fe_{21.2\text{-}21.9}$ $Ca_{38.6\text{-}39.2}$ $Mg_{39.7\text{-}39.5}$) and orthopyroxene ($Fe_{48.8\text{-}54.4}$ $Ca_{3.0\text{-}3.2}$ $Mg_{50.0\text{-}42.5}$). Using the analyses of magnetite-ilmenite pairs and the fO_2-T°C curves of Buddington & Lindsley (1964), calculated temperatures of crystallisation are 800-825°C, calculated fO_2 values are $10^{-(14.8 \text{ to } 15.4)}$ atmospheres, and the data points plot close to the quartz-magnetite-fayalite buffer curve (at 1 atmosphere). The fO_2-T°C estimates are very similar to those obtained for rhyolites from Mono Craters, California; the oxide-equilibration temperatures in these are probably below the liquidus temperatures (Carmichael 1976).

The main features of the major-element chemistry of these rocks are as follows (after Johnson & Smith, 1974).

(1) The rhyolites are alkali-rich, containing between 8.4 and 9.4 percent $Na_2O + K_2O$ (by weight). These values are similar to that of the average alkali-rhyolite composition (total-alkalies 8.86%) of Nockolds (1954), but they are higher than the alkali contents of the average rhyolite of Le Maitre (1976; 7.85%) and an average New Zealand rhyolite (7.42%; Ewart, Taylor & Capp, 1968).

(2) Plotted in the Quaternary system *Q-ab-or-an*, the TLP rocks form an elongate cluster of points in the one-feldspar field. The cluster trends away from the oligoclase section of the *ab-an* side line, and towards more *Q*- and *or*-rich compositions, closer to the low-pressure (less than about 5 kb) ternary minima in the system *Q-ab-or*. The rocks of Tuluman plot further from, and those of Pam nearer to, the ternary minima, and the Lou rocks generally fall between the two extremes. Clearly, sodic plagioclase has had a dominant influence on the evolution of the TLP series. Because of the increase in *Q* and *or* relative to *ab* and *an*, the ratio $100(Q + or)/(ab + an)$ is used below as a measure of the residual character of the TLP rocks (*qfr*, quartz-and-feldspars ratio).

(3) FeO + Fe_2O_3, TiO_2, and MgO contents are lower in rocks with higher *qfr* values, implying some influence of ferromagnesian minerals (pyroxene, or amphibole, or both) and iron-titanium oxides in the development of the series.

(4) There is a negative correlation between molecular CaO and $(Na_2O + K_2O)/Al_2O_3$ (PI) values, and by extrapolation of the trend to zero CaO the molecular proportions of $Na_2O + K_2O$ and Al_2O_3 are shown to be more or less equal. This relationship appears to be important, as it implies that the evolution of the series has been buffered with respect to these components (see below with reference to Fig. 7).

Rocks similar in major-element chemistry to the TLP rhyolites are known in continental volcanoes such as Tweed volcano in eastern Australia (Wilkinson, 1968; Ewart, Mateen, & Ross, 1976; Ewart, Oversby, & Mateen, 1977) and Summer Coon volcano in Colorado, western United States (Zielinski & Lipman, 1976). Alkali rhyolites are also found in the Salton Sea area of southern California (Robinson, Elders & Muffler, 1976), and on some volcanoes in western and southern Iceland (Sigurdsson, 1971; O'Nions & Grönvold, 1973). In both of these areas the rhyolites are associated with transitional basalts, are relatively abundant (forming bimodal rock suites with the basalts), and overlie regions of high heat flow near spreading axes.

Trace-element geochemistry

Trace-element data for the TLP rocks are listed in Tables 2 and 5, a correlation matrix and average values for the Table 2 values are given in Table 7, and abundances of selected trace elements are plotted relative to *qfr* values in Figure 2.

Large low-valency cations (Rb, Sr, Ba, Pb, Cs). Rb values are strongly and positively correlated with *qfr* values. K/Rb values (224-269) are close to the average crustal value of 230 reported by Taylor (1965), and decrease very slightly with increasing *qfr*, although the correlation is poor. Sr values are strongly and negatively correlated with *qfr*, although values between 72 and 88 ppm are notably absent. There is a three-fold variation in Rb/Sr values. Ba and *qfr* values are poorly

	10A	11	13*	16	17A	31	33	02	24	25	03	05	06	23	19	55	56	57A	59
SiO_2	69.55	69.47	70.31	69.41	69.57	70.40	70.57	71.39	73.28	73.55	72.85	71.80	71.71	70.96	70.60	73.40	73.70	73.49	73.63
TiO_2	.45	.45	.44	.44	.45	.36	.36	.31	.26	.26	.28	.29	.30	.30	.44	.26	.30	.22	.22
Al_2O_3	14.18	13.90	14.01	13.74	13.91	14.20	14.35	13.95	13.54	13.58	13.74	13.90	14.01	13.82	13.99	13.32	13.40	13.16	13.32
Fe_2O_3	.82	.90	1.08	.95	.89	.76	1.15	.58	.54	.48	.58	.27	.43	.68	.83	.48	.52	.47	.52
FeO	2.66	2.62	2.41	2.76	2.73	2.20	1.88	1.88	1.40	1.44	1.44	1.81	1.86	2.43	2.57	1.53	1.47	1.43	1.39
MnO	.10	.10	.09	.10	.10	.07	.09	.07	.07	.07	.07	.06	.07	.10	.10	.06	.06	.06	.06
MgO	.46	.49	.54	.76	.84	.45	.50	.55	.35	.38	.34	.45	.39	.37	.38	.13	.23	.10	.29
CaO	1.88	1.89	1.78	1.93	1.95	1.48	1.48	1.29	.98	1.01	1.11	1.26	1.21	1.27	1.55	.96	.85	.87	.85
Na_2O	5.39	5.38	5.26	5.32	5.29	5.20	5.24	5.06	4.85	4.84	4.94	4.95	5.04	5.43	5.36	4.77	4.65	4.77	4.74
K_2O	3.22	3.21	3.21	3.19	3.21	4.00	3.66	3.93	4.07	4.11	4.01	4.45	3.99	3.57	3.29	4.20	4.40	4.22	4.22
P_2O_5	.07	.13	.06	.06	.07	.05	.05	.04	.03	.03	.04	.04	.04	.04	.07	.02	.02	.01	.02
H_2O+	.25	.06	.19	.27	.23	.01	.06	.15	.20	.21	.19	.04	.21	.27	.20	.28	.31	.23	.28
H_2O-	.10	.10	.10	.12	.10	.27	.10	.21	.09	.12	.09	.18	.10	.07	.11	.13	.13	.08	.08
CO_2	.34	.24	.14	.32	.14	.19	.17	.27	.27	.11	.22	.16	.17	.33	.26	.14	<.05	.11	.19
TOTAL	99.47	98.94	99.62	99.37	99.48	99.64	99.66	99.68	99.93	100.19	99.90	99.66	99.53	99.64	99.75	99.68	100.04	99.22	99.81
$\frac{mol.\ (Na_2O + K_2O)}{mol.\ Al_2O_3}$	0.87	0.89	0.87	0.89	0.88	0.91	0.88	0.90	0.91	0.91	0.91	0.93	0.90	0.93	0.88	0.93	0.93	0.94	0.93
$\frac{100\ (Q + or)}{(ab + an)}$	79.2	80.5	83.6	81.0	80.3	93.4	88.9	99.7	115.8	115.4	109.5	109.7	101.3	88.6	84.4	121.1	126.5	123.4	122.7

*Analysis also given in Table II of Johnson & Smith (1974), but incorrectly labelled sample 11.

Table 1. Major-element analyses of 19 rocks from Tuluman, Lou, and Pam Islands.

	10A	11	13	16	17A	33	02	24	25	03	06	23	19	55		
Rb	115	110	99	110	109	134	141	150	152	139	138	122	116	154	155	150
Ba	764	756	798	751	772	821	812	792	791	774	831	824	800	820	807	814
Pb	16	8	15	11	8	9	8	9	9	8	9	10	15	8	8	9
Sr	96	95	93	88	89	93	72	60	60	68	69	68	89	49	47	45
K/Rb	232	242	269	241	244	227	231	225	224	239	240	243	235	226	226	234
Ba/Rb	6.64	6.87	8.06	6.83	7.08	6.13	5.76	5.28	5.20	5.57	6.02	6.75	6.90	5.32	5.21	5.43
Rb/Sr	1.20	1.16	1.06	1.25	1.22	1.44	1.96	2.50	2.53	2.04	2.00	1.79	1.30	3.14	3.30	3.33
La	39	43*	39	39	39	34	34	35	41*	31	40	42	40	37	37	36
Ce	93	95	94	92	91	80	84	79	84*	77	87	95	100	86	81	80
Y	51	50	52	50	51	40	39	35	35	36	38	50	51	37	38	38
La + Ce + Y	183	188	185	181	181	154	157	149	160	144	165	187	191	160	156	154
Th	12	13	13	11	12	13	14	15	13	14	13	12	13	12	16	15
U	3	2.9*	2	3	2.5*	2.7*	3	2	3.2*	4	3	3	2	3	4	3.3*
Zr	523	520	532	510	512	499	432	322	321	347	426	501	551	306	299	304
Nb	57	54	58	53	52	50	46	41	41	41	47	55	60	43	42	43
Th/U	4.0	4.5	6.5	3.7	4.8	3.5	4.7	7.5	4.1	3.5	4.3	4.0	6.5	4.0	4.0	4.5
Zr/Nb	9.18	9.63	9.17	9.62	9.85	9.98	9.39	7.85	7.83	8.46	9.06	9.11	9.18	7.12	7.12	7.07
Zn	77	75	54	73	72	56	53	50	51	48	55	74	73	50	50	49
Cu	6	4	8	6	10	6	5	<5	<5	<5	<5	<5	<5	<5	<5	<5
Ni	<5	<5	<5	<5	<5	<5	<5	<5	<5	<5	<5	<5	<5	<5	<5	<5
V	<5	<5	<5	<5	<5	<5	<5	<5	<5	<5	5	<5	<5	<5	<5	<5
Cr	27	26	26	27	28	27	26	23	23	24	25	24	25	26	25	24
Ga	18	18	19	17	17	19	17	15	17	15	16	17	19	16	17	16

† Determined by X-ray spectrometry, except values shown with asterisk which were obtained by spark-source mass spectrography.

Table 2. Trace-element analyses† of 16 rocks from Tuluman, Lou, and Pam Islands.

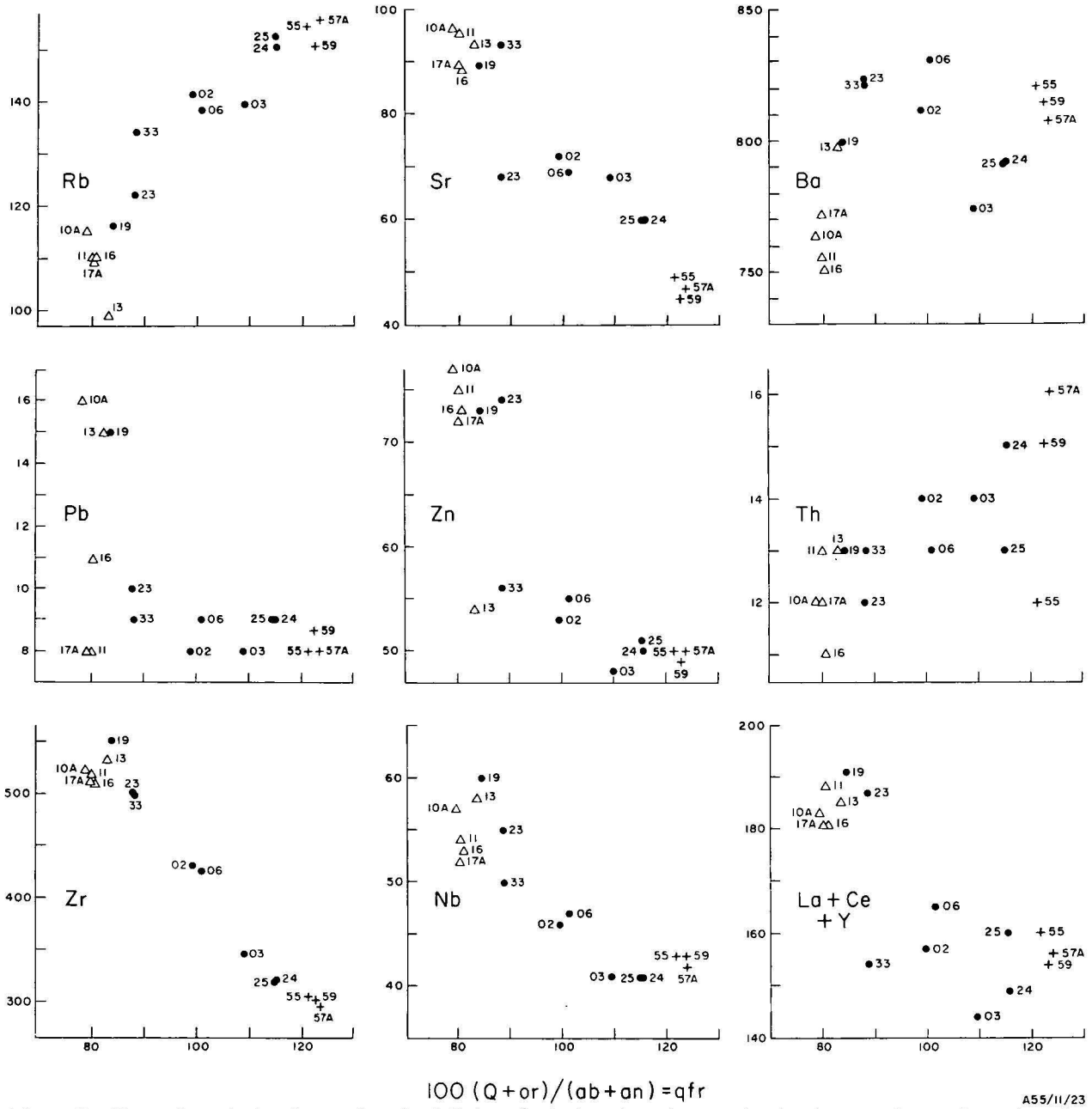

Figure 2. Trace-element abundances (ppm) plotted against *qfr* values (see text), showing sample numbers given in Table 2. Triangles: Tuluman Islands. Dots: Lou Island. Crosses: Pam Islands.

correlated, but the three rocks with the highest Ba values are in the intermediate *qfr* range. Most Pb values are 10 ppm or less. Cs abundances (determined for only five TLP rocks—see Table 5) generally increase as *qfr* increases. Also, Rb/Cs values are lowest in the two rocks with the highest *qfr* values.

The large-cation abundances in TLP rocks resemble those in the Salton Sea rhyolites (Robinson, Elders & Muffler, 1976), except that Ba and Sr contents are somewhat higher in the TLP rocks. Some Rb/Sr values in the TLP rocks are high for rhyolites, but nevertheless are much lower than those for the unusual highly fractionated rhyolites from Tweed volcano (Ewart, Mateen, & Ross, 1976). Compared to the average New Zealand rhyolite composition reported by Ewart, Taylor, & Capp (1968), the TLP rocks are lower in Sr and Ba, but have comparable Rb, Pb, and Cs contents.

The above large-cation relationships are all consistent with magma evolution controlled by fractionation of plagioclase—Rb and Cs being concentrated in more residual liquids, Sr and Pb being incorporated into the feldspar, and Ba possibly being incorporated into the K sites of the feldspars crystallised from more residual compositions (however see below).

Ferromagnesian and chalcophile elements (Zn, Cu, Ni, V, Cr, Ga). In the TLP rocks, only Zn, Cr and Ga are significantly above the limits of analytical detection, and all three elements correlate negatively with *qfr* at the 99.5 percent confidence level. The negative correlations support the major-element evidence that ferromagnesian minerals and Fe-Ti oxides have to some extent influenced the development of the TLP series. However, Ga was probably also incorporated in feldspar, and Zn and Ga may also have substituted in sulphide phases. Zn values appear to be distributed bimodally (Fig. 2).

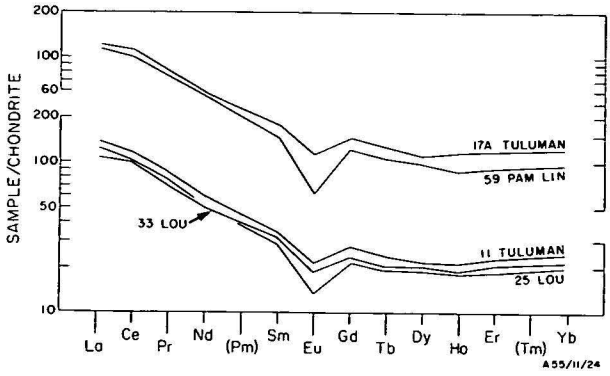

Figure 3. Chondrite-normalised rare-earth patterns for five TLP rocks. Data listed in Tables 2 and 5.

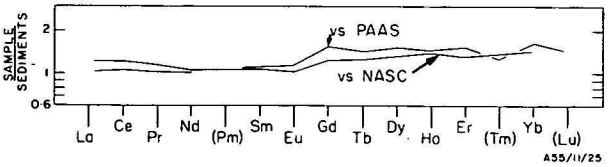

Figure 4. Rare-earth patterns for average of five samples shown in Figure 3, normalised against values for Post-Archaean Average Australian Sedimentary rock composite (PAAS; Nance & Taylor, 1976) and North American Shale Composite (NASC; Haskin, Frey, Schmitt, & Smith, 1966).

Large high-valency cations (Th, U, Zr, Nb, Hf). Th and U values are generally higher in rocks with higher *qfr*, but the correlations are poor. In contrast, Zr, Nb, and Zr/Nb are strongly and negatively correlated with *qfr*, and positively with one another, and with TiO_2 and normative apatite (*ap*) contents; accessory phases may have been responsible for these correlations (Table 7).

The abundances of Zr (mean = 432 ppm), Nb (mean = 49 ppm), and Hf (mean = 9.4 ppm) are all high in the TLP rocks compared to those in other rhyolites (cf. averages for New Zealand rhyolites given by Ewart, Taylor, & Capp, 1968: Zr = 160 ppm, Nb = 5.6 ppm, Hf = 4.5 ppm). They are even high compared to the values for the highly fractionated alkali rhyolites of Tweed volcano (Zr averages for three rhyolite types are 137, 282 and 330; Ewart, Mateen, & Ross, 1976), although similar and much higher values are known from basalt-pantellerite sequences (e.g. Boina volcano, Ethiopia; Barberi and others, 1975).

Rare-earth elements (REE) and yttrium. La + Ce + Y values are correlated negatively with *qfr* (Fig. 2), and positively with *ap*, Zr, and Nb values (Table 7). However, in Figure 2 (La + Ce + Y versus *qfr*) there is both a considerable scatter of points and a conspicuous absence of La + Ce + Y values in the interval 165-181 ppm. The samples in the high and low (La + Ce + Y) groups are generally the same as in the high and low-Sr and Zn groups. Chondrite normalised REE patterns for five rocks (Fig. 3) further verify that rocks from the high REE group (nos 11 and 17A from Tuluman) have the lowest *qfr* values (see also Table 5). These relationships are evidence for the influence of a phase or phases that has preferentially incorporated the REE relative to the magma (see below).

LREE (La-Sm) are enriched relative to HREE (Gd-Yb) in all five rocks in Table 2, but La/Yb and ΣLREE/ΣHREE values are greatest in the two rocks showing the highest *qfr* values (nos 25 and 59). All five samples have conspicuous negative Eu anomalies (Eu/Eu* = 0.46-0.70) indicating the pronounced influence of plagioclase. Eu anomalies are greatest in the two high-*qfr* rocks. Differences in Sr/Eu values are unsystematic. There is no evidence for the influence of phases that incorporate large amounts of the HREE (e.g., garnet).

The REE values are similar to those for estimates of average crustal concentrations, except that HREE values in the TLP rocks are about 1½ times as abundant (Fig. 4).

Strontium-isotope geochemistry

The initial (measured $^{87}Sr/^{86}Sr$ values for two TLP rocks (Table 8) are 0.7043 and 0.7044 (identical within analytical error). These values are lower than those obtained by Ewart & Stipp (1968) for the rhyolitic lavas of New Zealand (range 0.7045-0.7065, mean 0.7054), and are slightly higher than those for Quaternary volcanic rocks from other parts of the Bismarck Archipelago (range 0.7034-0.7042, mean 0.7038; Peterman, Lowder & Carmichael, 1970; Page & Johnson, 1974; Peterman & Heming, 1974).

Baluan basalts

The five analysed basalts from Baluan Island are all olivine and hypersthene normative (Table 3), but because their petrography is not obviously tholeiitic and *hy* contents are generally low, they have been termed 'mildly alkaline and transitional basalts' (Johnson & Smith, 1974; after Coombs, 1963) rather than olivine tholeiites. However, the order of crystallisation of phenocrysts is plagioclase-olivine-clinopyroxene, and the rocks are therefore 'plagioclase tholeiites' in the sense of Miyashiro, Shido, & Ewing (1969). All five basalts are fractionated: their Mg-numbers are low (52-60); FeOt/MgO values are all greater than 1.5; and Ni and Cr contents are conspicuously low, implying substantial fractionation of olivine and chrome spinel from plausible primary magmas (Table 9).

The principal difference between the analysed basalts is in the amounts of normative and of modal plagioclase. Two aphyric samples (nos. 38 and 42) are low in Al_2O_3 (less than 16%), but the others contain up to about 50 percent plagioclase phenocrysts and up to almost 21 percent Al_2O_3. Eu/Eu* values for an aphyric sample (42) and one for a plagiophyric sample (39) are 1.1 and 1.2 respectively (Table 5, Fig. 5), suggesting plagioclase accumulation and, for sample 42, implying either resorption of accumulated plagioclase or derivation from a mantle source with a positive Eu anomaly. The main difference in major-element chemistry between these two samples can be accounted for by about 31 percent plagioclase accumulation in sample 39. However, substitution of this value and the measured REE contents for the two rocks (Table 2) in the Rayleigh fractionation equation gives unusually high $D^{\text{plagioclase/liquid}}_{\text{Ce, Nd}}$ values, and no marked positive Eu anomaly (cf. Schnetzler & Philpotts, 1970). Thus, the two REE patterns (Fig. 5) do not appear to be closely related by plagioclase accumulation alone.

The compositions of tholeiitic basalts in marginal basins have been reported by Hart, Glassley & Karig (1972) from the Philippine Sea, and by Sclater and others (1971), and Hawkins (1976), from the Lau Basin, and their similarity to those of mid-ocean ridge basalts has been noted. However, although Baluan Island appears to have been built within the Bismarck Sea marginal basin, its basalts are clearly not of ocean-

	38	39	42	43	45	68C	69D	61	67
SiO_2	49.51	49.18	50.30	48.76	48.54	51.74	50.97	68.16	67.90
TiO_2	1.40	1.26	1.63	1.25	1.10	.79	.73	.83	.81
Al_2O_3	15.87	20.66	15.22	18.13	20.28	17.62	18.36	15.28	14.94
Fe_2O_3	1.91	2.08	2.07	2.24	1.83	2.36	2.53	1.63	1.60
FeO	8.51	6.55	9.62	6.93	6.21	5.78	5.17	2.20	2.15
MnO	.20	0.16	.21	.17	.15	.15	.15	.14	.15
MgO	6.86	3.97	5.79	5.89	4.63	6.59	6.61	1.08	1.23
CaO	11.99	12.27	10.54	12.61	12.92	11.31	12.28	3.01	3.00
Na_2O	2.67	3.03	3.18	2.65	2.73	2.52	2.35	5.84	5.92
K_2O	.45	0.53	.79	.48	.54	.32	.30	1.45	1.45
P_2O_5	.15	0.16	.20	.16	.13	.12	.11	.24	.22
H_2O+	.34	0.17	.14	.22	.15	.17	.14	.08	.17
H_2O-	.21	0.11	.14	.20	.10	.11	.08	.08	.11
CO_2	.05	0.08	.06	.02	.02	.05	<0.02	.04	.02
TOTAL	100.12	100.21	99.90	99.71	99.33	99.63	99.78	100.06	99.67
$\frac{mol.\ (Na_2O + K_2O)}{mol.\ Al_2O_3}$	0.31	0.27	0.40	0.27	0.25	0.25	0.23	0.73	0.76

Table 3. Major-element analyses of nine rocks from Baluan and Fedarb Islands.

	38	39	42	43	45	68C	68D	61	67
Rb	12	11	26	12	13	5	5	18	19
Ba	259	264	355	252	256	95	88	349	344
Pb	9	8	10	9	9	19	19	15	17
Sr	262	328	289	300	324	353	357	444	427
K/Rb	311	400	252	332	345	531	498	669	633
Ba/Rb	21.6	24.0	13.7	21.0	19.7	19.0	17.6	19.4	18.1
Rb/Sr	0.046	0.034	0.090	0.040	0.040	0.014	0.014	0.041	0.044
La	2	11*	13*	2	3	<1	5.0*	20	28*
Ce	17	26*	31*	16	9	7	11*	52	59*
Y	21	19	25	20	17	13	13	31	31
La + Ce + Y	40	56	69	38	29	20	29	103	118
Th	2	0.94*	1.5*	2	1	2	0.52*	3	2.1*
U	<1	0.23*	0.36*	1	<1	1	0.22*	1	1.2*
Zr	98	88	123	89	81	36	32	153	156
Nb	14	13	20	14	12	3	4	9	9
Th/U	—	4.1	4.2	2	—	2	2.4	3	1.8
Zr/Nb	7.00	6.77	6.15	6.36	6.75	12	8	17	17.3
Zn	81	70	89	71	63	68	59	82	91
Cu	119	91	75	66	65	92	87	23	25
Ni	61	21	16	34	23	72	70	<5	<5
V	249	175	274	215	172	213	172	30	30
Cr	208	47	31	91	56	149	145	25	26
Ga	15	18	18	16	19	16	17	18	17

† Determined by X-ray spectrometry, except values shown with asterisk which were determined by spark-source mass spectrography.

Table 4. Trace-element analyses† of nine rocks from Baluan and Fedarb Islands.

ridge type, because of the significantly higher abundances of most large-ion-lithophile elements (LILE). For example, K_2O values are up to 5 times greater, and Sr abundances twice as great, compared to equivalent values in ridge basalts, and Rb, Ba and Cs values are more than an order of magnitude greater (Table 9). Fractionation cannot be the dominant mechanism for these large differences in LILE concentrates. K/Rb, K/Ba, and K/Cs values in the Baluan rocks are much lower than those reported as typical, if not diagnostic, of ridge basalts (Table 9; Hart, 1976), and the Sr^{87}/Sr^{86} values, both 0.7044 (Table 8), are much higher (mainly 0.7020-0.7035 for ridge basalts; Hofmann & Hart, 1975). In addition, LREE are enriched relative to HREE (Table 5), and the REE patterns (Fig. 5) are therefore in striking contrast to the LREE-depleted patterns thought to be typical of 'normal' mid-ocean ridge basalts (e.g. Kay, Hubbard & Gast, 1970; Bryan and others, 1976).

Baluan basalts are much closer in composition to basalts from ocean islands than to mid-ocean ridge basalts (Table 9). Ocean-island basalts are typically enriched in many LILE (e.g. Hubbard, 1969), have higher Sr^{87}/Sr^{86} values (mainly 0.7030-0.7045; Hofmann & Hart, 1975), and lower K/Rb, K/Ba, K/Cs, and Zr/Nb values (e.g. Hart, 1976; Erlank & Kable, 1976). They are widely thought to have been derived from parts of the mantle which are richer in LILE than are those which give rise to much of the widespread mid-ocean-ridge volcanism.

Despite the chemical similarities to ocean-island rocks, the Baluan basalts have some marked differences: P_2O_5, TiO_2, Nb, and especially Zr, abundances are lower than in ocean-island rocks, and more closely resemble those of mid-ocean-ridge and island arc basalts. Gill (1976a, b), and Tarney, Saunders, & Weaver (1977) drew attention to the LILE characteristics of marginal basin basalts from the Lau Basin and Scotia Sea area, and interpreted some of them as being transitional between those of normal mid-ocean-ridge basalts and island-arc or ocean-island basalts. However, if inter-element relationships are regarded as being more important than absolute element abundances in the recognition of mantle sources (e.g. Sun & Hanson, 1976b) then the Baluan basalts are probably best regarded as hot-spot types, because their Zr/Nb values are identical to those of oceanic islands (Table 9).

	11	17A	33	25	59	39	42	68D	67
Cs	1.7	1.5	1.3	2.7	3.3	0.11	0.46	0.12	0.55
Hf	11	11	9.8	8.0	7.4	1.9	2.6	0.99	3.3
Rb/Cs	64.7	72.7	103	56.3	45.4	100	56.5	41.7	34.5
Zr/Hf	47.3	46.5	50.9	40.1	41.1	46.3	47.3	32.3	47.3
Pr	9.9	9.5	8.1	8.9	8.6	3.3	3.8	1.4	8.8
Nd	35	34	29	31	33	14	17	5.9	3.4
Sm	6.7	7.1	6.1	5.6	5.7	2.8	3.9	1.2	5.8
Eu	1.5	1.6	1.4	1.0	0.91	1.1	1.5	0.53	1.6
Gd	7.2	7.7	6.1	5.7[a]	6.4	3.1[a]	4.2[a]	1.6	4.9
Tb	1.2	1.3	1.0	0.96	1.0	0.54	0.72	0.27	0.93[a]
Dy	7.1	7.3	6.6	6.3	6.4	3.3	4.6	1.7	5.1
Ho	1.6	1.7	1.4	1.3	1.3	0.73	0.92	0.35	0.97
Er	4.9	5.1	4.4	4.0	4.0	1.9	2.6	0.97	2.9
Tm[a]	0.70	0.73	0.64	0.59	0.57	0.25	0.37	0.16	0.40
Yb	5.0	5.2	4.5	4.2	4.0	1.6	2.6	0.92	2.8
Lu[a]	0.81	0.80	0.71	0.68	0.65	0.23	0.40	0.14	0.43
ΣREE[b]	219.61	212.03	183.95	195.23	188.53	69.85	86.61	31.14	125.03
*Eu/Eu**	0.68	0.68	0.70	0.54	0.46	1.2	1.1	1.2	0.92
Sr/Eu	63.3	55.6	66.4	60.0	49.5	298	193	674	267
La/Yb	8.60	7.50	7.55	9.76	9.00	6.88	5.00	5.43	10.0
$\Sigma LREE$[b]	189.6	180.6	157.2	170.5	163.3	57.1	68.7	24.5	105
$\Sigma HREE$	28.51	29.83	25.35	23.73	24.32	11.65	16.41	6.11	18.43
$\Sigma LREE/\Sigma HREE$	6.65	6.05	6.20	7.18	6.71	4.90	4.19	4.01	5.70

a. Interpolated values, b. includes La and Ce values in Tables 2 and 4.

Table 5. Additional trace-element data for nine rocks from St Andrew Strait area.

Tuluman Islands

10A. Vesicular, partly crystalline, glassy rhyolite lava making up island of Cone 3.
11. Partly crystalline, glassy rhyolite lava from base of flow making up headland, southwestern coast of Tuluman Island.
13. Crystalline rhyolite lava from base of flow exposed in cliffs, southeastern coast of Tuluman Island.
16. Partly crystalline, glassy rhyolite lava from edge of 1956-57 lava flows, northwestern coast of Tuluman Island.
17A. Partly crystalline, glassy rhyolite lava from edge of 1956-57 lava flows, northeastern coast of Tuluman Island.

Lou Island

31. Crystalline rhyolite lava from flow of centre 1, 500 m south of extreme northeastern tip of island.
33. Crystalline rhyolite lava from same flow as 31, 100 m west of extreme northeastern tip of island.
02. Partly crystalline, glassy rhyolite lava from flow of centre 3, 700 m northeast of Solang village, northwestern coast.
24. Flow-banded, partly crystalline (including spherulites), glassy rhyolite lava probably from centre 3, 300 m east of Baun village, southeastern coast.
25. Flow-banded, partly crystalline, glassy rhyolite lava from flow of centre 3 (probably same flow as 24), 1.7 km east of Baun village, southeastern coast.
03. Flow-banded, partly crystalline, glassy rhyolite lava from flow of centre 7, 1.3 km southwest of Solang village, northwestern coast.
05. Partly crystalline, glassy rhyolite lava from flow of centre 8, directly west of high point marking centre 8, southwestern coast.
06. Obsidian (with bands of spherulites and numerous microlites) from rhyolite lava flow of centre 8, 2 km northwest of southern tip of island.
23. Flow-banded, partly crystalline, glassy rhyolite lava from flow of centre 8 at Monkol Point, southeastern coast.
19. Crystalline rhyolite lava from flow of centre 11, southern tip of island.

Pam Islands

55. Flow-banded, partly crystalline, glassy rhyolite lava from flow, southeastern coast of Pam Mandian.
56. Flow-banded, partly crystalline, glassy rhyolite lava from flow, northwestern coast of Pam Mandian.
57A. Flow-banded, partly crystalline, glassy rhyolite lava from flow, southwestern coast of Pam Lin.
59. Flow-banded, partly crystalline, glassy rhyolite lava from flow, western coast of of Pam Lin.

Baluan Island

38. Basalt lava from flow at Sabobarubay village, northwestern coast.
39. Basalt lava from small islet off Sone village, northwestern coast.
42. Basalt lava block from headland, 300 m north of twin scoria peaks, western coast.
43. Basalt lava from headland immediately south of twin scoria peaks, western coast.
45. Basalt lava from flow 1.5 km east-northeast of Bubanin village, southeastern coast.

Fedarb Islands

68C. Basalt from 1 m-wide dyke in cliff, southwestern coast of Sivisa.
68D. Basalt lava from flow in cliff, southwestern coast of Sivisa.
61. Dacite lava from northeastern part of flow making up Chokua.
67. Dacite lava from southwestern part of flow making up Small Sivisa.

Table 6. Rock-type and locality descriptions for samples whose analyses are listed in Tables 1-5.

Baluan Island may therefore be the marginal-basin equivalent of intra-oceanic volcanoes such as Hawaii and Reunion—that is, its development appears to have been independent of plate boundaries and the magmatic processes that accompany ocean-floor and marginal-basin distention. The Baluan rock compositions are consistent with the interpretation that St Andrew Strait overlies a mantle hot spot (Johnson & Smith, 1974).

Origin of TLP series

Baluan basalts parental to TLP rhyolites?

Some features of St Andrew Strait geochemistry are qualitatively consistent with the derivation of TLP rhyolites from parental Baluan-type basalts by crystal fractionation. $^{87}Sr/^{86}Sr$ values for both rock types are the same (Table 8), and the basalts are low in Rb, Ba, U,

	qfr	TiO_2	*ap*	*Rb*	*Ba*	*Pb*	*Sr*	*K/Rb*	*Ba/Rb*	*Rb/Sr*	*La*	*Ce*	*Y*	*La+Ce+Y*	*Th*	*U*	*Zr*	*Nb*	*Th/U*	*Zr/Nb*	*Zn*	*Cr*	*Ga*
qfr		—.942	—.809	.939	.450	—.529	—.951	—.559	—.888	.968	—.436	—.759	—.886	—.805	.676	.470	—.983	—.901	—.050	—.919	—.839	—.650	—.668
TiO_2			.842	—.935	—.590	.584	.947	.543	.873	—.926	.416	.761	.876	.797	—.639	—.524	.914	.868	.158	.808	.785	.704	.675
ap				—.783	—.605	.279	.826	.422	.686	—.805	.478	.656	.710	.691	—.455	—.355	.768	.691	.086	.726	.739	.476	.514
Rb					.514	—.585	—.879	—.763	—.973	.912	—.470	—.795	—.942	—.852	.613	.480	—.922	—.903	—.168	—.783	—.772	—.586	—.619
Ba						—.194	—.504	—.184	—.329	.482	—.157	—.266	—.440	—.340	.298	—.004	—.314	—.255	.022	—.320	—.498	—.309	—.070
Pb							.535	.400	.613	—.518	.296	.622	.628	.604	—.325	—.481	.578	.738	.363	.273	.446	.192	.595
Sr								.490	.818	—.975	.287	.620	.766	.662	—.574	—.490	.926	.817	.096	.906	.700	.649	.704
K/Rb									.836	—.577	.298	.518	.645	.567	—.311	—.326	.570	.593	.236	.446	.273	.275	.332
Ba/Rb										—.856	.483	.803	.925	.850	—.568	—.549	.903	.914	.242	.730	.678	.553	.669
Rb/Sr											—.328	—.665	—.789	—.700	.622	.499	—.943	—.826	—.123	—.934	—.721	—.568	—.620
La												.782	.587	.798	—.474	—.274	.447	.550	.068	.228	.640	.079	.401
Ce													.891	.982	—.638	—.491	.794	.896	.215	.522	.828	.379	.617
Y														.942	—.601	—.441	.889	.945	.145	.656	.869	.572	.657
La + Ce + Y															—.636	—.462	.842	.913	.170	.559	.869	.430	.636
Th																.283	—.631	—.588	.261	—.578	—.658	—.540	—.319
U																	—.521	—.544	—.783	—.397	—.296	—.177	—.425
Zr																		945	.107	.900	.812	.619	.741
Nb																			.197	.707	.817	.531	.777
Th/U																				—.033	—.045	—.245	.091
Zr/Nb																					.658	.619	.557
Zn																						.493	.488
Cr																							.504
Ga																							
Mean values		0.34	0.12	131	795	10	74	236	6.19	1.95	38	87	43	168	13	2.9	432	49	4.6	8.73	60	25	17
Standard deviation		0.09	0.07	19	25	3	18	11	0.85	0.80	3	7	7	16	1	0.6	98	7	1.2	1.01	11	2	1

qfr = 100 (Q + or)/(ab + an)
ap = normative apatite

Table 7. Correlation matrix and mean values for trace elements and selected petrological parameters for 16 rocks from Tuluman, Lou, and Pam Islands.

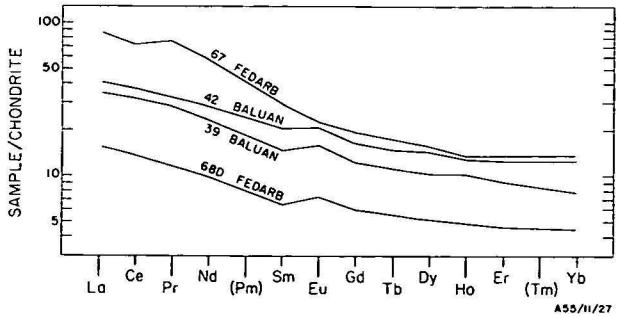

Figure 5. Chondrite-normalised rare-earth patterns for four rocks from Baluan and Fedarb Islands. Data listed in Tables 4 and 5.

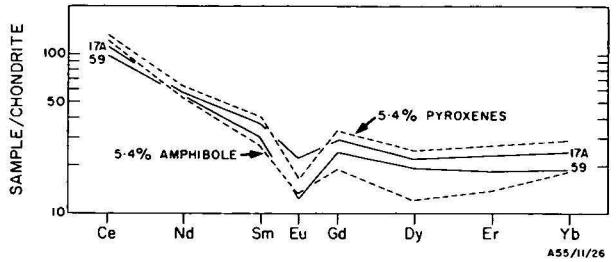

Figure 6. Chondrite-normalised rare-earth patterns for TLP rock samples 17A and 59 (solid lines) relative to two patterns for calculated values obtained after crystal extractions from sample 17A (see text).

Sample	*Island*	*Rock type*	$^{87}Sr/^{86}Sr$	*Reference*
16	Tuluman	rhyolite	0.7044	Page & Johnson(1974)
56	Pam Mandian		0.7043	
39	Baluan	basalt	0.7044	new analyses*
42	Baluan		0.7044	
68D	Sivisa		0.7033	
67	Small Sivisa	dacite	0.7033	

* R. W. Page (pers. comms. 1975, 1977). Analytical methods as described in Page & Johnson (1974). $2\sigma = 0.0001$.

Table 8. $^{87}Sr/^{86}Sr$ values for six rocks from St Andrews Strait area.

Th, Nb, and REE, and high in Cu, Ni, V, and Cr relative to the rhyolites. However, other lines of evidence are against crystal fractionation as a viable process:

(1) After extensive extraction of minerals containing different amounts of Ca, Al, Na and K, there appears to be no inherent reason why the TLP rhyolites should exhibit the striking 'buffered' relationship between molecular CaO and PI illustrated in Figure 7. Crystal fractionation might be expected to have produced peralkaline rocks (e.g. Barberi and others, 1975), or rhyolites low in PI values (e.g. Lowder & Carmichael, 1970), or perhaps even corundum-normative compositions, but not—by coincidence—rocks containing the same molecular amounts of Al_2O_3 and Na_2O+K_2O (after removal of all CaO by plagioclase fractionation; Johnson & Smith, 1974).

(2) In a basalt-to-rhyolite fractionation sequence, intermediate rocks may be expected to have erupted, but they appear to be absent.

(3) Abundances for Rb, Ba, and REE in the TLP rhyolites are apparently too low to have been derived by fractionation of Baluan-type basalts. Rigorous quantitative evaluation of possible fractionation relationships using crystal-extract calculations (e.g. Zielinski & Frey, 1970) is precluded by the apparent absence of the porphyritic rocks needed to follow the liquid line of descent. However, even assuming a bulk distribution coefficient ($D^{\text{minerals/liquid}}_{\text{Rb, Ba, REE}}$) of 0.2 (i.e. a very high value if the fractionating minerals were mainly olivine, clinopyroxene, orthopyroxene, and plagioclase), and only 95 percent crystallisation of the aphyric Baluan basalt 42, the values for Rb, Ba and REE calculated using the Rayleigh fractionation equation are greatly in excess of those found in the TLP rhyolites.

(4) The hypothetical fractionating process must be a highly efficient one. Large volumes of mafic magma would be required (probably two orders of magnitude greater than that for the rhyolites—see, for example, O'Nions & Grönvold, 1973), and the abundant, complementary cumulates from successive crystal extractions must be stored and effectively insulated from the phenocryst-poor rhyolites during their eruption.

(5) The Baluan basalts and TLP rhyolites were erupted from different volcanoes, implying independent courses of magmatic evolution, rather than development in the same magma chambers.

Crystal fractionation within the TLP series

In a qualitative sense, many of the relative differences in trace-element contents within the TLP series may be explained by extraction of appropriate minerals from a parental magma; each rock could be regarded as one member of a liquid line of descent, or the end product of a line of descent similar to those of the other TLP rocks. However, mineral-extract and trace-element-fractionation calculations do not provide results in support of this interpretation.

The normative mineral composition of sample 59 (a high *qfr* rock) can be derived from that of sample 17A (low *qfr*) by removal of about 18% plagioclase, 2.9% clinopyroxene, 2.5% orthopyroxene, 1.3% iron-titanium oxides, and 0.13% apatite. Using the Raleigh fractionation equation (e.g. Gast, 1968) and average distribution coefficients ($D^{\text{mineral/liquid}}_{\text{element}}$) for rhyolitic minerals collated by Arth & Hanson (1975), the concentrations of Sr, Rb, Ba and REE (i.e., elements whose D values are best known) have been calculated for a residual liquid resulting from the extraction of the above minerals (in the stated proportions) from a rock with the trace-element abundances in sample 59. The following conclusions are reached by comparing results with the trace-element abundances in sample 59.

(1) There is good agreement for Sr and Rb values (Sr = 47 ppm, Rb = 144 ppm for the calculated composition; Sr = 45 ppm, Rb = 150 ppm in sample 59).

(2) The calculated Ba content is 959 ppm, whereas the Ba content of sample 59 is 814. This discrepancy is probably not significant, however, because of uncertainty in the $D^{\text{plagioclase/liquid}}_{\text{Ba}}$ value used.

(3) Except for Eu, the calculated REE contents are all higher than those in sample 59 (Fig. 6). $D^{\text{apatite/liquid}}_{\text{REE values}}$ are known to be much greater than unity, but the difference in normative apatite content between samples 17A and 59 is too small to allow lower REE contents in the calculated liquid (see also Nagasawa & Schnetzler, 1971). Thus, the differences in normative mineral contents between samples 17 and 59 cannot account for the relative depletion in REE in sample 59.

$D^{\text{amphibole/liquid}}_{\text{REE}}$ values are also known to be greater than unity (e.g. Nagasawa & Schnetzler, 1971; Arth &

	Sample	Al_2O_3	FeOt/ MgO	Mg No.	Ni	Cr	K_2O	Na_2O/ K_2O	Rb	Ba	Sr	Cs	K/Rb	K/Ba	K/Cs x10⁻³	P_2O_5	TiO_2	Zr	Nb	Zr/Nb
BALUAN	42	15.22	2.06	52	16	31	0.79	4.02	26	355	289	0.46	254	19	14	0.20	1.63	123	20	6.15
	38	15.87	1.55	59	61	208	0.48	5.93	12	259	262	n.d.	308	14	—	0.15	1.40	98	14	7.00
	43	18.13	1.59	60	34	91	0.48	5.52	12	252	300	n.d.	333	16	—	0.16	1.25	89	14	6.36
	45	20.28	1.78	57	23	56	0.54	5.06	13	256	324	n.d.	346	18	—	0.13	1.10	81	12	6.75
	39	20.66	2.23	52	21	47	0.53	5.72	11	264	328	0.11	400	17	4	0.16	1.26	88	13	6.77
FEDARB	68C	17.62	1.27	67	72	149	0.32	7.88	5	95	353	n.d.	540	28	—	0.12	0.79	36	3	12.00
	68D	18.36	1.21	69	70	145	0.30	7.83	5	88	357	0.12	500	28	21	0.11	0.73	32	4	8.00
MORB		15.81	1.13	68	123	296	0.26	10.4	(1.02)	(12.2)	(124)	(0.013)	(1046)	(109)	(81)	0.15	1.39	(122)	(3.3)	(37)
OPTH		16.89	1.17	63	110	280	0.16	18.6	n.r.	9	122	n.r.	—	144	—	0.12	1.30	126	n.r.	—
OISB		15.20	1.89	59	372	124	0.60	4.2	⩽15	269	351	n.r.	(450)	19	—	0.34	2.63	(215)	(32)	(6.7)

FeOt = total iron as FeO.

Mg No. = (100 Mg^{2+})/(Mg^{2+} + Fe^{2+}), where Fe^{2+} is ferrous iron content calculated from reported FeO values.

n.d. = not determined, n.r. = not reported.

MORB: average values for mid-ocean ridge basalts, after Melsom & Thompson (1971); values in parenthesis are those given by Hart (1976) and Erlank & Kable (1976).

OPTH: average values for oceanic plagioclase tholeiites reported by Miyashiro, Shido, & Ewing (1969) and Thompson, Shido, & Miyashiro (1972).

OISB: ocean-island basalts; average values for 7 hypersthene-normative basalts with less than 7% MgO from Reunion Island, Indian Ocean (Upton & Wadsworth, 1972); values in parenthesis are averages for tholeiitic and alkali ocean-island basalts given by Erlank & Kable (1976) and Pearce & Cann (1973).

Table 9. Selected geochemical data for St Andrew Strait basalts, and comparative basalt data from other areas.

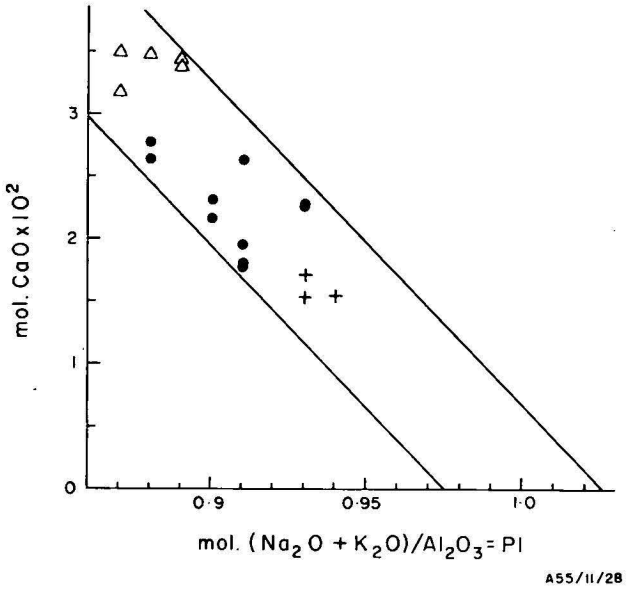

Figure 7. Molecular CaO versus PI (peralkalinity index) diagram. Triangles: Tuluman Islands. Dots: Lou Island. Crosses: Pam Islands. Two parallel lines contain all sample points, and correspond to PI value of 1 + 0.025 where CaO equals zero (see text).

Barker, 1976; Zielinski & Lipman, 1976), but even where 5.4 percent amphibole is added to the mineral-extract assemblage at the total expense of pyroxene the calculated REE values (using $D_{REE}^{amphibole/liquid}$ values for rhyolites; Arth & Hanson, 1975) do not conform with those for sample 59 (Fig. 6). There is good agreement for Nd, Sm, Eu, and Yb, but calculated Ce abundances, and Eu/Eu* values are still greater than that in sample 59; and Gd, Dy and Er are much lower than in sample 59. Appropriate amphibole-pyroxene mixtures, or systematically lower $D_{REE}^{amphibole/liquid}$ values would allow higher, calculated Gd, Dy, and Er values, but they would also raise values for the other REE. Thus, on the basis of $D_{REE}^{mineral/liquid}$ values known at present, there appears to be no likely combination of minerals that can account for the REE pattern of sample 59 by their removal from sample 17A.

Other possible models

Four other hypotheses for the derivation of felsic magmas are also considered inapplicable to the origin of the TLP rhyolites.

(1) Partial melting of old continental crust is precluded by the low $^{87}Sr/^{86}Sr$ values of the rhyolites, and by the presence of the volcanoes in a marginal basin several hundreds of kilometres from the nearest known continental material.

(2) For two reasons, partial melting of sediments is also an unlikely process: (a) the crust beneath St Andrew Strait is believed to consist mainly of igneous, rather than sedimentary rocks (see above); (b) the TLP rhyolites do not have the low Na_2O and high $Al_2O_3/(Na_2O + K_2O + CaO)$ values characteristic of granites thought to have been derived from metasedimentary sources (the 'S-type' granites of Chappell & White, 1974).

(3) Partial melting of upper mantle peridotite as a method of rhyolite production is precluded by the results of laboratory experiments. Silica-rich magmas at mantle pressures do not have the liquidus magnesian olivine required for mantle-derived magmas (e.g. Wyllie and others, 1976), and equilibrium glasses containing more than 70 percent SiO_2 have not been reported from experimental runs (e.g. Mysen and others, 1974).

(4) Liquid immiscibility is also regarded as an unlikely process. It may be important in magmas especially rich in iron and alkalies (e.g., Naslund, 1976), and may account for small-scale felsic layering found in parts of the Skaergaard intrusion (McBirney, 1975), but the process is unlikely to have had a major influence on igneous systems (e.g. Irvine, 1976). Many aspects of liquid immiscibility remain experimentally untested, and its application to the St Andrew Strait area introduces such problems as the identity of the magma that exsolves, as well as that of the second immiscible phase.

The most likely origin is considered to be partial melting of basaltic crust. If the small amounts of silica-rich residuum found in tholeiitic mafic rocks (e.g. Macdonald & Katsura, 1964; Wilkinson & Duggan, 1973) were melted along with other low-melting-point crystal fractions and extracted, compositions similar to those of the TLP rhyolites might be formed. This derivation would overcome several of the points listed above as objections to crystal fractionation—for example, no intermediate rocks need be produced, and no massive accumulations of residual crystals would be required. It would also account for the mol. CaO:PI relationship (Fig. 7): the first-formed liquid would be dominantly quartz and K-feldspar-rich, and mol. $Na_2O + K_2O$ would therefore be equal to mol. Al_2O_3, but as more plagioclase entered the melt, trends of increasing CaO and decreasing PI values would be generated away from the point where PI equals 1 (Johnson & Smith, 1974). The basaltic crust beneath St Andrew Strait is regarded as having formed sufficiently recently in the Bismarck Sea marginal basin that the $^{87}Sr/^{86}Sr$ values of the derivative liquids are not significantly different from those of the basalts of Baluan Island (Table 8).

Trace-element partitioning during crustal anatexis

Calculations have been made to determine some of the geochemical effects of basalt anatexis. The overall conclusion is that different degrees of partial melting of a more or less homogeneous source may account for the trace element abundances in the TLP rhyolites.

The formulations of Shaw (1970) for batch and fractional* melting were used to determine the Sr, Ba and Rb contents in liquids derived from a model mafic crust composed of plagioclase (60%), clinopyroxene (25%), olivine (7.5%) and orthopyroxene (7.5%), using the average distribution coefficients for these minerals tabulated by Arth & Hanson (1975, Table A1, for basaltic and andesitic rocks). Similar results for REE, Zr, and Nb have not been obtained because (1) the abundances of these elements appear to be controlled by accessory phases (see above), (2) the identity and abundance of these accessory minerals is not known, and (3) there is insufficient information on their distribution coefficients. However, because the accessories are regarded as refrac-

*** The fractional-melting equation is based on the assumption that infinitesimal amounts of liquid are continually removed from the source. Irrespective of the opinion that this process is geologically unrealistic (e.g. Arth, 1976), the results used in this study are for low degrees of melting (<5%) and the results for batch and fractional melting are quite similar. Widely different results are obtained only for large degrees of melting (>25%).**

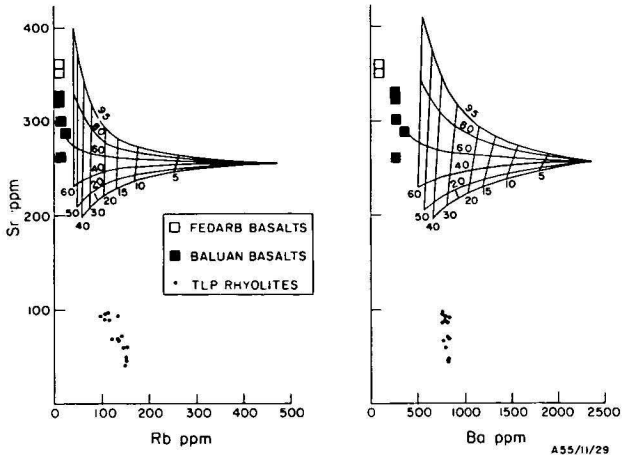

Figure 8. Sr-Rb-Ba relationships in St Andrew Strait rocks. Upright lines represent liquid compositions produced by the same degree of melting (5-60%) of mafic crust with the Sr, Rb, and Ba contents of Baluan basalt 42 (Table 4), and made up of 60% plagioclase, 25% clinopyroxene, 7.5% olivine, and 7.5% orthopyroxene. Curves converging to horizontal represent liquid compositions containing the same amount of melted plagioclase (1-95%). Curve 60 is modal-melting curve.

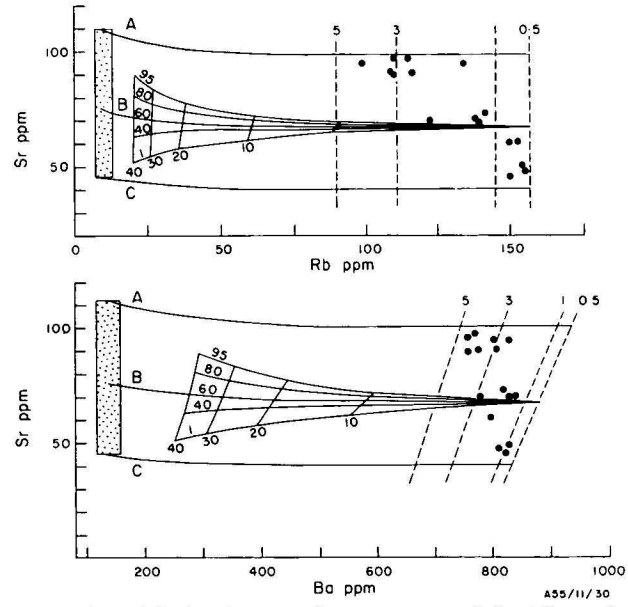

Figure 9. Calculated approximate ranges of Sr, Rb, and Ba (stippled areas) required to generate Sr, Rb and Ba contents of TLP rocks (solid dots) by small (0.5-5%) degrees of partial melting. Curves A, B, and C are selected modal-melting curves for the following compositions: A, Sr = 110 ppm, Rb = 9 ppm, Ba = 140 ppm; B, Sr = 75 ppm, Rb = 9 ppm, Ba = 133 ppm; C, Sr = 45 ppm, Rb = 9 ppm, Ba = 125 ppm. Dashed lines join points representing same melting percentages on curves A and C. Non-modal melting curves are shown for composition B: upright lines represent liquid compositions obtained by same degree of melting (10-40%); curves converging to horizontal represent compositions containing same amount of melted plagioclase (1-95%).

tory phases, the effect of increasing degrees of partial melting is considered to be an increase in the melting proportions of the minerals, and therefore an increase in the REE, Zr, and Nb abundances in the derivative liquids as their *qfr* values decrease (Fig. 2).

The Sr, Rb and Ba values of the TLP rhyolites cannot be generated by small degrees (0.5-5%) of batch melting from a mafic crust containing the same amounts of Sr, Rb and Ba as sample 42, an aphyric basalt from Baluan Island (Fig. 8). 10-40 percent partial melting is required to generate the same Rb and Ba contents, and even with 40 percent melting and only 1 percent plagioclase entering the melt, the calculated Sr content is at least twice as high as the TLP Sr values. The presumed mafic source of the TLP magmas is therefore not as high in Sr, Rb, and Ba as is the Baluan basalt. The inclusion of amphibole in the calculations does not appreciably affect this conclusion, and if added at the expense of plagioclase the calculated Sr values are even higher. More acceptable values are within the following ranges: Sr = 45-110 ppm, Rb = 7.5-12.5 ppm, Ba = 115-155 (Fig. 9). These ranges exclude all the analysed basaltic rocks from St Andrew Strait (Rb values for the Fedarb basalts fall within the calculated Rb range, but their Ba, and especially Sr values are far too high; their $^{87}Sr/^{86}Sr$ values are also too low—see below). The calculated ranges also exclude typical mid-ocean-ridge basalts which, although having comparable Sr abundances, are nevertheless much lower in Rb and Ba (e.g. Melsom & Thompson, 1971; Hart, 1976; Fleet, Henderson, & Kempe, 1976; see Table 9). Comparable Rb and Ba values, however, have been reported for basalts from, for example, the South Sandwich marginal basin (Tarney, Saunders, & Weaver, 1977), and therefore the calculated Rb and Ba abundances in the presumed basaltic crust beneath St Andrew Strait are consistent with the interpretation that marginal-basin basalts have some geochemical features transitional between those of mid-ocean ridge and island-arc or ocean-island basalts.

The Rb versus *qfr* relationship in the TLP rocks (Fig. 2) can be accounted for by increasing degrees of batch melting (0.5-5%) of a source containing about 9 ppm Rb (Fig. 9). In contrast, however, the strong enrichment in Sr as *qfr* values decrease cannot be accounted for by increased melting percentages using the equations of Shaw (1970), for a source with uniform Sr content. This conclusion is illustrated in Figure 9 where the dashed, equal-percent melting lines were selected from a range of results so that they cut across the bands of points representing TLP rocks at an acute angle as possible (without points representing degrees of melting falling outside the range 0.5-5%). This procedure maximises the possible effect of degrees of partial melting, but even under these conditions, the TLP trend is not at right angles to the dashed lines, and the variation in Sr therefore cannot be accounted for by different degrees of batch melting of the same source. Moreover, the non-modal melting curves for composition B (Fig. 9) at low degrees of partial melting are very close to the modal melting curve, indicating that the amount of plagioclase entering the liquid has a minimal effect on the Sr abundances. Non-modal melting would have a greater effect if the TLP magmas were generated by larger degrees of partial melting (10-40%) of crust of intermediate composition with Rb and Ba values similar to, or greater than, those of the aphyric Baluan basalt (Fig. 7). However, Sr contents must still be low—probably less than

100 ppm—and few intermediate igneous rocks have less than 100 ppm Sr.

The Sr versus *qfr* relationship may be due to partial melting of a source region characterised by a range of Sr contents. A more fractionated basaltic source would have higher Sr contents and, assuming the same thermal input as in a less fractionated (low Sr) source, a greater proportion of it would melt. For example, in Figure 9, 3-5 percent melting of a source with about 110 ppm Sr will produce a melt containing about 98 ppm Sr (i.e. similar to the Sr contents in low *qfr* TLP rhyolites) whereas 1 percent melting of a source with about 45 ppm Sr gives a melt containing only 40 ppm Sr (similar to values in high *qfr* TLP rocks). These percent-melting values and the Ba values for TLP rocks are also consistent with the high Sr source having relatively high Ba contents (compare curves A and C in Fig. 9). Similarly, the relatively fractionated source may have higher REE, Zr, and Nb contents (held in accessory minerals), and with 3-5 percent melting may produce magmas characterised by high REE, Zr, and Nb abundances compared to less fractionated sources. However, these arguments do not apply to Rb. As shown in Figure 9, if the fractionated source had a substantially higher Rb content than a less fractionated source with 9 ppm Rb, the lower Rb values in the TLP rocks require excessive melting percentages >5%). Rb contents in the rhyolites therefore appear to be strongly dependent on different degrees of melting, rather than different Rb contents in the source. Moreover, if a source composition characterised by ranges of trace element contents is the primary control for the ranges of abundances in the rhyolites, the crust must be laterally zoned, each volcano overlying crust characterised by particular trace-element contents. This is possible, but is regarded as a somewhat *ad hoc* and unsatisfactory explanation.

The equations of Shaw (1970) assume that the distribution coefficients do not change during partial melting. However, $D_{Sr}^{plagioclase/liquid}$ values are reported to be lower in plagioclase richer in anorthite (e.g., Arth & Hanson, 1975), presumably because Sr substitutes preferentially in K rather than Ca sites. Higher Sr abundances in liquids formed by higher degrees of partial melting may therefore be accounted for by a decrease in $D_{Sr}^{plagioclase/liquid}$ during partial melting as the feldspar becomes more calcic. Similarly, the Ba versus *qfr* relationship in which higher Ba abundances are in rocks with intermediate *qfr* values (Fig. 2) may be due to $D_{Sr}^{plagioclase/liquid}$ values initially dcreasing as the feldspar becomes significantly poorer in K.

In summary, therefore, the trace-element contents of the TLP rhyolites are probably best accounted for by different, but generally low (0.5-5%) degrees of partial melting of an essentially homogeneous basaltic source. However, the batch-melting formulation of Shaw (1970) does not strictly reproduce the required melting characteristics. A decrease in $D_{Sr, Ba}^{plagioclase/liquid}$ values, and an increase in the melting proportions of accessory phases containing REE, Zr, and Nb, are required as the degree of partial melting increases.

Fedarb rocks

The volcanic rocks of the Fedarb Islands are in marked compositional contrast to those of the other St Andrew Strait islands. The small size of the Fedarb Islands, and the limited extent of subaerial rock outcrop, prevent collection of samples that may be more representative of the volcano, but from the available data no close petrological relationship can be established between the basalts and dacite of the Fedarb group and the Baluan basalts and TLP rhyolites.

Compared to the olivine-normative basalts of Baluan, the quartz tholeiites of the Fedarb Islands are lower in K_2O, Na_2O, TiO_2, P_2O_5, Rb and Ba (Tables 3 and 4), lower in $^{87}Sr/^{86}Sr$ (Table 8) and REE (Table 5), and higher in K/Rb, Cu, Ni, Cr, and Mg-number (Tables 4 and 9); they therefore cannot have been produced by fractionation of olivine, clinopyroxene, and plagioclase from Baluan-type basalts. Furthermore, the different $^{87}Sr/^{86}Sr$ values (Table 8) preclude derivation of both basalt types from the same mantle source.

The Fedarb basalts are similar in some respects to mid-ocean ridge basalts. The low $^{87}Sr/^{86}Sr$ value (0.7033) is within the range for ridge basalts (e.g. Hofman & Hart, 1975), TiO_2 and P_2O_5 values are appropriately low, and K_2O values are only slightly higher than the characteristically low K_2O contents of ridge basalts (Table 9). Nevertheless, in the Fedarb basalts, Rb, Ba, Sr, and Cs are higher, K/Rb, K/Ba, and K/Cs are much lower, and in sample 68D LREE are enriched relative to HREE (Fig. 5; the REE pattern has a positive Eu anomaly—the sample contains plagioclase phenocrysts). The Fedarb tholeiites more closely resemble quartz tholeiites found in island-arc regions (e.g. Johnson, 1977), although the $^{87}Sr/^{86}Sr$ values is very slightly lower than those reported for rocks at the southern margin of the Bismarck Sea (range 0.7034-0.7041; Page & Johnson, 1974). Furthermore, FeO + Fe_2O_3 values are slightly higher (comparing rocks with the same SiO_2 content), and Mg-numbers are higher than for most south Bismarck Sea rocks.

The major-element composition of the Fedarb dacite (Johnson & Smith, 1974) and several aspects of its trace-element geochemistry, are consistent with a derivation from Fedarb-type quartz tholeiite basalt by crystal fractionation (although intermediate members of the fractionation sequence are not known. Rb, Ba, Rb/Sr, Cs, Hf, REE, Th, U, La/Yb are higher in the dacites, Cu, Ni, V, and Cr are lower (Tables 4 and 5, Fig. 5), and $^{87}Sr/^{86}Sr$ values are the same (Table 8). However, other aspects of the geochemistry are difficult to reconcile with a fractionation relationship between basalt and dacite. Despite the pronounced difference in normative anorthite content, the dacite contains more Sr than do the basalts, and the Eu anomaly for one dacite sample (Table 5) is not pronounced. Another anomalous feature is the higher K/Rb values of the dacite compared to the basalts. In view of the limited data available for the Fedarb rocks, the significance of these differences remains uncertain.

Conclusions

The four magma types represented in St Andrew Strait appear to have had largely independent lines of evolution. The basalts of Baluan Island are mantle derived, and have undergone crystal fractionation. Different degrees of partial melting of a basaltic source poorer in several LILE, but isotopically similar to the Baluan basalts, may account for chemical variation within the TLP rhyolites. On the other hand, the Fedarb Islands basalts are relatively primitive quartz tholeiites derived from mantle lower in $^{87}Sr/^{86}Sr$ than the mantle that gave rise to the Baluan basalts. The origin of the Fedarb dacite is uncertain; crystal fractionation of a Fedarb-type basaltic parent is one possibility, but partial

melting of crust in different composition to that underlying the TLP volcanoes cannot be discounted.

The Baluan basalts have compositional similarities to those found on oceanic islands that are believed to have formed from mantle hot spots. In addition, the TLP rocks resemble some rhyolites formed above the Iceland hot spot, that are also thought to have been derived by melting of young crust (e.g. O'Nions & Grönvold, 1973). By analogy, therefore, St Andrew Strait may be underlain by a diapir-like mass of peridotite which has produced not only basaltic volcanism, but also sufficient heat to partially melt overlying basaltic crust. This interpretation will remain a working hypothesis until detailed geophysical studies are made of the crust and upper mantle characteristics of the St Andrew Strait area.

Acknowledgements

We gratefully acknowledge the assistance of the following colleagues: R. A. Davies (sample collection), B. W. Chappell and R. Freeman (X-ray fluorescence spectrometric analysis), W. B. Nance and P. Muir (spark source mass spectrographic analysis), R. C. Price and R. H. MacDuff (computations), and R. J. Arculus (discussions, and criticism of draft manuscript). We thank B. W. Chappell and A. Ewart for reviewing the paper. The figures were drawn by M. Steele.

References

ARTH, J. G., 1976—Behaviour of trace elements during magmatic processes—a summary of theoretical models and their application. *Journal of Research of the US Geological Survey*, **4**, 41-7.

ARTH, J. G., & BARKER, F., 1976—Rare-earth partitioning between hornblende and dacitic liquid and implications for the genesis of trondjemitic-tonalitic magmas. *Geology*, **4**, 534-6.

ARTH, J. G., & HANSON, G. N., 1975—Geochemistry and origin of the early Precambrian crust of northeastern Minnesota. *Geochimica et Cosmochimica Acta*, **39**, 325-62.

BARBERI, F., FERRARA, G., SANTACROCE, R., TREUIL, M., & VARET, J., 1975—A transitional basalt—pantellerite sequence of fractional crystallization, the Boina Centre (Afar Rift, Ethiopia). *Journal of Petrology*, **16**, 22-56.

BRYAN, W. B., THOMPSON, G., FREY, F. A., & DICKEY, J. S., 1976—Inferred geologic settings and differentiation in basalts from the Deep-Sea Drilling Project. *Journal of Geophysical Research*, **81**, 4285-304.

BUDDINGTON, A. F., & LINDSLEY, D. H., 1964—Iron-titanium oxide minerals and synthetic equivalents. *Journal of Petrology*, **5**, 310-57.

CARMICHAEL, I. S. E., 1967—The iron-titanium oxides of salic volcanic rocks and their associated ferromagnesian silicates. *Contributions to Mineralogy and Petrology*, **14**, 36-64.

CHAPPELL, B. W., & WHITE, A. J. R., 1974—Two contrasting granite types. *Pacific Geology*, **8**, 173-4.

CONNELLY, J. B., 1974—A structural interpretation of magnetometer and seismic profiler records in the Bismarck Sea, Melanesian Archipelago. *Journal of the Geological Society of Australia*, **21**, 459-69.

CONNELLY, J. B., 1976—Tectonic development of the Bismarck Sea based on gravity and magnetic modelling. *Geophysical Journal of the Royal Astronomical Society*, **46**, 23-40.

COOMBS, D. S., 1963—Trends and affinities of basaltic magmas and pyroxenes as illustrated on the diopside-olivine-silica diagram. *Mineralogical Society of America Special Paper* **1**, 227-50.

ERLANK, A. J., & KABLE, E. J. D., 1976—The significance of incompatible elements in Mid-Atlantic Ridge basalts from 45°N with particular reference to Zr/Nb. *Contributions to Mineralogy and Petrology*, **54**, 281-91.

EWART, A., MATEEN, A., & ROSS, J. A., 1976—Review of mineralogy and chemistry of Tertiary central volcanic complexes in southeast Queensland and northeast New South Wales. *In* JOHNSON, R. W. (Editor), VOLCANISM IN AUSTRALASIA, 21-39. *Elsevier, Amsterdam.*

EWART, A., OVERSBY, V. M., & MATEEN, A., 1977—Petrology and isotope geochemistry of Tertiary lavas from the northern flank of the Tweed volcano, southeastern Queensland. *Journal of Petrology*, **18**, 73-113.

EWART, A., & STIPP, J. J., 1968—Petrogenesis of the volcanic rocks of the central North Island, New Zealand, as indicated by a study of Sr^{87}/Sr^{86} ratios, and Sr, Rb, K, U, and Th abundances. *Geochimica et Cosmochimica Acta*, **32**, 699-736.

EWART, A., TAYLOR, S. R., & CAPP, A. C., 1968—Trace and minor element geochemistry of the rhyolitic volcanic rocks, central North Island, New Zealand. *Contributions to Mineralogy and Petrology*, **18**, 76-104.

FLEET, A. J., HENDERSON, P., & KEMPE, D. R. C., 1976—Rare earth element and related chemistry of some drilled southern Indian Ocean basalts and volcanogenic sediments. *Journal of Geophysical Research*, **81**, 4257-268.

GAST, P. W., 1968—Trace element fractionation and the origin of tholeiitic and alkaline magma types. *Geochimica et Cosmochimica Acta*, **32**, 1057-86.

GILL, J. B., 1976a—Composition and age of Lau Ridge and Basin volcanic rocks: implications for evolution of inter-arc basins. *Geological Society of America—Bulletin* **87**, 1384-95.

GILL, J. B., 1976b—Evolution of the mantle: geochemical evidence from alkali basalt: comment and reply. *Geology*, **4**, 625-6.

HART, S. R., 1976—LIL element geochemistry, leg 34 basalts. *In* YEATES, R. S., & HART, S. R. (Editors), INITIAL REPORTS OF THE DEEP SEA DRILLING PROJECT, **34**, 283-8, *US Government Printing Office, Washington.*

HART, S. R., GLASSLEY, W. E., & KARIG, D. E., 1972—Basalts and seafloor spreading behind the Mariana island arc. *Earth and Planetary Science Letters*, **15**, 12-8.

HASKIN, L. A., FREY, F. A., SCHMITT, R. A., & SMITH, R. H., 1966—Meteoric, solar and terrestrial rare-earth distributions. *Physics and Chemistry of the Earth*, **7**, 169-321.

HAWKINS, J. W., Jr, 1976—Petrology and geochemistry of basaltic rocks of the Lau Basin. *Earth and Planetary Science Letters*, 28, 283-97.

HOFMANN, A. W., & HART, S. R., 1975—An assessment of local and regional isotopic equilibrium in a partially molten mantle. *Carnegie Institution of Washington—Yearbook* **74**, 195-210.

HUBBARD, N. J., 1969—A chemical comparison of ocean ridge, Hawaiian tholeiitic and Hawaiian alkalic basalts. *Earth and Planetary Science Letters*, **5**, 346-52.

IRVINE, T. N., 1976—Metastable liquid immiscibility and MgO-FeO-SiO_2 fractionation patterns in the system Mg_2SiO_4-Fe_2SiO_4-$CaAl_2SiO_2O_8$-$KAlSi_3O_8$-SiO_2. *Carnegie Institution of Washington—Yearbook* **75**, 597-611.

JOHNSON, R. W., 1977—Distribution and major-element chemistry of late Cainozoic volcanoes at the southern margin of the Bismarck Sea, Papua New Guinea. *Bureau of Mineral Resources, Australia—Report* **188**.

JOHNSON, R. W., & DAVIES, R. A., 1972—Volcanic geology of the St Andrew Strait islands, Papua New Guinea. *Department of Lands, Surveys and Mines, Papua New Guinea—Notes on Investigation* **72-002** (unpublished).

JOHNSON, R. W., & SMITH, I. E., 1974—Volcanoes and rocks of St Andrew Strait, Papua New Guinea. *Journal of the Geological Society of Australia*, **21**, 333-51.

KARIG, D. E., 1973—Comparison of island arc-marginal basin complexes in the north-west and south-west Pacific. *In* COLEMAN, P. J. (Editor), THE WESTERN PACIFIC ISLAND ARCS MARGINAL SEAS GEOCHEMISTRY, 355-64, *University of Western Australia Press, Perth.*

KAY, R., HUBBARD, N. J., & GAST, P. W., 1970—Chemical characteristics of oceanic ridge volcanic rocks. *Journal of Geophysical Research*, **75**, 1585-613.

LE MAITRE, R. W., 1976—The chemical variability of some common igneous rocks. *Journal of Petrology*, **17**, 589-637.

LOWDER, G. G., & CARMICHAEL, I. S. E., 1970—The volcanoes and caldera of Talasea, New Britain: geology and petrology. *Geological Society of America—Bulletin* **81**, 17-38.

MACDONALD, G. A., & KATSURA, T., 1964—Chemical composition of Hawaiian lavas. *Journal of Petrology*, **5**, 82-133.

MASUDA, A., NAKAMURA, N., & TANAKA, T., 1973—Fine structures of mutually normalized rare-earth patterns of chondrites. *Geochimica et Cosmochimica Acta*, **37**, 239-48.

MCBIRNEY, A. R., 1975—Differentiation of the Skaergaard intrusion. *Nature*, **253**, 691-4.

MELSON, W. G., & THOMPSON, G., 1971—Petrology of a transform fault zone and adjacent ridge segments. *Royal Society of London—Philosophical Transactions, Series A*, **268**, 423-41.

MIYASHIRO, A., SHIDO, F., & EWING, M., 1969—Diversity and origin of abyssal tholeiite from the Mid-Atlantic Ridge near 24° and 30° north latitude. *Contributions to Mineralogy and Petrology*, **23**, 38-52.

MYSEN, B. O., KUSHIRO, I., NICHOLLS, I. A., & RINGWOOD, A. E., 1974—A possible mantle origin for andesitic magmas: discussion of a paper by Nicholls and Ringwood. *Earth and Planetary Science Letters*, **21**, 221-9.

NAGASAWA, H., & SCHNETZLER, C. C., 1971—Partitioning of rare earths, alkali and alkaline earth elements between phenocrysts and acidic igneous magma. *Geochimica et Cosmochimica Acta*, **35**, 953-68.

NANCE, W. B., & TAYLOR, S. R., 1976—Rare earth element patterns and crustal evolution—1. Australian post-Archaean sedimentary rocks. *Geochimica et Cosmochimica Acta*, **40**, 1539-51.

NASLUND, H. R., 1976—Liquid immiscibility in the system $KAlSi_3O_8$-$NaAlSi_3O_8$-FeO-Fe_2O_3-SiO_2 and its application to natural magmas. *Carnegie Institution of Washington—Yearbook* **75**, 592-597.

NOCKOLDS, S. R., 1954—Average chemical composition of some igneous rocks. *Geological Society of America—Bulletin* **65**, 1007-32.

NORRISH, K., & CHAPPELL, B. W., 1967—X-ray fluorescence spectrography. *In* ZUSSMAN, J. (Editor), PHYSICAL METHODS IN DETERMINATIVE MINERALOGY, 161-214. *Academic Press, London.*

NORRISH, K., & HUTTON, J. Y., 1969—An accurate X-ray spectrographic method for the analysis of a wide range of geological samples. *Geochimica et Cosmochimica Acta*, **33**, 431-54.

O'NIONS, R. K., & GRÖNVOLD, K., 1973—Petrogenetic relationships of acid and basic rocks in Iceland: Sr-isotopes and rare-earth elements in late and postglacial volcanics. *Earth and Planetary Science Letters*, **19**, 397-409.

PAGE, R. W., & JOHNSON, R. W., 1974—Strontium isotope ratios of Quaternary volcanic rocks from Papua New Guinea. *Lithos*, **7**, 91-100.

PEARCE, J. A., & CANN, J. R., 1973—Tectonic setting of basic volcanic rocks determined using trace element analysis. *Earth and Planetary Science Letters*, **19**, 290-300.

PECK, L. C., 1964—Systematic analysis of silicates. *United States Geological Survey—Bulletin* **1170**.

PETERMAN, Z. E., & HEMING, R. F., 1974—Sr^{87}/Sr^{86} ratios from the Rabaul caldera, Papua New Guinea. *Geological Society of America—Bulletin* **85**, 1265-8.

PETERMAN, Z. E., LOWDER, G. G., CARMICHAEL, I. S. E., 1970—Sr^{87}/Sr^{86} ratios of the Talasea series, New Britain, Territory of New Guinea. *Geological Society of America—Bulletin* **81**, 39-40.

REYNOLDS, M. A., & BEST, J. G., 1976—Summary of the 1953-57 eruption of Tuluman volcano, Papua New Guinea. *In* JOHNSON, R. W. (Editor), VOLCANISM IN AUSTRALASIA, 287-296. *Elsevier, Amsterdam.*

ROBINSON, P. T., ELDERS, W. A., & MUFFLER, L. J. P., 1976—Quaternary volcanism in the Salton Sea geothermal field. Imperial Valley, California. *Geological Society of America—Bulletin* **87**, 347-60.

SCHNETZLER, C. C., & PHILPOTTS, J. A., 1970—Partition coefficients of rare earth elements and barium between igneous matrix materials and rock forming mineral phenocrysts—II. *Geochimica et Cosmochimica Acta*, **34**, 331-40.

SCLATER, J. G., HAWKINS, J. W., MAMMERICKX, J., & CHASE, C. G., 1971—Crustal extension between the Tonga and Lau Ridges: petrologic and geophysical evidence. *Geological Society of America—Bulletin* **83**, 505-18.

SHAW, D. M., 1970—Trace element fractionation during anatexis. *Geochimica et Cosmochimica Acta*, **34**, 237-343.

SIGURDSSON, H., 1971—Feldspar relations in a composite magma. *Lithos*, **4**, 231-8.

SUN, S.-S., & HANSON, G. N., 1976a—Rare earth element evidence for differentiation of McMurdo volcanics, Ross Island, Antarctica. *Contributions to Mineralogy and Petrology*, **54**, 139-55.

SUN, S.-S., & HANSON, G. N., 1976b—Evolution of the mantle: geochemical evidence from alkali basalt: comment and reply. *Geology*, **4**, 626-31.

TARNEY, J., SAUNDERS, A. D., & WEAVER, S. D., 1977—Geochemistry of volcanic rocks from the island arcs and marginal basins of the Scotia Arc region. *In* TALWANI, M., & PITMAN, W. C. III (Editors), ISLAND ARCS, DEEP SEA TRENCHES, AND BACK-ARC BASINS, 367-77. *American Geophysical Union, Washington, D.C.*

TAYLOR, B., 1975—The tectonics of the Bismarck Sea region. *B.Sc. Honours thesis, University of Sydney* (unpublished).

TAYLOR, S. R., 1965—The application of trace element data to problems in petrology. *In* AHRENS, L. H., PRESS, F., RUNCORN, S. K., & UREY, H. C. (Editors), PHYSICS AND CHEMISTRY OF THE EARTH, **6**, 133-213.

TAYLOR, S. R., & GORTON, M. P., 1977—Geochemical application of spark source mass spectrography III: element sensitivity, precision, and accuracy. *Geochimica et Cosmochimica Acta*, **41**, 1375-80.

THOMPSON, G., SHIDO, F., & MIYASHIRO, A., 1972—Trace element distributions in fractionated oceanic basalts. *Chemical Geology*, **9**, 89-97.

UPTON, B. G. J., & WADSWORTH, W. J., 1972—Aspects of magmatic evolution on Reunion Island. *Royal Society of London—Philosophical Transactions, Series A*, **271**, 105-30.

WILKINSON, J. F. C., 1968—The magmatic affinities of some volcanic rocks from the Tweed Shield volcano, S.E. Queensland - N.E. New South Wales. *Geological Magazine*, **105**, 275-289.

WILKINSON, J. F. G., & DUGGAN, N. T., 1973—Some tholeiites from the Inverell area, New South Wales, and their bearing on low pressure tholeiite fractionation. *Journal of Petrology*, **14**, 339-48.

WILLCOX, J. B., 1976—Structure of the Bismarck Sea. *Bureau of Mineral Resources, Australia — Record* **1976/59** (unpublished).

WYLLIE, P. J., HUANG, W.-L., STERN, C. R., MAALØE, S., 1976—Granitic magmas: possible and impossible sources, water contents, and crystallization sequence. *Canadian Journal of Earth Sciences*, **13**, 1007-19.

ZIELINSKI, R. A., & FREY, F., 1970—Gough Island: evaluation of a fractionation crystallization model. *Contributions to Mineralogy and Petrology*, **29**, 242-54.

ZIELINSKI, R. A., & LIPMAN, P. W., 1976—Trace element variations at Summer Coon volcano, San Juan Mountains, Colorado, and the origin of continental-interior andesites. *Geological Society of America—Bulletin* **87**, 1477-85.

BMR Journal of Australian Geology & Geophysics, 3, 1978, 71-76

Clay modelling of the Fitzroy Graben

L. K. Rixon

Parallel shear, generated by sliding tongue and grooved boards past each other with clay on top produced, initially—in addition to the commonly recognised conjugate strike slip faults—a set of gently plunging folds at 30-45° to the wrench zone. Essentially vertical Riedel shears may subsequently become part of reverse drag structures as rotation of the clay, in response to the shearing couple, introduces a tensional component.

A single right-lateral movement in the model has reproduced the orientation of the major faults and folds within the Fitzroy graben of the Canning Basin. Major features such as the offshore depression on the southern margin of the Leveque shelf and part of the Halls Creek mobile zone may have been produced, as simulated in the model, by major dextral wrenching and, in the case of the Leveque shelf, by later subsidence of basement rocks. Absorption of lateral movement by the Halls Creek mobile zone may account for the less deformed, more platform-like northeast Canning Basin.

Experiments on the formation of faults, folds, and fractures using deformed clay or wax models have been conducted by several workers, including Mead (1920), Cloos (1955, 1968), and Wilcox, Harding & Seely (1973). Two of the more important experiments are those of Cloos, who has established the reproducibility and constancy of fracture angles developed in strained clay models; and Wilcox and others, who in studying wrench tectonics have shown an agreement between the fractures predicted from the theoretical strain ellipse, and observed folds and faults, in both model and real situations.

Tchalenko (1970) has critically examined the similarities between shear zones of different magnitudes, from microscopic up to earthquake faults on a regional scale, and shown the remarkable similarity in structures at all scales and in greatly varying materials. His analysis supports the contention that modelling of structures is a valid exercise.

This paper demonstrates that both tensional and wrench structures produced in the laboratory (and recorded by the above authors) can be reproduced in the one model by simple shearing of clay. The similarity between the fault and fold patterns produced in the model and those mapped in and adjacent to the Fitzroy Graben suggests that wrench movements may have been significant in the development of the graben. Rattigan (1967), and Smith (1968), advanced hypotheses of dextral wrenching of basement blocks to explain the folds and associated fracture systems of the Fitzroy Graben. Similarly, Willcox and others (1973) suggested that the Fitzroy Graben is probably a right-lateral wrench graben. Lack of unequivocal geological or geophysical evidence for major basement wrenching has prompted this attempt to reproduce the structures of the Fitzroy Graben by simple shearing of clay, and thus to test the wrench hypothesis indirectly.

The Fitzroy Graben forms the northern portion of the Canning Basin, which lies between the Kimberley and Pilbara blocks of Western Australia. The area has been mapped by Guppy, Lindner, Rattigan & Casey (1958), and Veevers & Wells (1961). Rattigan (1967), and Smith (1968), summarised the regional geology with special reference to the boundary lineaments and structure within the graben, the main features of which are outlined below.

The northern and southern margins of the graben have been mapped as northwest-southeast-trending fault systems. Both systems consist of a group of named faults, including the Dummer Range, Dampier and Fenton faults in the south, and Pinnacle, Pender Bay, Markham, Mueller, and Beagle Bay faults in the north (Figure 8). Large vertical displacements have been seismically mapped across most of the major bounding faults, with displacement of more than 4000 m on the Pinnacle and Markham faults. The southeastern limit of the graben has not been clearly defined. Most of the faults at the eastern end of the graben are mapped as en echelon zones: the Stansmore Range fault, which extends northwest for more than 160 km from the eastern end of the graben, is the exception.

Folding within the cover rocks consists of east-west trending anticlinal and synclinal systems (Figure 8). The southern anticlinal belt (Guppy and others, 1958) consists of five culminations; the central anticlinal belt has two culminations, the axes of which are en echelon or sinuous, and gently plunging away from the culminations. They are referred to here as the St George Range and Grant Range anticlines respectively. The Millyit Syncline is an asymmetric southeast-plunging syncline (Towner, R. R., in press) south of the St George Range anticline.

Experimental techniques

The apparatus consisted of four tongue-and-groove floor boards, arranged on a base board so that they could be slid past each other. Basement wrenching can be simulated by laying a clay cake 2 or 3 cm thick on top of the boards, and generating shearing couples by sliding the underlying boards. Wrenching in pre-existing grabens or against growth faults can be simulated by fixing extra boards on top of the original boards. Controlled simultaneous movement of two or more boards was produced by a lever system, with a piece of wood placed across the ends of the boards to ensure their equal movement (Fig. 1); when such movement was not required the lever system was used without the end piece of wood.

Divergent wrenching was achieved by placing a piece of sheet steel (1 mm thick) diagonally across a join in the boards (Fig. 2). Movement of the underlying board in a parallel fashion produced oblique (divergent or convergent depending on the sense of movement) wrenching in the clay overlying the steel.

Friction between the clay and underlying boards was varied in some trials by placing thin plastic sheet or

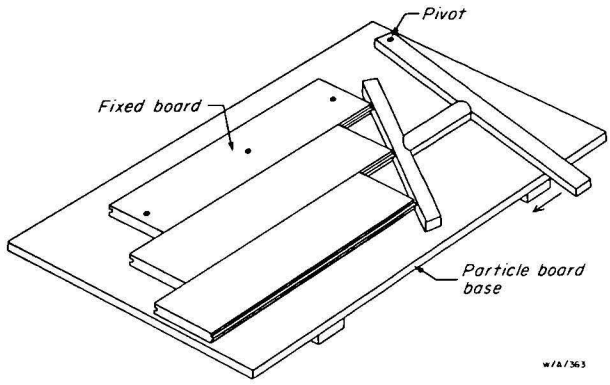

Figure 1. Board arrangement for simple parallel shear with controlled simultaneous movement.

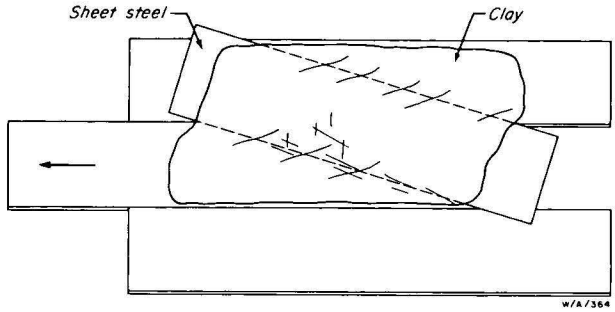

Figure 2. Diagonal arrangement of sheet steel ensures divergent wrenching in the overlying clay when the boards are moved in the direction indicated by the arrow above.

greaseproof paper between the two to enhance rotation and transmission of stress throughout the clay.

The red potters clay used for the experiment was prepared so that it had a tacky consistency, and clung tenaciously to the fingers. Development of both tensional and compressional features was enhanced by trowelling the clay surface with liberal quantities of water.

Structures observed in the model

Faults

Parallel shear, generated by sliding the tongue and grooved boards past each other with the clay on top, initially produced a conjugate set of strike slip faults with dihedral angle of about 60°, one set at 70-90° to the deforming couple (antithetic faults or conjugate Riedel shears), and one set at 10-30° to the couple (synthetic faults or Riedel shears).

Rotation of the strike-slip faults occurred on further application of the external shearing forces. Internal rotation and wedging of the clay for a right-lateral wrench tends to move the synthetic faults anti-clockwise parallel to the main wrench, while external rotation moves them away from the main wrench (Fig. 3). The resultant is little change in angle between the synthetic faults and the main wrench zone. Antithetic faults however have an internal rotation opposite to that of the synthetic faults, that is clockwise, and coupled with external clockwise rotation leads to rotation of these faults in a clockwise direction (Fig. 3). Thus synthetic faults remain favourably oriented in relation to the main wrench, so that they are able to accommodate large amounts of lateral movement—whereas antithetic faults become perpendicular to the

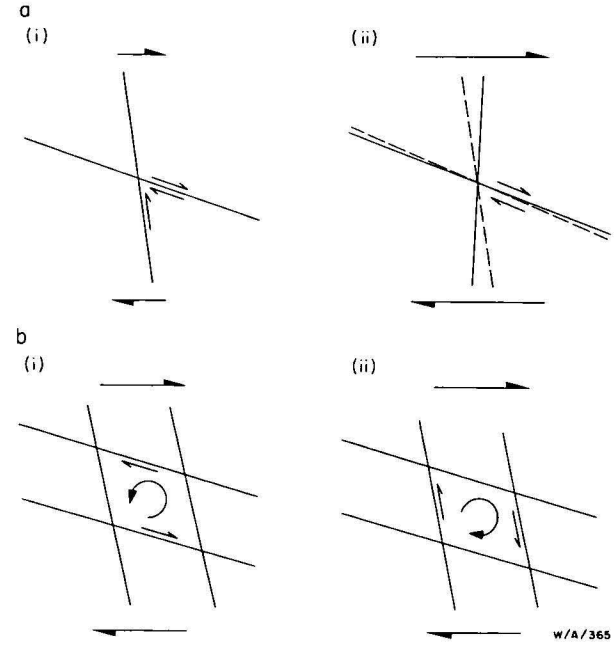

Figure 3. (a) Rotation of conjugate faults by shear movement. (i) Initial faults. (ii) Rotation after further movement. (b) Relative motions within individual shear blocks. (i) Internal rotation on synthetic faults. (ii) Internal rotation on antithetic faults.

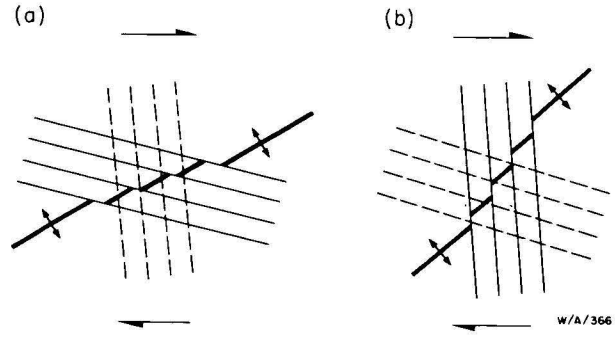

Figure 4. Rotation of fold axes by movement on either synthetic or antithetic faults. (a) Movement on synthetic faults results in clockwise rotation of the fold axis. (b) Movement on antithetic faults results in anticlockwise rotation of the fold axis.

wrench and can accommodate only small amounts of lateral movement. Further movement of the underlying boards caused the en echelon synthetic faults to coalesce into a major shear zone; still further movement leads to isolation of separate blocks within the main shear zone, either by development of shear lenses (Skempton, 1966) and/or by strong buckling of the adjacent synthetic faults and intervening clay. With the exception of strong buckling this sequence of events has been documented for shear zones of microscopic and mesoscopic scale (Morgenstem & Tchelenko, 1967) and postulated for large-scale earthquake faults (Tchelenko & Ambraseys, 1970). Buckling of strike-slip faults has been studied by Merzer & Freund (1975).

Divergent wrenching also developed a set of strike slip faults. However, tensional faults appeared first, with the orientation predicted by the strain ellipse—that is approximately 45°-50° to the shearing couple, bisecting the angle between the conjugate set. Sub-

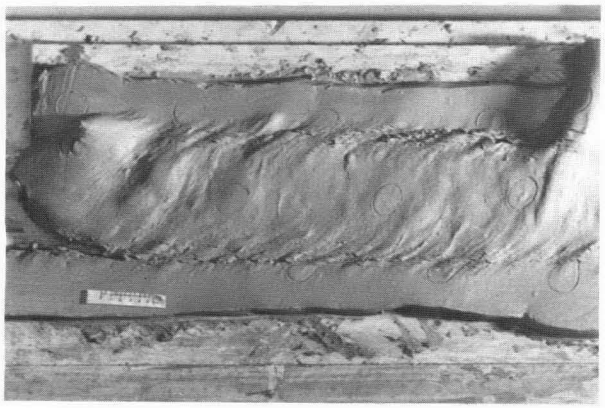

Figure 5. General view of one of the experimental trials showing the nature of the structures developed by simple parallel shear. The folding in the upper left and upper right of the clay represents the structural complexity in the King Sound area and the Halls Creek Mobile Zone respectively. The rift in the lower left corner of the clay represents the offshore depression south of the Leveque shelf.

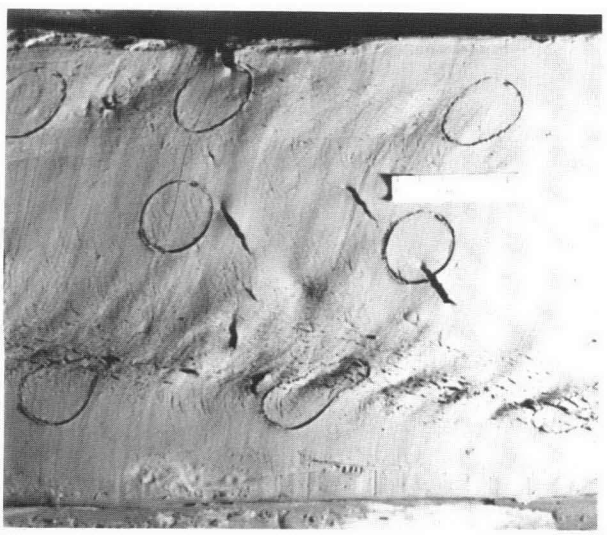

Figure 6. Simple divergent wrench model showing vertical tension faults which appear first and rotate before most of the conjugate shear faults become visible.

sequent movement quickly rotates these faults so that by the time the conjugate set appears the tensional set is at about 60° to the couple (Fig. 6).

Folds

Gently plunging folds developed at about 45° to the wrench zone, without the aid of plastic layers on or within the clay.

Close to the main shear zone, where rotation is maximal, the folds and antithetic faults were dragged into sigmoid shapes. Folds which first appeared at approximately 30°-45° to the wrench zone were rotated clockwise or anticlockwise depending on the predominance and relative displacement of either synthetic or antithetic faults, and plastic deformation. If synthetic faults predominate then slip is lateral and the folds are extended, reducing the angle between the fold axis and the wrench zone (Fig. 4a). If slip is largely on the antithetic faults and rotation anticlockwise for a dextral wrench then the angle between the folds and the main wrench increases in that zone (Fig. 4b). Thus folds with sinuous axes occur. The sinuosity is a function of relative movement on synthetic and/or antithetic faults.

Differential movement may occur along the wrench zone in response to varying resistances to movement when shearing forces are applied. A decrease in friction between the boards and clay at any position on the model may be accomplished by placing thin plastic sheet between the two at that position. Figure 5 shows the result of right-lateral wrench with increasing resistance to movement at the eastern end of the model. Compression produced folding of the clay and development of conjugate and tensional faults as predicted from the strain ellipse. Wrenching with extension usually lead to formation of graben-type structures with curving synthetic and antithetic faults.

Reverse Drag

Reverse drag (Hamblin, 1965) also called downbending, turnover, rollover, or sag is a structure often associated with down-to-basin faults, and refers to the beds on the downthrown block dipping into the fault plane in a manner exactly opposite to the flexure produced by drag.

These structures are best developed in areas of pure tension. Where transition from tensional to mainly wrench or strike-slip movement occurs, the curving master fault becomes vertical and displacement is strike-slip rather than dip or oblique-slip (Fig. 7).

External rotation

External rotation and deformation of the clay resulted in sigmoid shapes for the main fault zones in all the models. The major wrenches rotated clockwise upon application of dextral shearing forces. If the ends of the clay cakes were free to move simple rotation followed. However, if the ends were constrained either by wooden boards or by differential friction against the underlying boards (Fig. 5), then rifting occurred where rotation was away from the constraint or compressional folding, and overthrusting occurred where rotation was towards the constraint.

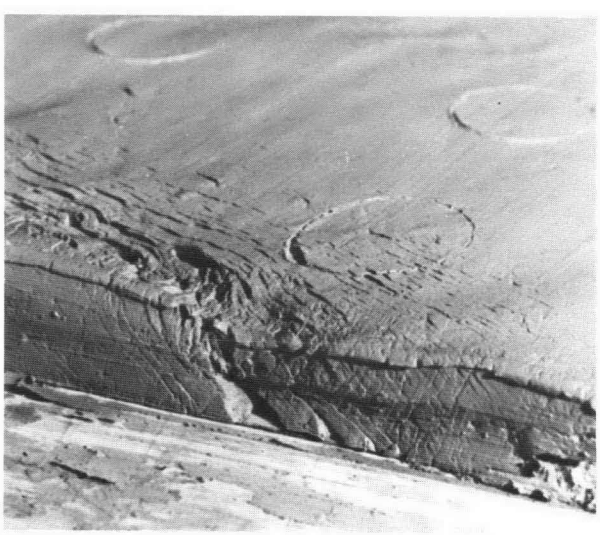

Figure 7. Close up view of reverse drag structures developed at the end of an essentially vertical wrench zone.

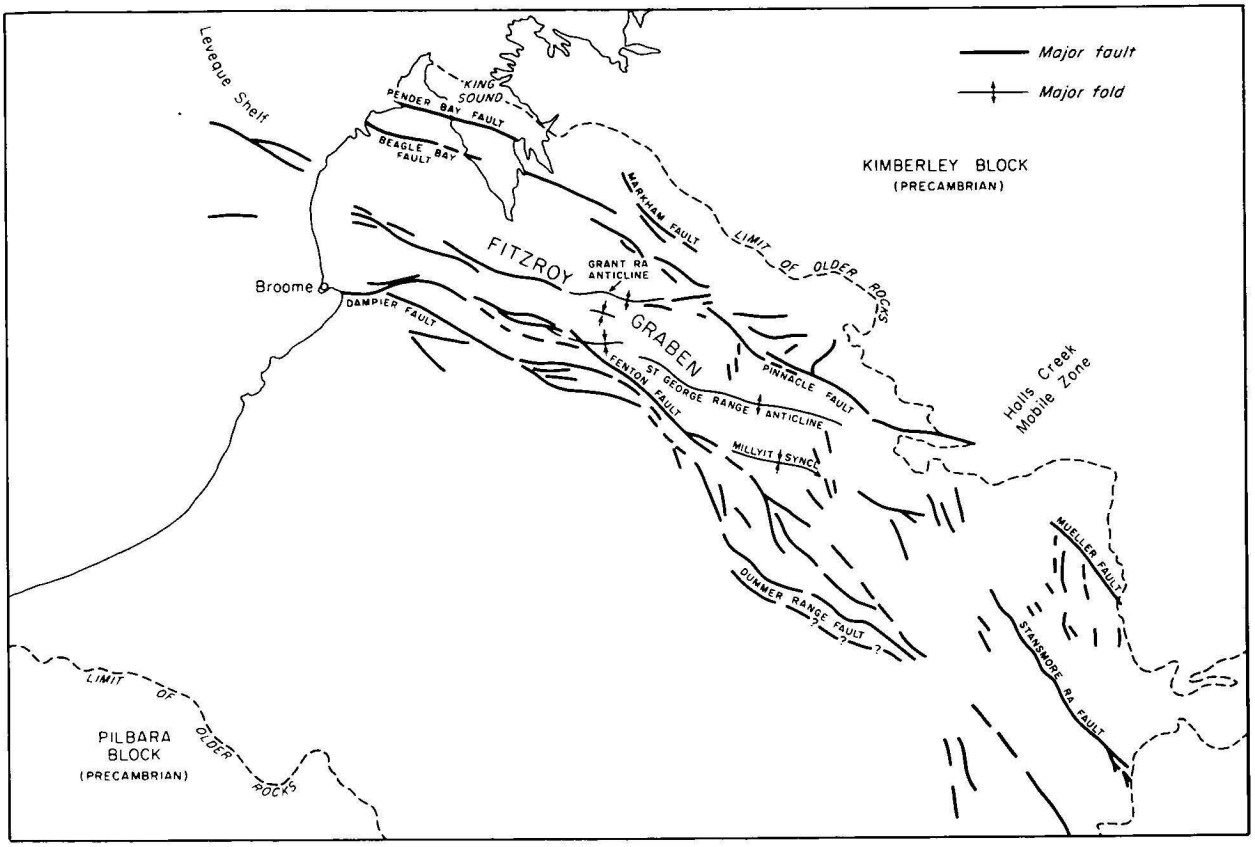

Figure 8. Structure of the Fitzroy Graben and associated tectonic elements. Fault system is subsurface (Lower Palaeozoic) and folds are surface mapped anticlines and synclines.

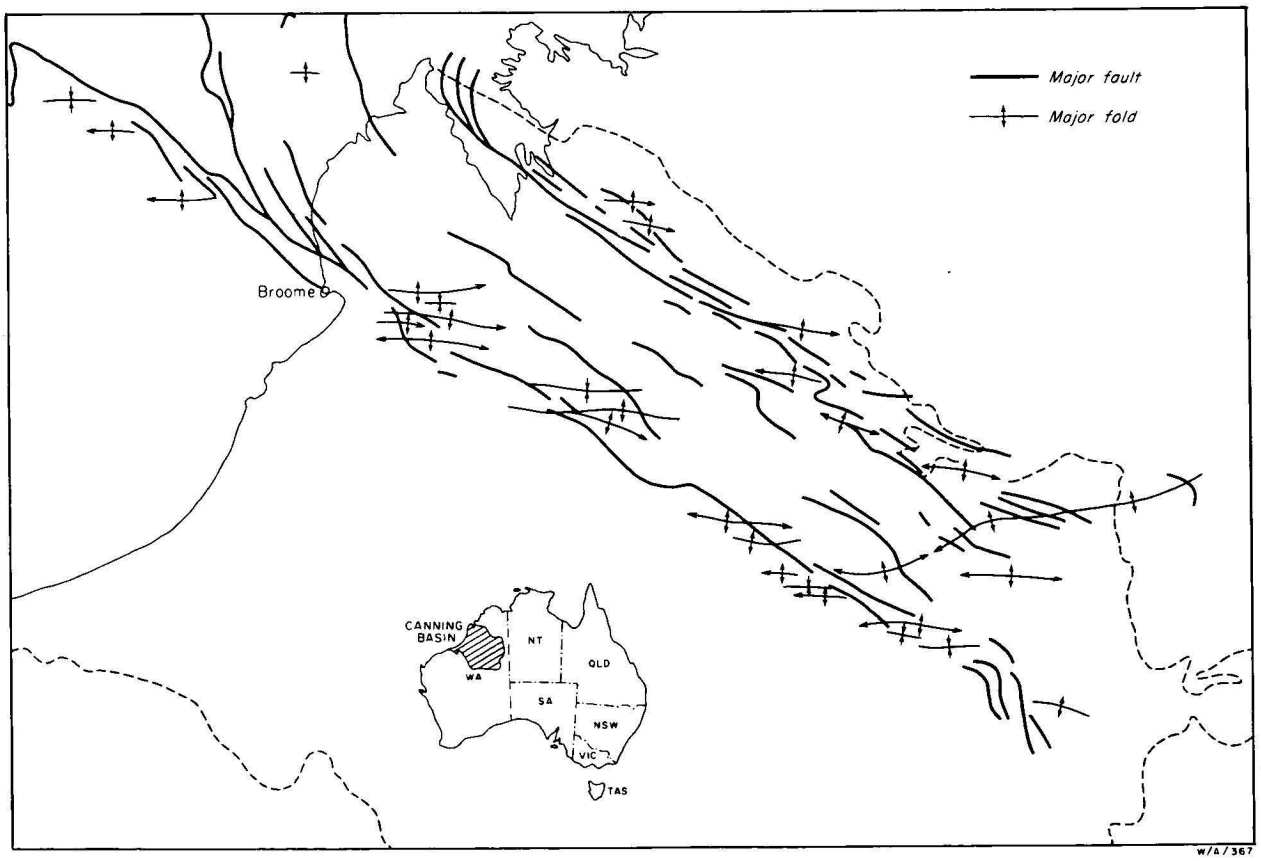

Figure 9. Major structures traced from a photograph of the clay cake that had been subjected to simple dextral shear. Coastline and limit of older rocks have been added for comparison with Figure 8.

The structural model applied to the Fitzroy Graben

The major fault systems of the Fitzroy Graben have been reproduced in a general fashion by the models. Comparison between the model and mapped structures can be made by referring to Figures 8 & 9. Figure 8 shows the subsurface basal Palaeozoic and possibly basement structure within the graben, and Figure 9 shows the major structures traced from a photograph of the model. North-south faults of the graben can be explained by tensional faulting as predicted from the theoretical strain ellipse for a dextral shear couple, and the faults at low angles to the fault system (synthetic) are the low-angle half of the conjugate set.

Reverse drag and rotating fault planes as described previously are present in Devonian rocks on both the Dummer Range and Pinnacle faults in areas where, according to the model, extension may be expected if dextral shear was a major tectonic influence.

The open upright style and gently plunging east-west axes of the major folds mapped in the cover rocks of the graben have been reproduced in the model by dextral shear. It seems likely that basement folds, although ill defined by seismic reflection traverses, will reflect the surface fold pattern. Seismic traverses approximately normal to and crossing the St George Range anticline reveal that the surface folds extend at least 4000 m below the surface into Late Palaeozoic rocks.

The King Leopold mobile belt (Fig. 8) has been simulated in the model by right lateral movement along the northern fault system. Simulation of the southern portion of the Halls Creek mobile belt has been achieved by increasing the resistance to movement at the eastern end of the model.

Moderately plunging folds at the western end of the northern fault system on the model (Fig. 7) were produced by compression caused by rotation of the central block against the northern block—which had been deliberately extended for that purpose. Structural complexity in the area north of King Sound is apparent from various geological and tectonic maps; the westward change in strike of the limits of uppermost Permian and Triassic sedimentary rocks shown on the maps corresponds to an area of relative uplift during the deposition of those rocks. This uplifted area may be analagous to the folded area on the model.

The pronounced arcuate V-shaped tear in the clay at the western end of the model (Fig. 5) is the result of dextral wrench movement, which caused clockwise rotation of the central block away from the southern block and coeval bifurcation of the southern wrench zone. This pattern of fractures is remarkably similar to the Fenton fault system, which bifurcates and runs offshore into the southern margin of the Leveque shelf. Clockwise rotation of the proto-Leveque Shelf may have caused initial basement rifting and bifurcation of the Fenton fault system which allowed subsidence of the southern part of the shelf under the load of subsequent sedimentation.

Basement subsidence in the graben has not been imitated by the models although some depression of the clay near the wrench zones is evident. The origin of the original basement weaknesses is unclear, but thickening of the post-Late Devonian sequence in the graben is evidence for subsidence since then. The causes of subsidence has yet to be determined.

Conclusions

The experiments have demonstrated the feasibility of basement wrenching as a likely cause of structures mapped in the Fitzroy Graben. A single right-lateral movement in the model has reproduced the orientation of major faults and folds within the graben. The large, open, upright, gently plunging folds developed in the model appear to have a similar style to those mapped in the cover rocks of Fitzroy Graben. Folding of basement rocks is not sufficiently well-defined by seismic reflection data to ascertain if there is any correlation between basement folds and the folds in the cover rocks.

Strike-slip faults that initially have vertical fault planes can develop into curving master faults, and become part of reverse drag structures in areas where deformation introduces a tensional component.

Major features such as the offshore depression on the southern margin of the Leveque Shelf, and part of the Halls Creek mobile zone, may have been produced, as simulated in the models, by major dextral wrenching, and in the case of Leveque Shelf by later subsidence, of basement rocks. Absorption of lateral movement by the Halls Creek mobile belt may account for the less deformed, more platform-like northeast Canning Basin.

Acknowledgements

I thank Dr M. J. Rickard of the Australian National University for the opportunity and the facilities to carry out the experiments, and members of the former Basins Study Group (BMR) for helpful discussion and encouragement.

The figures were drawn by R. R. Melsom.

References

CLOOS, E., 1955—Experimental analysis of fracture patterns. *Geological Society of America Bulletin,* **66**, 241-56.

CLOOS, E., 1968—Experimental analysis of Gulf coast fracture patterns. *American Association of Petroleum Geologists Bulletin,* **52**, 420-44.

MEAD, W., 1920—Notes on the mechanics of geologic structures: *Journal of Geology,* **28**, 505-23.

GUPPY, D. J., LINDNER, A. W., RATTIGAN, J. H., & CASEY, J. N., 1958—The geology of the Fitzroy Basin, Western Australia. *Bureau of Mineral Resources, Australia, Bulletin* **36**.

HAMBLIN, W. K., 1965—Origin of 'Reverse Drag' on the downthrown side of normal faults. *Geological Society of America Bulletin,* **76**, 1145-64.

MERZER, A. M., & FREUND, R., 1975—Buckling of strike-slip faults—in a model and in nature. *Geophysical Journal of the Royal Astronomical Society,* **43**, 517-30.

MORGENSTERN, N. R., & TCHALENKO, J. S., 1967—Microscopic structures in kaolin subjected to direct sheer. *Geotechnique,* **17**, 309-28.

RATTIGAN, J. H., 1967—Fold and fracture patterns resulting from basement wrenching in the Fitzroy depression, Western Australia. *Australasian Institute of Mining and Metallurgy, Proceedings,* **9**, 17-22.

SKEMPTON, A. W., 1966—Some observations on tectonic shear zones. *International Society for Rock Mechanics.* Congress 1st, Proceedings, Lisbon, **1**, 329-35.

SMITH, J. G., 1968—Tectonics of the Fitzroy wrench trough, Western Australia. *American Journal of Science,* **266**, 766-76.

TCHALENKO, J. S., 1968—The evolution of kink of bands and the development of compression textures in sheared clays. *Tectonophysics*, **6**, 159-74.

TCHALENKO, J. S., 1970—Similarities between shear zones of different magnitudes. *Geological Society of America Bulletin*, **81**, 1625-40.

TCHALENKO, J. S., & AMBRASEYS, N. N., 1970—Structural analysis of the Dasht-e Bayāz (Iran) earthquake fractures. *Geological Society of America Bulletin*, **81**, 41-60.

TOWNER, R. R., in press—Crossland, W.A.—1:250 000 Geological Series. *Bureau of Mineral Resources, Australia, Explanatory Notes*, **SE/51-16**.

VEEVERS, J. J., & WELLS, A. T., 1961—The geology of the Canning Basin, Western Australia. *Bureau of Mineral Resources, Australia, Bulletin*, **60**.

WILCOX, R. E., HARDING, T. P., & SEELY, D. R., 1973—Basic wrench tectonics. *American Association of Petroleum Geologists Bulletin*, **57**, 74-96.

BMR Journal of Australian Geology & Geophysics, 3, 1978, 76-79

Delny-Mount Sainthill Fault System, eastern Arunta Block, Central Australia

R. G. Warren

Introduction

The Delny-Mount Sainthill Fault System, a distinctive feature on satellite photographs, can be traced as a well-developed geological and geophysical feature extending some 130 km across the Arunta Block, central Australia. It has a slightly north-of-west trend, from 4 km south of Mount Thring (22°49′S, 136°02′E) to 5 km south of Delny Outstation (22°33′S, 134°49′S) (Figs 1, 2). The deformed nature of the rocks at Mount Sainthill was first noted by Smith and others (1960), who described a blastomylonite derived from nearby granite, and recorded the gradational contact between deformed and undeformed units. Shaw & Warren (1975) mapped the Delny section of the Fault System. The nature of the remainder of the Fault System and its continuity was recognised during rapid reconnaissance to provide data for interpretation of new coloured aerial photography in the 1976 field season.

Regional geology

The Arunta Block is considered to contain three major depositional units, each with probable stratigraphic significance, but recognised primarily by their distinctive lithologies (Shaw & Warren, 1975; Shaw & Stewart, 1976; Stewart & Warren, 1977, see Fig. 2). Division I consists principally of volcanogenic rocks and immature sediments, usually at the granulite grade of regional metamorphism. Division II (equated with the Warramunga Group in the Tennant Creek area) contains a larger proportion of derived sediments. Division III units (equivalent to Hatches Creek Group) contain mature quartzite and pelite. They overlie rocks of Division II unconformably.

In the region affected by the Delny-Mount Sainthill Fault System Division I is represented by the Kanandra Granulite, a unit of the Strangways Metamorphic Complex, cropping out mainly in a fault-bounded block extending eastward from south of Delny. It consists of garnetiferous felsic gneiss, with pods and thin layers of mafic granulite and lesser proportions of metasediments. South of the Fault System these granulites are intruded by small bosses of Mount Swan Granite (see below), but north of the Fault System they occur as rafts in the Mount Swan Granite (and possibly in the Dneiper Granite).

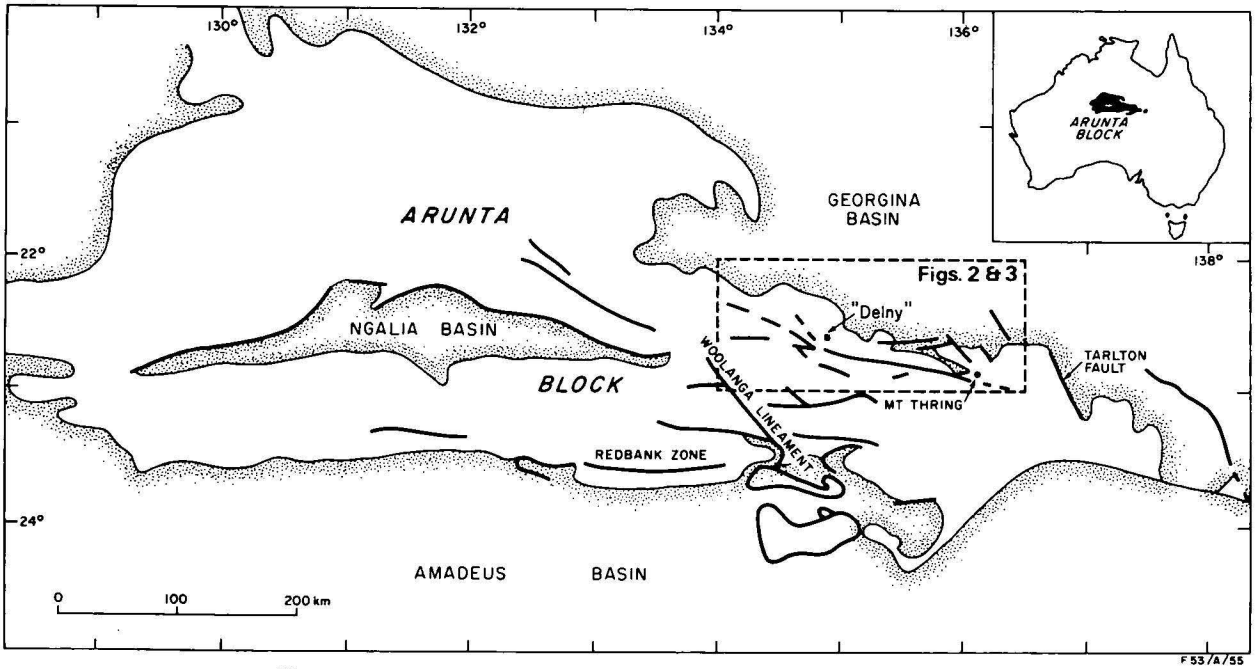

Figure 1. Major faults within the Arunta Block, central Australia.

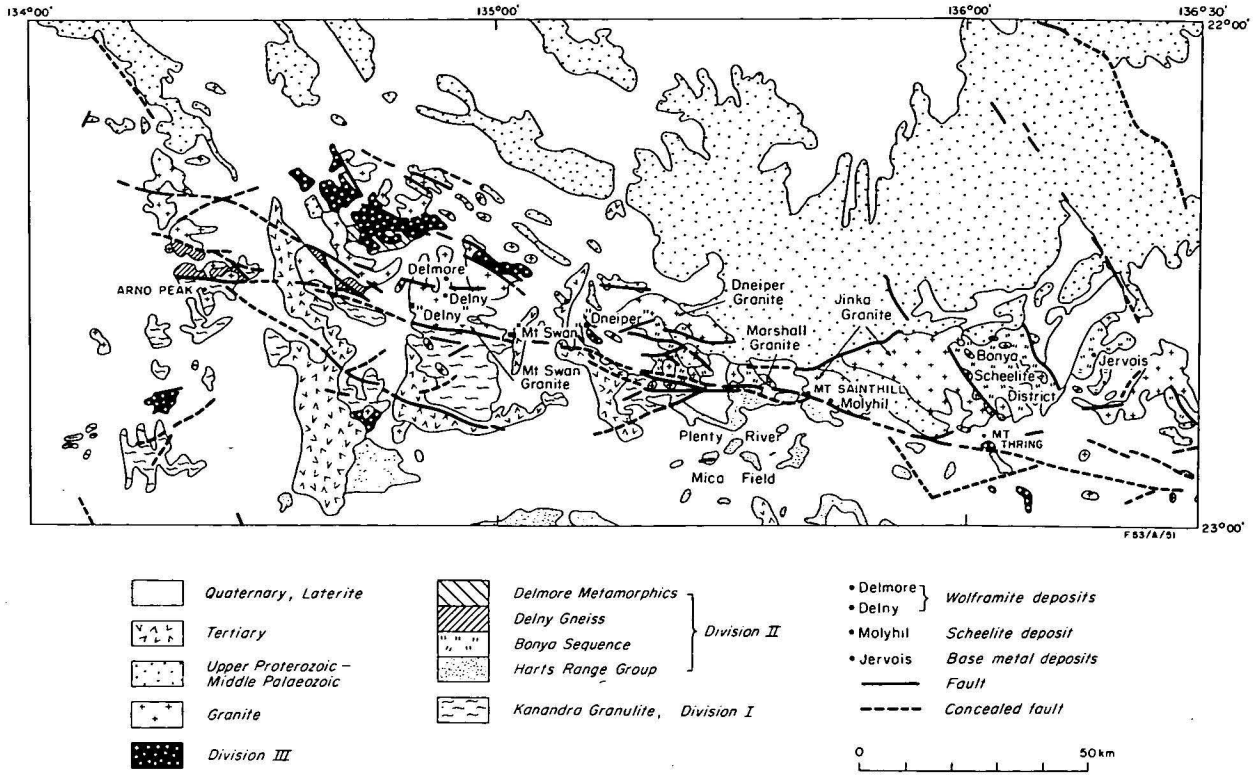

Figure 2. Regional geological setting of the Delny-Mount Sainthill Fault System.

The Harts Range Group (part of Division II) crops out in low hills rising above the Plenty River Plain to the south of the Fault System; it does not crop out north of the Fault System. The various units mapped by Joklik (1955) in the Harts Range can also be recognised in these hills, including garnet-biotite-quartz-oligoclase gneiss with minor mafic pods (Irindina Gneiss); calcareous gneiss and marble (Naringa Calcareous Member of the Irindina Gneiss and an unnamed unit); porphyroblastic felsic gneiss (Bruna Gneiss) and fine-grained leucocratic felsic gneiss (Entia Gneiss). The metamorphic grade rises from upper amphibolite to granulite towards the Fault System; retrograde metamorphism is superimposed immediately adjacent to the Fault System.

Northwest of Delny, Shaw & Warren (1975) delineated two metamorphic units in Division II: the Delny Gneiss, mainly potash-rich pelites; and the Delmore Metamorphics, a suite of calc-silicate gneisses and semi-pelitic gneisses.

In the Bonya Scheelite District, northeast of Mount Thring, Central Pacific Minerals N.L. (Bowen, Hensridge, & Paine, 1972) have mapped a sequence of two-mica schist, metamorphosed intermediate volcanics, calc-silicate gneiss, marble, amphibolite and magnetite quartzite, informally referred to as the Bonya sequence. A similar but less well exposed sequence to the east contains the Jervois ore bodies (Robertson, 1959).

The region north of the Fault System between these two areas is not yet mapped, but reconnaissance traverses suggest that the Bonya sequence persists west, and correlates with the Delny Gneiss and Delmore Metamorphics.

The regional metamorphic grade north of the Fault System is generally lower amphibolite, but locally it shows conditions verging on upper amphibolite (Shaw & Warren, 1975; Dobos, 1975).

Both the Harts Range Group and the Bonya sequence are assigned to Division II, as they contain a large proportion of clastic sediments. However the pelites in them are completely different: the Irindina Gneiss contains a predominance of oligoclase relative to potassium feldspar, whereas the pelites of the Bonya sequence are rich in muscovite, which, at the upper amphibolite to granulite grade of the Irindina Gneiss, would give rise to orthoclase-sillimanite assemblages. In general the chemical characteristics of the Harts Range Group are better known than those of the Bonya sequence. However, points such as the occurrence of scapolite (which is characteristic of calcareous units of the Harts Range Group) north of the Fault System only as a contact metasomatic mineral indicate that in the Bonya rocks the two units are indeed different.

Rocks of Division III have been mapped 12 kms north of Delny Outstation, where a lower pelitic unit (Ledan Schist) and an upper quartzite (Utopia Quartzite) crop out. Similar rocks crop out north of the Fault System near Dneiper homestead (22°37', 136°12'), immediately north of the Fault System at Mount Thring, and south of the Fault System, about 15 km southeast of Mount Thring. The metamorphic grade of these rocks is generally lower amphibolite, but reaches upper amphibolite southeast of Mount Thring.

Tectonically the Fault System is the northern limit of the Ambalindum Block of Shaw & Warren (1975) and, locally, the southern limit of the region of extensive granites (the northern Arunta zone of Stewart & Warren, 1977). Granite, making up about half the exposure north of the Fault System, ranges from gneissic and/or porphyritic to anisotropic. There are four named granites in the zone immediately north of the Fault System. From east to west these are the Jinka Granite, a coarse, even-grained, slightly gneissic granite; the Marshall Granite, a slightly gneissic leucogranite; the Dneiper Granite, a gneissic granite (probably a granite com-

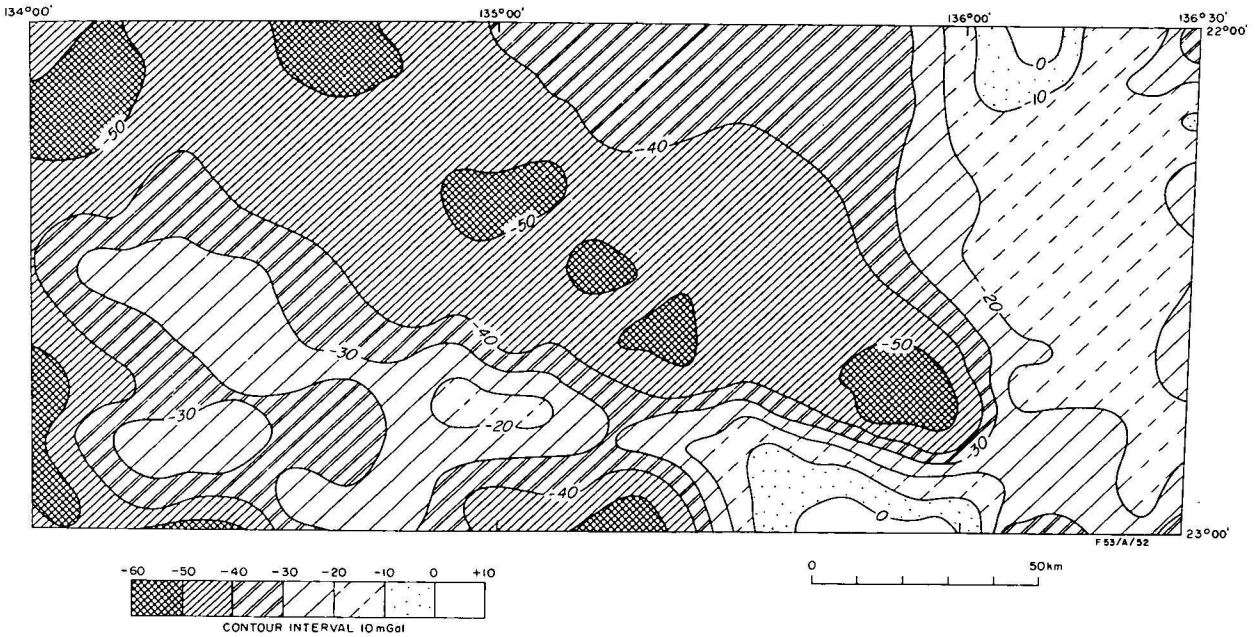

Figure 3. Distribution of Bouguer gravity anomalies in the vicinity of the Delny-Mount Sainthill Fault Zone (after the Gravity Map of Australia at 1:5 000 000).

plex); and the Mount Swan Granite, a porphyritic gneissic granite. In addition there are several other unnamed (and unmapped) granites in this zone. Outcrops of granite south of the Fault System take the form of small bosses intruding the Kanandra Granulite. In the west these are part of the Mount Swan Granite, but towards the eastern limits of the Kanandra Granulite the granites belong to the unnamed units (shown on the *extant* edition of the Huckitta 1:250 000 map as *Dneiper Granite*).

The Arunta Block north of the Fault System is overlain by platform sediments of late Proterozoic to Devonian age, including the Georgina Basin sequence.

In the late Mesozoic and early Tertiary this part of the Arunta Block was intensely and deeply weathered; in the middle to late Tertiary a number of small basins were filled by continental sediments.

Nature of the Fault System

The Fault System consists of a discontinuously exposed, anastomosing zone of deformed rocks, at some localities encompassing slivers of undeformed rocks. Zones of deformed rocks are commonly half a kilometre wide; at Mount Sainthill they exceed a kilometre in width. Generally the rocks within the deformed zones can be equated in composition with undeformed units away from the fault zone (cf. Smith and others, 1960), but there is a marked change in metamorphic facies from granulite or upper amphibolite to lower amphibolite and greenschist, and in fabric from granular to markedly layered and lineated. Segregation of quartz is not widespread, but where it has taken place the quartzose material has itself been deformed by later movements; the Delny section in particular contains mylonitic quartzite and refolded quartz veins. These features permit the tracing of the Fault System as a series of basement highs through an area of thin Tertiary sediments south of Mount Swan homestead. The rocks within the fault zones are less resistant to erosion, and tend to be less exposed than their undeformed counterparts; thus the Fault System generally occupies a topographic low. Towards Mount Thring the Fault System is very poorly exposed; south of Mount Thring (which contains mylonitic rocks but is not on the main Fault System) continuity with the Fault System is inferred from the juxtaposition in two adjacent monadnocks of units of Divisions II and III. A strong photolineament, traceable from the most easterly known outcrop of mylonitic rocks some 6 kms to the west, passes between the monadnocks. This photolineament continues through areas of sand cover for about 50 kms and is interpreted as a concealed fracture; but faults with a north-northwest trend parallel to the Tarlton Fault dominate this region.

West of Delny, the system may continue beneath Tertiary cover to link up with a major fault north of Arno Peak—perhaps adding another 60 km to its length.

Dips on the deformed rocks are steep (85°-65°S near Mount Sainthill, 80°N in parts of the Delny section), and lineations plunge steeply. This suggests at least that the later movements on the fault have had a major vertical component. At the Delny end of the Fault System the distribution of Mount Swan Granite and Kanadra Granulite suggests that a deeper level of the intrusive contact is exposed north of the Fault System, and hence that the cumulative effect of movement on the Fault System has been north-side-up, without any significant transcurrent component. The curvilinear nature of the fault traces is also at variance with transcurrent movements.

Geophysical expression

The Fault System forms a distinctive feature on regional aeromagnetic maps, mainly because of the contrast in magnetic characteristics of juxtaposed units. To the south, granulites of Division I give a magnetically disturbed but high response, whereas the Harts Range Group is magnetically quiet and low, with local contrast over calc-silicate horizons. North of the Fault System the Delny Gneiss and Delmore Metamorphics produce magnetically disturbed areas, whereas the

granites, particularly the Jinka Granite, give magnetic lows.

There is a marked gravity gradient across the Fault System (Fig. 3). To the north extensive granites correspond with Bouguer anomaly lows. Higher values south of the Fault System correspond to granulites of Division I and granulites in the Harts Range Group close to the Fault System.

The aeromagnetic and the regional gravity maps suggest that the Fault System ceases to be a major feature east of Mount Thring.

Age of the Fault System

There is no direct evidence for the age of the Fault System. The youngest units deformed within the system are granites with ages in excess of 1700 m.y. (L. P. Black, BMR, pers. comm.). The Redbank Zone, a wide belt of highly deformed rocks forming a major west-trending lineament near the south-central margin of the Arunta Block was initiated at about 1620 m.y. (Marjoribanks & Black, 1974). This is only one of the major structures within the Arunta Block to have been successfully dated so far. It trends more nearly east-west than does the Delny-Mount Sainthill Fault System, but the two are similar—both are wide, intensely deformed, and markedly retrogressed structures post-dating the major regional metamorphism. The Delny-Mount Sainthill Fault System does not cut the late Proterozoic-Middle Palaeozoic units, and is overlain by Tertiary sediments.

Economic implications

The Fault System separates the Harts Range Group from an extensive area of granites; it also separates a northern area more prospective for tungsten from the presently derelict Plenty River Mica Field in the Harts Range Group. The Bonya Scheelite District contains a number of metasomatic deposits of scheelite in calc-silicate skarns, introduced by pegmatites and granite (Bowen and others, 1971), and the Molyhil deposit (scheelite and molybdenite), about 6 km east-northeast of Mount Sainthill, is in roof pendants of calc-silicate skarn in the Jinka Granite. The Delny and Delmore wolframite deposits north of the western end of the Fault System are in roof pendants of meta-pelite and amphibolite in the Mount Swan Granite. Only a few traces of scheelite (at about 23°03'S, 135°05'E) have so far been found south of the Fault System.

The most important metallotect controlling the distribution of the fluorite and barite veins cutting the Jinka Granite north and northeast of Mount Sainthill was considered by Jensen (1971) to be proximity to the unconformity with the overlying late Proterozoic sediments. All known deposits are less than a kilometre from the present position of the unconformity, and at least some are demonstrably younger than the basal sediments of overlying units. Van Alstine (1976) has advanced a theory that fluorite deposits are clustered along major structures: it should be noted that the fluorite deposits are close to the north side of the Fault System.

The spatial relationship of the Mud Tank Carbonatite and the late Proterozoic Mordor Igneous Complex to the Woolanga Lineament (Fig. 1), a deep fracture in the south-central Arunta Block, has been noted by Langworthy & Black (in prep.). If the Delny-Mount Sainthill Fault System persists as a near vertical structure deep into the crust it may also serve as a conduit for similar intrusions. Presently the only indications of deep-source intrusions are three (separate) short references to high copper-chrome values or to small ultrabasic intrusions in the district (Hosking, 1972; Cooney, 1973; Geological Survey of the Northern Territory, 1976).

Acknowledgement

The figures were drawn by Jill Clarke and R. R. Melsom.

References

BOWEN, B. K., HENSTRIDGE, D. A., & PAINE, G. G., 1971—Jinka Plain E.L. 603. Geology, scheelite mineralization of the Bonya Bore area, Northern Territory. *Central Pacific Minerals N.L. Report* NT-39 (unpublished).

COONEY, R. G., 1973—Report on E.L. 339. *Neptide Mineral Exploration Pty Ltd* (unpublished).

DOBOS, S. K., 1975—Metamorphism in the northeast Arunta Block, N.T. *Geological Society of Australia, 1st Convention, Adelaide, May 1975*, Abstract, 38.

GEOLOGICAL SURVEY OF THE NORTHERN TERRITORY, 1976—Monthly summary of activities for August, 1976 (unpublished).

HOSKING, A. J., 1972—Exploration Licence 377 (Mopunga Range Prospect) Final Report. *ASARCO (Aust.) Pty Ltd* (unpublished).

JENSEN, C. J., 1971—Progress report on authority to prospect 2283. Sampling and evaluation of fluorite reefs A, C & E. Jinka Plain, Northern Territory. *Central Pacific Minerals N.L. Report* NT-48.

JOKLIK, G. F., 1955—The geology and mica-fields of the Harts Range, central Australia. *Bureau of Mineral Resources, Australia, Bulletin* **26**.

LANGWORTHY, A. P., & BLACK, L. P., in prep.—The Mordor Complex, a highly differentiated potassic intrusion with kimberlitic affinities in central Australia. *Bureau of ....Mineral Resources, Report.*

MARJORIBANKS, R. W., & BLACK, L. P., 1974—Geology and geochronology of the Arunta Complex, north of Ormiston Gorge, central Australia. *Journal of the Geological Society of Australia*, **21**, 291-300.

ROBERTSON, W. A., 1959—Jervois Range copper-lead deposits, Northern Territory. *Bureau of Mineral Resources, Australia, Record* **1959/103** (unpublished).

SHAW, R. D., & STEWART, A. J., 1976—Arunta Block—regional geology. *In* KNIGHT, L. C. (Editor), ECONOMIC GEOLOGY OF AUSTRALIA AND PAPUA NEW GUINEA: 1 METALS. *Australasian Institute of Mining and Metallurgy, Melbourne, Monograph Series* **5**, 437-42.

SHAW, R. D., & WARREN, R. G., 1975—Alcoota, N.T.—1:250 000 Geological Series. *Bureau of Mineral Resources, Australia, Explanatory Notes* **SF/53-10**.

SMITH, K. G., SMITH, J. W., WOOLLEY, D. R. G., & PULLEY, J. M., 1960—Progress report on the geology of the Marshall River Area, N.T. *Bureau of Mineral Resources, Australia, Record* **1960/34**.

STEWART, A. J., & WARREN, R. G., 1977—The mineral potential of the Arunta Block. *BMR Journal of Australian Geology & Geophysics* **2**, 21-34.

VAN ALSTINE, R. E., 1976—Continental rifts and lineaments associated with major fluorspar districts. *Economic Geology*, **71**, 977-98.

BMR Journal of Australian Geology & Geophysics, 3, 1978, 80-83

Buried reef structures in the Lennard Shelf, Canning Basin, Western Australia

J. S. Rasidi

Buried Upper Devonian reef has been found in Meda No. 1 borehole in the Lennard Shelf, Canning Basin. Frequency analysis made on seismic-record sections across the structure indicates an increase in the frequency of seismic reflection above the structure. The frequency increase is interpreted as indicating thinning of sedimentary layers caused by differential compaction commonly found above a reef. Analysis of a further sixteen selected seismic-record sections containing features suspected to be reef structures shows the presence of similar frequency anomalies on four of the seismic sections, and is suggestive of a further four buried reef structures in the Lennard Shelf.

Introduction

Upper Devonian reefs in the Canning Basin (Fig. 6) occur in the Lennard Shelf, a structural subdivision of the basin. Exposed at the surface, they are found in the limestone ranges where they are named the Windjana Limestone (Derrick & Playford, 1973). Evidence for the occurrence of reef structures buried in the subsurface in the Lennard Shelf has been found in Meda No. 1, in which a thick reef carbonate was intersected at depth. Although there are reasons to belive that the Meda No. 1 structure is only one of many buried reefs yet undiscovered in the area, extensive geophysical exploration and drilling have failed to locate other similar structures.

Geophysical methods for identifying buried reefs are well documented in the literature. The successful use of these methods is due largely to the physical characteristics of reefs and their effects on the overlying sediment. Reef geometry, the decrease in thickness (Yungul, 1961; Ferris, 1968), and the increase in seismic wave velocity within the sediment above a reef structure (Davis, 1973), give rise to some discrete expressions on seismic data recorded over the structure. Diffraction patterns from reef edges, a 'pull-up' effect due to velocity anomalies, and the disappearance of reflections from beds below the structure, are some of the more readily observable indications of the presence of reef structures. An increase in the frequency of seismic reflections, which is caused by the thinning of sedimentary layers caused by the differential compaction above reef structures, is usually only small and difficult to discern. Fitton & Long (1967) suggested that the presence of this small frequency variation is, however, an important diagnostic indicator of reef structures, and noted that it can be readily observed using a Laser Scan optical system.

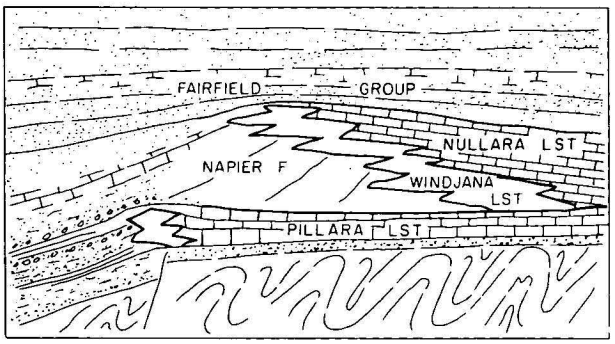

Figure 1. Relationships of stratigraphic units in the reef complex (after Playford, 1976).

This paper discusses the result of an investigation on whether seismic data over a known reef structure in the Lennard Shelf indicate an observable frequency anomaly, and also if other similar structures can be identified and mapped.

Acknowledgement

The figures were drawn by G. Butterworth.

Brief exploration history

Intensive petroleum exploration in the Lennard Shelf began at the end of 1956, when a combined reflection and refraction seismic survey was undertaken by West Australian Petroleum Pty Ltd. In 1958, Meda No. 1 was drilled to test a structure interpreted as a probable Devonian reef. About 350 m thick of Upper Devonian carbonate section, which in parts contain fragments of fauna indicative of reef facies (Pudovskis, 1962) was intersected at a depth of 1700 m. Several litres of paraffin-base crude oil were recovered from the Lower Carboniferous Fairfield Group, and a number of gas zones were intersected within the Upper Devonian carbonate section.

From 1959 to 1970, the search for petroleum in the area was directed almost exclusively to testing hydrocarbon potential of structures associated with Upper Devonian reef, but had disappointing results.

Stratigraphy

A summary of Upper Devonian and Lower Carboniferous stratigraphic nomenclature used in the Lennard Shelf and a diagrammatic section illustrating the relationship of the stratigraphic units are shown on Figure 1.

In Meda No. 1, the Upper Devonian reef facies Windjana Limestone is only thin. Where it occurs, it overlaps its marginal-slope equivalent, the Napier Formation, and is underlain by the back-reef equivalent, the Nullara Limestone (Playford, 1976). The top of the Upper Devonian reef complex, especially the Nullara Limestone, gives rise to a very prominent reflection (Fig. 3), which can be traced over a large area.

Method of investigation

Two seismic-record sections across the Meda No. 1 structure (lines AX and BP), and sixteen other sections containing features suspected to be reef structures, were selected and reduced to 35 mm film slides. To allow a

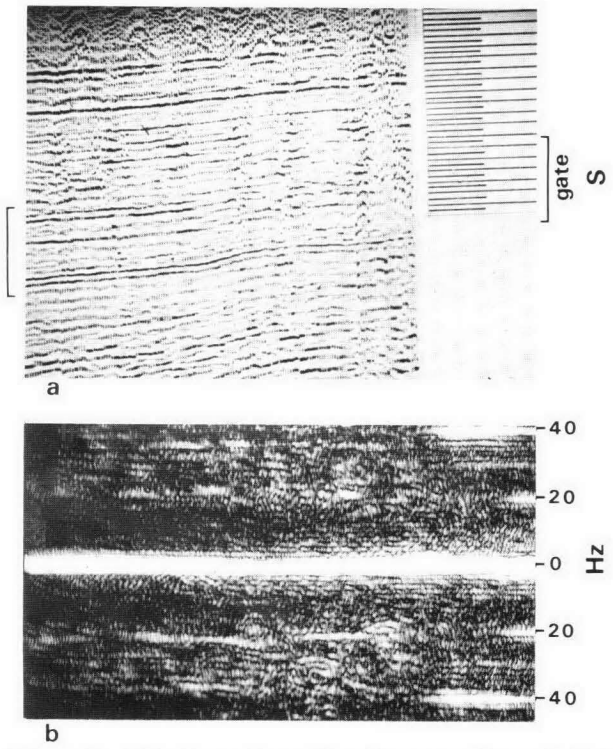

Figure 2. Seismic section with reference grids equivalent to 20 Hz and 40 Hz (A), and its optical spectrum (B).

good scan resolution for frequency of up to 40 cps, the vertical scale of the sections was reduced to 9 mm/s.

The basic principles and operation of the Laser Scan system, similar to the one used, have been described in detail by Dobrin and others (1965). A seismic-record section acts as a two-dimensional diffraction grating of variable grid spacing. An optical system is set up to produce a diffraction pattern at one of the optical planes in the system which is equivalent to the Fourier Transform of the seismic section. In Figure 2a, two reference grids representing frequency of 20 and 40 Hz are shown at the right-hand end of a seismic section. The display of two-dimensional Fourier Transform spectrum of the seismic section within the indicated gate is shown in Figure 2b. The calibration grids give bright lines at the 20 and 40 Hz positions of the transform.

The accuracy of determining the level at which lateral frequency variations occur is governed by the depth of the gate. It was observed that the optimum gate opening suitable for this analysis was about 0.400 s.

Results

Figure 3a shows a straight 6-fold seismic-record section for line AX through the Meda No. 1 structure. The strong reflection at about 1.00 s is from the top of the Nullara Limestone. The position of the reef structure in the section is indicated by the pull-up effect which can be seen at the centre of the picture. The display of the two-dimensional Fourier Transform spectrum for the full length of this record section is shown in Figure 3b. Figures 3c, d, e and f are the spectrum displays of the same record section, but only within the indicated gate c, d, e, and f respectively. It can be seen that high frequencies occur at the position of the structure. This concentration of higher

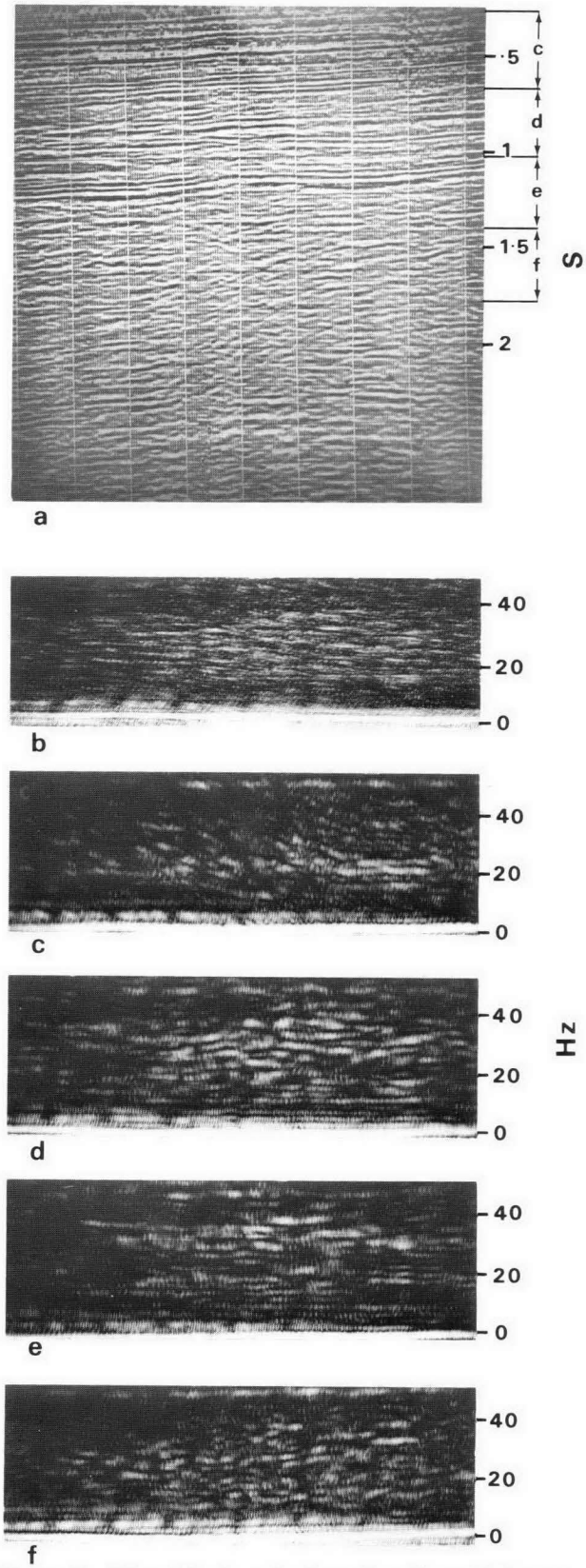

Figure 3. Line AX. A—seismic section, B—optical spectrum, C-F—optical spectrum of record section within indicated gates.

frequencies is seen most clearly in Figure 3d, which is the optical spectrum of reflection bands immediately above the reflection from the Nullara Limestone. In Figure 3e an increase in frequency from about 23 Hz

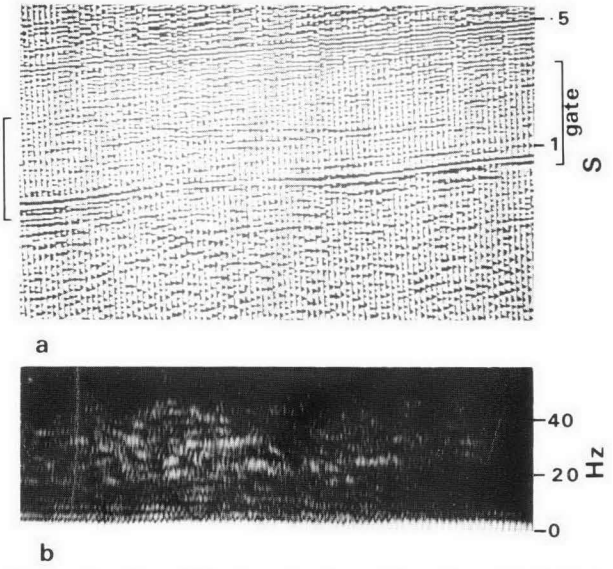

Figure 4. Line BP. A—seismic section, B—optical spectrum.

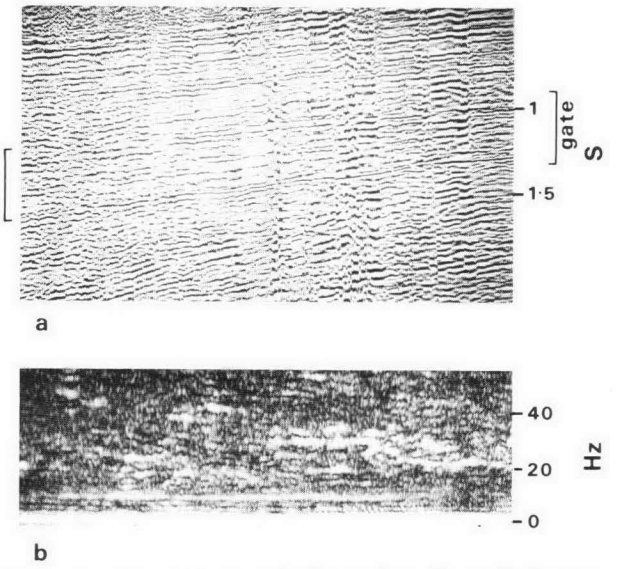

Figure 5. Line M. A—seismic section, B—optical spectrum.

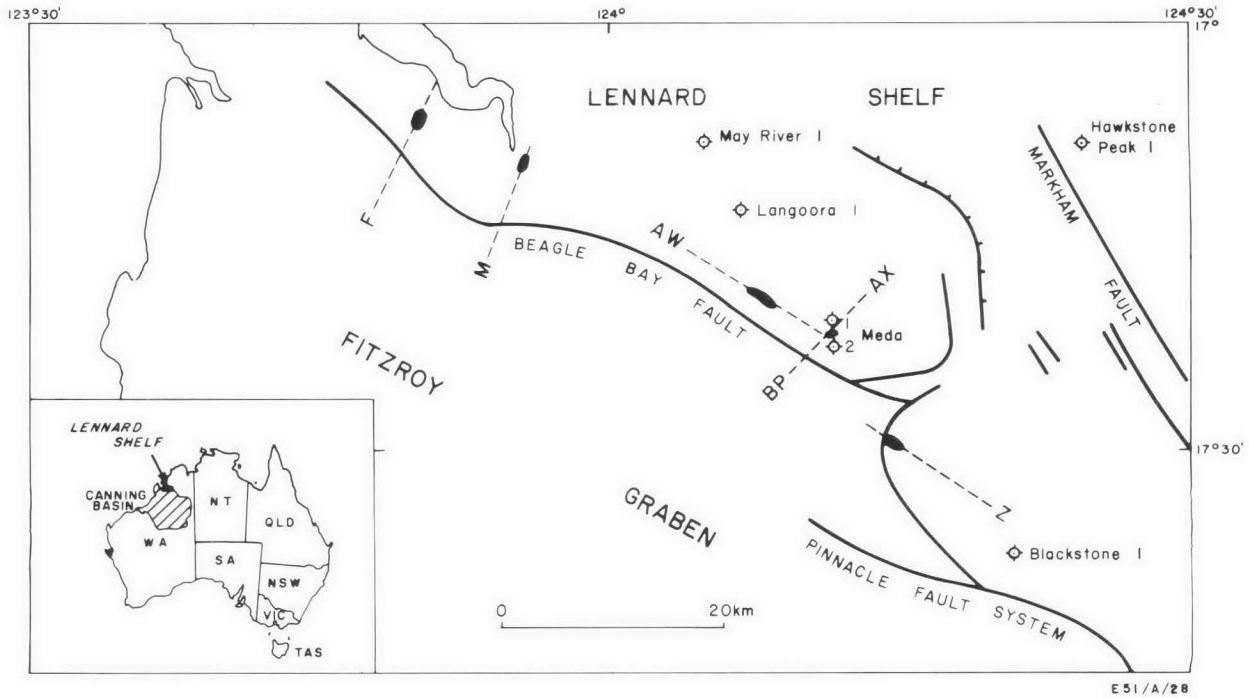

Figure 6. Probable reef structures in the Lennard Shelf.

to 28 Hz is weakly shown. However it is clear that no apparent frequency anomaly can be observed in the reflections from below the structure (Fig. 3f). This absence of anomalous increase in frequency spectra usually characterises seismic reflections from reef structure (Fitton & Long, 1967).

The transform spectrum of a 6-fold with TVD seismic-record section for line BP (which is through the Meda No. 1 structure) also shows a frequency increase from about 25 Hz to 32 Hz above the structure (Fig. 4). The direct association of the increase in seismic reflection frequency with the Meda No. 1 structure led to a conclusion that similar structures in the Lennard Shelf could probably be indentified from frequency variations of seismic reflections recorded over such structures.

The sixteen seismic-record sections containing features suspected to be reef structures were analysed with a 0.400 s gate set immediately above the reflection from the Nullara Limestone. Only four of these (Fig. 6) show clear lateral frequency changes. It is interesting to note the manner in which these frequency variations occur. For example on lines M and F, the dominant frequencies increase gradually from north to south (right to left, Figure 5), then drop abruptly at point A. If the increase in the frequency of seismic reflections is in fact related to the thinning of sedimentary layers above the structure, the gradual increase in frequency

suggest a gradual thinning of these layers. In a reef-structure regime it probably indicates the lagoon or back-reef part of the structure. Similarly, the sudden decrease in frequency may mark the fore-reef side of the structure.

Conclusions

The result of analyses made on seismic-records section across a known reef structure in the Lennard Shelf, Canning Basin, indicates an increase in the frequency of seismic reflections above the structure. This frequency anomaly was observed on both a straight 6-fold CDP, and a 6-fold with TVD records, suggesting that the frequency variations contained in the records are not adversely affected by the processes of record enhancement. The increase in the frequency of seismic reflections is considered to indicate the presence of thinning sedimentary layers due to differential compaction commonly occur above buried reef structures. The presence of frequency increases associated with the structures on four of the sixteen selected seismic-record sections analysed is suggestive of a further four buried reef structures similar to that intersected in Meda No. 1.

The lack of adequate reservoir rocks has been largely responsible for the disappointing record of petroleum exploration in the Canning Basin. Buried Upper Devonian reefs probably offer the best potential traps for hydrocarbon accumulation in the basin.

References

DAVIS, T. L., 1973—Geophysical study of Alberta's Keg River reefs. *Oil and Gas Journal*, **71**, 46-50.

DERRICK, G. M., & PLAYFORD, P. E., 1973—Lennard River, Western Australia—1:250 000 Geological Series. *Bureau of Mineral Resources, Australia, Explanatory Notes* (2nd edition), **SE/51-8**.

FERRIS, CRAIG, 1968—Gravity and compaction anticlines are key to oil finding. *Oil and Gas Journal*, **66**, 110-13.

FITTON, J. C., & LONG, J. A., 1967—Reef interpretation by frequency analysis. *Canadian Society of Exploration Geophysicists*, **3**, 5-23.

LYON, P. L., & DOBRIN, M. B., 1971—Seismic Exploration for Stratigraphic Traps. *In* KING, R. E. (Editor), Stratigraphic Oil and Gas Fields Classification Exploration Methods and Case Histories. *American Association of Petroleum Geologists, Memoir* **16**, 225-43.

PLAYFORD, P. E., 1976—Devonian reef complexes of the Canning Basin, Western Australia. *25th International Geological Congress, Excursion Guide No.* **38A**.

PUDOVSKIS, V., 1965—Meda No. 1 Well, Western Australia. *Bureau of Mineral Resources, Australia, Petroleum Search Subsidy Act Publication* **7**.

YUNGUL, S. H., 1961—Gravity prospecting for reefs, effect on sedimentation and differential compaction. *Geophysics*, **26**, 45-56.

R76/1403(1) Cat. No. 77 7123 2

BMR Symposium

These annual symposia stress work of relevance to industry. The Seventh Symposium will be held in Canberra in the Academy of Science Building on 2, 3, and 4 May 1978, and will be opened by the Hon. Kevin Newman, M.P., Minister for National Development. The program is given below: for further particulars write to the Director (attention Mrs E. Young, Bureau of Mineral Resources, P.O. Box 378, Canberra City, ACT 2601; or phone (062) 49 9615.

Tuesday, 2 May

Australia's non-renewable energy resources—L. C. Ranford.

The logic that underlies a feasibility study and calculations for mining projects—J. C. Erskine and E. L. Smith.

The calculation and expression of national estimates of inferred mineral resources—J. W. Cottle.

An example of a national mineral appraisal: lead and zinc—D. F. Sangster (Geological Survey of Canada).

Assessment of 1:100 000 scale geological mapping of Precambrian terrains in northern and central Australia—Panel chaired by D. Blake.

Subdivision of the Precambrian—K. A. Plumb.

Configuration and composition of basement of the Pine Creek Geosyncline, Northern Territory—D. H. Tucker.

Advances in the understanding of the stratigraphy of the Pine Creek Geosyncline, Northern Territory—I. H. Crick and P. G. Stuart-Smith.

Wednesday, 3 May

Petroleum resource assessment methods—D. J. Forman.

Maturation of petroleum source rocks in Australia: results of the BMR-CSIRO studies, 1977—J. D. Gorter.

Enhanced recovery: a general discussion with possible application to Australian oilfields—B. A. McKay.

A seismic investigation of the eastern margin of the Galilee Basin, Queensland—J. Pinchin.

Lead and zinc in carbonate rocks—prospects in the Georgina Basin, Northern Territory and Queensland—J. J. Draper.

Western Victoria, a geothermal energy prospect?—J. P. Cull.

Gravity evidence for abrupt changes in mean crustal density at junctions of Australia's crustal blocks—P. Wellman.

The use of microfossils in Precambrian correlation; problems and principles—M. D. Muir.

Geoscience in Australia—today and tomorrow—L. C. Noakes, Director.

Crustal structure in Australia from explosion seismology—D. Denham and D. M. Finlayson.

Tectonic setting of kimberlites in southeast Australia—John Ferguson and L. P. Black.

Thursday, 4 May Workshops

Involvement of government organisations in geochemical surveys.
Convener—K. R. Walker.

Georgina Basin, Northern Territory and Queensland.
Convener—A. R. Jensen.

Contents

Notes